The Gran Sasso National Laboratory

The Gran Sasso National Laboratory (LNGS) is the largest underground laboratory in the world for experiments in particle and astroparticle physics. It is one of four INFN national laboratories and it is used as a worldwide facility by scientists (presently 900 in number) from 24 countries.

Its location is between the towns of L'Aquila and Teramo, about 120 km from Rome. The underground facilities are located on a side of the ten kilometres long freeway tunnel crossing the Gran Sasso Mountain. They consist of three large experimental halls, each about 100 m long, 20 m wide and 15 m high and service tunnels for a total volume of about 180,000 cubic metres.

The average 1400 m rock coverage gives a reduction factor of one million in the cosmic ray flux; moreover, the neutron flux is thousand times less than on the surface, thanks to the smallness of the Uranium and Thorium content of the dolomite rocks of the mountain.

The headquarters and the support facilities, including the general electric and safety services, library and meeting halls, canteen, computing and networking services, mechanical, electronic and chemical shops, low radioactivity service, assembly halls, offices and administration department, are located on the surface.

The mission of the Laboratory is to host experiments that require a low background environment in the field of astroparticle physics and nuclear astrophysics and other disciplines that can profit by its characteristics and of its infrastructures.

The geographic location (inside the National Park of Gran Sasso - Monti della Laga) and the special operating conditions (underground, near a highway tunnel and in close proximity of water basins) demand that special attention is paid to the safety and environmental aspects of the activities.

Main research topics of the present scientific programme are: neutrino physics with neutrinos naturally produced in the Sun and in Supernova explosion and neutrino oscillations with a beam from CERN (CNGS program), search for neutrino mass in neutrinoless double beta decays, dark matter search, nuclear reactions of astrophysical interest.

The activity in the year 2004 returned almost to normal, with respect to 2003, thanks to the special safety works started by the Government Commissioner.

Solar neutrino physics is one of the main research sectors of the laboratory. After the glorious life of GALLEX and GNO, the focus is now on Borexino, which is dedicated mainly to the measurement of the Be line component of the solar neutrino spectrum. The construction of the main detector and of its ancillary facilities, restarted during 2004, in parallel with the safety works in Hall C. The nylon vessels were inserted and inflated in the stainless steel sphere, which was closed and is now ready for filling.

The solar models are based on data and extrapolations; in particular the thermonuclear cross sections of the involved reactions are not measured in the relevant energy range but rather extrapolated from higher energies.

The direct measurements are made very difficult by the very low values of the cross sections. LUNA published the results of the cross section measurements of the reaction

^{14}N (p,γ) ^{15}O down to the energy of the nucleosynthesis in the stars, using the new 400 kV accelerator. This is the slowest reaction in the CNO cycle and, as such determines the contribution of this cycle to solar burning and neutrino production. The LUNA results suggest a new estimate of age of the globular clusters, which are the oldest stars in the Galaxy.

Elementary particles are different from their antiparticles because their charges - not only the electric ones, but all of them - are opposite. The standard model assumes that neutrinos have only one charge, the lepton number. But, if this charge is not conserved, neutrinos and antineutrinos can be two states of the same particle. In this case well-specified nuclides would decay through the neutrino-less double beta channel. The Laboratory hosts today experiments searching for these very rare decays, employing different and complementary techniques, and it is preparing new important activities. The Heidelberg-Moscow experiment with a sensitive mass of 11 kg of enriched ^{76}Ge was the most sensitive experiment in the world and accumulated data for a 75 kg y exposure.

CUORICINO, which employs TeO_2 bolometers for a total of 42 kg and started taking data in 2003, has continuously operated in 2004. It is the most sensitive running experiment today.

The Laboratory approved two new experiments: CUORE, which brings the CUORICINO technique to a mass of more than 200 kg of TeO_2 bolometers, and GERDA planning to employ 500 kg of enriched ^{76}Ge. These activities represent the state of the art of the field.

From astronomical observations, we know that most of the matter in the Universe is not made of nuclei and electrons as normal matter. It is called dark matter, because it does not emit light, and its nature is unknown. Probably, its constituents, elementary particles that interact only very weakly with the rest (they are called WIMPs,) have not been yet discovered; they are around us, invisible, waiting to be discovered. The search for WIMPs is very difficult and requires a very low background environment and the development of advanced background reduction techniques. The search is going on in many experiments worldwide. At Gran Sasso several experiments, using different techniques, are active and new experiments have been approved and started operating in 2004.

DAMA/LIBRA employs NaI crystals to detect the WIMPs by means of the flash of light produced in the detector by an Iodine nucleus recoiling after having been hit by a WIMP, a very rare phenomenon. To distinguish these events from the background, DAMA searches for an annual modulation of the rate, a behaviour that has several aspects that are peculiar of the searched effect and not of the main backgrounds. With its about 100 kg sensitive mass, DAMA was the only experiment world wide sensitive to the annual modulation signature. After the conclusion of the experiment, results were published confirming a signal of annual modulation. The larger experiment LIBRA, with 250 kg sensitive mass, continued regularly to take data along all the year.

CRESST searches for WIMPs with a cryogenic technique, looking for a very tiny temperature increase in the detector, due to the energy deposited by nuclei hit by the WIMPs. After the final design, the CRESST2 $CaWO_2$ detector has been installed.

The GENIUS project proposes the use of one ton enriched Germanium with a strong reduction of the background for dark matter searches, double beta decay and other searches. A small test facility GENIUS-TF has been approved so far, with 40 kg of natural Germa-

nium operated in liquid Nitrogen.

Two new dark matter experiments, WARP and XENON were approved during 2004. They are based on the simultaneous detection of the ionization and scintillation signals in, respectively, liquid argon and liquid xenon. WARP performed during the year preliminary measurements underground with a small (2.3 l) prototype.

One of the major committments of the Gran Sasso Laboratory in the next decennium will be the search of tau neutrino appearance on the artificial neutrino beam being built at CERN in Geneva, the CERN Neutrinos to Gran Sasso (CNGS) project. The beam will be directed through the Earth crust to Gran Sasso at 732 km distance. Beam is foreseen to be ready in the Summer of 2006. The OPERA experiment is designed for the direct observation of tau neutrinos resulting from oscillations of the muon neutrino of the beam. This search requires both micrometer scale resolution, obtained with modern emulsion techniques and large sensitive mass (1800 t) obtained with Pb sheets interleaved by emulsion layers. In 2004 the installation in Hall C has continued regularly, even in presence of the interference represented by the water-proofing of the floor of Hall C.

ICARUS is a general-purpose detector, with a broad physics programme, based on the novel concept of the liquid Argon time-projection chamber. After the development of the "definitive project" and of the risk analysis, completed in 2003, the 600 ton module was transported from Pavia to our underground Laboratory in December 2004. The main activity of the theory group, staff and visitor scientists, has been focused on astroparticle physics, including solar and Supernova neutrinos, massive neutrinos, ultra high energy cosmic rays, topological defects and relativistic astrophysics. Important activity took place also in particle phenomenology and computer simulations of Lattice Field Theories.

The Gran Sasso Laboratory is recognized by Europe as a large scientific infrastructure. In December 2004 LNGS completed the EC contract number HPRI-CT-2001-00149 (within Framework Programme 5) for Transnational Access support in the action "Access to Research Infrastructures". This contract allowed to support access to LNGS for non-italian european scientists for more than 4500 person-days during 3 years.

In April 2004 a new EU contract started (RII3-CT-2003-505818) within Framework Program 6. The new contract is involving LNGS as one of the leader paricipants in the Integrated Infrastructure Initiative (I3) called ILIAS.
The main goal of ILIAS (Integrated Large Infrastructures for Astroparticle Physics) is to pull together all of Europe's leading infrastructures in Astroparticle Physics to produce a focused, coherent and integrated project to improve the existing infrastructures and their operation as well as to organize and structure the scientific community to prepare the best infrastructures for the future.

Gran Sasso, July 2005

The Director of the Laboratory
Prof. E. Coccia

BOREXINO. SOLAR NEUTRINO PHYSICS

Borexino collaboration

H. Back[n], M. Balata[b], A. de Bari[e], A. de Bellefon[o], G. Bellini[a], J. Benziger[c], S. Bonetti[a], C. Buck[j], B. Caccianiga[a], L. Cadonati[d], F.P. Calaprice[d], G. Cecchet,[e], M. Chen,[r], D. D'Angelo[h], A. Derbin[m], A. Etenko[s], F. von Feilitzsch[h], R. Ford[b], D. Franco[a], C. Galbiati[d], S. Gazzana[b], M.G. Giammarchi[a], M. Göger-Neff[h], A. Goretti[a], C. Grieb[h], B. Harding[d], G. Heusser[j], A. Ianni,[d], A.M. Ianni[c], H. de Kerret[o], S. Kidner[d], J. Kiko[j], T. Kirsten[j], G. Korga[a], G. Korschinek[h], H. de Kerret[o], D. Kryn[o], M. Laubenstein[b], C. Lendvai[h], E. Litvinovich[s], P. Lombardi[a], I. Machulin[s], S. Malvezzi[a], I. Manno[k], G. Manuzio[i], F. Masetti[g], U. Mazzucato[g], K. McCarty[d], E. Meroni[a], L. Miramonti[a], M.E. Monzani[a], V. Muratova[m], L. Niedermeier[h], L. Oberauer[h], M. Obolensky[o], F. Ortica[g], M. Pallavicini[i], L. Papp[a], L. Perasso[i], P. Pfeiffer[j], A. Pocar[d], R.S. Raghavan[l], G. Ranucci[a], A. Razeto[i], A. Sabelnikov[s], C. Salvo[i], S. Schönert[j], T. Shutt[d], H. Simgen[j], M. Skorokhvatov[s], O. Smirnov[m], A. Sotnikov[m], S. Sukhotin[s], Y. Suvorov[s], V. Tarasenkov[s], R. Tartaglia,[b], G. Testera[i], D. Vignaud[o], B. Vogelaar[n], V. Vyrodov[s], B. Williams[n], W. Wojcik[q], O. Zaimidoroga[m], G. Zuzel[q]

[a]Dip. di Fisica dell'Università and Infn Milano - Italy
[b]Laboratori Nazionali del Gras Sasso, Assergi (Aq) - Italy
[c]Dept. of Chemical Engineering, Princeton University - NJ USA
[d]Dept. of Physics, Princeton University - NJ USA
[e]Dip. di Fisica dell'Università and Infn Pavia - Italy
[f]Dept. of Physics, Massachusetts Institute of Technology - MA USA
[g]Dip. di Chimica dell'Università and Infn Perugia - Italy
[h]Technische Universität München - Germany
[i]Dip. di Fisica dell'Università and Infn Genova - Italy
[j]Max Planck Inst. für Kernphysik, Heidelberg - Germany
[k]KFKI-RMKI Research Institute for Particle & Nuclear Physics, Budapest - Hungary
[l]Bell Laboratories, Lucent Technologies, Murray Hill - NJ USA
[m]J.I.N.R. Dubna - Russia
[n]Dept. of Physics, Virginia Polytechnic Institute - VA USA
[o]Laboratoire de Physique Corpusculaire et Cosmologie, Paris - France
[p]I.R.M.M. - EURATOM, Geel - Belgium
[q]Institute of Physics, Jagellonian University, Kracov - Poland
[r]Dept. of Physics, Queen's University, Ontario - Canada
[s]RRC Kurchatov Institute, Moscow - Russia

Abstract

Borexino is a solar neutrino detector in commissioning phase in Hall C of LNGS. We summarize here the status of the project and the main technical achievements obtained in these years of development.

1 Introduction

Borexino is a real time experiment which plans to study the low energy (sub-MeV) solar neutrinos. The main experimental goal is the study of the 0.862 MeV ^{7} Be solar neutrino line through the neutrino-electron elastic scattering reaction. The maximum energy of the recoiling electron is 664 KeV and the experimental design threshold will be at 250 KeV. The detection reaction will be observed in a large mass of well shielded liquid scintillator. The main problem of a real time experiment with such a low energy threshold is the natural radioactivity which is present in any environment and in any material. For these reasons an intense R&D program has been carried out in the last ten years to develop methods for selecting low radioactivity materials and/or purify them. An effort in this field has to be complemented by a comparably thorough research in the field of detection and measurement of very low radioactivity levels.
The development of purification methods has been focused on the costituents of the liquid scintillator. Four main methods have been developed: distillation, water extraction, stripping with ultrapure N_2, solid gel column (Si gel, Al gel) adsorption. Significant results have been achieved by the Collaboration as for example: $10^{-16} - 10^{-17}$ (g of contaminants/g of material) for ^{232}Th and ^{238}U family and a few microBq of Rn-222 in gases and liquids.
In addition the organic solvent selected by the collaboration shows a ^{14}C presence not exceeding 10^{-18} in its ratio to ^{12}C. This impurity is particularly important because it cannot be removed by chemical purification methods.
For the measurements of these ultralow radioactivity levels, dedicated methods were developed. In addition to small-scale techniques (Ge underground detectors installed in Rn free environment, Inductively Coupled Plasma Mass Spectometer, high sensitivity Neutron Activation, Atomic Absortion Spectroscopy etc...), a Counting Test Facility (CTF), has been constructed on purpose and operated in the Hall C of LNGS. The Counting Test Facility features 4 tonnes of liquid scintillator viewed by 100 photomultipliers and shielded by 1000 tons of ultrapure water.
The sensitivities reached are summarized below and correspond to the lowest radioactivity levels obtained by the Borexino Collaboration, in preparation of the experiment:

- Bulk material radiopurities of 10^{-10} g/g for ^{238}U and ^{232}Th, $\sim 10^{-5}$ for ^{nat}K, few tenths of mBq/kg for ^{60}Co, have been measured with Ge detectors in construction materials such as stainless steel, photomultipliers, metal and plastic gaskets, products for PMT sealing, etc...
- Radon emanations of 10 μBq/m^2 from plastic materials, 0.1 mBq/m^3 for Rn-222 and 1 mBq/m^3 for Ra-226 in water, below 1 mBq/m^3 for the N_2 used for scintillator purification.
- Radiopurity levels of a few times 10^{-15} g/g ^{238}U, ^{232}Th and ^{40}K have been reached with ICMPS in measuring the Borexino shielding water.

- few ppt for ^{238}U and ^{232}Th have been obtained in the Nylon bulk measurements.
- The radiopurity of the scintillator itself was measured to be at the level of few 10^{-16} g/g for ^{238}U, ^{232}Th and $\sim 10^{-18}$ for ^{14}C/^{12}C in the Counting Test Facility.
- Bulk radiopurity levels of $10^{-13} - 10^{-14}$ g/g for Au, Ba, Ce, Co, Cr, Cs, Ga, Hg, In, Mo, Rb; less than few 10^{-15} g/g for Cd, Sb, Ta, W; $10^{-16} - 10^{-17}$ g/g for La, Lu, Re, Sc, Th; less than 1x10^{-17} g/g for U, have been reached by mean of Neutron Activation followed by a β-γ coincidence analysis selection applied to the scintillator.
- Kr and Ar contamination in nitrogen at 0.005 ppm (for Ar) and 0.06 ppt (for Kr) were obtained and measured with noble gas mass spectrometry.

These results were a milestone in the development of the Borexino detector and technique. Several of these concepts were incorporated in the construction of the high purity systems for the treatment of the most critical liquid, the scintillator of the experiment.

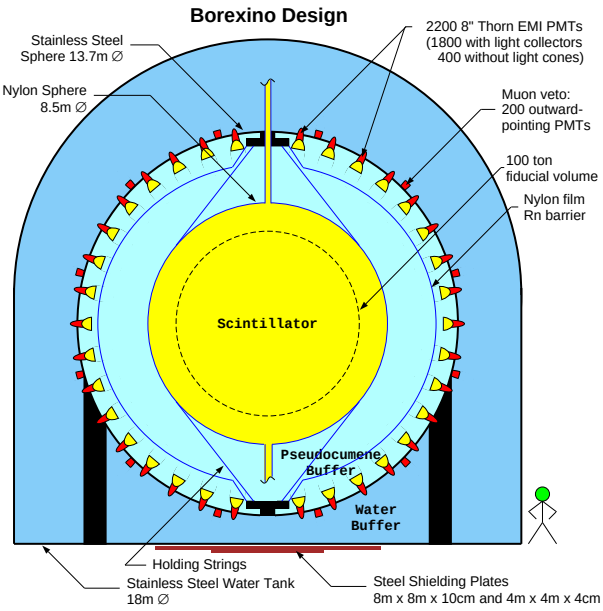

Figure 1: Schematic view of the Borexino detector.

2 The Borexino Detector

Borexino is an unsegmented scintillation detector featuring 300 tonnes of well shielded liquid ultrapure scintillator viewed by 2200 photomultipliers (fig. 1). The detector core is a transparent spherical vessel (Nylon Sphere, 100μm thick), 8.5 m of diameter, filled with 300 tonnes of liquid scintillator and surrounded by 1000 tonnes of high-purity buffer liquid. The scintillator mixture is PC and PPO (1.5 g/l) as a fluor, while the buffer liquid will be PC alone (with the addition of DMP as light quencher). The photomultipliers are supported by a Stainless Steel Sphere, which also separates the inner part of the detector from the external shielding, provided by 2400 tonnes of pure water (water buffer).

An additional containment vessel (Nylon film Radon barrier) is interposed between the Scintillator Nylon Sphere and the photomultipliers, with the goal of reducing Radon diffusion towards the internal part of the detector.
The outer water shield is instrumented with 200 outward-pointing photomultipliers serving as a veto for penetrating muons, the only significant remaining cosmic ray background at the Gran Sasso depth (about 3500 meters of water equivalent). The innermost 2200 photomultipliers are divided into a set of 1800 photomultipliers equipped with light cones (so that they see light only from the Nylon Sphere region) and a set of 400 PMT's without light cones, sensitive to light originated in the whole Stainless Steel Sphere volume. This design greatly increases the capability of the system to identify muons crossing the PC buffer (and not the scintillator).
The BOREXINO design is based on the concept of a graded shield of progressively lower intrinsic radioactivity as one approaches the sensitive volume of the detector; this culminates in the use of 200 tonnes of the low background scintillator to shield the 100 tonnes innermost Fiducial Volume. In these conditions, the ultimate background will be dominated by the intrinsic contamination of the scintillator, while all backgrounds from the construction materials and external shieldings will be negligible.
BOREXINO also features several external systems and conceived to purify the experimental fluids (water, nitrogen and scintillator) used by the experiment.

3 Status of the project

The Borexino detector is essentially completed, as well as the vast majority of the purification and ancillary plants, which will be re-commissioned after the long stop due to the judicial sequestration, ended with the de-sequestration occurred an August 2004.
The decrease of judicial contraints (already during the first half of 2004) allowed the installation of the most crucial component of the detector, the Nylon Sphere devoted to hold the scintillator. This installation was completed in May 2004 and was followed by the mounting of the last hardware components in the Stainless Steel Sphere (the remaining phototupes) and in the Stainless Steel Water Tank (almost all of the Muon Veto).

The experimental activity is now focused to bring the detector in the operational phase which foresees a first water filling followed by the final scintillator data taking.

4 Borexino and Neutrino Physics

Borexino will be studying solar neutrino physics below the 1 MeV threshold, where the Large Mixing Angle suppresion pattern becomes vacuum dominated. This is in contrast with the "matter dominated" situation of the B-8 neutrinos, the only component observed in real-time up to now.
The expected Be-7 solar neutrino rates is close to 30 counts/day. With a sizeable number of real-time expected events, Borexino can also study several time-dependences of the solar neutrino signal, including day-night and seasonal variations.
Finally, a 10% accuracy measurement of the Be-7 line will be of great importance to

measure the relative solar model parameter whose uncertainty is at present of the order of 50%.

Other physics topics can be investigated with high sensitivity with the Borexino detector, such as Supernova neutrinos, neutrino magnetic moment, terrestrial neutrinos...

Physics results already obtained with the Counting Test Facility, confirm the validity and the sensitivity of the Borexino technique.

5 List of articles published in year 2004

1. H.O. Back et al. *New experimental limits on violations of the Pauli exclusion principle obtained with the Borexino Counting Test Facility.* Accepted by Eur. Phys. Journal C.

2. H.O. Back et al. *A high-density and high-flashpoint organic liquid scintillator for applications in low-energy particle-astrophysics experiments.* Sbmitted to Nuclear Instr. & Methods A.

References

[1] G. Alimonti et al., *Science and technology of Borexino: a real-time detector for low energy solar neutrinos*, Astroparticle Physics 16 (2002) 205.

[2] C. Arpesella et al., *Measurements of extremely low radioactivity levels in BOREXINO*, Astroparticle Physics 18 (2002) 1.

DAMA. DARK MATTER SEARCH

DAMA collaboration:
P. Belli[a], R. Bernabei[a,@], A. Bussolotti[a,*], F. Cappella[a,b],
F. Montecchia[a], F. Nozzoli[a], R. Cerulli[b],
A. d'Angelo[c,d], A. Incicchitti[c], A. Mattei[c,*], D. Prosperi[c],
C.J. Dai[e], H.H. Kuang[e], H.L. He[e], J.M. Ma[e], Z. P. Ye[e,f]

in neutron measurements: M.Angelone[g], P.Batistoni[g], M.Pillon[g]

in some by-product results: F. Danevich[h], V.I. Tretyak[h]

[a]Dip. di Fisica, Università di Roma "Tor Vergata" and INFN-Roma2, 00133 Roma, Italy;
[b]Laboratorio Nazionale del Gran Sasso, INFN, 67010 Assergi (Aq), Italy;
[c]Dip. di Fisica, Università di Roma "La Sapienza" and INFN-Roma, 00185 Roma, Italy;
[d]Scuola di Specializzazione in FISICA SANITARIA, Università di Roma "Tor Vergata", 00133 Rome, Italy;
[e]IHEP, Chinese Academy, P.O. Box 918/3, Beijing 100039, China;
[f]University of Zhao Qing, Guang Dong, China;
[g]ENEA - C. R. Frascati, P.O. Box 65, 00044 Frascati, Italy;
[h]Institute for Nuclear Research, 252650 Kiev, Ukraine.

@ Spokesperson
* technical staff

Abstract

DAMA is investigating various rare processes by developing and using several kinds of radiopure scintillators. The main experimental set-ups are: i) the $\simeq$ 100 kg NaI(Tl) set-up (DAMA/NaI), which completed its data taking in July 2002; this set-up has allowed to reach many results on various rare processes and, in particular, it has pointed out with high C.L. (6.3 σ) a model independent evidence for the presence of a dark matter particle component in the galactic halo; ii) the new $\simeq$ 250 kg NaI(Tl) LIBRA (Large sodium Iodide Bulk for RAre processes) set-up (DAMA/LIBRA), now running; iii) the $\simeq$ 6.5 kg liquid Xenon pure scintillator (DAMA/LXe), in operation; iv) the R&D installation (DAMA/R&D) for measurements on prototype PMTs and detectors and for small scale experiments, in operation. Moreover, in the framework of devoted R&D for higher radiopure

detectors and PMTs, sample measurements are carried out by means of the low background Ge detector of the DAMA experiment (DAMA/Ge) and in some cases at Ispra. In the following main arguments and the activity in 2004 are summarized.

1 DAMA/NaI

The DAMA/NaI set-up [1, 2, 3] had as main aim the investigation of the presence of a Dark Matter particle component in the galactic halo by exploiting the model independent annual modulation signature (see refs. [4, 5, 6, 7, 2, 8, 9, 10, 3] and in the 2004 publication list). The same experimental set-up also achieved several other results both on Dark Matter particle investigations with other approaches and on many other different rare processes (see refs. [11, 12, 13, 14, 15, 16, 17, 18] and in the 2004 publication list).

DAMA/NaI has been a pioneer experiment running at LNGS for about a decade and investigating as first the Dark Matter particle annual modulation signature with suitable exposed mass, sensitivity and control of the running parameters.

1.1 Investigation on the particle Dark Matter presence in the galactic halo by exploiting the annual modulation signature.

The presence of a model independent positive evidence in the data of DAMA/NaI has firstly been reported by the DAMA collaboration at the TAUP conference in 1997 [19] and published also in [4], confirmed in [5, 6], further confirmed in [7, 2, 8, 9, 10] and conclusively confirmed, at end of experiment in 2003 (see ref. [3] and in the 2004 publication list). During seven independent experiments (total exposure: 107731 kg $\times$ day) each one during one annual cycle, DAMA/NaI has pointed out the presence of a modulation satisfying the many peculiarities of a particle Dark Matter induced effect, reaching an evidence at 6.3 σ C.L. (Fig. 1); details can be found in ref.[3] and in the 2004 publication list. A careful investigation of all the known possible sources of systematic and side reactions has been carried out. No systematic effect or side reaction able to account for the observed modulation amplitude and to satisfy all the requirements of the signature has been found or suggested by anyone.

On the basis of the obtained 6.3 σ model-independent result, corollary investigations can also be pursued on the nature of the Dark Matter particle candidate. This latter investigation is instead model-dependent. Thus, it should be handled in the most general way as we have pointed out along the time (see [4, 5, 6, 7, 2, 8, 9, 10, 3] and the 2004 publication list). Details on the model-dependent corollary analyses can be found in ref. [3] and in the 2004 publication list as well as devoted discussions to correctly understand the results obtained in corollary model dependent quests for the candidate particle and the real validity of any claimed model-dependent comparison in the field. It is worth to note that – although many possible scenarios for the astrophysical, nuclear and particle Physics assumptions as well as parameters uncertainties have been considered in the corollary model-dependent analyses presented in ref. [3] and in the 2004 publication list – the reported allowed volumes/regions are not exhaustive of the many existing possibilities, which at present level of knowledge cannot be disentangled. In particular, we have

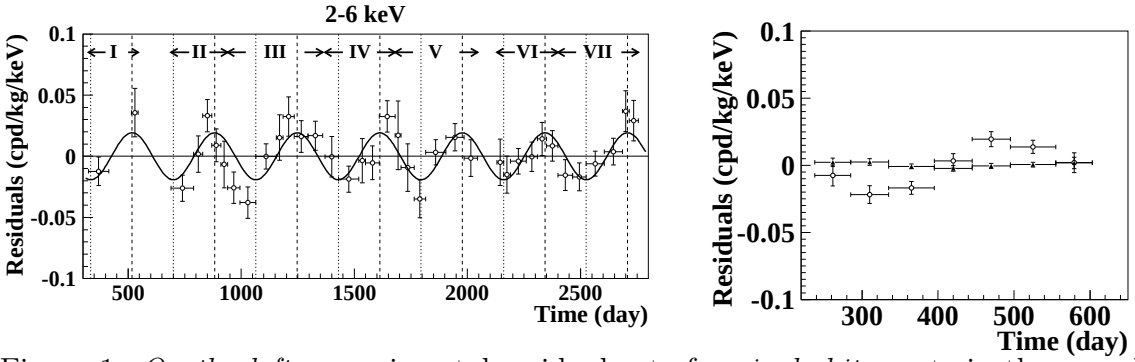

Figure 1: *On the left*: experimental residual rate for *single-hit* events in the cumulative (2–6) keV energy interval as a function of the time over 7 annual cycles (total exposure 107731 kg $\times$ day). The experimental points present the errors as vertical bars and the associated time bin width as horizontal bars. The superimposed curve represents the cosinusoidal function behaviour expected for a WIMP signal with a period equal to 1 year and phase exactly at 2^{nd} June; the modulation amplitude has been obtained by best fit. A careful investigation of all the known possible sources of systematic and side reactions has been carried out. No systematic effect or side reaction able to account for the observed modulation amplitude and to satisfy all the requirements of the signature has been found. *On the right*: experimental residual rates over seven annual cycles for *single-hit* events (open circles) – class of events to which WIMP events belong – and over the last two annual cycles for *multiple-hits* events (filled triangles) – class of events to which WIMP events do not belong – in the (2–6) keV cumulative energy interval. They have been obtained by considering for each class of events the data as collected in a single annual cycle and using in both cases the same identical hardware and the same identical software procedures. The initial time is taken on August 7^{th}. The obtained result offers an additional strong support for the presence of a Dark Matter particle component in the galactic halo further excluding any side effect either from hardware or from software procedures or from background. For more, see ref. [3] and the 2004 publication list.

considered some of the many possible model frameworks regarding: i) the nature of the Dark Matter particle; ii) its real coupling with ordinary matter (mixed SI&SD, purely SI, purely SD or *preferred inelastic*) iii) the right form factors and related parameters for each target nucleus; iv) the right spin factor for each target nucleus; v) the real scaling laws (see ref. [20]); vi) the real halo model and related parameters; vii) the real values of the experimental and theoretical parameters within their uncertainties; etc. As an example, we remind that not only large differences in the measured rate can be expected when using target nuclei sensitive to the SD component of the interaction (such as e.g. ^{23}Na and ^{127}I) with respect to those largely insensitive to such a coupling (such as e.g. ^{nat}Ge, ^{nat}Si, ^{nat}Ar, ^{nat}Ca, ^{nat}W, ^{nat}O), but also when using different target nuclei although all – in principle – sensitive to such a coupling, depending on the unpaired nucleon (compare e.g. the odd-spin isotopes of Xe, Te and those with small abundance of Ge, Si, W with the Sodium and Iodine cases) [3].

Some of the obtained allowed regions or slices of allowed volumes obtained in the corollary model-dependent analyses are reported in [3] and in the 2004 publication list; here, we only show in Fig. 2 the particular case of a candidate with dominant SI interaction

for the model frameworks considered in ref. [3]. The same figure also shows for comparison the theoretical expectations for the neutralino candidate in MSSM with gaugino mass unification at GUT scale released, as in ref. [21].

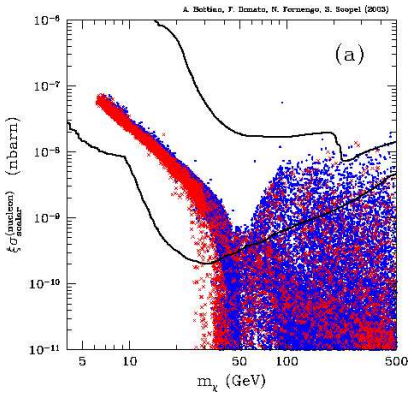

Figure 2: Figure taken from ref. [21]: theoretical expectations of $\xi\sigma_{SI}$ versus m_W in the purely SI coupling for the particular case of a neutralino candidate in MSSM with gaugino mass unification at GUT scale released; in this case neutralino masses down to $\simeq 6$ GeV are possible still taking into account the accelerator bounds. The curve is the region allowed by the DAMA/NaI result for the model frameworks given in ref. [3]. For other possible scenarios and other interaction types – however far from being exhaustive of all the possibilities – see ref. [3] and the 2004 publication list.

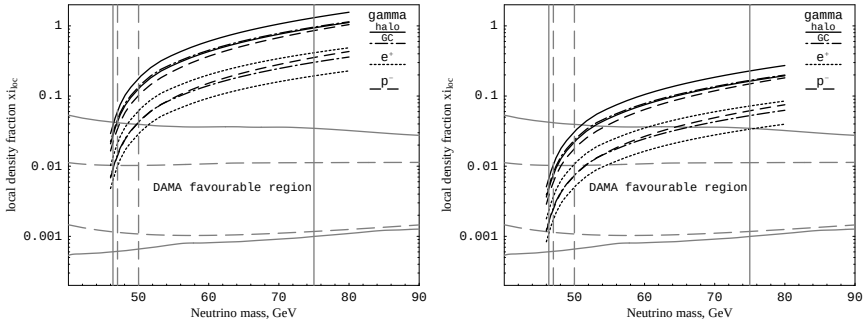

Figure 3: Figure taken from ref. [27] : Case of a subdominant heavy 4^{th} neutrino candidate in the plane local density fraction versus the heavy neutrino mass (of course, neutrino masses above 45 GeV have been considered with the respect to the LEP results about the width of the Z^0 boson). The favorable region in the considered scenario for this candidate, as obtained from the DAMA/NaI data (grey dashed line when using the Evan's halo model; solid line when using the other halo models), and the best-fit density parameters deduced from cosmic gamma-radiation (from halo and galactic center), positron and antiproton analysis are shown (left panel). The effect of the inclusion of possible neutrino clumpiness is also reported (right panel). See ref. [27] for details.

We remind that no experiment is available whose result can be directly compared in a model independent way with the one of DAMA/NaI. As regards some claimed model-dependent comparisons by experiments insensitive to the annual modulation signature, where exposures orders of magnitude lower that the one by DAMA/NaI, different target

nuclei, etc. are used, specific discussions can be found e.g. in ref.[3] and in the 2004 publication list. They already account, as a matter of fact, for the model dependent claims by [22], [23], [25, 26] and [24], which are based - even assuming the experimental results and the associated uncertainties as they give - on a single model-dependent scenario where all the astrophysical, nuclear and particle physics assumptions and experimental/theoretical parameters are fixed at a single selected choice (highly questionable in most of the aspects) and on the uncorrect, partial and unupdated quotation of the corollary model dependent aspects of the DAMA/NaI model independent result. Moreover, the existing interactions and scenarios to which those experiments are largely insensitive – on the contrary of DAMA/NaI – are ignored.

On the other hand, some positive hints are present in indirect detection experiments; in fact, an excess of positrons and of gamma's in the space has been reported with the respect to a modellised background; they are not in contraddiction with the DAMA/NaI result. As an example, recently, it has been suggested [27] that these positive hints and the effect observed by DAMA/NaI can also be described in a scenario with multi-component Dark Matter in the galactic halo, made of a subdominant component of heavy neutrinos of the 4^{th} family and of a sterile dominant component (see Fig. 3).

Other scenarios on the nature of the candidate particle, on astrophysical, nuclear and particle Physics assumptions are under studies also in the light of the future DAMA/LIBRA data releases, as briefly mentioned in the following.

1.2 Search for spontaneous transition of nuclei to a superdense state

During year 2004 an exposure collected by DAMA/NaI has been analysed in order to search for spontaneous transition of nuclei to a superdense state.

In fact, from the very beginning of nuclear physics it was debated the possible existence of superdense nuclear states with $\rho_s > \rho_0$ [28, 29, 30, 31], where ρ_0 is the average density which is almost the same for all nuclei due to the structure of nuclear forces. It was argued that the energy of a nucleus as a function of its density, $E(\rho)$, must have a minimum for the normal density ρ_0. A transition to the superdense state can occur if $E(\rho)$ has a second minimum for $\rho = \rho_s$. The possible existence of superdense states was discussed in some pioneering works [32], in connection with the so called "pion condensation" phenomenon. More recently this argument has been developed by many authors (see for example ref. [33]).

To realise the density transition $\rho_0 \to \rho_s$, it must be overcome a potential barrier U_0 whose shape and height cannot be reliably predicted on the basis of the present knowledge. In this framework a nucleus (or a part of a nucleus) can be metastable and spontaneously can go over to the superdense state.

In the past several experimental works employing different techniques have been devoted to determine limits for the probability λ of the $\rho_0 \to \rho_s$ transition and for the effective height U_0 of the potential barrier [34, 35]. A simple model, allowing to connect U_0, λ, ρ_0 and ρ_s, can be considered by adopting the ideas developed in refs. [29, 32, 36], where it was postulated that the transition can occur as a consequence of nuclear volume

oscillations (hydrostatic compression). According to ref. [36], the relation:

$$U_0(MeV) = \frac{7.2 \cdot 10^4}{A^{\frac{5}{3}}} \left(1 + \frac{1}{55} \cdot ln \frac{\tau}{10^{20} y}\right) \cdot \left[1 - \left(\frac{\rho_0}{\rho_s}\right)^{\frac{1}{3}}\right]^{-2}$$

can be written; where $\tau = \lambda^{-1}$ is the lifetime of the process in years.

Our search has been carried out by using data collected deep underground by DAMA/NaI for an an exposure of 33834 kg · day. The experimental approach has been similar to the one previously exploited in ref. [37], where characteristic γ-radiation, accompaining the occurrence of the searched transition in NaI(Tl), has been looked for. In particular, a possible transition of Sodium and Iodine nuclei to a superdense state, releasing a ΔE larger than 10 MeV through γ radiation, has been considered. Thus, the data have been analysed searching for events with multiplicity larger than or equal to two and with total released energy, ΔE, larger than 10 MeV. The required features have been satisfied by 1551 events in the given exposure; these events can largely be ascribed to the background due to high energy muons surviving the mountain shielding.

A cautious approach has been considered in order to obtain the lifetime lower limits

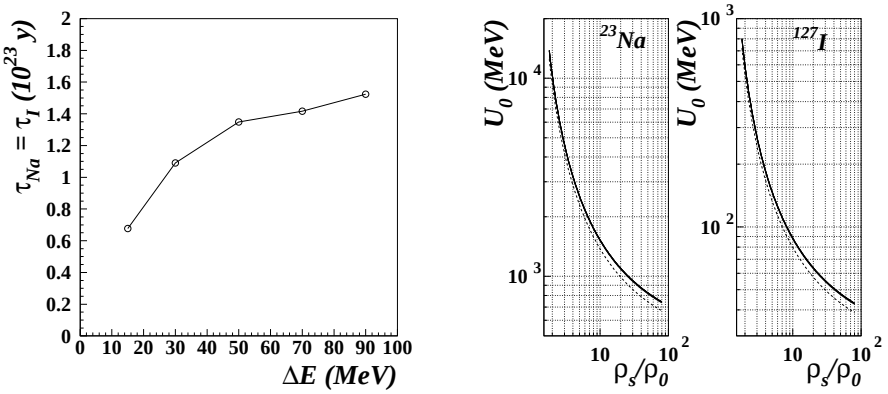

Figure 4: *Left panel*: obtained lifetime lower limits (90% C.L.) on the considered process in Sodium and Iodine nuclei as a function of the energy release, ΔE. *Right panels*: obtained lower limits (90% C.L.) on the barrier potential, U_0, as for the Sodium and Iodine nuclei (continuous lines); the behaviours for the various energy releases are practically indistinguishable. The dashed lines are the lower limits for U_0 as calculated from the previous best limits in ref. [37]. We note that, although the restriction on τ is increased of about 3 orders of magnitude (thanks to the deeper experimental site, to the much larger exposure, to the effective shielding of the detectors and to the strong improvements in the detectors' radiopurity, occurred during the last decades), the restriction on U_0 is modestly increased because of the logarithmic dependence.

(90% C.L.) for Sodium and Iodine nuclei – as a function of ΔE – depicted in fig. 4–*left panel* in the range (15 – 90) MeV. From these restrictions, one can derive lower limits for the barrier potential, U_0, as reported for the Sodium and Iodine nuclei in fig. 4–*right panels*.

2 DAMA/LIBRA

The large merits of highly radiopure NaI(Tl) set-up have been demonstrated in the practice by DAMA/NaI. In 1996 DAMA proposed to realize a ton set-up [38] and a new R&D project for highly radiopure NaI(Tl) detectors was funded at that time and carried out for several years in order to realize as an intermediate step the second generation experiment, successor of DAMA/NaI, with an exposed mass of about 250 kg. As a result of this second generation R&D effort for NaI(Tl) radiopurification (by exploiting new material selections, new chemical/physical radiopurification of NaI and TlI powders and new protocols), the new experimental set-up, DAMA/LIBRA (Large sodium Iodide Bulk for RAre processes), $\simeq$250 kg highly radiopure NaI(Tl) crystal scintillators (matrix of twenty-five $\simeq$ 9.70 kg NaI(Tl) crystals), was funded and realised. After the completion of the DAMA/NaI data taking in July 2002, the dismounting of DAMA/NaI occurred and the installation of DAMA/LIBRA started. In particular, the experimental site as well as many components of the installation itself have been implemented (environment, shield of PMTs, wiring, HP Nitrogen system, cooling water of air conditioner, electronics and DAQ, etc.). In particular, all the Cu parts have been chemically etched before their installation following a new devoted protocol and maintained in HP Nitrogen atmosphere until the installation. All the procedures performed during the dismounting of DAMA/NaI and the installation of DAMA/LIBRA detectors have been carried out in HP Nitrogen atmosphere.

As previously for DAMA/NaI, an hardware/software system to continuosly monitor the running conditions is also operative; in particular, several probes are read out by the data acquisition system and stored with the production data. Moreover, self-controlled computer processes are operational to automatically control several parameters and to manage alarms.

Fig. 5 – *left panel* shows the energy distribution of the ^{241}Am source as measured by one of the new DAMA/LIBRA detectors (σ/E = 6.7% at 59.5 keV).

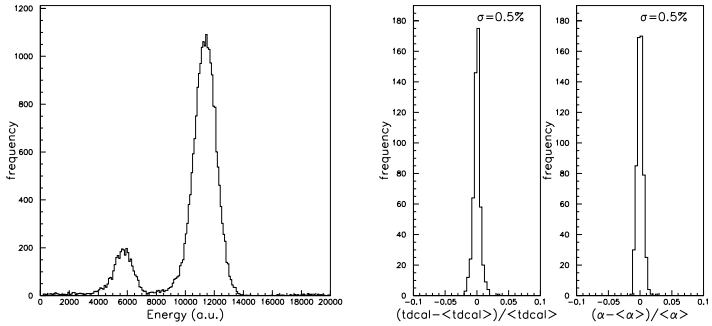

Figure 5: *Left panel*: energy distribution of the ^{241}Am source as measured by one of the new highly radiopure DAMA/LIBRA NaI(Tl) detectors (σ/E = 6.7% at 59.5 keV). *Right panels*: examples of the stability of the calibration factor (*tdcal*) and of the ratio of the peaks' positions (α) of the measured energy distribution of the ^{241}Am source during about one year of data taking.

DAMA/LIBRA is taking data since March 2003 and the first data release is planned at time when an exposure larger than that of DAMA/NaI will have been collected and

analysed in all the aspects. Just as an example of the quality of the data taking, Fig. 5 – *right panels* show the stability of the calibration factor and of the ratio of the peaks' positions of the ^{241}Am source during about one year of data taking.

The highly radiopure DAMA/LIBRA set-up is a powerful tool for further investigation on the Dark Matter particle component in the galactic halo having many intrinsic merits (see e.g. the 2004 reference list), a larger exposed mass, an higher overall radiopurity and improved performances with the respect to DAMA/NaI. Thus, DAMA/LIBRA will further investigate the 6.3 σ C.L. model independent evidence pointed out by DAMA/NaI with increased sensitivity in order to reach even higher C.L.. Moreover, it will also offer an increased sensitivity to improve corollary quests on the nature of the candidate particle, trying to disentangle at least among some of the many different possible astrophysical, nuclear and particle physics models as well as to investigate other new possible scenarios.

In the following some of the main topics – not yet well known at present and which can affect whatever corollary model dependent result and comparison – will be mentioned. They will be addressed by the highly radiopure DAMA/LIBRA in a way often unique and always reliable, cheap and competitive. As an example, we remind here:

- *the possible effects induced on the Dark Matter particles distribution in the galactic halo by contributions from satellite galaxies tidal streams.* Recently it has been pointed out [39] that contributions to the Dark Matter particles in the galactic halo should be expected from tidal streams from the Sagittarius Dwarf elliptical galaxy. Considering that this galaxy was undiscovered until 1994 and considering galaxy formation theories, one has to expect that also other satellite galaxies do exist and contribute as well. In particular, the Canis Major satellite Galaxy has been pointed out as reported in 2003 in ref. [40]; it can, in principle, play a very significant role being close to our galactic plane. At present, the best way to investigate the presence of a stream contribution is to determine more accurately the phase of the annual modulation, t_0, as a function of the energy; in fact, for a given halo model t_0 would be expected to be (slightly) different from 152.5 d and to vary with energy (see Fig.6).

- *the effects induced on the Dark Matter particles distribution in the galactic halo by the possible existence of caustics.* It has been shown that the continuous infall of Dark Matter particles in the galactic gravitational field can form caustic surfaces and discrete streams in the Dark Matter particles halo [41]. The phenomenology to point out a similar scenario is analogous to that in the previous item.

- *the detection of possible "solar wakes".* As an additional verification of the possible presence of contributions from streams of Dark Matter particles in our galactic halo, DAMA/LIBRA can investigate also the gravitational focusing effect of the Sun on the Dark Matter particle of a stream. In fact, one should expect two kinds of enhancements in the Dark Matter particles flow: one named "spike", which gives an enhancement of Dark Matter particle density along a line collinear with the direction of the incoming stream and of the Sun, and another, named "skirt", which gives a larger Dark Matter particle density on a surface of cone whose opening angle depends on the stream velocity.

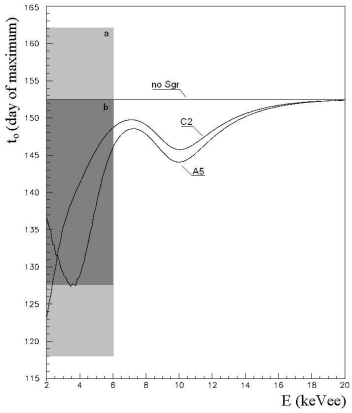

Figure 6: Expected behaviours of the phase, t_0, of the annual modulation signal as function of the energy when considering: i) only galactic halo ("no Sgr"); ii) galactic halo ($C2$ halo model with $v_0 = 220$ km/s, ρ_0 equal to the maximum value for this model) and a contribution from Sagittarius Dwarf galaxy ("C2"); iii) galactic halo ($A5$ halo model with $v_0 = 220$ km/s, ρ_0 equal to the maximum value for this model) and a contribution from Sagittarius Dwarf galaxy ("A5"). The contributions from Sagittarius Dwarf galaxy have been taken in both cases with a density equal to 4% of ρ_0. The light shadow region is the final result of DAMA/NaI on the t_0 value for the cumulative energy interval (2 – 6) keV, while the dark shadow region is the expectation on t_0 assuming an experiment with the same features as DAMA/NaI, an exposure of $3 \cdot 10^5$ kg $\cdot$ day and the same central value for t_0.

Moreover, other topics will be further addressed by the highly radiopure DAMA/LIBRA, such as the study (i) on the velocity and spatial distribution of the Dark Matter particles in the galactic halo (for details see the discussions in refs. [3, 10] and in the 2004 reference list); (ii) on possible structures as clumpiness with small scale size; (iii) on the coupling(s) of the Dark Matter particle with the ^{23}Na and ^{127}I target-nuclei; (iv) on the nature of the Dark Matter particles (susy particles in various scenarios, a neutrino of a fourth family, particles from multi-dimensional Kaluza-Klein like theories, Mirror Dark Matter, self-interacting dark matter, axion-like particles, ...); (v) on scaling laws and cross sections (recently, it has been pointed out [20] that, even for the neutralino candidate, the usually adopted scaling laws could not hold); etc.

A large work will be faced by DAMA/LIBRA when a suitably large exposure will have been collected. In addition, it is the intrinsecally the most sensitive experiment in the field of Dark Matter so far because of its radiopurity, exposed mass and high duty cycle. These qualities will also allow DAMA/LIBRA to further investigate with higher sensitivity several other different rare processes.

3 R&D-III and beyond

An R&D activity to develop higher radiopure detectors is continuously carried out, in particular towards the creation of ultimate radiopure NaI(Tl) detectors. Some studies on their applications are/have been also carried out (see ref. [38, 42] and 2004 publication list).

Actually, a third generation R&D towards a ton NaI(Tl) set-up, we proposed in 1996, has been funded and is in progress. In particular, during year 2004 some corollary investigations have been carried out and measurements and analysis to qualify new special low background PMTs without any glass and ceramics have been realized.

4 DAMA/LXe

As regard the LXe experiment, following the former Xelidon experiment on R&D developments of liquid Xenon detectors in latest 80's, DAMA considered many years ago (see e.g. ref. [43]) the use of the liquid Xenon as target-detector material for particle dark matter investigations and realized several LXe prototype detectors using natural Xenon. Then, it preliminarily put in measurement the set-up employed in the data taking of ref. [44, 45] by using Kr-free Xenon enriched in ^{129}Xe at 99.5%. This set-up was significantly upgraded at fall 1995 and again – deeply – in summer 2000, when the handling of Kr-free Xenon enriched in ^{136}Xe at 68.8% and in ^{134}Xe at 17.1% was also introduced. Main features of the set-up are described in ref. [46]. Investigations on several rare processes have been carried out with time passing in the various configurations [44, 45, 46, 47, 48, 49, 50, 51, 52, 53, 54, 55, 56]. The set-up is in operation. Note that – on the contrary of the NaI(Tl) case – plans for enlarging its exposed mass have never been considered because of the technical reasons (specific of liquid xenon detectors) pointed out several times in the past (see e.g. [57]).

After the upgrading mentioned in the LNGS activity report 2003, the $\simeq$ 6.5 kg liquid Xenon set-up has been put again in measurements in summer 2004. Moreover, continuing the preliminary data analysis described in the LNGS activity report 2003, the already available data have also been analysed in order to investigate possible tri-nucleon decays into invisible channels in ^{136}Xe [58].

4.1 The search for tri-nucleon decays into invisible channels in ^{136}Xe

The data, collected above the threshold of 550 keV during 8823.54 h with the set-up filled with the Xenon enriched in ^{136}Xe at 68.8%, have been considered to investigate possible tri-nucleon (NNN) decays into invisible channels for the ^{136}Xe isotope: disappearance or decay to neutrinos, Majorons, etc. [58]. The approach is similar to the one exploited in [53] at the first time; it consists in a real-time search for radioactive decay of unstable daughter nuclei created as result of the NNN disappearance in parent nucleus. If the half-life of the daughter nucleus is of order of 1 s or greater, such a decay will be time-resolved from prompt products in case they were emitted and observed in the detector. The considered experimental approach assures an high detection efficiency and a branching ratio $\sim$ 1 with the respect to other different approaches necessarily pursued with very large mass apparata. Moreover, all the achieved limits hold in the present approach for every invisible decay channel, including "disappearance" in extra-dimensions or decay in particles which weakly interact with the matter.

As a consequence of NNN decays in ^{136}Xe, when the daughter de-excitation occurs only by γ emission, the isotopes given in Table 1 are produced (on the contrary, the emission of heavy particles such as p, n or α will give rise to the formation of nuclei with lower A and Z values).

Table 1: Daughter nuclei produced in NNN decays in ^{136}Xe when the de-excitation of the daughter nucleus occurs by γ emission. All the produced nuclei are radioactive and at least one β^- decay occurs. The half-life times of the isotopes involved in the four decay chains vary from 2.5 minutes (^{133}Sb) and 5.243 days (^{133}Xe) assuring that the chains are in equilibrium and that subsequent decays are well separated in time.

Decay	daughter nucleus	subsequent decays
nnn	^{133}Xe	$^{133}\text{Xe} \xrightarrow{\beta^-} {}^{133}\text{Cs}$
nnp	^{133}I	$^{133}\text{I} \xrightarrow{\beta^-} {}^{133}\text{Xe} \xrightarrow{\beta^-} {}^{133}\text{Cs}$
npp	^{133}Te	$^{133}\text{Te} \xrightarrow{\beta^-} {}^{133}\text{I} \xrightarrow{\beta^-} {}^{133}\text{Xe} \xrightarrow{\beta^-} {}^{133}\text{Cs}$
ppp	^{133}Sb	$^{133}\text{Sb} \xrightarrow{\beta^-} {}^{133}\text{Te} \xrightarrow{\beta^-} {}^{133}\text{I} \xrightarrow{\beta^-} {}^{133}\text{Xe} \xrightarrow{\beta^-} {}^{133}\text{Cs}$ **

** given here only the main part of the chain.

Since previous searches for NNN decays into invisible channels are not available, there are no reference criteria to evaluate the effective objects number, N_{ogg}^{eff}, in the ^{136}Xe nucleus, whose decay would produce the investigated daughter nucleus (objects means NNN groups). Thus, in this preliminary research we have cautiously assumed $N_{ogg}^{eff} = 1$ for all the NNN processes (*nnn*, *nnp*, *npp* and *ppp*), as done in the preliminary researches on the NN decays into invisible channels in ref. [59]. The value of N_{ogg}^{eff} enters in the evaluation of the lifetime, τ, of the studied processes: $\tau = \frac{\epsilon_{\Delta E} \cdot N_{nucl} \cdot N_{ogg}^{eff} \cdot T}{S_{\Delta E}}$, where $N_{nucl} = 2.00 \cdot 10^{25}$ is the number of ^{136}Xe nuclei; $T = 8823.54$ h is the time of measurement, $S_{\Delta E}$ is the number of events which can be ascribed to the decay process searched for in the considered energy window, ΔE, while $\epsilon_{\Delta E}$ is the related detection efficiency.

The result of a $nnn \rightarrow$ *invisible channels* decay in the ^{136}Xe nucleus is the creation of the ^{133}Xe isotope, which is unstable, has $T_{\frac{1}{2}} = 5.243$ days and β^- decays in ^{133}Cs (stable) with $Q_{\beta^-} = 427.4$ keV. Since the maximum energy released in this process is below the 550 keV energy threshold of the present measurements, this decay process cannot be investigated here.

As a consequence of a $nnp \rightarrow$ *invisible channels* decay in the ^{136}Xe nucleus, a ^{133}I nucleus is instead created in the sensitive volume of DAMA/LXe. This isotope β^- decays in ^{133}Xe with $T_{\frac{1}{2}} = 20.8$ hours and $Q_{\beta^-} = 1770$ keV; the ^{133}Xe is also unstable and decays in ^{133}Cs, which closes the chain. An event generator able to simulate the full decay schema of the ^{133}I has been realized and used with EGS4 package [60] to estimate the energy distribution expected for this β^- decay in our liquid xenon set-up. The signal to be searched for in case of a *nnp* decay into invisible channels in ^{136}Xe is given by the sum of this energy distribution and the one which would be obtained simulating the β^- decay of ^{133}Xe, which in the present specific case do not play any role because under the experimental energy threshold. As it can be seen in fig. 7a) , at energies above the experimental energy threshold, the signal does not present any distinctive structure;

thus, the lower limit on the lifetime of the process has been evaluated by following a very cautious procedure (used also in the investigation of other rare processes). In fact, it has been required that – in no energy interval – the number of events which could be ascribed to the investigated process can exceeds the number of measured events, N, plus $n \times \sqrt{N}$ (where n gives the C.L.). The more selective region in the present case is ΔE = 1100 - 1150 keV; it contains 35 events, which gives rise to the upper limit (90% C.L.) $S_{\Delta E} < 42.6$ events and being $\epsilon_{\Delta E}$ =3.0% gives:

$$\tau_{nnp} > 1.4 \cdot 10^{22} \text{ years (90\%C.L.)}.$$

The signal corresponding to a lifetime equal to the obtained limit value is shown in fig. 7a) superimposed to the experimental energy distribution.

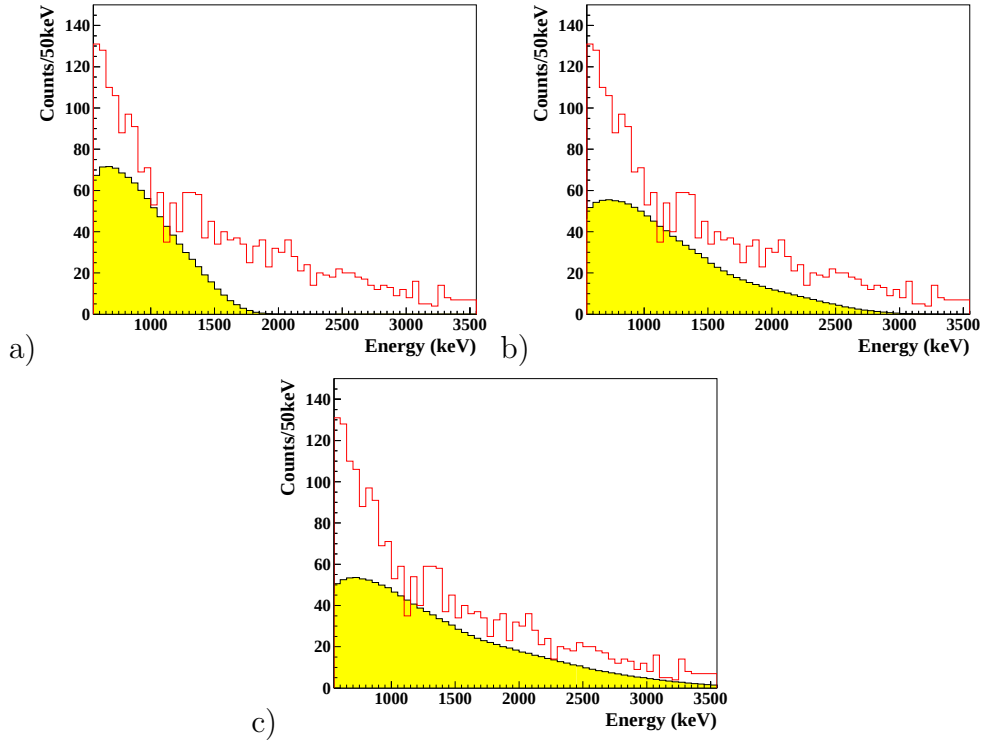

Figure 7: Comparisons between the experimental energy distribution collected during 8823.54 h with the DAMA/LXe set/up and the expected signals (colored area) for: a) $nnp \rightarrow$ *invisible channels* decay in ^{136}Xe for $\tau_{nnp} = 1.4 \cdot 10^{22}$ years; b) $npp \rightarrow$ *invisible channels* decay in ^{136}Xe for $\tau_{npp} = 2.7 \cdot 10^{22}$ years; c) $ppp \rightarrow$ *invisible channels* decay in ^{136}Xe for $\tau_{ppp} = 3.6 \cdot 10^{22}$ years. See text.

In the case of the process $npp \rightarrow$ *invisible channels* decay in the ^{136}Xe nucleus, a ^{133}Te nucleus is created. The ^{133}Te β^- decays in ^{133}I with $T_{\frac{1}{2}} = 12.5$ minutes and $Q_{\beta^-} = 2920$ keV. To simulate this process in our liquid xenon set-up EGS4 package [60] and an event generator able to generate the complex decay schema of ^{133}Te (with $\sim$ 40 levels of ^{133}I filled in β^- decays of the ^{133}Te and $\sim$ 200 different transitions in the subsequent de-excitation process) have been employed. A ^{133}Te decay is followed by the β^- decays of the ^{133}I and of the ^{133}Xe; the chain can be considered in equilibrium and the single events are well separated in time. Thus, each possible *npp* decay in ^{136}Xe is associated to a signal

given by the sum of the energy distributions expected for the β^- decays of the ^{133}Te, of the ^{133}I and of the ^{133}Xe (this latter, as already mentioned, gives here signal under the experimental energy threshold and, therefore, is not considered). Also in this case (fig. 7b)) the expected signal does not show any particular structures in the energy region where experimental data are available for the data analysis; thus, following the same cautious procedure considered above, one gets that the more selective energy window is ΔE = 1100 - 1150 keV which contains 35 events, giving rise to the upper limit: $S_{\Delta E} < 42.6$ events (90% C.L.); in this case the efficiency is: $\epsilon_{\Delta E}$ =5.7%. Thus, one can derive:

$$\tau_{npp} > 2.7 \cdot 10^{22} \text{ years (90\%C.L.)}.$$

The signal corresponding to a lifetime equal to the found limit value is shown in 7b) superimposed to the experimental energy distribution.

Finally, a possibile *ppp* $\rightarrow$ *invisible channels* decay process in ^{136}Xe will create the ^{133}Sb nucleus in the liquid xenon. This isotope β^- decays with $T_{\frac{1}{2}}$ = 2.5 minute and Q_{β^-} = 4003 keV. As it can be derived from the decay schema of the ^{133}Sb, this process gives rise to the production of ^{133}Te nuclei in the fundamental state (82.4%) and in the ^{133m}Te metastable state at 334 keV (17.6%). The full decay chain generated by the ^{133}Sb is summarized in the following schema:

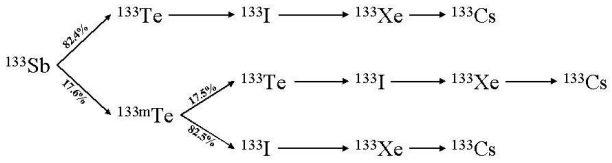

With simple calculation one can get that a possible *ppp* $\rightarrow$ *invisible channels* in ^{136}Xe is followed by a serie of β^- decays weighted according to the following formula:

$$1 \times^{133} \text{Sb} + 0.855 \times^{133} \text{Te} + 0.176 \times^{133m} \text{Te} + 1 \times^{133} \text{I} + 1 \times^{133} \text{Xe}.$$

The decay schema and the energy distributions expected for the ^{133}Te, ^{133}I and ^{133}Xe isotopes have been already summarized above, while the response function of the β^- decay of ^{133}Sb has been evaluated by using EGS4 package [60] and an event generator able to simulate the whole decay schema. The last process to be simulated to obtain the expected energy distribution as described in the previous formula is the ^{133m}Te decay. This isotope has $T_{\frac{1}{2}}$ = 55.4 minutes; in the 17.5% of the cases it goes to the ^{133}Te fundamental state, while in the remaining 82.5% it β^- decays in ^{133}I. The event generator realized for the ^{133m}Te isotope accounts both for the transition to the fundamental state of the ^{133}Te and the whole β^- decay schema.

The signal expected for the *ppp* $\rightarrow$ *invisible channels* in ^{136}Xe can be obtained by summing according to the previous formula the energy distributions of the related nuclide decays and is shown in fig. 7c) superimposed to the experimental data (also in this case the signal associated to the ^{133}Xe decay is below the experimental threshold). Considering the shape of the expected energy distribution, the same cautious procedure followed above has been considered. Also in this case the most sensitive energy window is ΔE = 1100 - 1150 keV which contains 35 events, giving rise to the upper limit: $S_{\Delta E} < 42.6$ eventi (90% C.L.); the detection efficiency is: $\epsilon_{\Delta E}$ =7.6%. One obtains:

$$\tau_{ppp} > 3.6 \cdot 10^{22} \text{ years (90\%C.L.)}.$$

The signal corresponding to a lifetime equal to the found limit is given in fig. 7c) superimposed to the experimental energy distribution.

In conclusion, new experimental limits have been set on the NNN decay processes in ^{136}Xe.

5 DAMA/R&D

The DAMA/R&D set-up has been upgraded several times and is used for tests on prototype PMTs and/or detectors and for small scale experiments mainly devoted to the search for double beta decay processes in various isotopes, such as ^{40}Ca, ^{46}Ca, ^{48}Ca, ^{106}Cd, ^{130}Ba, ^{136}Ce, ^{138}Ce, ^{142}Ce (see refs. [61, 62, 63, 64, 65, 66] and in 2004 publication list). Both the active and the passive source techniques have been exploited as well as – sometimes – the coincidence technique.

During year 2004 the measurements on the radiopurity of new PMT prototypes without any glass and ceramic components have been completed. Then, the DAMA/R&D set-up has been upgraded by installing a new automatized system for the opening/closure of the hard shield; moreover, the work for a new DAQ system has been started. Some preliminary measurements related to new small scale experiments in preparation have also been carried out. In addition, new results have been published on the basis of the measurements carried out deep underground by using a BaF_2 crystal scintillator; they are summarized in the following (see in the 2004 publication list).

Moreover, some investigations on new possible scintillators are also carried out both for possible further investigations on other double beta decay processes and on other applications [67].

5.1 Performances of a BaF_2 detector and its application to the search for $\beta\beta$ decay modes in ^{130}Ba

By exploiting the coincidence technique (which allows to significantly reduce the background, typically high in commercial BaF_2 detectors), the potentiality of BaF_2 detectors in the search for neutrinoless double beta decay modes in ^{130}Ba ($Q_{\beta\beta}$ = 2610 keV [68]) has been investigated. A 3615 g BaF_2 crystal scintillator (natural abundance of ^{130}Ba: 0.106%), manufactured in China, and two low background NaI(Tl), working in coincidence, have taken data deep underground during 4253 h. The experimental set-up has been installed inside the low background DAMA/R&D set-up. A charge ADC channel was acquired for each detector, while the signals from the BaF_2 were also registered by a 160 MSa/s Transient Digitizer over a time window of 3125 ns.

In the present experiment mostly the 310 nm component of the scintillation light was collected by PMT and the features presented in the following refer to this experimental condition since some of them (e.g. α/β light ratio and features of the pulse shape discrimination) depend on the sensitivity to the different emission wavelengths.

The considered hardware trigger condition: $BaF_2.and.(NaI1.or.NaI2)$, has allowed to investigate also some properties of the BaF_2 detector in the used set-up. In particular, the α/β light ratio and the pulse shape discrimination capability between α and β particles

have been studied by considering Bi-Po events – able to satisfy the coincidence trigger – induced by internal ^{232}Th and ^{238}U contaminations. Similar events have been identified by using the pulse information recorded by the Transient Digitizer (note that since its time window is 3125 ns, Bi-Po events from ^{232}Th chain were mostly recorded). The results are discussed in the reference quoted in the 2004 publication list and summarized in Fig. 8. In Fig. 8e) the α/β pulse shape discrimination capability of the used BaF_2 detector is shown as a function of the energy (in keV electron equivalent).

Finally, the Bi-Po events also allow to quantify the radioactive contaminations of ^{212}Bi and ^{214}Bi in the BaF_2 crystal scintillator. In fact, considering the running time (4253 h) and the detection efficiencies (calculated by a MonteCarlo code using EGS4 package [60]) contaminations of 0.4 Bq/kg and 1.4 Bq/kg are obtained for ^{212}Bi and ^{214}Bi, respectively. They correspond to 100 ppb (or 0.01 $\alpha \cdot s^{-1} \cdot cm^{-3}$) of ^{232}Th and to 110 ppb (or 0.05 $\alpha \cdot s^{-1} \cdot cm^{-3}$) of ^{238}U if the chains are assumed to be in equilibrium. These results show that the levels of residual contaminations in commercial BaF_2 detectors are still very high for direct low background applications; thus, possible efforts to significantly reduce them have to be considered.

Various coincidence patterns suitable to investigate several possible double beta decay modes in ^{130}Ba have been considered. In the following the more sensitive ones, which have allowed to obtain the experimental limits reported in Table 2, are listed:

- $2\beta^+0\nu(0^+ \rightarrow 0^+)$ – Case a): a signal in the BaF_2 detector in coincidence with signal(s) in NaI(Tl) in the energy window: 481 – 541 keV ($\pm$ 1 σ around 511 keV). Case b): triple coincidence among BaF_2, NaI1 and NaI2; the same energy window as case a) is considered for the NaI(Tl) detectors.

- $2\beta^+0\nu(0^+ \rightarrow 2_1^+)$ – Case c): as case a), but the energy window for the signal(s) in the NaI(Tl) is: 481 – 567 keV (511 keV minus 1 σ and 536 keV – 2_1^+ excitation energy – plus 1 σ, respectively). Case d): triple coincidence among BaF_2, NaI1 and NaI2; the same energy window as case c) is considered for the NaI(Tl) detectors.

- $EC\beta^+0\nu(0^+ \rightarrow 0^+)$ – as previous case a).

- $EC\beta^+0\nu(0^+ \rightarrow 2_1^+)$ – as previous case c).

- $EC\beta^+0\nu(0^+ \rightarrow 2_2^+)$ – Case e): as case a), but the energy window for the signal(s) in the NaI(Tl) is 481 – 618 keV (511 keV minus 1 σ and 586 keV – transition energy from 2_2^+ to 2_1^+ states – plus 1 σ, respectively).

- $EC\beta^+0\nu(0^+ \rightarrow 4^+)$ – Case f): as case a), but the signal(s) in NaI(Tl) should be either in the 481 – 567 keV energy window or in the 635-703 keV one. As regards the first energy interval see above, while the second one corresponds to $\pm$ 1 σ around 669 keV (transition energy from 4^+ to 2_1^+ states).

The experimental energy distributions measured by the BaF_2 detector (rejection of the *coincidence* Bi-Po events already applied) for the cases from a) to f) are given in the reference quoted in the 2004 publication list, where are also reported the energy distributions expected from a signal in each one of the considered double beta decay mode as calculated by a MonteCarlo code using the EGS4 package [60].

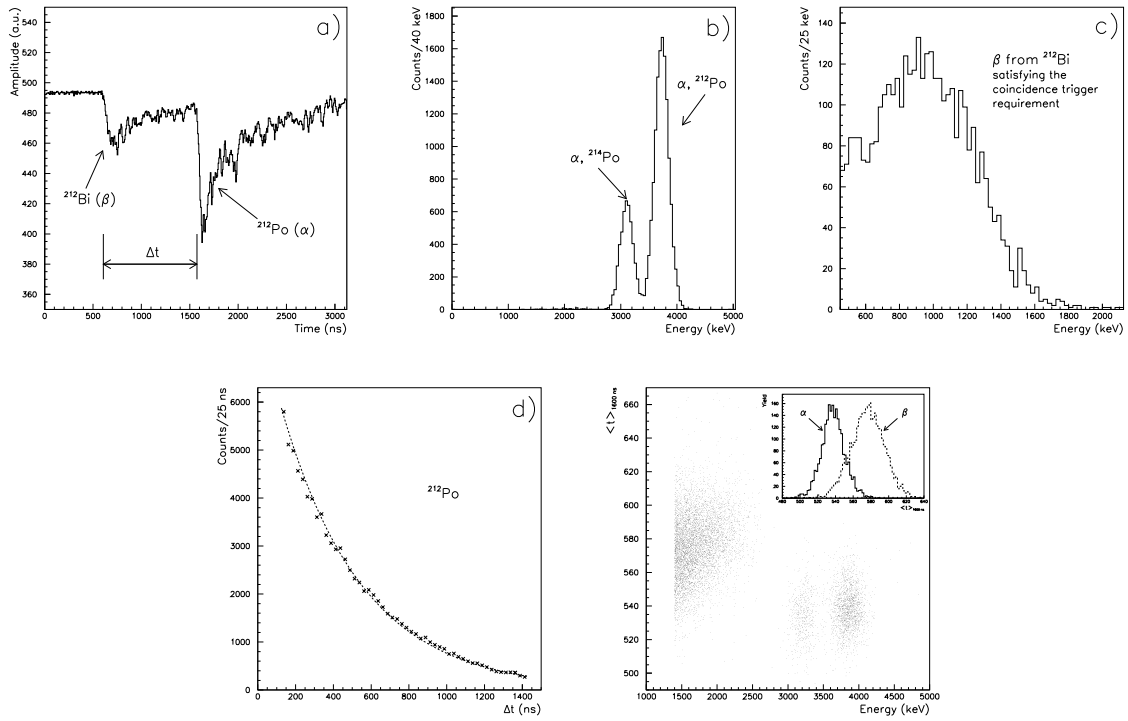

Figure 8: a) typical pulse shape of a Bi-Po event satisfying the hardware coincidence trigger as recorded by the Transient Digitizer. Note that the fast component of the BaF_2 scintillation light is here mostly suppressed by optical interfaces and by the response of the PMT and of the electronic chain; Δt is the measured delay time between the β and α pulses; b) energy distribution (in keV electron equivalent) of the α particles from the ^{212}Po and from the ^{214}Po decays; c) energy distribution of ^{212}Bi β decays. The end-point of 1521 keV corresponds to the ^{212}Bi β decay into the first excited level of ^{212}Po, giving a γ of 727 keV in one NaI(Tl); d) measured Δt distribution of the Bi-Po events from ^{212}Bi. From these data the half-life of the ^{212}Po α decay is: $T_{1/2}$ = (297 $\pm$ 1) ns, in agreement with the value available in literature (299 $\pm$ 2 ns [69]). e) α/β pulse shape discrimination capability of the used BaF_2 detector (310 nm slow component of the scintillation light mostly collected) as a function of the energy; keV means keV electron equivalent. As a discrimination indicator we consider the first momentum of the time distribution of each pulse calculated, within 1600 ns averaging time, according to: $< t >_{1600} = \frac{\Sigma_i h_i t_i}{\Sigma_i h_i}$ with t_i i^{th} time bin and h_i the corresponding pulse height. Note that the first momentum of the time distribution of a pulse would be exactly its decay constant in case of a pure exponential shape when considering an infinite averaging time. In the inset the normalized distributions of the discrimination indicator for the β and α events, respectively, are shown as obtained in the present experimental condition where mostly the 310 nm slow component of the BaF_2 scintillation light is collected. The found features are consistent with those measured e.g. in refs. [70, 71] in analogous experimental conditions. It is worth to note that instead a more efficient pulse shape discrimination capability with different features is obtained in set-ups where also the fast UV component is efficiently collected and suitably processed since the electrons appreciably excite it, while alpha particles do not (see e.g. ref. [72]). For details see in the 2004 publication list.

Table 2: Results obtained on some of the double beta decay modes in ^{130}Ba by exploiting the coincidence technique. The BaF_2 energy window considered in the fit for each decay mode is reported in the third column. See the 2004 publication list.

Decay mode	Selection criteria	BaF_2 energy window (MeV)	N_d (10^4)	τ_{limit} (y) (90% C.L.)
$2\beta^+0\nu(0^+ \to 0^+)$	case a)	(1.9 - 2.3)	(2.1±2.8)	$1.0 \cdot 10^{17}$
$2\beta^+0\nu(0^+ \to 0^+)$	case b)	(0.95 - 1.80)	(3.2±3.5)	$0.7 \cdot 10^{17}$
$2\beta^+0\nu(0^+ \to 0^+)$	combined		(2.5±2.2)	$1.1 \cdot 10^{17}$
$2\beta^+0\nu(0^+ \to 2_1^+)$	case c)	(1.9 - 2.3)	(1.2±4.1)	$0.8 \cdot 10^{17}$
$2\beta^+0\nu(0^+ \to 2_1^+)$	case d)	(0.95 - 1.80)	(-2.8±4.3)	$1.4 \cdot 10^{17}$
$2\beta^+0\nu(0^+ \to 2_1^+)$	combined		(-0.7±3.0)	$1.5 \cdot 10^{17}$
$EC\beta^+0\nu(0^+ \to 0^+)$	case a)	(1.9 - 2.3)	(1.0±1.3)	$2.0 \cdot 10^{17}$
$EC\beta^+0\nu(0^+ \to 2_1^+)$	case c)	(1.9 - 2.3)	(0.7±2.0)	$1.6 \cdot 10^{17}$
$EC\beta^+0\nu(0^+ \to 2_2^+)$	case e)	(1.9 - 2.3)	(-4.9±4.3)	$2.0 \cdot 10^{17}$
$EC\beta^+0\nu(0^+ \to 4^+)$	case f)	(1.9 - 2.3)	(-4.5±6.0)	$1.1 \cdot 10^{17}$

The number of background events in coincidence is still relevant because of the very high level of residual radioactive contaminants in the BaF_2 commercial detector. This can be mainly ascribed to double coincidences from standard contaminants such as e.g. ^{208}Tl (e.g. 583 and 2614 keV γ's), ^{214}Bi (mainly 609 – 1120 keV γ's) with Δt larger than the time window used in the Bi-Po events rejection procedure, Compton events satisfying the coincidence, etc.

The obtained results are summarized in Table 2 For details refer to the reference quoted in the 2004 publication list.

We note that the new experimental limits (90% C.L.) for the $0\nu(0^+ \to 0^+)$ decay modes are modest with respect to those achieved for other isotopes, but they represent a significant improvement with respect to the ones previously available for the same decay modes in ^{130}Ba. The experimental limits on ^{130}Ba decay modes involving excited states are, instead, set here for the first time.

6 DAMA/Ge

Various R&D developments to improve low background set-ups and scintillators as well as new developments for higher radiopure PMTs are regularly carried out. The related measurements on samples are usually performed by means of the DAMA low background Ge detector, specially realized with a low Z window. It is operative deep underground in the low background facility of the Gran Sasso Laboratory. Some selected materials are in addition measured at ISPRA facility.

During year 2004 a significant improvement of the DAMA/Ge installation has been started.

7 Conclusions

In conclusion, the main activities during year 2004 can be summarized as in the following:

I. Further presentation and general corollary investigations on the basis of the final model independent result on the particle Dark Matter investigation by DAMA/NaI have been and are in progress. Moreover, further analyses to investigate some nuclear rare processes have been carried out; in particular, the result on the search for spontaneous transition of nuclei to a superdense state have been published.

II. The new DAMA/LIBRA set-up is collecting data.

III. The DAMA/LXe set-up has taken data in the second part of the year 2004 and some further data analyses have been carried out on previously available exposure.

IV. The DAMA/R&D set-up has been employed for new measurements on PMT prototypes and preliminary measurements for new small scale experiments. Moreover, the data analysis on data collected with a BaF_2 scintillator have been published.

V. The DAMA/Ge set-up is in progress of upgrading.

8 List of Publications during 2004

1. R. Bernabei, P. Belli, F. Cappella, F. Montecchia, F. Nozzoli, A. Incicchitti, D. Prosperi, R. Cerulli, C.J. Dai, H.H. Kuang, J.M. Ma, Z.P. Ye, *DAMA/NaI results*, in publication on the Proceed. of the NOON04 Int. Conf., Tokyo, February 2004.

2. R. Bernabei, P. Belli, F. Cappella, F. Montecchia, F. Nozzoli, A. Incicchitti, D. Prosperi, R. Cerulli, C.J. Dai, H.H. Kuang, J.M. Ma, Z.P. Ye, *DAMA/NaI results*, in publication on the Proceed. of the Rencontre de Morions "Electroweak Interactions and unified theories", La Thuile, March 2004.

3. R. Bernabei, P. Belli, F. Cappella, F. Montecchia, F. Nozzoli, A. Incicchitti, D. Prosperi, R. Cerulli, C.J. Dai, H.H. Kuang, J.M. Ma, Z.P. Ye, *Very low background scintillators in DAMA project: results and perspectives*, in publication on the Proceed. of the CALOR04 Int. Conf., Perugia, April 2004.

4. R. Bernabei, P. Belli, F. Cappella, F. Montecchia, F. Nozzoli, A. d'Angelo, A. Incicchitti, D. Prosperi, R. Cerulli, C.J. Dai, H.H. Kuang, J.M. Ma, Z.P. Ye, *The new DAMA/LIBRA and beyond*, to appear on the Proc. of the Workshop on "Frontier Objects in Astrophysics and Particle Physics", Vulcano, May 2004.

5. R. Bernabei, P. Belli, F. Cappella, F. Montecchia, F. Nozzoli, A. Incicchitti, D. Prosperi, R. Cerulli, C.J. Dai, H.H. Kuang, J.M. Ma, Z.P. Ye, *Signature for signals from the Dark Universe*, to appear on the Proc. of the Workshop on "Frontier Objects in Astrophysics and Particle Physics", Vulcano, May 2004.

6. R. Cerulli, P. Belli, R. Bernabei, F. Cappella, F. Nozzoli, F. Montecchia, A. d'Angelo, A. Incicchitti, D. Prosperi, C.J. Dai, *Performances of a BaF_2 detector and its application to the search for $\beta\beta$ decay modes in ^{130}Ba*, Nucl. Instr. & Meth. A525 (2004) 535-543.

7. R. Bernabei, *La materia oscura dell'Universo e la sua investigazione*, Il Nuovo Saggiatore, vol. 21 no. 3-4 (2004) 32.

8. R. Bernabei, P. Belli, F. Cappella, F. Montecchia, F. Nozzoli, A. Incicchitti, D. Prosperi, R. Cerulli, C.J. Dai, H.H. Kuang, J.M. Ma, Z.P. Ye, *Direct search for Dark Matter*, in publication on the Proceed. of the "Frontier Science 2004" Int. Conf., Frascati, June 2004.

9. F. Cappella, R. Bernabei, P. Belli, F. Montecchia, M. Amato, G. Ignesti, A. Incicchitti, D. Prosperi, R. Cerulli, C.J. Dai, H.L. He, H.H. Kuang, J.M. Ma, G.X. Sun, Z. Ye, *Searches for Q-balls, for neutral Strong Interacting Massive Particles and for neutral nuclearites with DAMA/NaI*, in publication on the Proceed. of the "Frontier Science 2004" Int. Conf., Frascati, June 2004.

10. F. Nozzoli, R. Bernabei, P. Belli, A. Incicchitti, *Anisotropic scintillators for particle Dark Matter direct detection*, in publication on the Proceed. of the "Frontier Science 2004" Int. Conf., Frascati, June 2004.

11. R. Bernabei, P. Belli, F. Montecchia, F. Nozzoli, A. Incicchitti, D. Prosperi, R. Cerulli, C.J. Dai, H.L. He, H.H. Kuang, J.M. Ma, S. Scopel, *Search for solar axions by Primakoff effect in NaI crystals*, in publication on the Proceed. of the "Frontier Science 2004" Int. Conf., Frascati, June 2004.

12. R. Bernabei, *Dark Matter searches*, to appear in the Proc. of 7th School on non-accelerator Astroparticle Physics (ICTP04), Trieste, August 2004.

13. R. Bernabei, P. Belli, F. Cappella, F. Montecchia, F. Nozzoli, A. Incicchitti, D. Prosperi, R. Cerulli, C.J. Dai, H.H. Kuang, J.M. Ma, Z.P. Ye, *DAMA results and perspectives*, to appear in the Proc. of PASCOS04, Boston, August 2004

14. R. Bernabei, P. Belli, F. Cappella, F. Montecchia, F. Nozzoli, A. Incicchitti, D. Prosperi, R. Cerulli, C.J. Dai, H.H. Kuang, J.M. Ma, Z.P. Ye, *DAMA: results and perspectives*, to appear in the Proc. of IDM04, Edinburgh, September, 2004.

15. R. Bernabei, P. Belli, F. Cappella, F. Montecchia, F. Nozzoli, A. Incicchitti, D. Prosperi, R. Cerulli, C.J. Dai, H.H. Kuang, J.M. Ma, Z.P. Ye, *Dark Matter particles in the galactic halo: results and implications from DAMA/NaI*, to appear on Int. J. Mod. Phys. D, arXiv:astro-ph/0501412

16. R. Bernabei, P. Belli, F. Cappella, F. Nozzoli, F. Montecchia, A. d'Angelo, A. Incicchitti, D. Prosperi, R. Cerulli, C.J. Dai, H.H. Kuang, J.M. Ma, Z.P. Ye, *Search for spontaneous transition of nuclei to a superdense state*, Eur. Phys. J. A23 (2005) 7-10.

17. R. Bernabei, P. Belli, F. Cappella, F. Nozzoli, F. Montecchia, A. Incicchitti, D. Prosperi, R. Cerulli, C.J. Dai, H.H. Kuang, J.M. Ma, Z.P. Ye, *DAMA/NaI results on Dark Matter particles by annual modulation signature*, in publication on the Proceed. of the DARK04 Int. Conf., College Station , TX, USA, October 2004.

18. R. Bernabei, P. Belli, F. Cappella, F. Nozzoli, F. Montecchia, A. d'Angelo, A. Incicchitti, D. Prosperi, R. Cerulli, C.J. Dai, H.H. Kuang, J.M. Ma, Z.P. Ye, *DAMA/LIBRA and Beyond*, in publication on the Proceed. of the DARK04 Int. Conf., College Station , TX, USA, October 2004.

References

[1] R. Bernabei et al., Il Nuovo Cimento A112 (1999) 545.

[2] R. Bernabei et al., Eur. Phys. J. C18 (2000) 283.

[3] R. Bernabei et al., La Rivista del Nuovo Cimento 26 n.1 (2003) 1-73 (*astro-ph/0307403*) and references therein.

[4] R. Bernabei et al., Phys. Lett. B424 (1998) 195.

[5] R. Bernabei et al., Phys. Lett. B450 (1999) 448.

[6] P. Belli et al., Phys. Rev. D61 (1999) 023512.

[7] R. Bernabei et al., Phys. Lett. B480 (2000) 23.

[8] R. Bernabei et al., Phys. Lett. B509 (2001) 197.

[9] R. Bernabei el al., Eur. Phys. J. C23 (2002) 61.

[10] P. Belli et al., Phys. Rev. D66 (2002) 043503.

[11] R. Bernabei et al., Phys. Lett. B389 (1996) 757.

[12] R. Bernabei et al., Il Nuovo Cimento A112 (1999) 1541.

[13] R. Bernabei et al., Phys. Rev. Lett. 83 (1999) 4918.

[14] F. Cappella et al., Eur. Phys. J.-direct C14 (2002) 1.

[15] R. Bernabei et al., Phys. Lett. B515 (2001) 6.

[16] R. Bernabei et al., Phys. Lett. B408 (1997) 439.

[17] P. Belli et al., Phys. Rev. C60 (1999) 065501.

[18] P. Belli et al., Phys. Lett. B460 (1999) 236.

[19] R. Bernabei et al., Nucl. Phys. B (Proc. Suppl.) 70 (1999) 79.

[20] G. Prezeau et al., Phys. Rev. Lett. **91**, 231301 (2003).

[21] A. Bottino et al., Phys. Rev. D69 (2004) 037302.

[22] CDMS coll., *astro-ph/0405033*; *Phys. Rev. Lett.* **84** (5699) 2000 .

[23] EDELWEISS coll., in the Proc. of NDM03, Japan (2003); *Phys. Lett.* **B 513** (15) 2001 .

[24] CRESST coll., *astro-ph/0408006*

[25] N. Smith, talk given at IDM02, York, september 2002.

[26] R. Luscher , talk given at Moriond, march 2003.

[27] K. Belotsky et al., *hep-ph/0411093*.

[28] E. Feenberg and H. Primakoff, Phys. Rev. 70 (1946), 980.

[29] A. R. Bodmer, Phys. Rev. D4 (1971), 1601.

[30] T. D. Lee and G. C. Wick, Phys. Rev. D9 (1974), 2291.

[31] T. D. Lee, Rev. Mod. Phys. 47 (1975), 267.

[32] A. B. Migdal, Zh. Eksp. Theor. Fiz. 61 (1971), 2209 [Sov. Phys. JETP 34 (1972), 1184]; A. B. Migdal et al., Zh. Eksp. Theor. Fiz. 66 (1974), 443 [Sov. Phys. JETP 39 (1974), 212]; A. B. Migdal, Rev. Mod. Phys. 50 (1978) 107.

[33] A. Akmal and W.R. Pandharipande, *Phys. Rev.* **C 56** (2261) 1997

[34] G. N. Flerov et al., Yad. Fiz. 20 (1974), 472 [Sov. J. Nucl. Phys. 20 (1975), 254]; W. Grimm et al., Phys. Rev. Lett. 26 (1971), 1040, 1408; V. M. Gorbachev et al., Osnovnye kharakteristiki izotopov tyazhelykh elementov, SPRAVOCHNIK (fundamental characteristics of isotopes of heavy elements, reference manual), Atomizdat, 1970; E. Bukhner et al., Yad. Fiz. 52 (1990), 305 [Sov. J. Nucl. Phys. 52 (1990), 193].

[35] V. M. Galitskii, Usp. Fiz. Nauk 120 (1976) No.1 [Sov. Phys. Usp. 19 (1976), 769].

[36] L.A. Mikaèlyan and M. D. Skorokhvatov, Yad. Fiz. 25 (1977), 1164 [Sov. J. Nucl. Phys. 25 (1977), 618].

[37] V.I. Aleshin et al., Pis'ma Zh. Eksp. Theor. Fiz. 24 (1976) No. 2 [JETP Lett. 24 (1976), 100].

[38] R. Bernabei et al., Astrop. Phys. 4 (1995) 45; R. Bernabei, "Competitiveness of a very low radioactive ton scintillator for particle Dark Matter search", in the volume *The identification of Dark Matter*, World Sc. pub. (1997) 574.

[39] K. Freese et. al. astro-ph/0309279; Phys. Rev. Lett. **92**, 11301 (2004).

[40] R.A. Ibata et al., Mon. Not. Roy. Astr. Soc. **348**, 12 (2004).

[41] F.S. Ling, P. Sikivie, S. Wick, astro-ph/0405231.

[42] I.R. Barabanov et al., Astrop. Phys. 8 (1997) 67; I.R. Barabanov et al., Nucl. Phys. B546 (1999) 19; I.R. Barabanov et al., New Journal of Physics 3 (2001) 5.1.

[43] P. Belli et al., Il Nuovo Cimento A103 (1990) 767.

[44] P. Belli et al., Il Nuovo Cimento C19 (1996) 537.

[45] P. Belli et al., Astrop. Phys. 5 (1996) 217.

[46] R. Bernabei et al., Nucl. Instr. & Meth. A482 (2002) 728.

[47] P. Belli et al., Phys. Lett. B387 (1996) 222 and Phys. Lett. B389 (1996) 783 (erratum).

[48] R. Bernabei et al., Phys. Lett. B436 (1998) 379.

[49] R. Bernabei et al., Eur. Phys. J.-direct C11 (2001) 1.

[50] R. Bernabei et al., New Journal of Physics 2 (2000) 15.1.

[51] P. Belli et al., Phys. Rev. D61 (2000) 117301.

[52] P. Belli et al., Phys. Lett. B465 (1999) 315.

[53] R. Bernabei et al., Phys. Lett. B493 (2000) 12.

[54] R. Bernabei et al., Phys. Lett. B527 (2002) 182.

[55] R. Bernabei et al., Phys. Lett. B546 (2002) 23.

[56] R. Bernabei et al., in the volume "Beyond the Desert 2003", Springer (2003), 365-374.

[57] R. Bernabei et al., in the volume "Cosmology and particle Physics", AIP ed. (2001) 189.

[58] F. Cappella, PhD thesis, Univ. Roma "Tor Vergata" (2005).

[59] C. Berger et al., Phys. Lett. B269 (1991) 227

[60] W. R. Nelson et al., SLAC-265, UC-32 (E/I/A).

[61] R. Bernabei et al., Il Nuovo Cimento A110 (1997) 189.

[62] R. Bernabei et al., Astrop. Phys. 7 (1997) 73.

[63] P. Belli et al., Nucl. Phys. B563 (1999) 97.

[64] P. Belli et al., Astrop. Phys. 10 (1999) 115.

[65] R. Bernabei et al., Nucl. Phys. A705 (2002) 29.

[66] P. Belli et al., Nucl. Instr. & Meth. A498 (2003) 352.

[67] R. Bernabei et al., Eur. Phys. J. C28 (2003) 203.

[68] V.I. Tretyak, Yu.G. Zdesenko, At. Data Nucl. Data Tables 61 (1995) 43; 80 (2002) 83.

[69] Y. Akovali, Nuclear data sheet 84 (1998) 1.

[70] L.E. Dinca et al., Nucl. Inst. & Meth. A486 (2002) 141.

[71] T.A. DeVol and R.A. Fjeld, Nucl. Inst. & Meth. A353 (1994) 28.

[72] E. Slunga et al., Nucl. Inst. & Meth. A469 (2001) 70.

G.N.O.
Gallium Neutrino Observatory

M. Altmann[a], M. Balata[b], P. Belli[c], E. Bellotti[d],
R. Bernabei[c], E. Burkert[e], C. Cattadori[d],
R. Cerulli[c], M. Chiarini[e], M. Cribier[g], S. d'Angelo[c],
G. Del Re[f], K. Ebert[h], F. von Feilitzsch[a], N. Ferrari[b],
A. Germeroth[e], W. Hampel[e], F.X. Hartmann[e], E. Henrich[h],
G. Heusser[e], L. Ioannucci[b], F.Kaether[e], J. Kiko[e],
T. Kirsten[e], T. Lachenmaier[a], J. Lanfranchi[a],
M. Laubenstein[b], P. Mögel[e], D. Motta[d,e],
S. Nisi[b], J. Oehm[e], L. Pandola[b], W. Potzel[a],
H. Richter[e], S. Schoenert[e], M. Wojcik[i], L. Zanotti[d]

[a] Physik Department E15, Technische Universität München (TUM),
James-Franck Straße, D-85748 Garching b. München, Germany
[b] INFN, Laboratori Nazionali del Gran Sasso (LNGS),
S.S. 17/bis Km 18+910, I-67010 L'Aquila - Italy
[c] Dip. di Fisica, Università di Roma "Tor Vergata" and INFN, Sez. Roma II,
Via della Ricerca Scientifica, I-00133 Roma - Italy
[d] Dip. di Fisica, Università di Milano "Bicocca", and INFN Sez. Milano,
Via Emanueli, I-20126 Milano - Italy
[e] Max-Plank-Institut für Kernphysik (MPIK), P.O.B. 103980,
D-69029 Heidelberg - Germany
[f] Dip. di Ingegneria Chimica e Materiali, Università dell'Aquila,
Località Monteluco di Roio, L'Aquila - Italy
[g] DAPNIA/Service de Physique de Particules, CE Saclay,
F-91191 Gif-sur-Yvette Cedex - France
[h] Institut für Technische Chemie, Forschungszentrum Karlsruhe (FZK),
Postfach 3640, D-76021 Karlsruhe, Germany
[i] Instiytut Fizyki, Uniwersytet Jagiellonski,
ul. Reymonta 4, PL-30059 Krakow, Poland

Abstract

The GNO (Gallium Neutrino Observatory) monitored the low energy solar neutrino flux with a 30 tons gallium detector at LNGS. The experiment is now terminated after altogether 58 solar exposure runs that were performed between May 20, 1998 and April 9, 2003. The final result for GNO is $62.9^{+5.5}_{-5.3}$(stat)±2.5(syst) SNU (1σ). Overall, gallium-based observations at LNGS (first in GALLEX, later in GNO) lasted from May 14, 1991 through April 9, 2003. The joint results from 123 runs in GALLEX and GNO is 69.3±5.5 SNU (1σ). The distribution of the individual run results is consistent with the hypothesis of a neutrino flux which is constant in time.

The various activities performed during 2004 are also discussed in this report. They include the data taking for a set of 6 solar runs extrected by the SAGE experiment at Baksan, Russia, and shipped at Gran Sasso for counting.

1 Introduction

The Gallium Neutrino Observatory (GNO) experiment at the Laboratori Nazionali del Gran Sasso (LNGS) has recorded solar neutrinos with energies above 233 keV via the inverse EC reaction $^{71}\mathrm{Ga}(\nu_e, e)^{71}\mathrm{Ge}$ in a 100-ton galliun chloride target (containing 30 tons of gallium) from May 1998 to April 2003. The energy threshold is well below the maximum energy of the so-called *pp* neutrinos, that represent the bulk of solar neutrinos and account for 90% of the total flux.

The data taking has been now terminated and the gallium chloride solution has been removed from the hall A of the undeground Laboratory in December 2004. Together with the preceding GALLEX obvservations, low energy solar neutrino recordings were acquired for more than a full solar cycle (1991-2003, with a break in 1997); the bulk production rate is determined from 123 solar runs (65 from GALLEX and 58 from GNO) with a accuracy of ±5.5 SNU.

The result and its precision will remain without competition from eventually upcoming low-threshold real-time experiments for many years to come. It recorded a fundamental astrophysical quantity, i.e. the neutrino luminosity of the Sun. Lack of these data would have a very negative impact on the interpretation of the results from forthcoming second generation solar neutrino experiments such as BOREXINO. In the astrophysical context the gallium results shed light also on the relative contributions of the pp-I, pp-II and CNO cycles to the solar luminosity, and on the agreement of the energy production derived from the photon and neutrino luminosities. In section 2 we describe the GNO solar neutrino observations and the results obtained from data analysis. In section 3 we discuss the experimental activities performed in 2004. In section 4 we discuss the implication of the results in the context of solar neutrino physics and neutrino oscillations.

2 The detector and the results

The GNO experiment detects solar neutrinos via the reaction $^{71}\mathrm{Ga}(\nu_e, e)^{71}\mathrm{Ge}$, which has a threshold of 233 keV. The detector is sensitive mainly to pp-neutrinos (53% of the

interaction rate according to the standard solar model [1]), with smaller contributions to the signal from ^{7}Be ν (27%), ^{8}B ν (12%), and CNO ν (8%). The target consists of 101 tons of a $GaCl_3$ solution in water and HCl, containing 30.3 tons of natural gallium; this amount corresponds to $\sim 10^{29}$ ^{71}Ga nuclei. The ^{71}Ge atoms produced by solar neutrinos (at a rate of about 0.7 per day, one half of the amount predicted by solar models) are extracted from the gallium tank every 4 weeks [2] and introduced in low-background gas proportional counters [3] as germane gas (GeH_4). The decay of ^{71}Ge (EC, τ=16.5 days) produces a signal in the counters consisting of a point-like ionization at 10.4 keV, or 1.1 keV (K-shell or L-shell electron capture respectively). The signal is recorded by fast digitizers to allow background reduction by pulse shape analysis [4]. The solar neutrino interaction rate on ^{71}Ga is deduced from the number of ^{71}Ge atoms observed. For a complete description of the experimental procedure see [5].
The gallium detector was operated between 1991 and 1997 by the GALLEX Collaboration: 65 "solar runs" were performed. The solar neutrino capture rate on ^{71}Ga was measured with a global uncertainty of 10% as: 77.5 $\pm$6.2(stat.)$^{+4.3}_{-4.7}$(syst.) SNU[1] (1 σ) [5]. After maintenance of the chemical plants and renovation of the DAQ and electronics, a new series of measurements was started in April 1998, within the GNO (Gallium Neutrino Observatory) project [6], using the same 30-ton Gallium target.

2.1 Solar neutrino observations

GNO started solar neutrino observations in May 1998: 58 solar runs and 12 blank runs were succesfully performed and counted. The total GNO solar neutrino exposure is 1687 days. During this time the statistical analysis identifies a total of 258 decaying ^{71}Ge atoms, 239 of them (or 4.1 per run) due to solar neutrinos. The mean ^{71}Ge count rate per run at the start of counting is $\sim$ 0.27 counts/day; this may be compared with the time-independent background rate in the acceptance window, which is on average as low as 0.06 counts/day. The total result, which is obtained after subtraction of 4.55 SNU for side reactions (see Ref. [7]) and after correction of the geometrical modulation effect, is

$$62.9^{+5.5}_{-5.3}(\text{stat})\pm 2.5(\text{syst})\ \text{SNU}\ (1\sigma)\ [8].$$

The total systematic error amounts to 2.5 SNU (1σ); it is still dominated by the error on the counting efficiencies, but is substantially lower than in GALLEX (4.5 SNU) thanks to several experimental activities performed in GNO (absolute calibrations with ^{69}Ge activity, z-scanning, neural-network-based pulse shape analysis, re-evaluation of the Rn-cut inefficiency), as described in the previous annual reports [9, 10, 11, 12, 13, 14]. The energy spectrum of all the events observed in the 58 GNO solar runs (see Fig. 1) is well consistent with the expectation from ^{71}Ge decay: a clear excess of events in the L- and K-peak occurring in the first $\sim 3\tau$ of ^{71}Ge can be seen. The time distribution of the candidate events in the GNO runs is also compatible with the expectation of a ^{71}Ge signal and a constant background (see Fig. 2). The experimental distribution (dots) has been superimposed with the best-fit curve obtained from the maximum likelihood analysis and the corresponding $\pm 1\sigma$ error band.

Table 1 summarizes the basic results for GNO, GALLEX and for a combined analysis

[1] 1 SNU (Solar Neutrino Unit) = 10^{-36} captures per second and per absorber nucleus

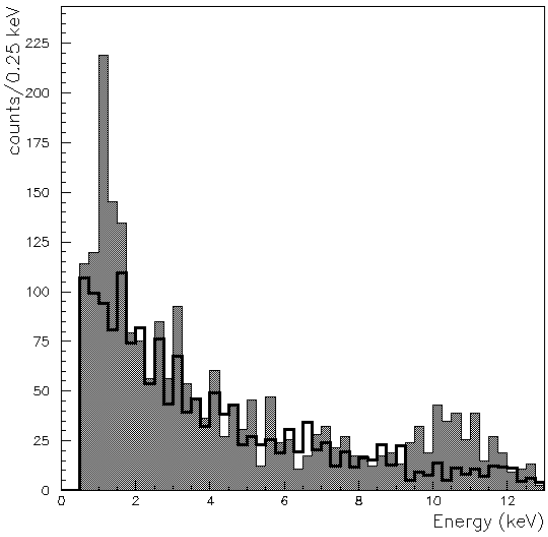

Figure 1: Energy distribution for all the events observed in the GNO solar runs SR1-SR58. The shaded histogram contains events occurred in the first 50 days ($\sim 3\tau$) of counting. The thick-line histogram includes events occurred after the first 50 days of counting (normalized).

of GALLEX and GNO together. The joint GALLEX+GNO result after 123 solar runs is

$$69.3 \pm 5.5 \text{ SNU } (1\sigma),$$

with errors added in quadrature [8]. This is in good agreement with the latest result from the SAGE experiment, $66.9^{+5.3}_{-5.0}$ SNU (1σ) [15]. The results of all 123 individual GNO and GALLEX runs (corrected for side reactions and geometrical effects) are displayed in Fig. 3.

The measured interaction rate is lower than the value expected from *pp* neutrinos only, which, for a large class of solar models, is almost independent from the details of the models themselves. Therefore, as discussed in section 4, the gallium results strongly support by themselves that the solution of the solar neutrino problem must be found in the ν physics domain.

2.2 Time constancy and annual modulation

The Gallium-solar neutrino interaction rate has been estimated under the assumption of a neutrino flux costant in time. This assumption must be justified even so there are presently no attractive models that predict a time variable neutrino emission from the Sun. Observation of such a variation on a short (i.e. non-secular) time scale would signal rather new and unexpected solar neutrino physics, but it cannot be excluded *a priori*.

For this reason the GALLEX/GNO data were analyzed for possible time variation during

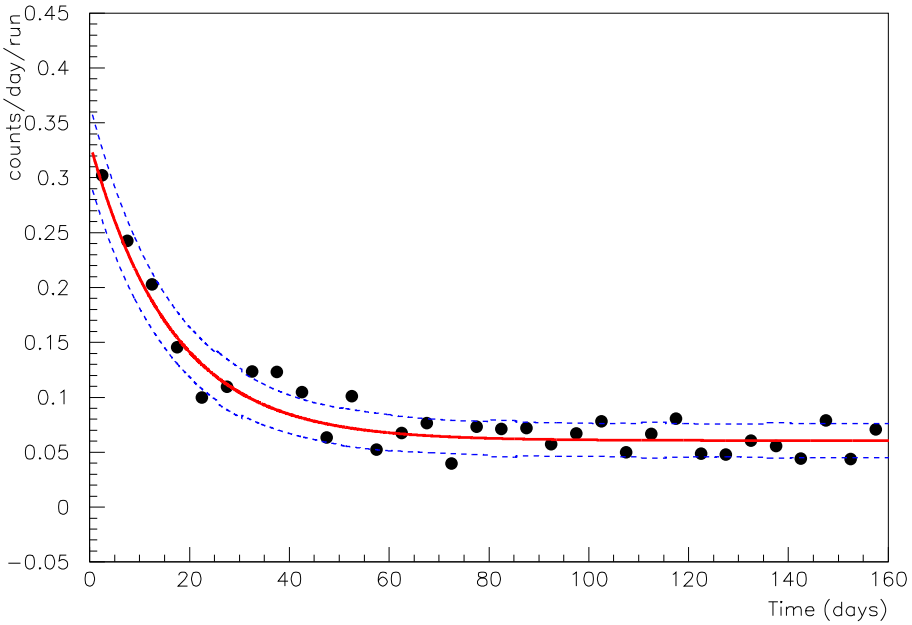

Figure 2: Counting rate of ^{71}Ge candidates vs. time.

Table 1: Results from GALLEX and GNO. Statistical and systematic errors combined in quadrature.

	GNO	GALLEX	GNO+GALLEX
Time period	05/98-04/03	05/91-01/97	05/91-0403
Net exposure time (d)	1687	1594	3281 (8.98 yrs)
Number of runs	58	65	123
L only (SNU)	$68.2^{+8.9}_{-8.5}$	74.4±10	70.9±6.6
K only (SNU)	$59.5^{+6.9}_{-6.6}$	79.5±8.2	67.8±5.3
Result (all) (SNU)	$62.9^{+6.0}_{-5.9}$	$77.5^{+7.6}_{-7.8}$	69.3±5.5

the 12-year-long data taking period. The scatter plots of the single run results for GNO, GALLEX and GALLEX+GNO are shown in Fig. 4. They are compatible with the Monte Carlo generated distributions of single run results for a constant production rate (62.9, 77.5 and 69.3 SNU respectively) under the typical solar runs conditions (efficiencies, exposure time, etc.): the Kolmogorov-Smirnov confidence levels are 82%, 38% and 51% respectively.

One approach to check for the time-constancy of the capture rate is the application of the likelihood-ratio test (see [7]). The resulting goodness-of-fit confidence levels are 25.1% for GNO, 24.2% for GALLEX and 5.6% for GALLEX+GNO.

The data were also analyzed in term of correlation with the seasonal Earth-Sun distance variation: since the eccentricity of the Earth orbit is $\varepsilon = 0.0167$ and the solar neutrino flux varies as $1/d^2$ for purely geometrical reasons, the expected modulation has amplitude

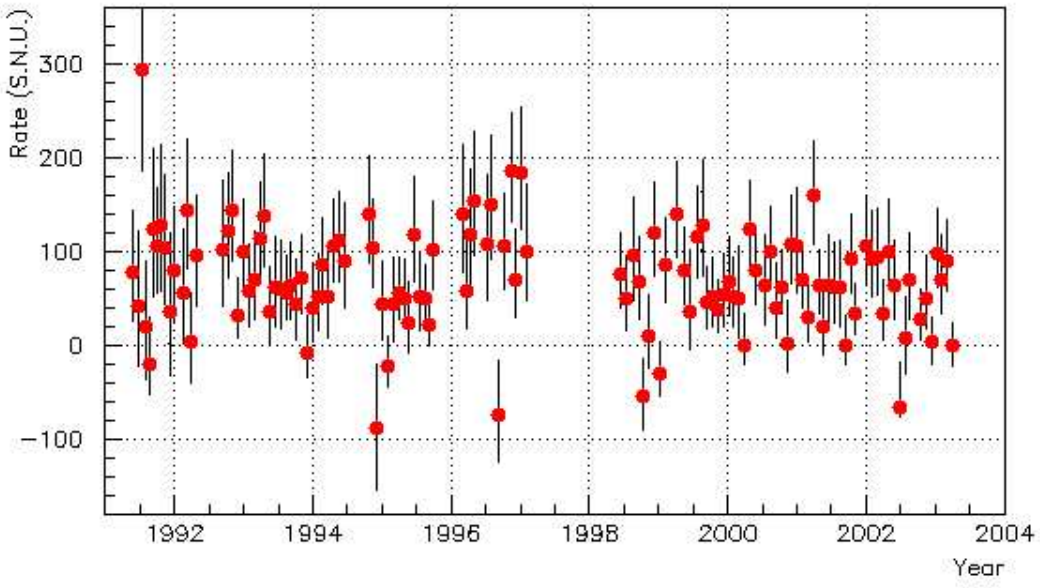

Figure 3: Davis plot of the 123 single Gallex and GNO solar runs.

$2\varepsilon = \pm 3.3\%$ (i.e. about 7% between aphelion and perihelion). The 123 solar runs of Gallex and GNO were divided in six groups, according to the period of the year in which they were performed: in this way each set includes solar runs of similar Sun-Earth distance. The analysis was then separately performed for the six groups, in order to reconstruct the gallium rate profile vs. d (see Fig. 5) between the perihelion (0.983 AU) and the aphelion (1.017 AU). The same plot shows the expected modulation, assuming that the mean signal at 1 AU is 69.3 SNU; the Neyman-Pearson test confidence level is about 69% ($\chi^2 = 3.0$ with 5 d.o.f.).
It is also possible to evaluate the solar signal of the runs performed during winter (which is defined as the 3 months preceding plus the 3 months following the perihelion, January 4^{th}) and summer. The result obtained for the 66 winter runs of Gallex and GNO is $R_W = 66.5 \pm 5.5 \pm 3.5$ SNU (1σ) while it is $R_S = 74.1 \pm 6.3 \pm 3.6$ SNU (1σ) for the 57 summer runs; the experimental W-S difference is hence

$$\Delta_{W-S} \;=\; -7.6 \pm 8.4 \text{ SNU}$$

(the systematic errors cancel out, being the same for the two datasets), which is consistent within 1.2 σ with the pure geometrical case, i.e. $\Delta_{W-S} = +2.3$ SNU.

2.3 Time series analysis

In recent years it has been suggested [16, 17] that the solar neutrino capture rate measured by the gallium radiochemical experiments shows a time variability with characteristic frequency $\sim 13.5\,\text{year}^{-1}$, resembling that of rotation of the solar magnetic fields. Since this variability would be an indication for the presence of sub-dominant magnetic interactions of *pp* neutrinos in the solar convective zone [17], a dedicated search for possible time

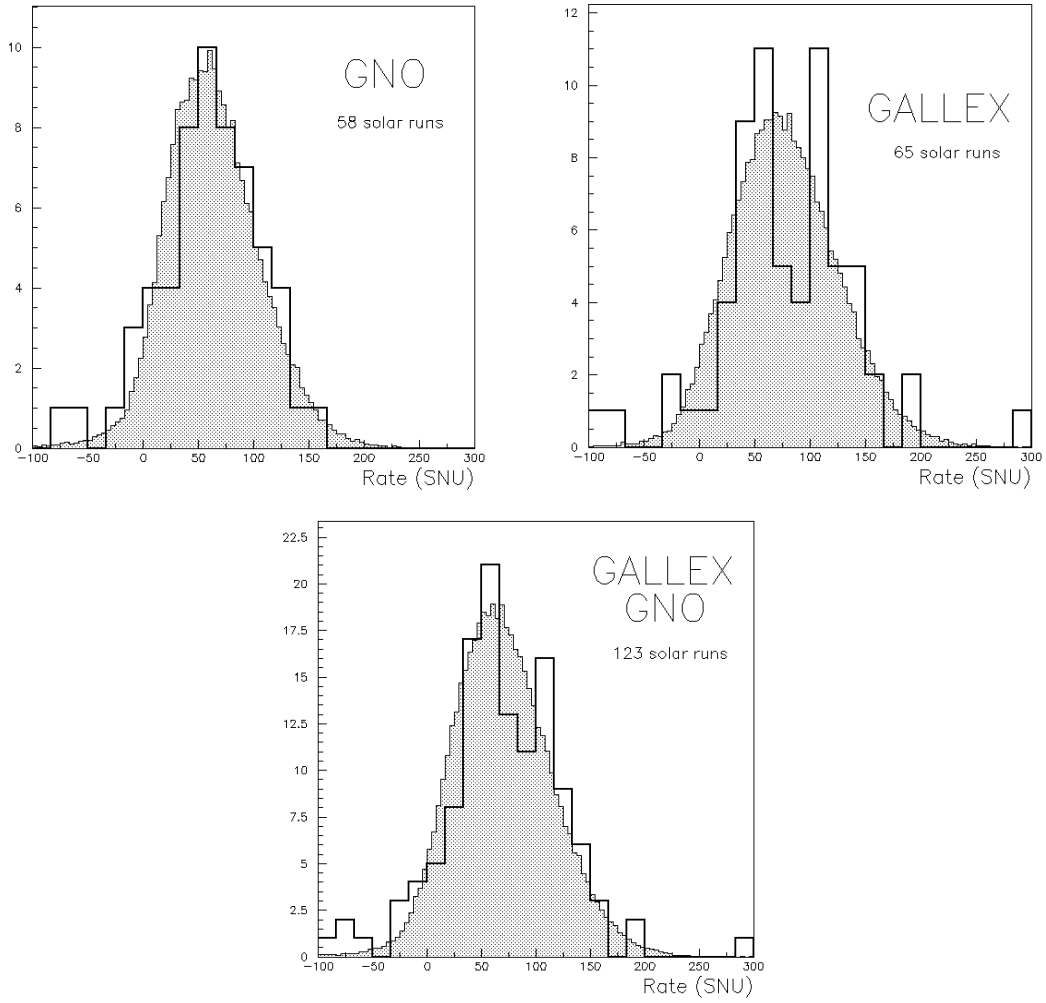

Figure 4: Single run distribution for GNO, GALLEX and GALLEX+GNO superimposed with the corresponding Monte Carlo simulations (shaded histograms).

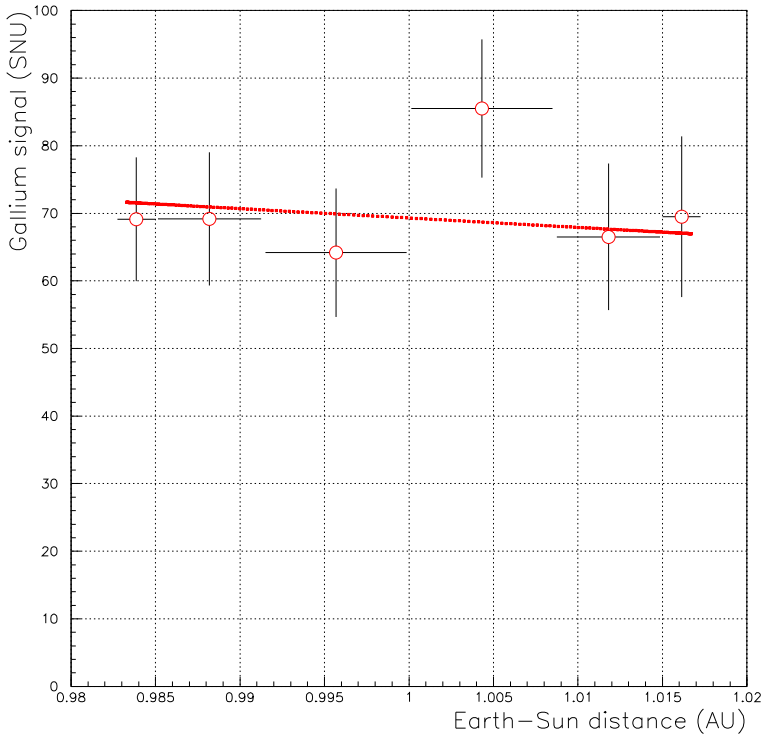

Figure 5: Ga signal vs. heliocentric distance of the Earth.

modulations in the Gallex and GNO data was performed [18] using different methods (i.e. Lomb-Scargle and maximum likelihood).
The Lomb-Scargle periodogram of the 123 solar runs of Gallex and GNO is statistically consistent with the expectations of a constant interaction rate. Since no positive signal of time periodicity is found, it is possible to set an exclusion plot. In the assumption of sinusoidal time modulations

$$n(t) \;=\; n_0[1 + A\sin(2\pi\nu t + \varphi)] \tag{1}$$

with $0 \leq A \leq 1$, the experimental data rule out (see Fig. 6) variations with low frequency and large amplitude. As expected, a general feature of radiochemical experiments is a rapid loss of sensitivity for variations over periods shorter than the exposure time.

An other option is to apply the maximum likelihood method to the time list of the ^{71}Ge candidate events in the single solar runs, including a time-modulated term in the likelihood function. The general maximum likelihood method [19] has then been applied to the case of a production rate periodically varying as in Eq. (1). The best-fit from the 123 solar runs is (statistical errors only) n_0=69.1±6.1 SNU, A=0.57±0.38, ν=13.9±0.4 year^{-1} and φ= -0.3±1.0 rad[4]. The hypothesis of modulated solar neutrino flux can then be compared with that of stationary flux by means of the likelihood ratio test. The resulting $-2\ln\lambda = 3.40$ corresponds to a p-value of 33.4%. Fig. 7 shows the likelihood

[4]The time origin is conventionally set to May 14^{th}, 1991, i.e. to the start of exposure of the first Gallex run.

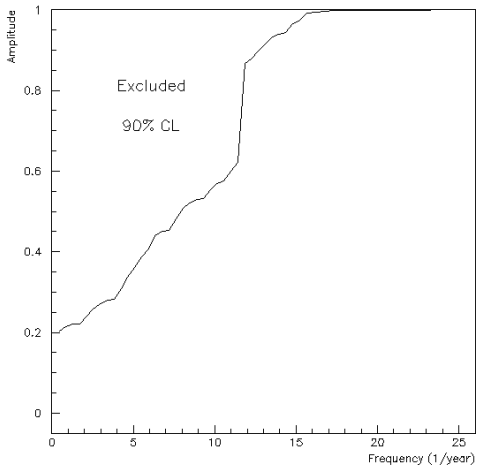

Figure 6: 90% CL exclusion plots in the frequency/amplitude plane derived from the Gallex/GNO dataset.

spectrum $-2 \ln \lambda$ obtained fixing the frequency and fitting all the other parameters.
Given the present sensitivity, the experimental Gallex/GNO data are hence statistically consistent with the expectation of a solar neutrino capture rate constant over the whole data taking period (> 10 y). Although this fact does not invalidate other hypotheses that might give a better a time-dependent fit, the data allow to set some restrictions on low-frequency periodical modulations.
The results of 12 years of solar neutrino observations call for a continuous monitoring of the low-energy solar neutrino flux with ever increasing sensitivity over very long time periods, in a spirit comparable to the motivations for a continuous observation of solar surface phenomena.

3 Experimental activity during 2004

3.1 z-scanning

During 2003 it was realized a small set-up devoted to the systematic measurement of the detection efficiencies of the miniaturized proportional counters used in the GNO experiment as a function of the coordinate along the anode wire. Four counters, with different cathode materials, have been selected for the z-scanning and the longitudinal gas-gain curve has been succesfully measured. This procedure can assure a better knowledge of these quantities, previously extrapolated for all the counters from a few determinations, and verify the goodness of the response of repaired counters. In particular, an automatic system allows to measure the response of the counter longitudinally at given steps with a collimated X-ray source of fixed intensity and to collect at each position the pulses profiles and the energy distribution measured by the exposed counter. The X-ray tube is mounted on a motor step – that allows to move the source in the z direction with a precision of

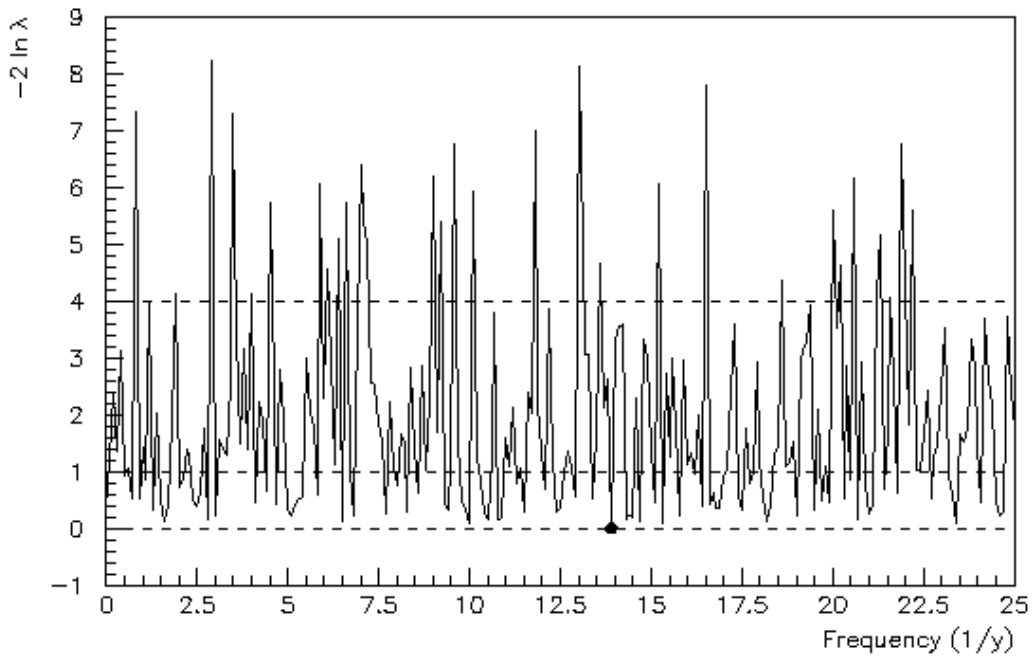

Figure 7: Likelihood spectrum $-2\ln\lambda(\nu)$ from the Gallex/GNO dataset vs. frequency. All the other parameters are left free in the fit. The black dot marks the best-fit point. The dashed lines correspond to the 1σ and 2σ levels.

few microns – and the proportional counter settled in a plexiglas support.
The results obtained for all the counters are reported in Fig. 5. As expected, the response of the proportional counters gets significantly worse approaching the edges of the detector. In particular, the peak position moves toward lower channels and the energy resolution becomes poorer. Anyhow, for every counter, the two edge regions are narrow with a typical width of about 1.5 mm and the response between these regions is very good and stable with a typical energy resolution at $\simeq 5$ keV: $\sigma/\mathrm{E} \simeq 13\%$ for $FC93$ and $FE112$ and $\sigma/\mathrm{E} \simeq 10\%$ for $SC136$ and $SC151$. These values are consistent with the typical energy resolution ($\sigma/\mathrm{E} \simeq 5\%$ at 10 keV and $\simeq 19\%$ at 1 keV) obtained from routine calibrations in the GNO experiment, when the Cerium X-rays irradiate homogeneously the whole body of the counter. Only the counter $SC136$ has an appreciable non-completely uniform behaviour along the z direction (see the relative peak position behaviour); this can be ascribed to some extent to loss of detector quality in its repairing procedure and shows that similar measurements may be crucial in some cases. Figs. 6a) and 6b) give, as an example, the measured energy spectra obtained by positioning the collimated X-ray source in the middle and at one edge of the counter $SC136$, respectively. The degradation of the counter response at the cathode edges is evident and can allow to quantify the effect for precise determinations.

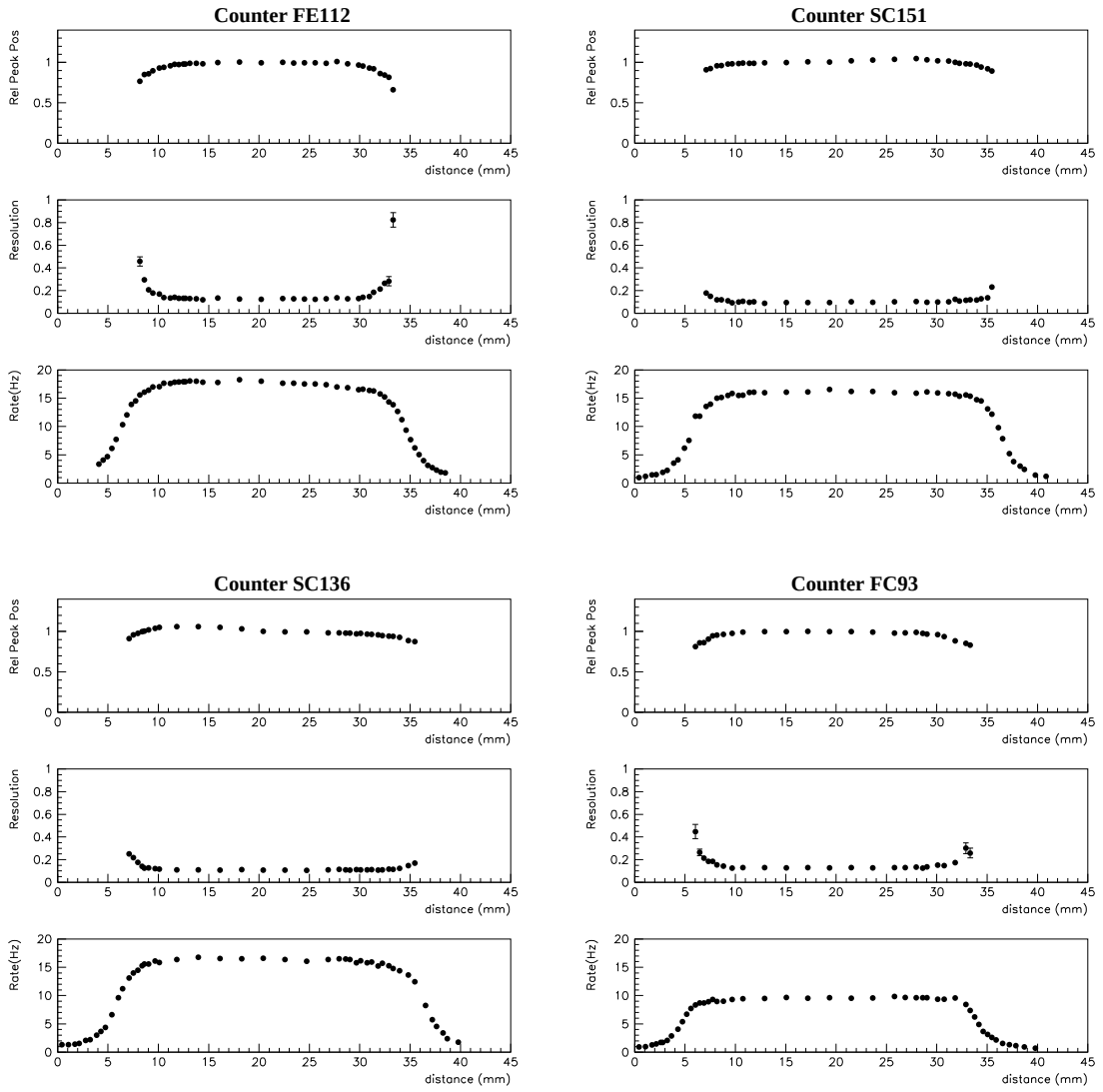

Figure 8: Measured counting rates, peak relative positions and energy resolutions (σ/E) of the $\simeq$ 5 keV peak as obtained by calibrating along the z axis four miniaturized proportional counters with different cathode materials. See text.

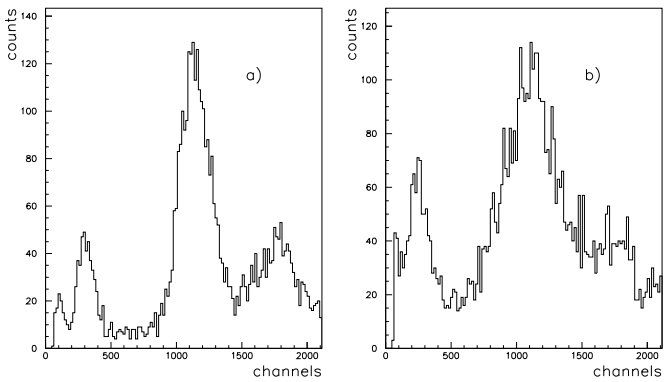

Figure 9: Energy spectra collected by irradiating the $SC136$ proportional counter with the collimated X-ray source located in the middle of the counter (a) and at one of its edges (b).

3.2 Counting of SAGE runs

In November 2003, the SAGE Collaboration, given the availability at Gran Sasso of the GNO counting facility, asked the help of the GNO Collaboration for counting a few solar runs extracted from the SAGE gallium target in Baksan. Between April and September 2004, in coincidence with the ^{37}Ar neutrino source experiment at Baksan, six samples of Ge extracted from part of the SAGE target were sent to Gran Sasso. Germanium was then synthetized in germane, inserted in a proportional counter and counted using the same procedures (x-ray calibrations, test pulses) developed for GNO. Even the subsequent analysis was performed with the GNO techniques (neural selection, Radon cut, etc.). Although the counted samples are real solar runs, and then usable for the SAGE overall analysis, the experiment was aiming to verify the feasibility of the transport, with particular care to possible systematics. It was demonstrated that the time delay between the end of exposure and the start of counting can be as short as 54 hours, to be compared with 34 hours of standard SAGE runs. The main characteristics of the six solar runs are summarized in Tab. 2. For the runs performed in coincidence with the ^{37}Ar experiment, the source contribution to the ^{71}Ge production rate must be subtracted [20]. The preliminary results of the six runs are shown in Tab. 3; they are in good agreement with what expected from solar neutrinos, once taken into account the target mass, the exposure time and the source correction. The effects of cosmogenic activation of the carrier[2] during the transport flight (Mineralnye Vody - Moscow - Rome) turn out to be negligible: the Gran Sasso measurements show that the background level (0.057 counts/run with pulse shape analysis) and the overflow rate do not differ from the typical GNO values, implying that the operations of extraction and transport of germanium from SAGE do not bring radioactive contaminations in the counting gas nor affect the set-up background.

[2]The carrier used in SAGE is ^{nat}Ge and then it contains 21.2% of the stable ^{70}Ge isotope.

Table 2: Summary of the characteristics of the SAGEGNO solar runs counted at Gran Sasso.

Label	Date of extr.	Exposure time (days)	Target mass (tons)	Counter	Target-to-counter yield (%)	Detection/ selection eff. (%)	Source subtraction (SNU)
SR01	22-apr-04	24	48.3	sc136	66	71.3	-
SR02	16-may-04	23	22.3	si106	91	62.6	18.5
SR03	24-jun-04	38	22.0	si108	96	60.9	11.7
SR04	25-jul-04	25	21.9	fc093	100	63.8	5.9
SR05	23-aug-04	29	21.9	fc174	96	62.9	3.4
SR06	25-sep-04	33	42.4	fc126	78	62.7	1.6

Table 3: Preliminary results of the SAGE solar neutrino runs counted at LNGS, corrected for geometrical and source effects. Runs marked with (*) are still counting. Statistical errors only.

Label	Counting time (days)	Number of ^{71}Ge candidates	Bck rate (L+K) (counts/day)	Rate (SNU)	^{71}Ge excess	Residual background
SR01	227	19	0.0649	64^{+46}_{-35}	4.4	14.6
SR02	204	9	0.0267	73^{+67}_{-50}	3.6	5.4
SR03	166	10	0.0386	90^{+77}_{-59}	4.1	5.9
SR04	135(*)	13	0.0841	33^{+75}_{-64}	1.7	11.3
SR05	106(*)	10	0.0456	133^{+75}_{-64}	5.3	4.7
SR06	72(*)	9	0.1257	-12^{+47}_{-31}	0.0	9.0
combined		70	0.0566	59^{+23}_{-21}	19.6	50.4

4 The role of GALLEX and GNO in the solar neutrino research

The results from GALLEX followed by GNO have played a central role both for neutrino physics and astrophysics.

4.1 Particle physics

If the LMA(MSW) oscillation scenario pintpointed by solar experiments and by KamLAND is correct, the basic oscillation mechanism changes at a neutrino energy of about 2 MeV from the MSW matter mechanism (above 2 MeV) to the vacuum oscillation mechanism (below 2 MeV). This transition has not been checked yet in a model-independent way. The gallium result fits very well in the oscillation scenario. If one subtracts the ^{8}B neutrino contribution as measured by SNO [21] from the gallium signal and calculates the suppression factor P with respect to the BP04 SSM [1], the result is $P = 0.556 \pm 0.071$. Assuming vacuum oscillations, P is given by $P = 1 - 0.5 \sin^2(2\theta)$; this yields $\theta = 35.2^{+9.8}_{-5.4}$ degrees. Although such an estimate is quite approximate, it is in good agreement with the latest determination (32.0 ± 1.6 degrees [22]), which essentially comes from ^{8}B neutrinos (i.e. matter effects dominate). Furthermore, in addition to the dominant LMA(MSW) conversion mechanism, the possible existence of a sterile neutrino and/or flavour-changing neutrino matter interactions other than the MSW effect can be investigated using low-energy solar neutrinos [23, 24, 25].

4.2 Astrophysics

In the present experimental scenario, the gallium radiochemical experiments have almost no impact on the determination of the neutrino oscillation parameters. On the astrophysical side the situation is different, because gallium experiments, thanks to the very low energy threshold, are still the only source of experimental information about sub-MeV neutrinos (in particular about the fundamental pp-neutrinos). These experiments can test the consistency of the (electromagnetic) solar luminosity with the observed neutrino fluxes.

It has to be noticed that in the last year the LUNA Collaboration measured the ^{14}N,p cross section down to 70 keV [26]; the direct consequence in the neutrino sector is the 40-50% decrease of the N and O fluxes relatively to the predictions of the BP04 SSM (see the Franec model [27]). Solar neutrino fluxes are constrained by the so called "luminosity constraint"

$$L_{sun} = \sum_i \Phi_i \cdot \alpha_i, \tag{2}$$

where $L_{sun} = 8.53 \cdot 10^{11}$ MeV cm^{-2}s^{-1} is the solar luminosity, and α_i are the energy released in photons per emitted neutrino of type i (pp, ^{7}Be, etc.). This assumes that nuclear fusion reactions are the only energy production mechanism inside the Sun, which is in a quasi-steady state. Apart from this basic assumption, the luminosity contraint

does not depend on the solar model. The fractional CNO luminosity is defined by

$$\frac{L_{CNO}}{L_{sun}} = \frac{\Phi_O \cdot \alpha_O + \Phi_N \cdot \alpha_N}{\sum_i \Phi_i \cdot \alpha_i}. \tag{3}$$

It can be inferred from the measured gallium rate

$$R_{Ga} = N_{target} \cdot \sum_i \int \sigma(E) \cdot \frac{d\Phi_i(E)}{dE} P_{ee}(E) dE, \tag{4}$$

where $\sigma(E)$ is the ν capture cross section on Ga, $\frac{d\Phi_i(E)}{dE}$ is the differential flux of solar neutrinos of species i and $P(E)$ the electron neutrino survival probability. In performing this calculation the following assumptions have been made:

1. the ^{8}B electron neutrino flux is measured with a precision of the order of 12% by SNO [21];

2. the electron neutrino survival probability as a function of energy is determined by mass-driven flavour oscillations and can be calculated from the oscillation parameters presently determined by SNO and Kamland;

3. the ^{7}Be neutrino flux is not directly measured up to now, but is assumed to be equal to te BP04 SSM prediction [1], with an uncertainty of 12%. The ^{7}Be predicted value will hopefully be replaced in the next years by a measured number, provided by Borexino or Kamland;

4. the neutrino capture cross section on ^{71}Ga is theoretically calculated [28];

5. the neutrino flux ratios pep/pp and ^{13}N/^{15}O are fixed from nuclear physics and kinematics with negligible uncertainties.

With the assumpion above listed and taking into account the present uncertainties, we can extract from the gallium capture rate measured by GALLEX/GNO the following constraint on the CNO solar luminosity:

$$\frac{L_{CNO}}{L_{sun}} < 6.5\% \ (3\sigma).$$

The result for the CNO luminosity taking into account the gallium rate measured by GALLEX and GNO is graphically shown in Figure 10; it is in good agreement with the prediction of the BP04 solar models $L_{CNO} = 1.6 \pm 0.6\%$ ($L_{CNO} = 0.8\%$ in the Franec SSM). It has to be stressed again that in order to obtain the results above we assumed that the ^{7}Be neutrino flux is known with a 12% uncertainty. Presently this flux is not experimentally measured but calculated by SSM, and the limits above can be considered as an important self-consistency test of the SSM, the oscillation scenario, and the gallium data. In the future, when a direct determination of the ^{7}Be neutrino flux becomes available, the Ga rate will become a direct experimental determination of the *pp* (and CNO) luminosity in neutrinos [29].

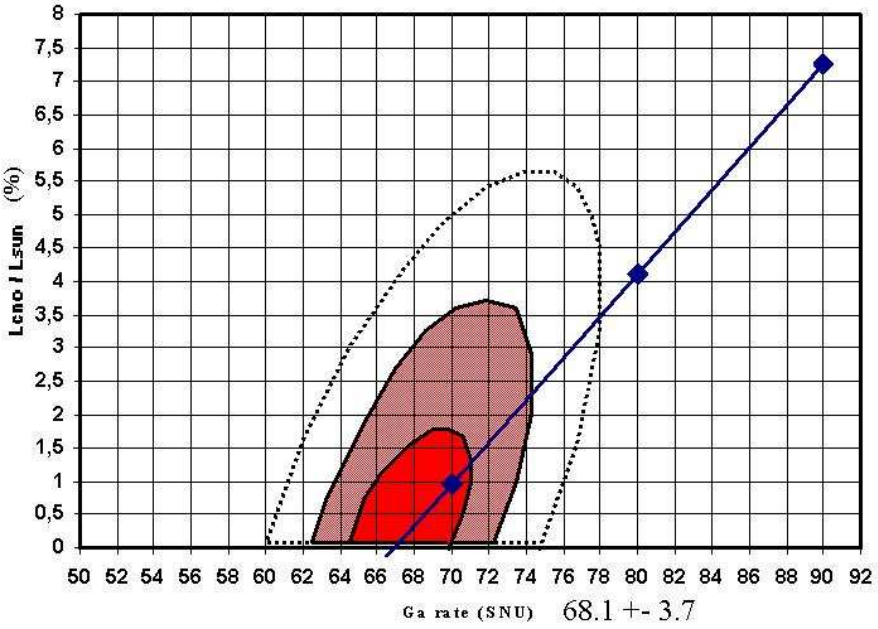

Figure 10: Scatter plot of the fraction CNO solar luminosity (%) vs. gallium rate, evaluated as described in the text. The countours represent respectively the 1σ, 2σ and 3σ limits allowed by the GALLEX/GNO experimental results. The luminosity contraint is graphically represented by the straight line.

5 Conclusions

The data taking of the GNO experiment has been terminated in 2003; the gallium chloride target has been removed from the hall A of the underground laboratory in December 2004. During 2004 the activity was focused on data analysis and interpretation, including the search for time modulation. Moreover, ancillary experimental measurements were carried on for the characterization of proportional counters (z-scanning). In the second part of 2004, six solar extractions from the SAGE solar neutrino experiment were succesfully counted in the GNO facility at Gran Sasso.

6 List of Publications

1. GNO collaboration, "GNO progress report for 2003", LNGS annual Report 2003, LNGS/EXP-01/04 (2004)

2. L. Pandola *et al.*, *Neural network analysis for proportional counters events*, Nucl. Instr. Meth. A **522** (2004), 521

3. L. Pandola, *Search for time modulations in the Gallex/GNO solar neutrino data*, Astrop. Phys. **22** (2004) 219

4. P. Belli et al., *Response of low-noise miniaturized proportional counters in the keV region*, in press on Nucl. Instr. Meth. A, preprint LNGS/EXP−08/04

5. GNO Collaboration, M. Altmann et al., *Complete results for five years of GNO solar neutrino observations*, submitted to Phys. Lett. B

6. N. Ferrari et al., *The GNO experiment*, Nucl. Phys. B (Proc. Suppl.) **143 C** (2005) 561, in press

7. C.M. Cattadori et al., *Results from radiochemical experiments, with main emphasis on the gallium ones*, Nucl. Phys. B (Proc. Suppl.) **143 C** (2005) 3, in press

7 List of Conference Presentations

1. C.M. Cattadori, *Results from radiochemical experiments, with main emphasis on the gallium ones*, XXI International Conference on Neutrino Physics and Astrophysics, Paris (2004)

8 Theses

1. L. Pandola, *Measurement of the solar neutrino interaction rate on ^{71}Ga with the radiochemical experiment GNO at Laboratori Nazionali del Gran Sasso*, Ph. D. Thesis, Università degli Studi dell'Aquila.

References

[1] J.N. Bahcall and M.H. Pinsonneault, Phys. Rev. Lett. 92 (2004) 121301; J.N. Bahcall et al., Astroph. J. 555 (2001) 990

[2] E.Henrich, K.H.Ebert, Angew. Chemie Int. Ed. (Engl.) 31 (1992) 1283; E.Henrich et al., "GALLEX, a challenge for chemistry", Proc. IV Int'l. Solar Neutrino Conf., ed. W.Hampel, MPI Kernph., Heidelberg (1997) 151-162.

[3] R. Wink et al. Nucl. Inst. and Meth. A329 (1993) 541.

[4] L. Pandola *at al.*, Nucl. Instr. Meth. A 522 (2004), 521

[5] GALLEX collaboration, Phys.Lett. B285 (1992) 376; Phys.Lett. B314 (1993) 445; Phys.Lett. B327 (1994) 377; Phys.Lett. B342 (1995) 440; Phys.Lett. B357 (1995) 237; Phys.Lett. B388 (1996) 384, Phys.Lett. B447 (1999) 127.

[6] E.Bellotti et al., GNO collaboration, LNGS report INFN/AE-96-27.

[7] GNO collaboration, M. Altmann *et al.*, "GNO solar neutrino observations: results for GNO I", Phys.Lett.B 490(2000), 16;

[8] GNO Collaboration, M. Altmann *et al.*, submitted to Phys. Lett. B (2005)

[9] GNO collaboration, LNGS annual report 1998, pag. 55-69.

[10] GNO collaboration, LNGS annual report 1999, pag. 57-68.

[11] GNO collaboration, LNGS annual report 2000, pag. 57-68.

[12] GNO collaboration, LNGS annual report 2001, pag. 79-94.

[13] GNO collaboration, LNGS annual report 2002, pag. 57-76.

[14] GNO collaboration, LNGS annual report 2003, pag. 79-99.

[15] SAGE Collaboration, J.N. Abdurashitov *et al.*, Poster at XXI International Conference on Neutrino Physics and Astrophysics, Paris (2004), to be published on Nucl. Phys. B (Proc. Suppl.)

[16] P.A. Sturrock and M.A. Weber, Astroph. J. 565 (2002), 1366

[17] D.O. Caldwell and P.A. Sturrock, Nucl. Phys. B (Proc. Suppl.) 124 (2003), 239

[18] L. Pandola, Astropart. Phys. 22 (2004) 219

[19] B.T. Cleveland, Nucl. Instr. Meth. 214 (1983), 453

[20] F. Kaether, *The SAGE source experiment - influence on solar runs*, GNO internal note (2004), unpublished; B.T. Cleveland, *Contribution of the ^{37}Ar source to the SAGE@GNO runs*, internal note (2005), unpublished

[21] SNO collaboration, Phys.Rev.Lett. 87 (2001) 071301; Phys.Rev.Lett. 89 (2002) 011302; Phys. Rev. Lett. 92 (2004) 181301

[22] J. Bahcall and C. Peña-Garay, New J. Phys. 6 (2004) 63

[23] M. Cirelli *et al.* Nucl. Phys. B 708 (2005) 215

[24] P. de Holanda and A. Smirnov, Phys. Rev. D 69 (2004) 113002

[25] A. Friedland *et al.*, Phys. Lett. B 594 (2004) 347

[26] LUNA collaboration, nucl-ex/0312015.

[27] S. Degl'Innocenti et al., Phys. Lett. B 590 (2004) 13

[28] J.N.Bahcall, Phys.Rev.C56 (1997) 3391.

[29] J.N. Bahcall, C. Pena-Garay, JHEP 0311 (2003) 004

ICARUS T600: landing at GranSasso Laboratory

S. Amerio[a], S. Amoruso[b], M. Antonello[c], P. Aprili[d], M. Armenante[b], F. Arneodo[d], A. Badertscher[e], B. Baiboussinov[a], M. Baldo Ceolin[a], G. Battistoni[f], B. Bekman[g], P. Benetti[h], M. Bischofberger[e], A. Borio di Tigliole[h], R. Brunetti[h], R. Bruzzese[b], A. Bueno[e,i], E. Calligarich[h], F. Carbonara[b], D. Cavalli[f], F. Cavanna[c], P. Cennini[j], S. Centro[a], A. Cesana[k,f], C. Chen[l], D. Chen[l], D.B. Chen[a], Y. Chen[l], R. Cid[i], D.B. Cline[m], K. Cieślik[n], A.G. Cocco[b], D. Corti[a], Z. Dai[e], C. De Vecchi[h], A. Dąbrowska[n], A. Di Cicco[b], R. Dolfini[h], A. Ereditato[b], A. Ferella[c], A. Ferrari[j,f], F. Ferri[c], G. Fiorillo[b], S. Galli[c], D. Garcia Gamez[i], Y. Ge[e], D. Gibin[a], A. Gigli Berzolari[h], I. Gil-Botella[e], K. Graczyk[o], L. Grandi[h], A. Guglielmi[a], K. He[l], J. Holeczek[g], X. Huang[l], C. Juszczak[o], D. Kiełczewska[p,q], J. Kisiel[g], T. Kozłowski[p], H. Kuna-Ciskal[r], M. Laffranchi[e], J. Łagoda[q], Z. Li[l], B. Lisowski[m], F. Lu[l], J. Ma[l], G. Mangano[b], G. Mannocchi[s,t], M. Markiewicz[n], A. Martinez de la Ossa[i], C. Matthey[m], F. Mauri[h], A.J. Melgarejo[i], A. Menegolli[h], G. Meng[a], M. Messina[e], J.W. Mietelski[n], C. Montanari[h], S. Muraro[f], S. Navas-Concha[e,i], M. Nicoletto[a], J. Nowak[o], C. Osuna[i], S. Otwinowski[m], Q. Ouyang[l], O. Palamara[d], D. Pascoli[a], L. Periale[s,t], G. Piano Mortari[c], A. Piazzoli[h], P. Picchi[u,t,s], F. Pietropaolo[a], W. Półchłopek[v], M. Prata[h], T. Rancati[f], A. Rappoldi[h], G.L. Raselli[h], E. Rondio[p], M. Rossella[h], A. Rubbia[e], C. Rubbia[h], P. Sala[f], R. Santorelli[b], D. Scannicchio[h], E. Segreto[c], Y. Seo[m], F. Sergiampietri[m,w], J. Sobczyk[o], N. Spinelli[b], J. Stepaniak[p], R. Sulej[x], M. Szeptycka[p], M. Szarska[n], M. Terrani[k,f], G. Trinchero[s,t], R. Velotta[b], S. Ventura[a], C. Vignoli[h], H. Wang[m], X. Wang[b], J. Woo[m], G. Xu[l], Z. Xu[l], X. Yang[m], A. Zalewska[n], J. Zalipska[p], C. Zhang[l], Q. Zhang[l], S. Zhen[l], W. Zipper[g]

[a] *Università di Padova e INFN, Padova, Italy*

[b] *Università Federico II di Napoli e INFN, Napoli, Italy*

[c] *Università dell'Aquila e INFN, L'Aquila, Italy*

[d] *INFN - Laboratori Nazionali del Gran Sasso, Assergi, Italy*

[e] *Institute for Particle Physics, ETH Hönggerberg, Zürich, Switzerland*

[f] *Università di Milano e INFN, Milano, Italy*

[g] *Institute of Physics, University of Silesia, Katowice, Poland*

[h] *Università di Pavia e INFN, Pavia, Italy*

[i] *Dpto de Física Teórica y del Cosmos & C.A.F.P.E., Universidad de Granada, Granada, Spain*

[j] *CERN, Geneva, Switzerland*

[k] *Politecnico di Milano (CESNEF), Milano, Italy*

[l] *IHEP - Academia Sinica, Beijing, People's Republic of China*

[m] *Department of Physics, UCLA, Los Angeles, USA*

[n] *H.Niewodniczański Institute of Nuclear Physics, Kraków, Poland*

[o] *Institute of Theoretical Physics, Wrocław University, Wrocław, Poland*

[p] *A.Soltan Institute for Nuclear Studies, Warszawa, Poland*

[q] *Institute of Experimental Physics, Warsaw University, Warszawa, Poland*

[r] *Institute of Mechanics and Machine Design, Cracow University of Technology, Kraków, Poland*

[s] *IFSI, Torino, Italy*

[t] *INFN Laboratori Nazionali di Frascati, Frascati, Italy*

[u] *Università di Torino, Torino, Italy*

[v] *University of Mining and Metallurgy, Kraków, Poland*

[w] *INFN, Pisa, Italy*

[x] *Warsaw University of Technology, Warszawa, Poland*

Abstract

The ICARUS T600 detector is the largest liquid Argon TPC ever built, with a size of about 500 tons of fully imaging mass. The design and assembly of the detector relied on industrial support and represents the applications of concepts matured in laboratory tests to the kton scale.

The detector was developed to act as an observatory for astroparticle and neutrino physics at the Gran Sasso Underground Laboratory and a second generation nucleon decay experiment.

The ICARUS T600 was commissioned in 2001 for a technical run performed at surface in the Pavia INFN site. During this period all the detector features were extensively tested with an exposure to cosmic–rays. During 2004 the detector was moved from Pavia to the LNGS underground site. In this report a description of the ICARUS T600 is first given, followed by short description of the transportation operation.

1 Introduction

The technology of the Liquid Argon Time Projection Chamber (LAr TPC), first proposed by C. Rubbia in 1977 [1], was conceived as a tool for a completely uniform imaging with high accuracy of massive volumes. The operational principle of the LAr TPC is based on the fact that in highly purified LAr ionization tracks can be transported practically undistorted by a uniform electric field over macroscopic distances. Imaging is provided by a suitable set of electrodes (wires) placed at the end of the drift path continuously sensing and recording the signals induced by the drifting electrons.

Non–destructive read–out of ionization electrons by charge induction allows to detect the signal of electrons crossing subsequent wire planes with different orientation. This provides several projective views of the same event, hence allowing space point reconstruction and precise calorimetric measurement.

The LAr TPC was developed in the context of the ICARUS programme and currently finds its application in studies concerning some of the major issues of particle and astroparticle physics:

- the study of solar and atmospheric neutrino interactions;
- the study of nucleon decay for some channels predicted by GUTs;
- the detection of neutrinos following a Supernova explosion;
- the study of neutrino oscillations with beams from particle accelerators.

After the original proposal, the feasibility of the technology has been first demonstrated by an extensive R&D programme, which included ten years of studies on small LAr volumes and five years of studies with several prototypes of increasing mass[2, 3, 4, 5, 6, 7, 8, 9, 10, 11, 12, 13, 14, 15, 16].

The second step was represented by the construction of the T600 module[17]: a detector employing about 600 tons of liquid Argon to be operated at LNGS. This step–wise strategy allowed to progressively develop the necessary know–how to build a multi–kton liquid Argon detector.

The realization of the T600 detector (from design to construction) lasted about four years and culminated with the full test of the experimental set–up, carried out at surface during 2001. This test demonstrated the maturity of the project. All technical aspects of the system, namely cryogenics, LAr purification, read–out chambers, detection of LAr scintillation light, electronics and DAQ had been tested and performed as expected. Statistically significant samples of cosmic–ray events (long muon tracks, spectacular high–multiplicity muon bundles, electromagnetic and hadronic showers, low energy events) were recorded. The subsequent analysis of these events, carried out in 2002-03, has allowed the development and fine tuning of the off–line tools for the event reconstruction and the extraction of physical quantities. It has also demonstrated the performance of the detector in a quantitative way, issuing in a number of papers published in 2003:

- Analysis of the liquid Argon purity in the T600 detector [18];
- Observation of very long ionizing tracks [19];
- Measurement of the muon decay spectrum [20];
- Study of ionization quenching in liquid Argon [21];

A detailed description of the T600 detector and of its technical performance as obtained from the acceptance tests has been reported on a dedicated milestone paper [22]: *"Design, construction and tests of the ICARUS T600 detector"*, published by the ICARUS Collaboration on N.I.M. A 527 (2004), p. 329.

In agreement with the indications from LNGS the T600 detector has been moved from Pavia to the LNGS underground site (Hall B) during December 2004 with a special transportation. This delicate operation was successfully accomplished by a common effort of the Icarus Collaboration and of the LNGS technical staff.

2 Detector overview

Extracted from "Design, construction and tests of the ICARUS T600 detector", ICARUS Collaboration, N.I.M. A 527 (2004), p. 329.

ICARUS T600 (Fig. 1) is composed of a large cryostat split into two identical, adjacent half–modules, each one with internal dimensions of 3.6 m (width) × 3.9 m (height) × 19.6 m (length). Each half–module houses an inner detector made of two Time Projection Chambers, the field shaping system, monitors and probes, and of a system for the LAr scintillation light detection. The half–modules are externally surrounded by thermal insulation layers. In the following, we shall refer to each half–module as "T300". The full scale test reported was carried on after the commissioning of one T300.

Dimensions and shape of the cryostat were defined by the requirement that the LAr containers (cold vessels) had to be transported through the Italian highways into the underground Gran Sasso Laboratory and installed there. In order to collect significant samples of solar and atmospheric neutrino events, the ICARUS Collaboration adopted a solution with two coupled containers with dimensions corresponding to a total LAr volume of about 550 m^3.

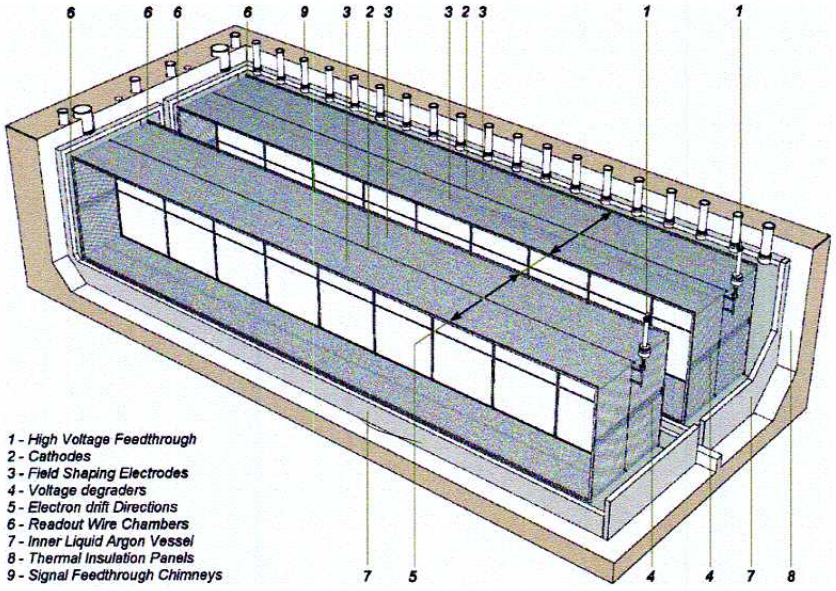

Figure 1: Artist cutaway view of the ICARUS T600 detector.

Outside the detector are located the read–out electronics, on the top side of the cryostat, and the cryogenic plant composed of a liquid Nitrogen (LN_2) cooling circuit and of a system of purifiers needed to achieve the required LAr purity.

The inner detector structure of each T300 consists of two TPCs (called *left* and *right* chambers) separated by a common cathode. Each TPC is made of three parallel wire–planes, 3 mm apart, oriented at 60 degrees with respect to each other, with a wire pitch of 3 mm, as shown in Fig. 2. The three wire planes of each TPC are held by a sustaining frame (see Fig. 3) positioned onto the longest walls of the half–module. The total number of wires in the T600 detector is 53248. The read–out of the signals induced on the TPC wires by the electron drift allows a full three–dimensional (3D) image reconstruction of the event topology.

A uniform electric field perpendicular to the wires is established in the LAr volume of each half–module by means of a high voltage (HV) system, as required to allow and guide the drift of the ionization electrons. The system is composed of a cathode plane, parallel to the wire planes, placed in the center of the LAr volume of each half–module at a distance of about 1.5 m from the wires of each side. This distance defines the maximum drift path (see Fig. 3). The HV system is completed by field shaping electrodes to guarantee the uniformity of the field along the drift direction, and by a HV feedthrough to set the required voltage on the cathode. At the nominal voltage of 75 kV, corresponding to an electric field of 500 V/cm, the maximum drift time in LAr is about 1 ms.

The top side of the cryostat hosts the exit flanges equipped with cryogenic feedthroughs for the electrical connection of the wires with the read–out electronics, and for all the internal instrumentation (PMTs, LAr purity monitors, level and temperature probes, etc.).

The electronic chain is designed to allow for continuous read–out, digitization (with a sampling time of 0.4 μs) and wave–form recording of the signals from each wire of the TPC. It is composed of three basic units, see Fig. 4, serving 32 channels:

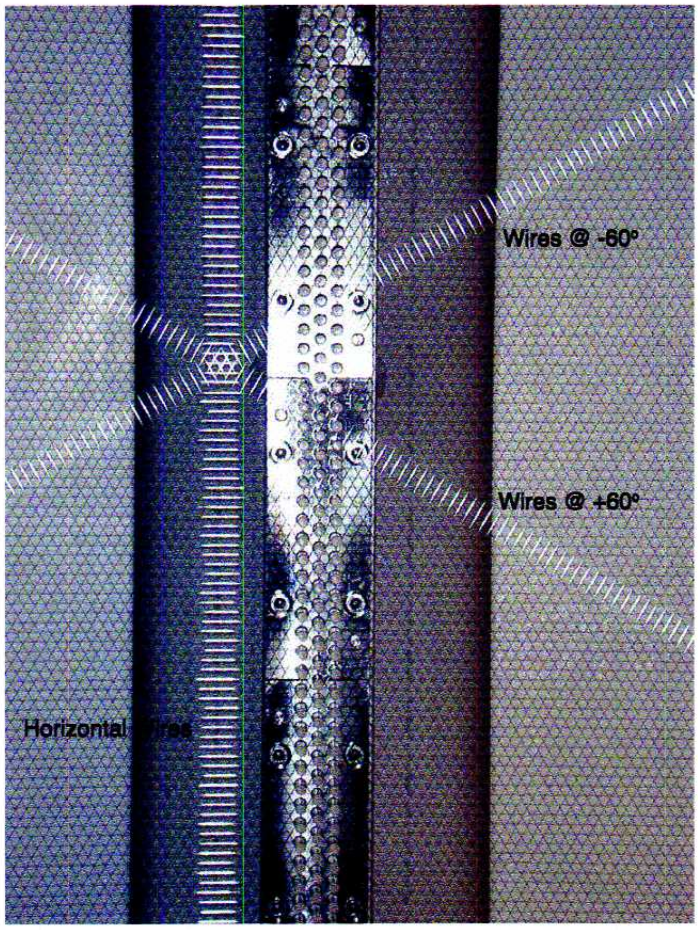

Figure 2: Picture of the three wire planes of a TPC installed in the T600 detector.

1. the decoupling board receives analog signals from the TPC wires via vacuum tight feedthrough flanges and passes them to the analog board. It also provides biasing of the wires and distribution of calibration signals;

2. the analog board houses the signal amplifiers, performs 16:1 multiplexing and the data conversion (10 bit) at a 40 MHz rate;

3. the digital board uses custom programmable chips (two per board) specially developed for ICARUS, called DAEDALUS, that implement a hit finding algorithm. Each board receives the multiplexed digital data via an external serial–link cable.

Ionization in LAr is accompanied by scintillation light emission. Detection of this light can provide an effective method for absolute time measurement of the event, as well as an internal trigger signal. A system to detect this LAr scintillation light has been implemented based on large–surface (8") PMTs directly immersed in the LAr, see Fig. 5.

The spatial reconstruction of ionizing tracks inside the LAr volume is performed by the simultaneous exploitation of the charge and of the light release following the energy loss processes of charged particles which cross the detector:

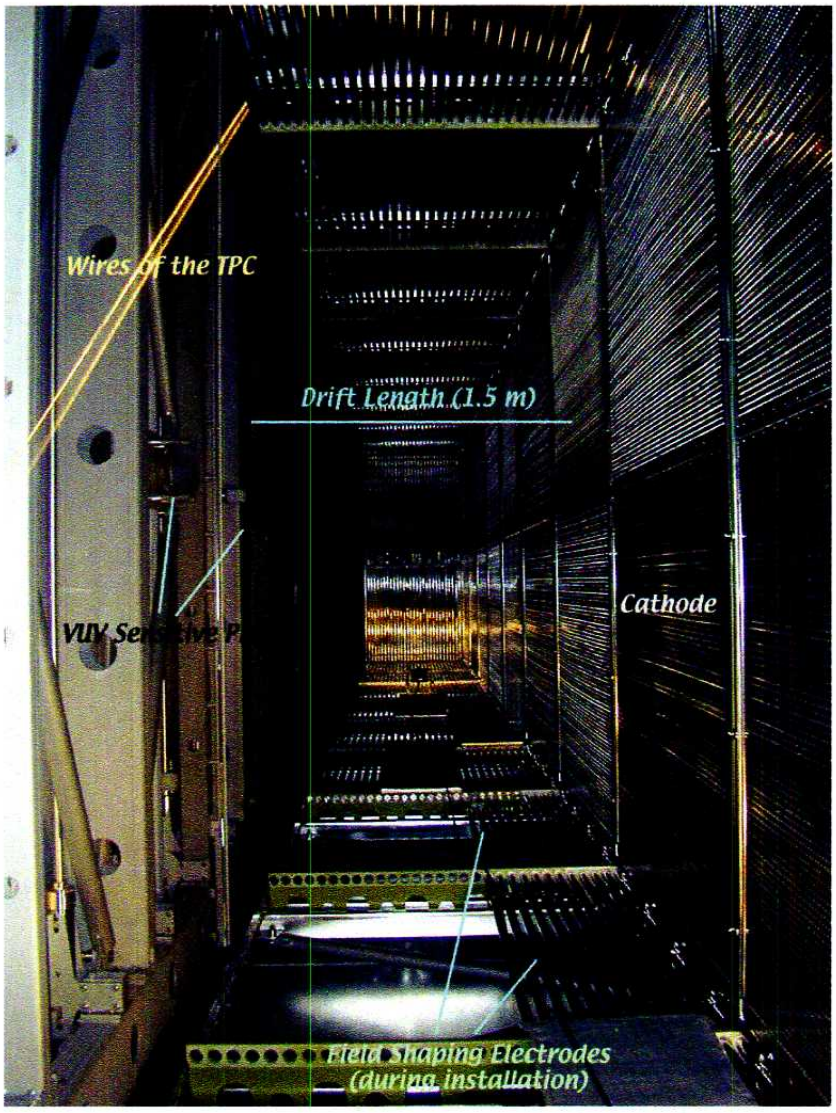

Figure 3: Picture of the inner detector layout inside the first half–module: the cathode (vertical plane on the right) divides the volume in two symmetric sectors (*chambers*). The picture refers to the left sector where wires and mechanical structure of the TPC and some photo–multipliers (PMTs) are visible.

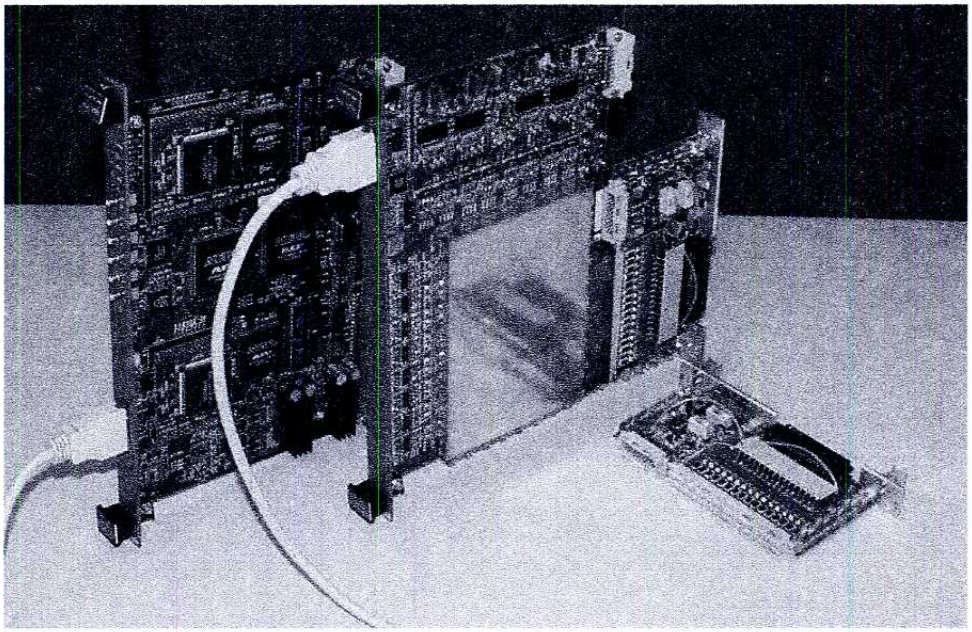

Figure 4: The three basic electronics modules: the small decoupling board (DB) that receives 32 analog signals from the chamber via the feedthrough and passes them to the analog board; the analog board (V791 by CAEN) that houses the amplifiers for 32 channels; the digital board (V789 by CAEN) Arianna that has the two DAEDALUS VLSI, mounted on small piggy back PCBs.

1. electrons from ionization induce detectable signals on the TPC wires during their drift motion towards and across the wire planes (wire coordinate);

2. UV photons from scintillation provide a prompt signal on the PMTs that allows the measurement of the absolute drift time and, hence, of the distance traveled by the drifting electrons (drift coordinate).

In this way, each of the planes of the TPC provides a two–dimensional projection of the event image, with one coordinate given by the wire position and the other by the drift distance. The Collection view of a spectacular cosmic–ray event composed of many parallel tracks is displayed in Fig. 2. The event extends up to the full length (about 18 m) and drift (1.5 m) of the detector, as shown in the upper image. The zoomed regions show several electromagnetic and hadronic showers, muon tracks and low energy electrons from γ-conversion.

The various projections have a common coordinate (the drift distance). A full 3D reconstruction of the event is obtained by correlating the signals from two different planes at the same drift distance.

The calorimetric measurement of the energy deposited by the ionizing particle in the LAr volume is obtained by collecting information from the last of the three wire planes, working in charge collection mode.

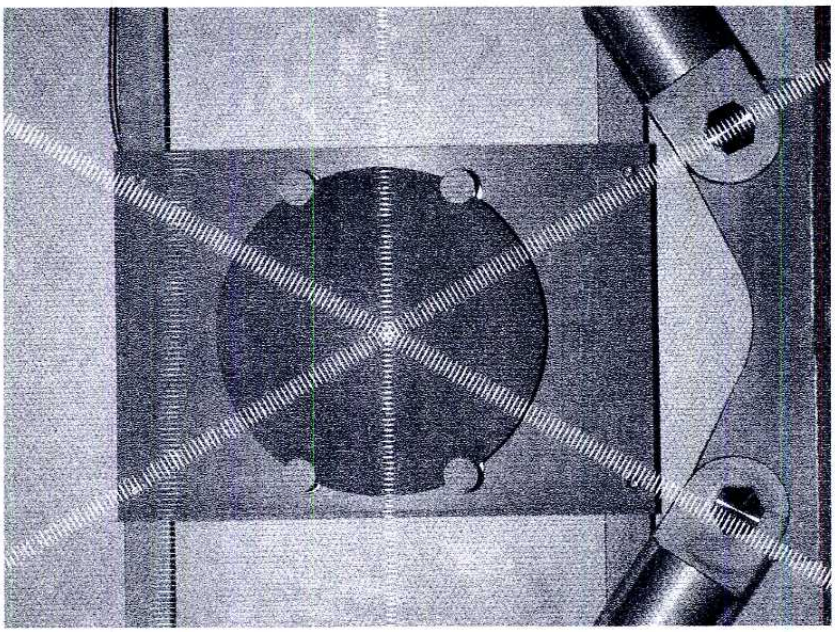

Figure 5: Picture one of the PMTs visible behind the three wire planes.

3 Transportation to LNGS

On September 12th 2004, the LNGS management, considering the current development of the civil works in the underground laboratory by "Protezione Civile" and in agreement with the INFN authorities, indicated to the Icarus Collaboration the period from November 29th to December 19th 2004 as a possible first time window for the transportation of the two T300 half-modules to LNGS.

Following this indication the Collaboration immediately activated the transportation procedure already defined with a specialized company (Fumagalli Trasporti). This operation consists in a number of subsequent steps:

- preparation of the special convoy with the first T300 module at the Pavia INFN site.
- transportation on route (about 600 km) from Pavia to Assergi (from A14 highway - Teramo side).
- entry in LNGS underground site.
- positioning in Hall B
- same sequence of operations for the second T300 module.

In Fig. 7 a schematic view of the special convoy for the T300 modules is shown.

All the steps for the entry procedure at LNGS and for the positioning in Hall B have

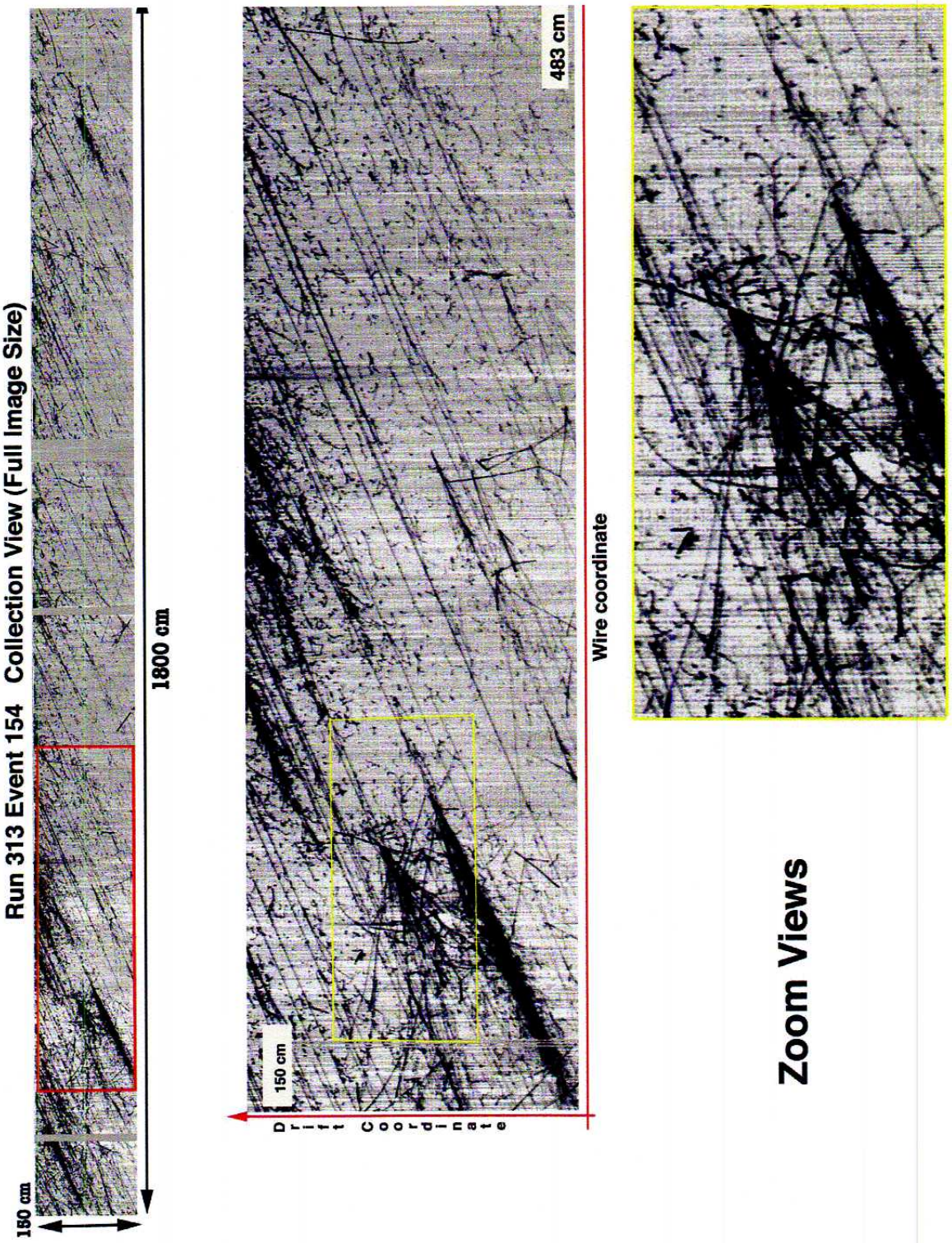

Figure 6: Run 313, Event 154, Collection view. Extensive air shower.

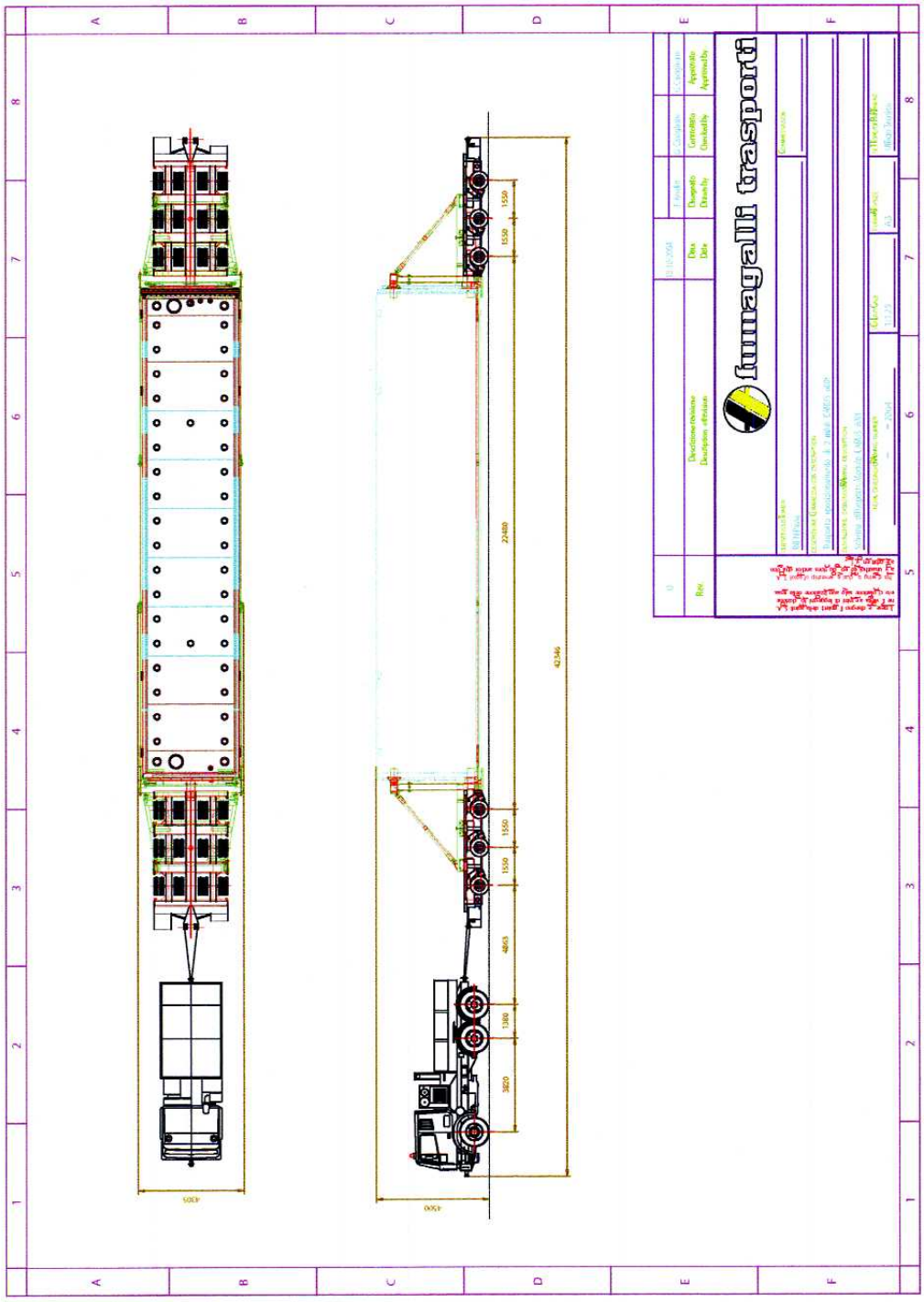

Figure 7: Schematic view of the special convoy for the transportation of the ICARUS T300 modules.

been carefully analyzed and simulated, taking into account the real dimensions of the pathway from the highway tunnel to the experimental site, as reported in Fig. 8 and Fig. 9.

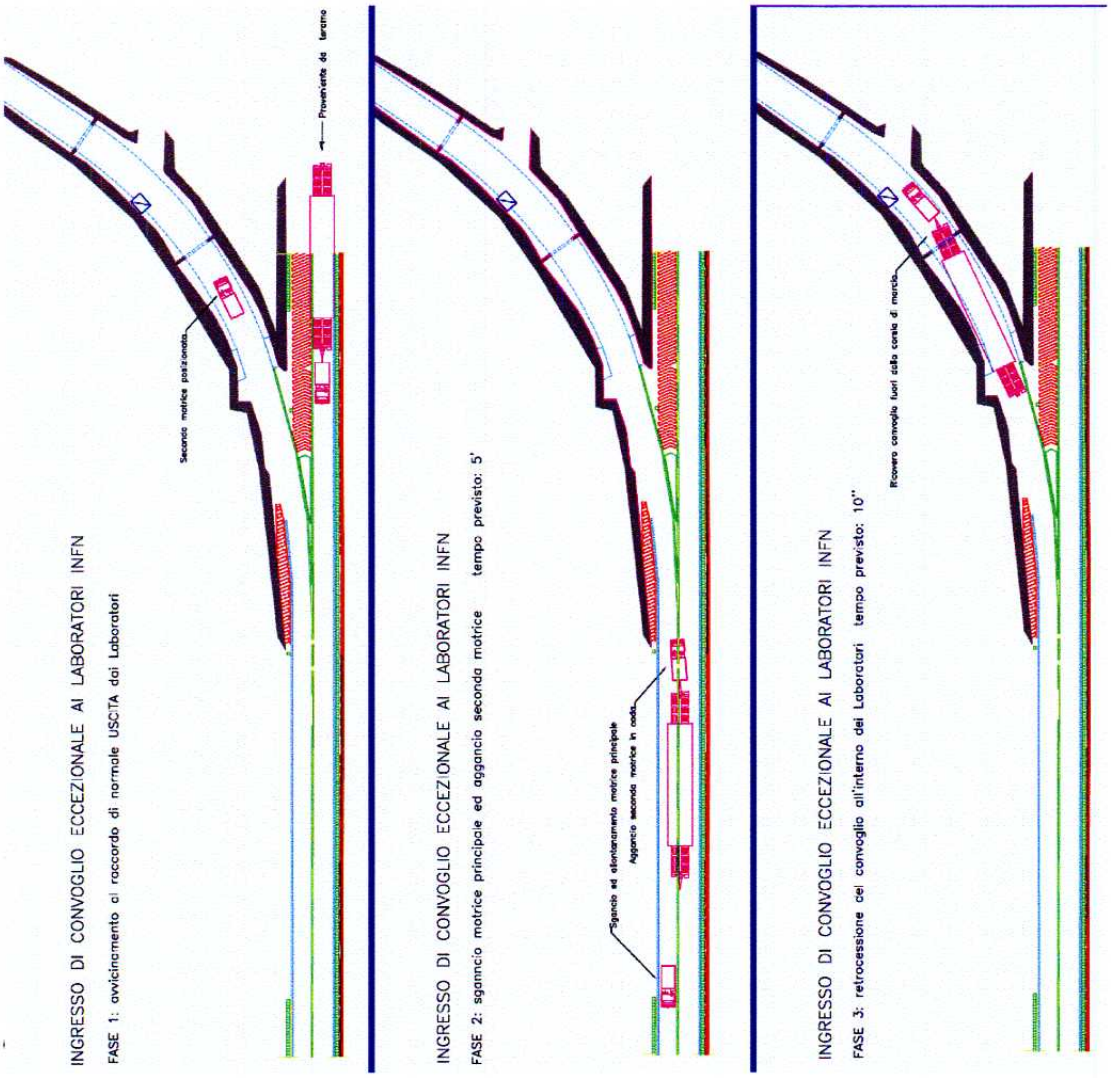

Figure 8: Schematic view of the entry procedure of the ICARUS T300 modules at LNGS.

The transportation procedure, according to the program described above, started on November 28th. The subsequent steps strictly followed the agreed time schedule here reported:

- *November 28th, 2004* - Departure of the first T300 module from the Pavia INFN experimental site, Fig. 11.
- *December 3rd, 2004* - Arrival of the first T300 module at the GranSasso underground lab, positioning at the entrance of Hall B, Fig. 11..

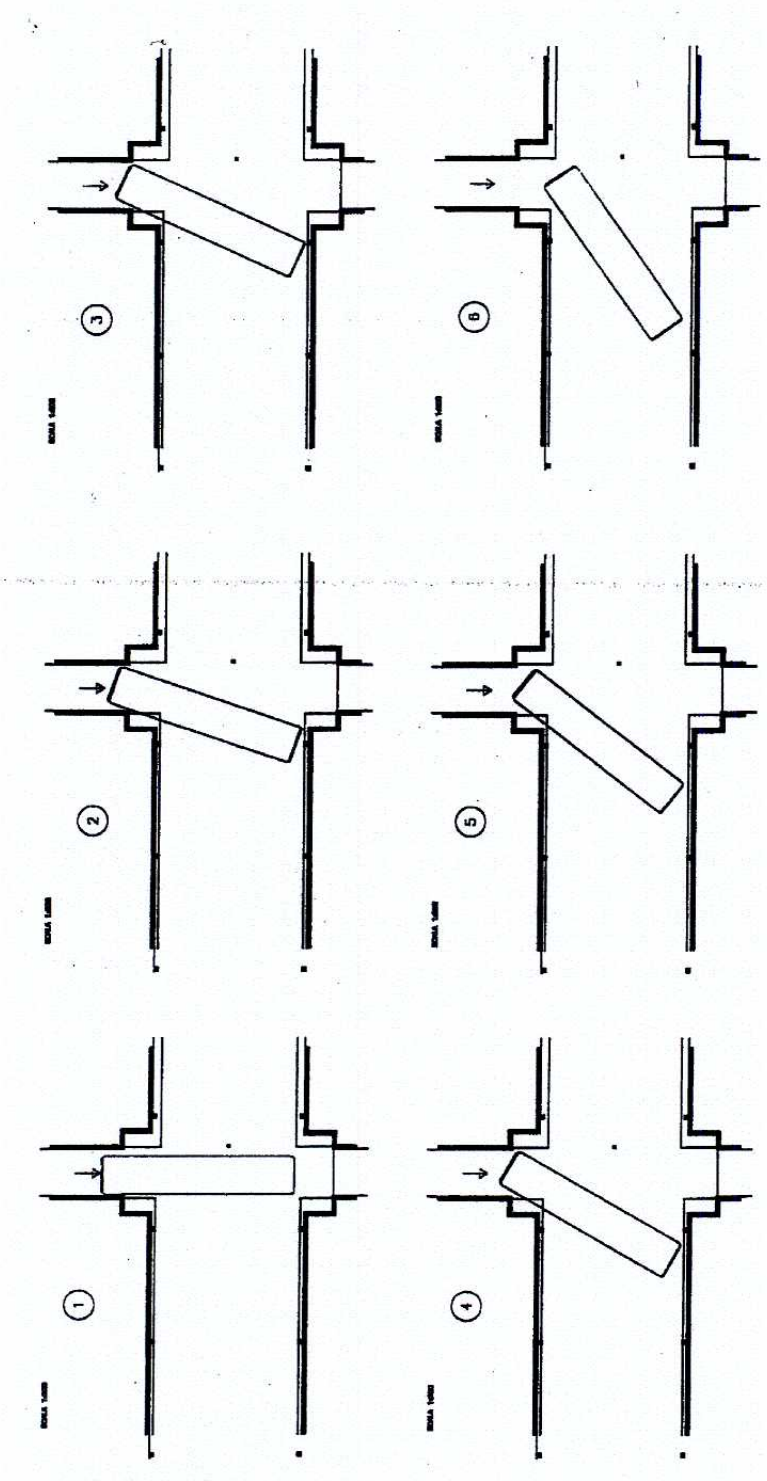

Figure 9: Schematic view of the entry procedure of the ICARUS T300 modules in Hall B.

- *December 4th, 2004* - Rotation of the first T300 module along the Hall B main axis and positioning in a defined temporary location (preliminary parking position).
- *December 14th, 2004* - Departure of the second T300 module from the Pavia INFN experimental site.
- *December 17, 2004* - Arrival of the second T300 module at the GranSasso underground lab, positioning at the entrance of Hall B.
- *December 18th, 2004* - Rotation of the second T300 module along the Hall B main axis and positioning in a defined temporary location (preliminary parking position).

The preliminary parking position for the two T300 modules is located a few meters upstream the T1200 area in preparation, see Fig. 10. In Fig. 13 the two T300 modules positioned in their preliminary parking position is shown, as at the conclusion of the transportation procedure on December 18th, 2004.

Finally, it has been agreed to move (on January 17th to 19th 2005) the two T300 modules from the preliminary parking position to the actual parking position (at the edge of the T1200 area) indicated in Fig. 10.

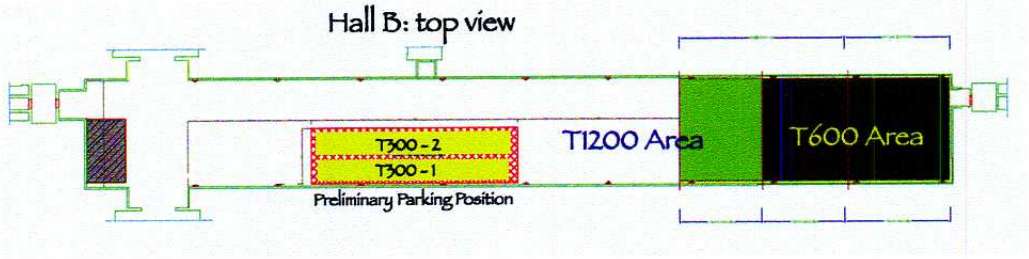

Figure 10: Top view of the LNGS Hall B with indication of the preliminary parking position, dashed area, where the two T300 module have been temporary located at the end of the transportation procedure.

4 Conclusions

We have presented a brief description of the ICARUS T600 detector, a large–mass Liquid Argon TPC meant as the basic unit for a multi-kton astroparticle observatory and neutrino detector to be installed in the underground Gran Sasso Laboratory.

An extended technical run with the T600 detector has been performed at surface in the Pavia INFN site during 2001. The design, the description of the basic components, assembly, start–up and test-run procedures of the detector have been recently published, as well as the demonstration of the off–line event reconstruction capabilities. The detector space and energy resolution, particle identification and full events reconstruction have been also the subjects of several analyses published during the last two years.

The main conclusion from the test is that the measurements and the experimental results demonstrate that it is feasible to master all technical issues related to the construction and operation of a large size LAr TPC, within and sometimes beyond the design specifications.

The major event during 2004 was the successful transportation of the T600 detector from Pavia to the INFN Gran Sasso Underground Laboratory. This delicate operation required the definition of a dedicated procedure and a careful organization of the many related logistic aspects both at Pavia and at LNGS.

The installation of the ancillary infrastructures in the LNGS Hall B is presently under way. The re-assembly of the detector components will be the main goal of the activity during 2005.

References

[1] C. Rubbia, *The Liquid-Argon Time Projection Chamber: A New Concept For Neutrino Detector*, CERN–EP/77–08, (1977).

[2] P. Benetti *et al.* [ICARUS Collaboration], *A 3 Ton Liquid Argon Time Projection Chamber*, Nucl. Instrum. Meth. A **332**, (1993) 395.

[3] P. Cennini *et al.* [ICARUS Collaboration], *Performance Of A 3 Ton Liquid Argon Time Projection Chamber*, Nucl. Instrum. Meth. A **345**, (1994) 230.

[4] F. Arneodo *et al.* [ICARUS Collaboration], *The ICARUS 50 l LAr TPC in the CERN neutrino beam*, arXiv:hep-ex/9812006.

[5] F. Arneodo *et al.* [ICARUS Collaboration], *First Observation Of 140-Cm Drift Ionizing Tracks In The Icarus Liquid-Argon Tpc*, Nucl. Instrum. Meth. A **449**, (2000) 36.

[6] F. Arneodo *et al.* [ICARUS Collaboration], *Determination Of Through-Going Tracks' Direction By Means Of Delta-Rays In The Icarus Liquid Argon Time Projection Chamber*, Nucl. Instrum. Meth. A **449**, (2000) 42.

[7] P. Cennini *et al.* [ICARUS Collaboration], *Detection Of Scintillation Light In Coincidence With Ionizing Tracks In A Liquid Argon Time Projection Chamber*, Nucl. Instrum. Meth. A **432**, (1999) 240.

[8] F. Arneodo *et al.* [ICARUS Collaboration], *Performance Evaluation Of A Hit Finding Algorithm For The Icarus Detector*, Nucl. Instrum. Meth. A **412**, (1998) 440.

[9] P. Cennini *et al.* [ICARUS Collaboration], *A Neural Network Approach For The Tpc Signal Processing*, Nucl. Instrum. Meth. A **356**, (1995) 507.

[10] P. Cennini *et al.* [ICARUS Collaboration], *Improving The Performance Of The Liquid Argon Tpc By Doping With Tetramethyl Germanium*, Nucl. Instrum. Meth. A **355**, (1995) 660.

[11] P. Benetti *et al.* [ICARUS Collaboration], *A 3D Image Chamber For The Lar Tpc On Multilayer Printed Circuit Board*, Nucl. Instrum. Meth. A **346**, (1994) 550.

[12] P. Benetti *et al.* [ICARUS Collaboration], *Argon Purification In The Liquid Phase*, Nucl. Instrum. Meth. A **333**, (1993) 567.

[13] A. Bettini *et al.* [ICARUS Collaboration], *A Study Of The Factors Affecting The Electron Lifetime In Ultrapure Liquid Argon*, Nucl. Instrum. Meth. A **305**, (1991) 177.

[14] S. Bonetti *et al.* [ICARUS Collaboration], *A Study Of The Electron Image Due To Ionizing Events In A Two-Dimensional Liquid Argon Tpc With A 24-Cm Drift Gap*, Nucl. Instrum. Meth. A **286**, (1990) 135.

[15] F. Arneodo *et al.* [ICARUS Collaboration], *Performance Of The 10 m^3 Icarus Liquid Argon Prototype*, Nucl. Instrum. Meth. A **498**, (2003) 293.

[16] F. Arneodo *et al.* [ICARUS Collaboration], *Detection Of Cerenkov Light Emission In Liquid Argon*, Nucl. Instrum. Meth. A **516** (2004), 348.

[17] ICARUS Collaboration, *A First 600 Ton ICARUS Detector Installed At The Gran Sasso Laboratory*, Addendum to Proposal by the ICARUS Collaboration, LNGS–95/10, (1995).

[18] S. Amoruso *et al.* [ICARUS Collaboration], *Analysis Of The Liquid Argon Purity In The ICARUS T600 TPC*, Nucl. Inst. Meth., A **516**, (2004) 68.

[19] F. Arneodo *et al.* [ICARUS Collaboration], *Observation Of Long Ionizing Tracks With The ICARUS T600 First Half-Module*, Nucl. Inst. Meth., A **508**, (2003) 287.

[20] S. Amoruso *et al.* [ICARUS Collaboration], *Measurement Of The Muon Decay Spectrum With The ICARUS T600 Liquid Argon TPC*, Eur. Phys. J., C 33 (2004) 233.

[21] S. Amoruso *et al.* [ICARUS Collaboration], *Study Of The Electron Recombination In Liquid Argon With The ICARUS TPC*, Nucl. Inst. Meth., A 523 (2004) 275.

[22] S. Amerio *et al.* [ICARUS Collaboration], *"Design, construction and tests of the ICARUS T600 detector"*, Nucl. Inst. Meth., A 527 (2004) 329.

LVD. LARGE VOLUME DETECTOR

LVD Collaboration

N.Y.Agafonova[9], M.Aglietta[14], E.D.Alyea[7], P.Antonioli[1], G.Badino[14], G.Bari[1], M.Basile[1], V.S.Berezinsky[9], M.Bertaina[14], R.Bertoni[14], G.Bruni[1], G.Cara Romeo[1], C.Castagnoli[14], A.Chiavassa[14], J.A.Chinellato[3], L.Cifarelli[1], F.Cindolo[1], A.Contin[1], V.L.Dadykin[9], E.A. Dobrynina[9], L.G.Dos Santos[3], R.I.Enikeev[9], W.Fulgione[14], P.Galeotti[14], M.Garbini[1], P.L.Ghia[5,14], G.Giuliani[5,14], P.Giusti[1], F.Gomez[14], F.Grianti[4], G.Iacobucci[1], E.Kemp[3], E.V.Korolkova[9], V.B.Korchaguin[9], V.V.Kuznetsov[9], M.Luvisetto[1], A.S.Malguin[9], H.Menghetti[1], N.Mengotti Silva[3], C.Morello[14], R.Nania[1], G.Navarra[14], K.Okei[10], L.Periale[14], A.Pesci[1], P.Picchi[14], I.A.Pless[8], A.Porta[14], A.Romero[14], V.G.Ryasny[9], O.G.Ryazhskaya[9], O.Saavedra[14], K.Saitoh[13], G.Sartorelli[1], M.Selvi[1], N.Taborgna[5], N.Takahashi[12], V.P.Talochkin[9], G.C.Trinchero[14], S.Tsuji[11], A.Turtelli[3], P.Vallania[14], S.Vernetto[14], C.Vigorito[14], L.Votano[4], T.Wada[10], R.Weinstein[6], M.Widgoff[2], V.F.Yakushev[9], G.T.Zatsepin[9], A.Zichichi[1]

[1] *University of Bologna and INFN-Bologna, Italy*
[2] *Brown University, Providence, USA*
[3] *University of Campinas, Campinas, Brazil*
[4] *INFN-LNF, Frascati, Italy*
[5] *INFN-LNGS, Assergi, Italy*
[6] *University of Houston, Houston, USA*
[7] *Indiana University, Bloomington, USA*
[8] *Massachusetts Institute of Technology, Cambridge, USA*
[9] *Institute for Nuclear Research, Russian Academy of Sciences, Moscow, Russia*
[10] *Okayama University, Okayama, Japan*
[11] *Kawasaki Medical School, Kurashiki, Japan*
[12] *Hirosaki University, Hirosaki, Japan*
[13] *Ashikaga Institute of Technology, Ashikaga, Japan*
[14] *IFSI-INAF, Torino; University of Torino and INFN-Torino, Italy*

Abstract

The Large Volume Detector (LVD) in the INFN Gran Sasso National Laboratory, Italy, is a ν observatory mainly designed to study low energy neutrinos from the gravitational collapse of galactic objects.

The experiment has been monitoring the Galaxy since June 1992, under increasing larger configurations: in January 2001 it has reached its final active mass $M = 1$ kt. LVD is one of the largest liquid scintillator apparatus for the detection of stellar collapses and, together with SNO and SuperKamiokande, it is part of the SNEWS network.

1 Introduction

LVD, located in Hall A of the INFN Gran Sasso National Laboratory, is a multipurpose detector consisting of a large volume of liquid scintillator interleaved with limited streamer tubes in a compact geometry. The major purpose of the LVD experiment is the search for neutrinos from Gravitational Stellar Collapses (GSC) in our Galaxy [1].

In spite of the lack of a "standard" model of the gravitational collapse of a massive star, the correlated neutrino emission appear to be well established. At the end of its burning phase a massive star ($M > 8M_{\odot}$) explodes into a supernova (SN), originating a neutron star which cools emitting its binding energy $E_B \sim 3 \cdot 10^{53}$ erg mostly in neutrinos.

The largest part of this energy, almost equipartitioned among neutrino and antineutrino species, is emitted in the cooling phase: $E_{\bar{\nu}_e} \sim E_{\nu_e} \sim E_{\nu_x} \sim E_B/6$ (where ν_x denotes generically $\nu_\mu, \bar{\nu}_\mu, \nu_\tau, \bar{\nu}_\tau$ flavors). The energy spectra are approximatively a Fermi-Dirac distribution, but with different mean temperatures, since ν_e, $\bar{\nu}_e$ and ν_x have different couplings with the stellar matter: $T_{\nu_e} < T_{\bar{\nu}_e} < T_{\nu_x}$. LVD is able to detect $\bar{\nu}_e$ interactions with protons, which give the main signal of supernova neutrinos, with a very good signature. Moreover, it can detect ν_e through the elastic scattering reactions with electrons, and it is also sensitive to neutrinos of all flavors detectable through neutral and charged currents interactions with the carbon nuclei of the scintillator. The iron support structure of the detector can also act as a target for electron neutrinos and antineutrinos. The products of the interaction can exit iron and be detected in the liquid scintillator. The amount of neutrino-iron interaction can be as high as about 20% of the total number of interactions.

The described features of stellar collapses are in fact common to all existing models and lead to rather model independent expectations for supernova neutrinos. Thus, the signal observable in LVD, in different reactions and due to different kinds of neutrinos, besides providing astrophysical informations on the nature of the collapse, is sensitive to intrinsic ν properties, as oscillation of massive neutrinos and can give a contribution to define some of the neutrino oscillation properties still missing.

2 The LVD experiment

2.1 The detector

The LVD experiment has been in operation since 1992, under different increasing configurations. During 2001 the final upgrade took place: LVD became fully operational, with

an active scintillator mass $M = 1000$ t. LVD now consists of an array of 840 scintillator counters, 1.5 m^3 each, arranged in a compact and modular geometry. There are two subsets of counters: the external ones (43%), operated at energy threshold $\mathcal{E}_h \simeq 7$ MeV, and inner ones (57%), better shielded from rock radioactivity and operated at $\mathcal{E}_h \simeq 4$ MeV. In order to tag the delayed γ pulse due to n-capture, all counters are equipped with an additional discrimination channel, set at a lower threshold, $\mathcal{E}_l \simeq 1$ MeV.
During 2004, we started the re-calibration of the whole array, aiming at setting $\mathcal{E}_h$ at the same value for both internal and external counters, namely at ≈ 5 MeV.
In figure 1 a front view of the ν telescope is visible.

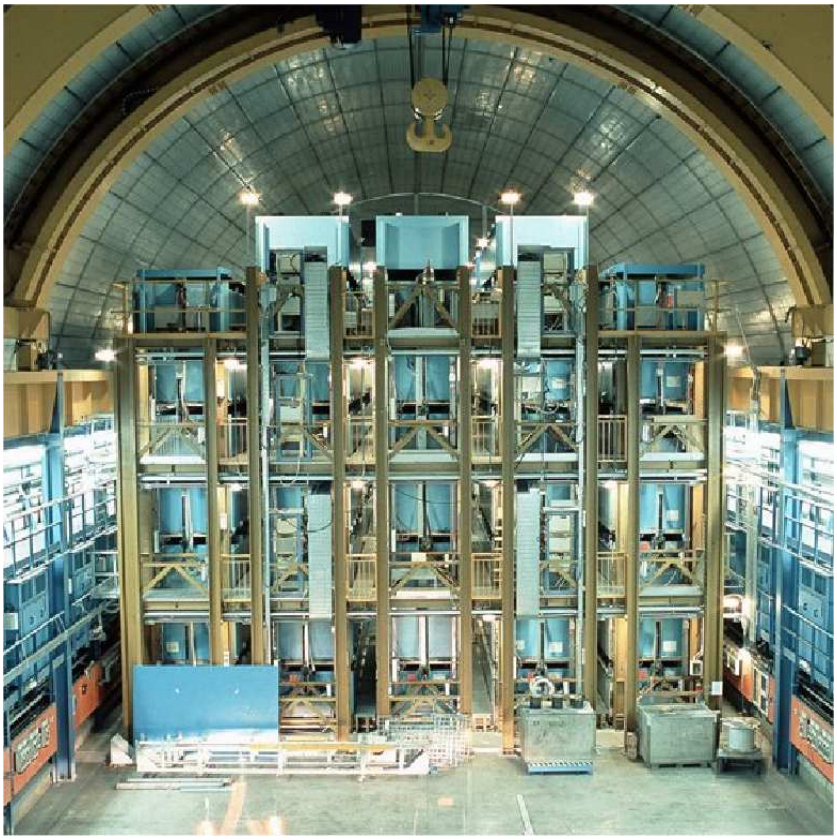

Figure 1: Front view of the LVD detector

Relevant features of the detector are:
(*i*) good event localization and muon tagging;
(*ii*) accurate absolute and relative timing: $\Delta t_{abs} = 1\,\mu$s, $\Delta t_{rel} = 12.5$ ns;
(*iii*) energy resolution: $\sigma_E/E = 0.07 + 0.23 \cdot (E/\text{MeV})^{-0.5}$;
(*iv*) very high duty cycle, i.e. $> 99.3\%$ in the last five years;
(*v*) fast event recognition.

2.2 SN neutrino interactions

The observable neutrino reactions in the liquid scintillator (LS) are:

- *(1)* $\bar{\nu}_e p, e^+ n$, (physical threshold $E_{\bar{\nu}_e} > 1.8\ MeV$) observed through a prompt signal from e^+ above threshold $\mathcal{E}_h$ (detectable energy $E_d \simeq E_{\bar{\nu}_e} - 1.8$ MeV $+2m_e c^2$), followed by the signal from the $np, d\gamma$ capture ($E_\gamma = 2.2$ MeV), above $\mathcal{E}_l$ and with a mean delay $\Delta t \simeq 180\ \mu$s. The cross section for this reaction has been recently recalculated [2] with a better treatment of the $10 - 100$ MeV region, i.e. the SN neutrino energy. The efficiency for the prompt signal is $\epsilon_{\bar{\nu}_e p, e^+ n} = 95\%$, while for the neutron capture is 50%.

- *(2)* ν_e ^{12}C,^{12}N e^-, (physical threshold $E_{\nu_e} > 17.3\ MeV$) observed through two signals: the prompt one due to the e^- above $\mathcal{E}_h$ (detectable energy $E_d \simeq E_{\nu_e} - 17.3$ MeV) followed by the signal, above $\mathcal{E}_h$, from the β^+ decay of ^{12}N (mean life time $\tau = 15.9$ ms). The efficiency for the detection of the ^{12}N beta decay product is 90%.

- *(3)* $\bar{\nu}_e$ ^{12}C,^{12}B e$^+$, (physical threshold $E_{\bar{\nu}_e} > 14.4\ MeV$) observed through two signals: the prompt one due to the e^+ (detectable energy $E_d \simeq E_{\bar{\nu}_e} - 14.4\,\text{MeV} + 2m_e c^2$) followed by the signal from the β^- decay of ^{12}B (mean life time $\tau = 29.4$ ms). As for reaction *(2)*, the second signal is detected above the threshold $\mathcal{E}_h$ and the efficiency for the detection of the ^{12}B beta decay product is 75%.

- *(4)* $\overset{(-)}{\nu}_\ell$ ^{12}C, $\overset{(-)}{\nu}_\ell$ ^{12}C* ($\ell = e, \mu, \tau$), (physical threshold $E_\nu > 15.1\ MeV$), whose signature is the monochromatic photon from carbon de-excitation ($E_\gamma = 15.1$ MeV), above $\mathcal{E}_h$, detected with a 55% efficiency. Cross sections for reactions (2), (3) and (4) are taken from [16].

- *(5)* $\overset{(-)}{\nu}_\ell$ e^-, $\overset{(-)}{\nu}_\ell$ e^-, which yields a single signal, above $\mathcal{E}_h$, due to the recoil electron.

The LVD detector presents an iron support structure made basically by two components: the tank (mean thickness: 0.4 *cm*) which contains the LS and the "portatank" (mean thickness: 1.5 *cm*) which hosts a cluster of 8 tanks. Indeed, the higher energy part of the ν flux could be detected also with the $\nu(\bar{\nu})$Fe interaction, which results in an electron (positron) that could exit iron and release energy in the LS.

The considered reactions are:

- *(6)* ν_e ^{56}Fe,^{56}Co e^-. The mass difference between the nuclei is $\Delta_{m_n} = m_n^{\text{Co}} - m_n^{\text{Fe}} = 4.055$ MeV; moreover the first Co allowed state is at 3.589 MeV. Other higher energy allowed states are present in Cobaltum 56, indeed we consider $E_{e^-}^{\text{kin}} = E_{\nu_e} - \Delta_{m_n} - E_{\text{level}} - m_e$ MeV, where E_{level} is the energy difference between the excitation level and the ground state level: it can take values: $3.589, 4.589, 7.589, 10.589\ MeV$. A number of gammas are produced in the interaction, depending on the excitation level considered.

  A full simulation of the LVD support structure and LS geometry has been developed in order to get the efficiency for electron and gammas, generated randomly in the iron structure, to reach the LS with energy higher than $\mathcal{E}_h$. It is greater than 20% for $E_\nu > 30$ MeV and grows up to 70% for $E_\nu > 100$ MeV. On average, the electron energy detectable in LS is $E_d \simeq 0.45 \times E_\nu$.

- *(7)* $\bar{\nu}_e$ ^{56}Fe,^{56}Mn e^+, the energy threshold is very similar to reaction *(6)* and the same efficiency is considered.

The cross section for reactions *(6),(7)* are taken respectively from [17] and [18].

The number of all the possible targets present in the LVD detector is listed in table 1.

Table 1: Number of targets in the LVD detector.

Target Type	Contained in	Mass	Number of targets
Free protons	Liquid Scintillator	1000 t	9.34 10^{31}
Electrons	LS	1000 t	3.47 10^{32}
C Nuclei	LS	1000 t	4.23 10^{31}
Fe Nuclei	Support Structure	710 t	7.63 10^{30}

3 LVD and its experimental activity in 2004

3.1 Operation on the detector

3.1.1 Re-calibration and upgrade

Starting from April 2004, LVD has undergone a systematic program of maintenance, re-calibration and upgrade. Thanks to the high modularity of the detector (which consists of three large modules - named "towers"), this process has not influenced at all the duty cycle, and great attention has been given in limiting the reduction of the effective mass. The re-calibration of the PMTs is realized through the use of a ^{60}Co source moved from counter to counter: beside for recovering the gain matching of the almost 2500 PMTs, this operation is meant for changing the PMTs gains and equalizing them between internal and external counters. On the other side, the upgrade concerns the electronics, tuned to get the threshold matching for all the counters, both internal and external ones.
The program, which will finally result in a more uniform and sensitive detector, has been realized starting from the first tower: this is now completely re-calibrated and upgraded, while the program on the rest of the detector will be completed within June 2005. We show in fig. 2 and 3 the distributions of the estimated new thresholds[1] in tower 1, for

[1]The single counter spectrum, in the low-energy part, i.e. below 10 MeV, can be fitted by a function describing the natural radioactivity spectrum, folded with the detector response. The latter can be approximated by a gaussian integral function

$$\frac{1}{\sqrt{2\pi}} \int_{-\infty}^{x} exp(\frac{-y^2}{2}) dy$$

where

$$y = \frac{E - E_{th}}{\sigma_E}$$

being E_{th} the threshold and $\sigma_E$the energy resolution. With respect to the radioactivity spectrum shape, we adopt a power-law form, with exponent fixed to -4.5, which best describes the LVD counters spectra. E_{th} can thus be estimated, being a free parameter in the combined fit (power-law plus gaussian) to the spectrum of each counter.

internal and external counters, respectively: the average value is around 5 MeV for all of them.

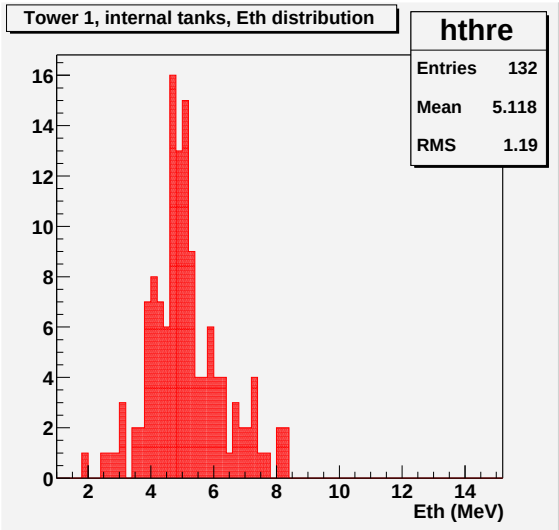

Figure 2: Distribution of estimated thresholds for internal counters of tower 1.

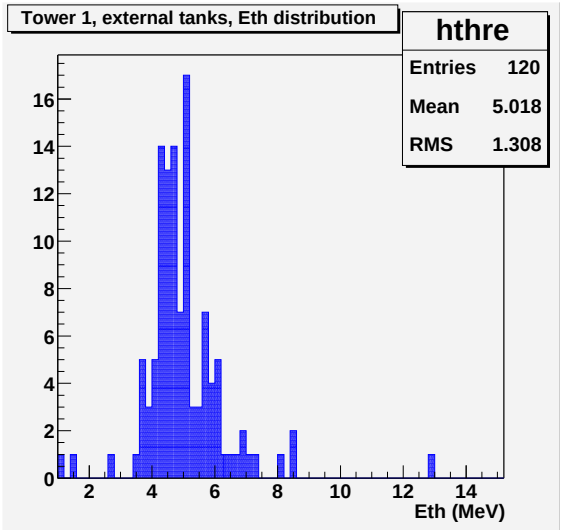

Figure 3: Distribution of estimated thresholds for external counters of tower 1.

3.1.2 Test facility

The change of the PMTs gain, which is the result of the calibration and upgrade of LVD, allows to accomplish a higher efficiency for the neutron capture detection. To make systematic measurements on this issue, we have set up a test facility in the mounting hall. This facility includes several LVD counters, which are used for different kinds of test. One of them is dedicated to the measurement of the neutron detection from a neutron source (^{252}Cf): the efficiency is measured as a function of a tunable threshold in the counter electronics.
Other two counters are dedicated to the study of Gd-loaded scintillator, as part of a R&D program which is on-going in LVD.

3.2 Supernova physics

3.2.1 Monitoring

LVD has been continuously monitoring the Galaxy since 1992 in the search for neutrino bursts from GSC [2]. Its active mass has been progressively increased from about 330 t in 1992 to the present 1000 t, always guaranteeing a sensitivity to GSC up to distances $d = 20$ kpc from the Earth, even for the lowest ν-sphere temperature.
The telescope duty cycle has been continuously improving since 1992. As it can be seen in Fig.4, in the last five years the average duty cycle was $> 99.3\%$.

Since the LVD sensitivity is higher than expected from GSC models, even if the source is at a distance of 20 kpc and for soft neutrino energy spectra, we can conclude that no

[2]The results of this search have been periodically updated and published[3, 4, 5, 6, 7, 8]

gravitational stellar collapse has occurred in the Galaxy in the whole period of observation: the resulting upper limit to the rate of GSC at 90% c.l. is 0.2 event/yr.

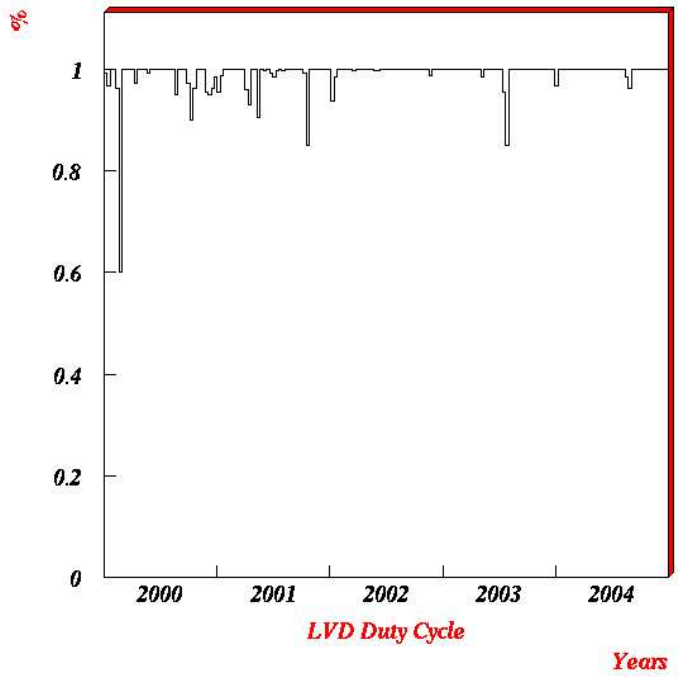

Figure 4: LVD duty cycle during year 2000-2004.

The reliability of LVD to detect and recognize on-line ν-bursts with different characteristics, has been tested by inducing clusters of pulses - with different multiplicity and duration - in the LVD counters. The cluster injector, consisting of a generator of light pulses in a certain number of counters, allowed us to evaluate the system efficiency in detecting and disentangling bursts from the background, even with different background conditions. Moreover, the on-line algorithm is continuously checked through the high-rate mode of the supernova monitor used for the SNEWS.

3.2.2 SNEWS

The SNEWS (SuperNova Early Warning System)[13, 15] is a collaboration among several neutrino-sensitive experiments. The primary goal of SNEWS is to provide the astronomical community with a prompt alert for a galactic supernova. An additional goal is to optimize global sensitivity to supernova neutrino physics, by such cooperative work as downtime coordination.
The charter member experiments of SNEWS are LVD in Italy, Super-K in Japan and SNO in Canada. Representatives from Amanda, IceCube, KamLAND, Borexino, Mini-Boone, Icarus, OMNIS and LIGO participate in the SNEWS working group, and will eventually join the active members of the network.
There is currently a single coincidence server, hosted by Brookhaven National Laboratory. We expect that additional machines will be deployed in the future. The BNL computer

continuously runs a coincidence server process, which waits for alarm datagrams from the experiments' clients, and provides an alert if there is a coincidence within a specified time window (10 seconds for normal running). A scheme of "GOLD" and "SILVER" alerts has been implemented: GOLD alerts are intended for automated dissemination to the community; SILVER alerts will be disseminated among the experimenters, and require human checking.
As of today, SILVER alerts only between LVD and Super-K are activated.
Up to now, no inter-experiment coincidence, real or accidental, has ever occurred (except during a special high rate test mode), nor any core collapse event been detected within the lifetimes of the currently active experiments.

3.2.3 Effects of neutrino oscillations

The observation of a neutrino burst due to the explosion of a galactic supernova can add precious informations about neutrino mass and mixing scenarios, in a complementary way with respect to solar, atmospheric and terrestrial ν experiments.
The signal at LVD from a SN exploding at $D = 10$ kpc for 3-flavor ν oscillation, assuming the LMA-MSW solution for solar ν, and normal or inverted mass hierarchy has been calculated [9] [10] [11]. For a normal mass hierarchy (NH) scheme, ν (not $\bar{\nu}$) cross two resonance layers: one at higher density (H), which corresponds to $\Delta m^2_{\rm atm}, U^2_{e3}$, and the other at lower density (L), corresponding to $\Delta m^2_{\rm sol}, U^2_{e2}$. For inverted mass hierarchy (IH), transitions at the higher density layer occur in the $\bar{\nu}$ sector. Given the energy range of SN ν (up to ~ 100 MeV) and considering a star density profile $\rho \propto 1/r^3$, the adiabaticity condition is always satisfied at the L resonance for any LMA solution, while at the H resonance, this depends on the value of U^2_{e3}. When $U^2_{e3} \geq 5 \cdot 10^{-4}$ the conversion is completely adiabatic, meaning that the flip probability between two adjacent mass eigenstates is null ($P_h = 0$). In the adiabatic case and NH, the $\bar{\nu}_e$ produced in the SN core arrive at Earth as ν_1, and they have a high ($U^2_{e1} \simeq cos^2\theta_{12} \simeq 0.7$) probability to be detected as $\bar{\nu}_e$. On the other hand, the original $\bar{\nu}_x$ arrive at Earth as ν_2 and ν_3 and are detected as $\bar{\nu}_e$ with probability $U^2_{e2} \simeq sin^2\theta_{12}$. Given the higher energy spectrum of $\bar{\nu}_x$ this configuration results in a larger number of interactions, with respect to the no-oscillation case, due to the increasing cross sections with energy. In the adiabatic-IH case the detected $\bar{\nu}_e$ completely come from the original $\bar{\nu}_x$ flux in the star and the number of interactions is still greater.
The oscillations scheme can be summarized as: $F_e = P_h U^2_{e2} F^0_e + (1 - P_h U^2_{e2}) F^0_x$ and $F_{\bar{e}} = U^2_{e1} F^0_{\bar{e}} + U^2_{e2} F^0_{\bar{x}}$ for normal hierarchy; $F_e = U^2_{e2} F^0_e + U^2_{e1} F^0_x$ and $F_{\bar{e}} = P_h U^2_{e1} F^0_{\bar{e}} + (1 - P_h U^2_{e1}) F^0_{\bar{x}}$ for inverted hierarchy, where F^0_{any} are the original neutrino fluxes in the star and F_{any} are the observed ν fluxes. One can notice that, in the antineutrino channel, the non adiabatic ($P_h = 1$), IH case, is equivalent to the NH case (which does not depend on adiabaticity). Earth matter effects are quite weak given the current value of Δm^2_{12}. They are more relevant in the ν than in the $\bar{\nu}$ channel. The effect in reaction *(1)* could be detected if compared with a high statistic sample (i.e. SK) or if a larger number of events is available, i.e. a closer SN.

3.3 Study of the muon-induced neutron background

3.3.1 Neutron signature

The LVD apparatus can detect neutrons with the same signature of the inverse beta decay reaction. High energy neutrons could cause a liquid scintillator proton to recoil (prompt HET signal), and are then thermalized and finally captured by the liquid scintillator protons with the emission of the 2.2 MeV gamma (delayed LET signal). Taking into account the energy transfer in the interaction between neutron and proton, the proton quenching and the value of the high energy threshold in the core of the detector, we estimate that the neutrons detected in this way have energies greater than about 20 MeV.
The background to the neutron detection is due to the accidental coincidences between the high energy signals and the low energy ones. This background, however, has a flat distribution of the delay between the two signals and can be estimated by fitting the time delay distribution.

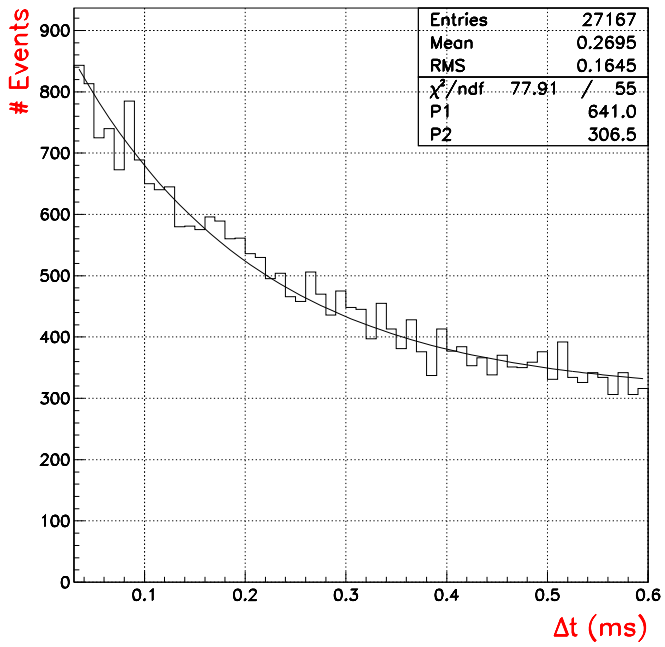

Figure 5: Time delay distribution between the high energy signals and the following low energy one detected in the same counter of the detector. From the distribution we can separate the neutron interaction from the accidental coincidences (see text).

An example of this distribution is shown in figure 5; we can fit the data with the curve

$$\frac{dN}{dt} = P1 \cdot e^{\frac{-t}{\tau}} + P2$$

where $\tau = 185\ \mu s$. From the first parameter we obtain the number of neutron interactions, while the second takes into account the number of accidental coincidences.

3.3.2 Analysis and results

We have analyzed the neutron production in association to single muon events, that is events with only one reconstructed track, from 1994 to 2002, for a total sample of more than 7 millions of single muons events.
First we have evaluated the production of neutrons per counter per event at various distances from the muon track; the distance is defined as the distance between the reconstructed muon track and the center of the counter where the neutron is detected. Notice that in the counters traversed by the muon track we require, in addition to the high energy signal associated to the muon a second one associated to the recoiling proton. Neutron candidates are selected with the procedure described in the previous section; at each distance the background contribution is evaluated by fitting the time delay distribution between the HET signal and the LET ones. The result obtained is shown in fig. 6; we were able to evaluate the neutron production up to 22 m from the muon track.

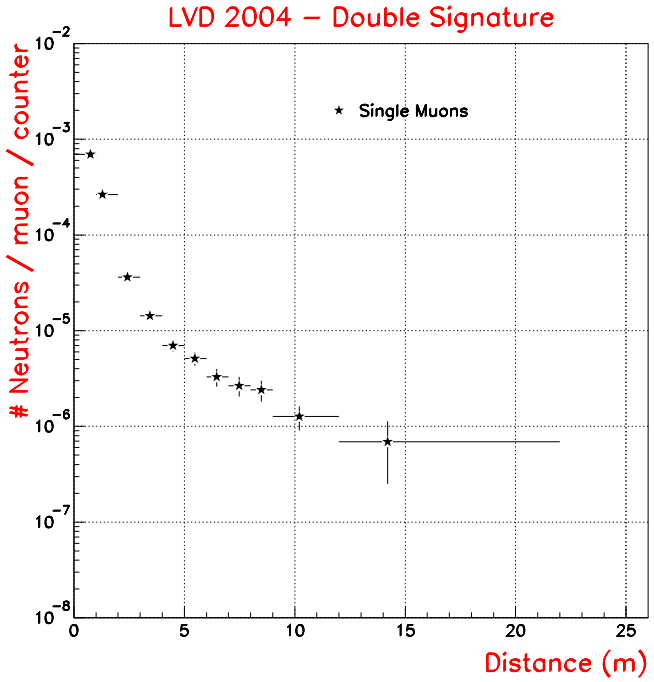

Figure 6: Number of neutrons detected per muon per counters as a function of the distance from the muon track.

Due to the non homogeneous distribution of the scintillator in the LVD detector the behavior observed in figure 6 has to be studied with a detailed Montecarlo simulation which is under development. To estimate the neutron energy spectrum, we studied the number of neutrons detected as a function of the energy released in the scintillator from the recoiling proton. The result is shown in figure 7; the data are well fitted by the power law spectrum:

$$\frac{dN}{dE} = A \times E^{-\alpha}$$

where $A = (1.6 \pm 0.1) \cdot 10^{-5}$ and $\alpha = (1.18 \pm 0.02)$; the errors are statistical only.

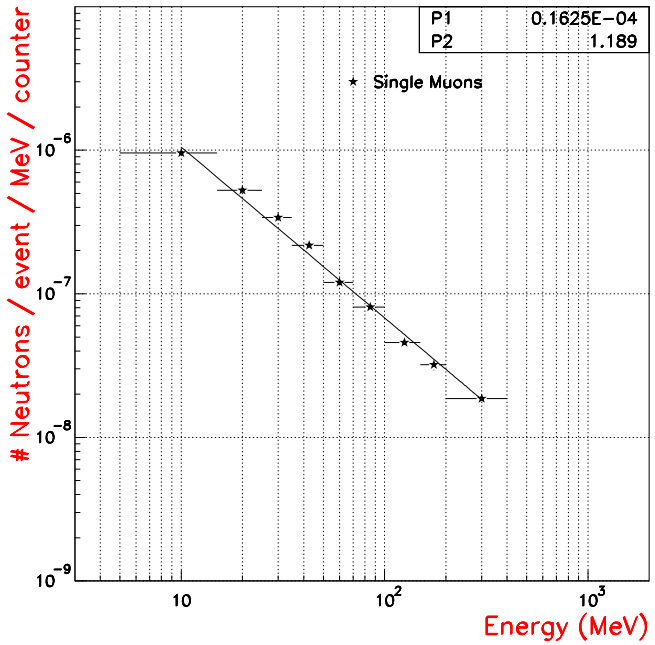

Figure 7: Number of neutrons detected per muon per counters as a function of the proton recoil energy.

Finally we evaluate the neutron production as a function of the muon track length in scintillator. The preliminary result is shown in figure 8.

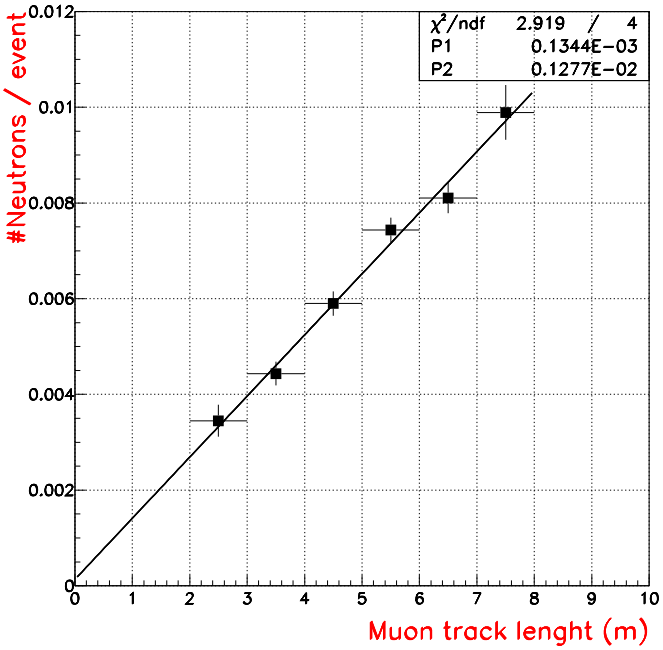

Figure 8: Number of neutrons per events detected as a function of the muon track length in scintillator; the main production of neutron is due to the muon interaction with the detector nuclei.

The data are well fitted by:

$$y = 0.13 \cdot 10^{-3} + 0.13 \cdot 10^{-2} \cdot L$$

where the first parameter takes into account the neutron production in the rock, as it is independent from the muon track length inside the liquid scintillator, while the second parameter takes into account the increase in the neutron production with the muon track length in scintillator. Comparing the two values we can conclude that the neutron production in the core of the experiment is mostly due to the interaction of muons with the detector nuclei (Fe,C).

4 List of publications in 2004

- *CNGS beam monitor with the LVD detector.*
  Nuclear Instruments and Methods in Physics Research A 516 (2004) 96-103
  `hep-ex/0304018`

- *Search for low energy neutrinos in correlation with the 8 events observed by the EXPLORER and NAUTILUS detectors in 2001.*
  Astronomy & Astrophysics 421 (2004) 399
  `astro-ph/0403207`

- *Study of the effect of neutrino oscillation on the supernova neutrino signal with the LVD detector*
  Nucl. Phys. Proc. Suppl., 138 (2005) 115

- *CNGS beam monitor with the LVD detector*
  Nucl. Phys. Proc. Suppl., 138 (2005) 424

- *Study of muon-induced neutron background with the LVD detector at LNGS*
  submitted as Neutrino 2004 conference proceeding (to be published on Nucl. Phys. Proc. Suppl.)

- *1992-2004: search for neutrino bursts from collapsing objects with LVD*
  submitted as Neutrino 2004 conference proceeding (to be published on Nucl. Phys. Proc. Suppl.)

- *Study of muon-induced neutron background with the LVD detector at LNGS*
  submitted as IDM2004 conference proceeding (to be published by World Scientific Ltd.)

References

[1] LVD Collaboration, Il Nuovo Cimento **A105** (1992) 1793

[2] A. Strumia, F. Vissani, `astro-ph/0302055`.

[3] LVD Collaboration, 23th ICRC Conf.Proc.,HE 5.1.1,Vol.4,468,1993

[4] LVD Collaboration, 24th ICRC Conf.Proc., HE 5.3.6,Vol.1,1035,1995

[5] LVD Collaboration, 25th ICRC Conf.Proc., HE 4.1.12,1997

[6] LVD Collaboration, 26th ICRC Conf.Proc., HE 4.2.08,Vol.2,223,1999

[7] LVD Collaboration, 27th ICRC Conf.Proc., HE230,1093,2001

[8] LVD Collaboration, 28th ICRC Conf.Proc., HE2.3,1333,2003

[9] LVD Collaboration, Nucl. Phys. B Proc. Sup. 110 (2002) pp 410-413, astro-ph/0112312

[10] A. Zichichi, *The most powerful scintillator supernova neutrino detector*, talk presented at the symposium *LVD: the First Ten Years*, LNGS, 28-29 October, 2002).

[11] LVD Collaboration, 28th ICRC Conf.Proc., HE2.3,1297,2003

[12] C.Lunardini and A.Yu.Smirnov, hep-ph/0106149

[13] http://hep.bu.edu/∼snnet/

[14] SNEWS Subgroup "Proposal for an Automated Supernova Alert for the Astronomical Community"

[15] P. Antonioli et al., New J. Phys., 6 (2004) 114

[16] M. Fukugita, Phys. Lett. B 212:139 , (1988)

[17] E. Kolbe, K. Langanke, `nucl-th/0003060`.

[18] J. Toivanen et al., *Nuclear Physics A* **694** (2001), 395-408.

[19] Astone P., Babusci D., Bassan M., et al., 2002, Class. Quant. Grav. 19, 5449

[20] Burrows A., Klein D., Gandhi R. 1992, Phys. Rev. D, 45, 3361

[21] Thorne, K.S., 1988, "Gravitational radiation", Cambridge Univ. Press, Cambridge (MA)

[22] Muller, E. Class. Quant. Grav. 1997, 14, 1455

[23] Fulgione, W., Mengotti-Silva, N., & Panaro, L. 1996, Nucl. Instr. Meth., A, 368, 512

[24] Montanet, L., et al., 1994, Phys. Rev., D, 50, 1173

[25] Kocharov et al., Il Nuovo Cimento C **14** (1991) 417.

[26] LVD collaboration, Proc. 28 ICRC, Tsukuba, HE 2.2, 1251, (2003).

[27] Khalchukov et al, *Il Nuovo Cimento C* **6**, 320 (1983).

[28] Aglietta et al., *Il Nuovo Cimento A* **105**, 1793 (1992).

LUNA. Laboratory for Underground Nuclear Astrophysics

D.Bemmerer[1,12], R.Bonetti[2], C.Broggini[1*], F.Confortola[3], P.Corvisiero[3], H.Costantini[3], J.Cruz[4], A.Formicola[5], Z.Fülöp[6], G.Gervino[7], A.Guglielmetti[2], C.Gustavino[5], G.Gyürky[6], G.Imbriani[8], A.P.Jesus[4], M.Junker[5], A.Lemut[3], R.Menegazzo[1], A.Ordine[8], P.Prati[3], V.Roca[8], D.Rogalla[9], C.Rolfs[10], M.Romano[8], C.Rossi Alvarez[1], F.Schümann[10], E.Somorjai[6], O.Straniero[11], F.Strieder[10], F.Terrasi[9], H.P.Trautvetter[10]

[1] INFN, Padova, Italy
[2] Università di Milano, Dipartimento di Fisica and INFN, Milano, Italy
[3] Università di Genova, Dipartimento di Fisica and INFN, Genova, Italy
[4] Centro de Fisica Nuclear, Universidade de Lisboa, Portugal
[5] Laboratori Nazionali del Gran Sasso, Assergi, Italy
[6] ATOMKI, Debrecen, Hungary
[7] Politecnico di Torino, Dipartimento di Fisica and INFN, Torino, Italy
[8] Università di Napoli, Dipartimento di Fisica and INFN, Napoli, Italy
[9] Dipartimento di Scienze Ambientali, Seconda Univerità di Napoli, Caserta, Italy
[10] Institut für Experimentalphysik III, Ruhr-Univerität Bochum, Germany
[11] Osservatorio Astronomico di Collurania, Teramo, and INFN, Napoli, Italy
[12] Inst. für Atomare Physik und Fachdidaktik, Technische Univ. Berlin, Germany

Abstract

LUNA is measuring fusion cross sections down to the energy of the stellar nucleosynthesis. The activity during this year has been focused on the study of ^{14}N(p,γ)^{15}O and on the preparation of the ^{3}He(^{4}He,γ)^{7}Be experiment. In particular, ^{14}N(p,γ)^{15}O, the key reaction of the CNO cycle, has been measured down to a center of mass energy of about 70 keV, entering the energy window where the CNO burning takes place in stars.

*Spokesperson

Introduction

Nuclear reactions that generate energy and synthesize elements take place inside the stars in a relatively narrow energy window: the Gamow peak. In this region, far below the Coulomb energy, usually below 100 keV, the reaction cross-section σ(E) drops almost exponentially with decreasing energy E:

$$\sigma(E) = \frac{S(E)}{E}\, exp(-2\,\pi\,\eta), \tag{1}$$

where $S(E)$ is the astrophysical factor and η is the Sommerfeld parameter, given by $2\,\pi\,\eta = 31.29\,Z_1\,Z_2(\mu/E)^{1/2}$. Z_1 and Z_2 are the nuclear charges of the interacting particles in the entrance channel, μ is the reduced mass (in units of amu), and E is the center of mass energy (in units of keV).

The extremely low value of the cross-section, from pico to femto-barn and even below, has always prevented its measurement in a laboratory at the Earth's surface, where the signal to background ratio would be too small because of cosmic ray interactions. Instead, the observed energy dependence of the cross-section measured at high energies is extrapolated to the low energy region, leading to substantial uncertainties. In particular, there might be a change of the reaction mechanism or there might be the contribution of narrow or sub-threshold resonances, not accounted for by the extrapolation, but which could completely dominate the reaction rate at the Gamow peak.

In addition, another effect can be studied at low energies: the electron screening. The electron cloud surrounding the interacting nuclei acts as a screening potential, thus reducing the height of the Coulomb barrier and leading to a higher cross-section. The screening effect has to be measured and taken into account in order to derive the bare nuclei cross-section, which is the input data to the models of stellar nucleosynthesis.

In order to explore this new domain of nuclear astrophysics we have installed two electrostatic accelerators underground at LNGS: a 50 kV accelerator and a 400 kV one. The qualifying features of both the accelerators are a very small beam energy spread and a very high beam current even at low energy.

Outstanding results obtained up to now are the only existing cross-section measurements within the Gamow peak of the sun: $^3He(^3He, 2p)^4He$ [1] and $d(p,\gamma)^3He$ [2]. The former plays a big role in the proton-proton chain, largely affecting the calculated solar neutrino luminosity, whereas the latter is the reaction that rules the proto-star life during the pre-main sequence phase.

With these measurements LUNA has shown that, by going underground and by using the typical techniques of low background physics, it is possible to measure nuclear cross sections down to the energy of the nucleosynthesis inside stars.

In the following we report on the activity during the year 2004, which has been mainly dedicated to the study of $^{14}N(p,\gamma)^{15}O$ and to the preparation of the experimental apparatus to measure ^{3}He(^{4}He,γ)^{7}Be.

1 The ^{14}N(p,γ)^{15}O reaction

^{14}N(p,γ)^{15}O (Q=7.297 MeV) is the slowest reaction of the CNO cycle, the key one to determine the age of the globular clusters, which are the oldest systems in the Galaxy, as well as to predict the CNO neutrino flux from the Sun.

As a matter of fact, during most of its life, a low mass star burns H in the center via the pp chain. However, when the central H mass fraction reduces down to 0.1, the nuclear energy produced by the H-burning becomes not sufficient and the stellar core must contract to extract some energy from its gravitational field. Then, the central temperature (and the density) increases and the H-burning switches from the pp-chain to the more efficient CNO-burning. Thus, the escape from the main sequence is powered by the onset of the CNO burning, whose bottleneck is the ^{14}N(p,γ)^{15}O reaction. In particular, a rate modification of this reaction changes the luminosity of the turn off point in the Hertzsprung-Russell diagram of a globular cluster. The luminosity of this point gives then the age of the cluster: the higher the cross section is, the younger is the age, for a given turn off luminosity.

In the center of the sun the CNO cycle is also partially active. Then a fraction of the total neutrino flux comes from the β-decay belonging to the cycle. Obviously, the total amount of CNO solar neutrinos directly depends on the value of the ^{14}N(p,γ)^{15}O cross section. CNO neutrinos from the Sun play an important role in the solar neutrino experiment detecting neutrinos of about 1 MeV energy, e.g. BOREXINO, where the CNO neutrino flux was calculated to account for about 20 % of the expected neutrino signal.

At solar energies the cross section of ^{14}N(p,γ)^{15}O is dominated by a subthreshold resonance at -504 keV. At higher energies, more than 100 keV, the cross section is dominated by the resonance at $E_R = 259$ keV with transitions to the the ground state of ^{15}O or to its excited states at 5.18 MeV, 6.18 MeV and 6.79 MeV energy. The status of the ^{14}N(p,γ)^{15}O determination before the LUNA measurement is described in the 2003 LNGS Annual Report. This year our results have been published [3] to cover the proton energy region from 140 keV to 400 keV . Very briefly, the experiment was performed by sending a proton beam on a solid nitrogen target (TiN) and by measuring the γ-rays with a HPGe detector. The analysis of the transitions to the 6.79 MeV exicited state and to the ground state provided a new value for the extrapolated S-factor.

In particular, we have obtained a total S-factor $S_{tot}(0) = 1.7 \pm 0.1$ (statistical) $\pm$0.2(systematic) $keV \cdot b$. Our value can be compared with 1.77 ± 0.2 $keV \cdot b$ from the theoretical paper [4] and 1.70 ± 0.22 $keV \cdot b$ from [5], where the asymptotic normalization coefficients for $^{14}N + p \rightarrow^{15} O$ have been determined by measuring the $^{14}N(^3He, d)^{15}O$ proton transfer reaction at an incident energy of 26.3 MeV. The LUNA result is smaller than the value given in most recent compilations: $3.5^{+0.4}_{-1.6}$ $keV \cdot b$ [6] and 3.2$\pm$0.8 $keV \cdot b$ [7]. The astrophysical consequences are significant: the CNO neutrino yield in the Sun is decreased by about a factor two [9][10][11] and the age of the oldest Globular Clusters is increased by 0.7-1 Gyr [8][9] with respect to the current estimates.

In order to perform the R-matrix fit to our data we had to use also the high energy data of [12] (corrected to take into account the summing effect). The careful evaluation of this data has suggested the need of studying the energy region above 400 keV. As

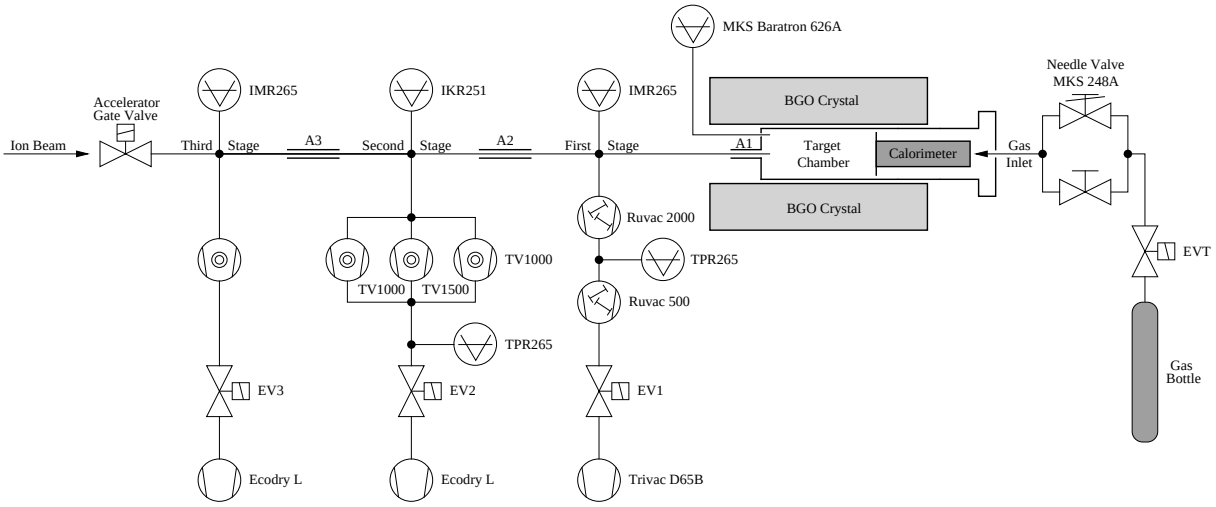

Figure 1: ^{14}N(p,γ)^{15}O windowless gas target schematic diagram.

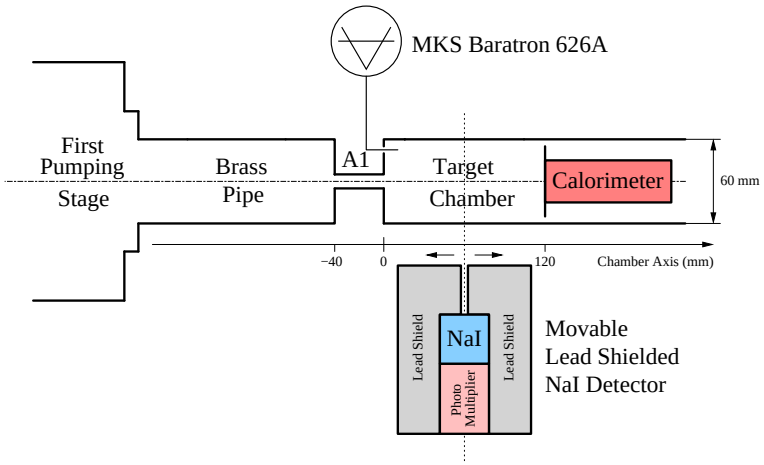

Figure 2: The set-up used to measure the beam heating effect.

a consequence, a new set of measurements has been made at the 500 kV and 4 MV tandem accelerators of the Dynamitron Tandem Laboratory (DTL-Bochum) in the energy range between 500 keV and 1.7 MeV (at such energies it is not necessary to perform the experiment underground because of the high reaction rate). We are now analysing this data which will then be used, together with the ones obtained in Gran Sasso, to perform the R-matrix fit to each of the transitions which contribute to the ^{14}N(p, γ)^{15}O cross section.

1.1 The gas target set-up

In order to reduce the region where the cross section is obtained by extrapolation, we have explored the proton energy range below 140 keV. For this it is essential to have both a γ-ray detector with very high efficiency, to compensate for the rapidly decreasing cross

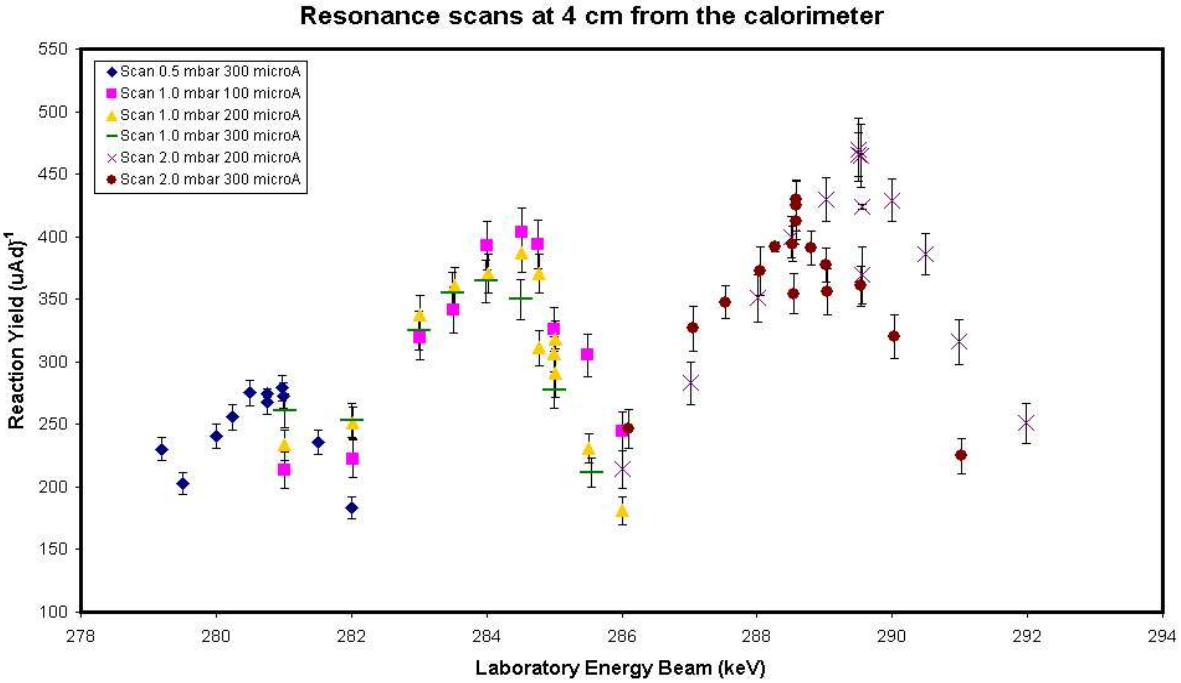

Figure 3: The yield of ^{14}N(p,γ)^{15}O at 4 cm from the calorimeter for different pressures and currents.

section, and a very pure and thin ^{14}N target, to suppress the beam induced background and to minimize the straggling on the energy loss. In addition, the target must be stable for the long time required by the low energy measurements. All this has been achieved with the same 4π BGO summing detector [13] (about 65% efficiency and 8% resolution in the energy region between 6.5 and 8 MeV) used in the measurement of $d(p,\gamma)^3He$ [2] and with a new windowless gas target. A schematic diagram of the gas target is shown in Fig. 1. The ion beam enters the target chamber through three apertures of high impedance (A_3–A_1, Fig. 1) and it is stopped in a beam calorimeter placed at the downstream part of the chamber. The chamber is designed to fit inside the central hole (diameter $\phi = 6\ cm$) of the BGO crystal detector.

When using a gas target, there is the problem to determine the real density along the beam axis inside the interaction chamber. During the data taking the pressure has been monitored by a capacitance gauge with a 0.25% accuracy; measurements have been performed to correctly estimate the gas density starting from this information. In the first step, to estimate the target density whithout the beam, the gas pressure and temperature have been measured by using a test chamber with transversal holes along the beam axis direction. We found an exponential increase (pressure dependent) of the temperature along the beam axis with higher values near the calorimeter (which is kept at high temperature and radiates energy). Such a result shows that there is a noticeable density reduction in target regions closer to the calorimeter which has to be taken into account.

A further effect to be considered is due to the beam heating of the gas [14] along the

beam path. Figure 2 shows the set-up we used to measure such effect in our experiment. The small NaI detector is movable along the beam axis and it is shielded with lead. From the position of the E_R=259 keV ^{14}N(p,γ)^{15}O resonance along the axis (Figure 3) we obtain the energy loss and, from this, the target nuclei density. In the standard measurement conditions the beam heating effect is not negligible and it has to be included in the data analysis.

The measurement has been completed during the summer, by covering the centre of mass energy range from 250 keV to about 70 keV. For the first time a direct measurement of the ^{14}N(p, γ)^{15}O cross section has been made in the region where the CNO burning takes place in astrophysical conditions. In particular, at the lowest energy we had a rate of about 30 events/day: 10 coming from the reaction and 20 from the natural background (the beam induced background is completely suppressed at such energies). The total number of collected ^{14}N(p, γ)^{15}O events in the first bin amounts to about 500. The analysys of this data is still in progress.

2 The ^{3}He(^{4}He, γ)^{7}Be reaction

^{3}He(^{4}He, γ)^{7}Be is the next reaction which will be studied in LUNA. ^{3}He(^{4}He,γ)^{7}Be is the key reaction for the production of ^7Be and ^8B neutrinos in the Sun. The joint effort of all experiments on solar neutrinos and solar physics has finally cast light on the long-standing solar neutrino puzzle. As a consequence, we can now go back to the original motivation of solar neutrino detection: the study of the Sun. The error on $S_{3,4}$ is, at the moment, the main limitation to the extraction of physics from the ^8B neutrino flux measurement. For instance, a 5% determination of $S_{3,4}$ would allow a study of the central region of the Sun with an accuracy better than the one given by helioseismology [15].

At present, the ^{3}He(^{4}He,γ)^{7}Be reaction has been studied in the energy range $E_{c.m.} \geq 107\ keV$ (see [16] and References therein). The capture reaction ($Q-value = 1.586\ MeV$) is dominated, at low energies, by the non-resonant direct capture mechanism to the ground state and to the 429 keV first excited state of ^{7}Be. One expects to observe two primary γ-ray transitions, $DC \rightarrow 0$ and $DC \rightarrow 429\ keV$ with the latter followed by a 429 keV secondary transition. An independent determination of the number of ^{7}Be nuclei produced in the reaction requires the detection of the 478 keV γ-ray activity of the first excited state in the daughter nucleus ^{7}Li populated by the EC decay of ^{7}Be ($T_{1/2}$=53.29$\pm$0.07 d). Both methods have been used in the past to determine the absolute cross section σ(E) but the results obtained from the measurements of the induced ^{7}Be activity are systematically higher (more than $3\frac{1}{2}$ standard deviations) than the values obtained from the measurements of the prompt capture γ-rays transitions.

We decided to reinvestigate the ^{3}He(^{4}He,γ)^{7}Be reaction with high accuracy (relative error $\leq$ 5%) and to extend at lower energies ($E_{c.m.} \simeq 70\ keV$, 100-150 keV for the off-line radioactive decay measurements) the data set used to extrapolate the S(E) factor at zero energy. The measurements will include the detection of the prompt capture γ-rays as well as the 478 keV γ-ray produced in the EC decay of the ^{7}Be (see Fig.4).

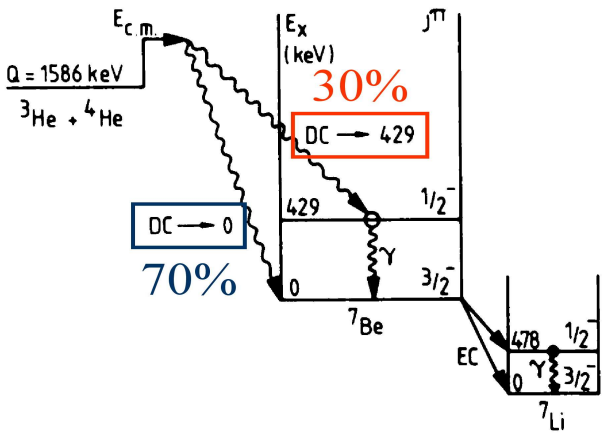

Figure 4: Level scheme of ^{7}Be near the ^{3}He+^{4}He threshold. The ^{3}He(^{4}He,γ)^{7}Be capture reaction is expected to proceed predominantly via the direct capture (DC) mechanism into the ground state and the 429 keV excited state. The EC decay of the ^{7}Be ground state will populate the level at 478 keV in ^{7}Li with a branching ratio=10.45±0.04%.

2.1 Experimental Equipment and Setup

A strong reduction of the background is required in order to study ^{3}He(^{4}He,γ)^{7}Be at low energy (i.e. measure a cross section in the range of pico to femto-barn). In particular, background events should be reduced as much as possible in the Regions Of Interest (ROI) that correspond to the primary γ-ray transitions for the on-line measurements and in the region around 478 keV for the off-line radioactive decay measurements. The natural shielding provided by the LNGS underground laboratory is very efficient to reduce the background at high energy but an additional shield is required to suppress background events from the laboratory walls (mainly 1460 and 2614 keV from ^{40}K and ^{232}Th chain) and air (Radon).

Extensive montecarlo simulations have been performed to define the best geometry and layout of the shield surrounding a large volume HPGe detector and to optimize the background soppression. Moreover, all materials close to the detector have been carefully selected to be radioactively pure by measuring their activity at the low background laboratory of the LNGS. The final layout consists of a lead shield surrounding an inner shield of OFHC copper and placed inside a plastic box filled with Nytrogen.

2.2 Gas target chamber

A new gas target has been designed, a box of 60 x 13 x 11 cm entirely built of OFHC copper to reduce the background. During the measurements we will have a ^{4}He beam on a ^{3}He gas target (with the gas continuosly purified). The beam will enter the target through a 7 mm copper collimator and, after a 30 cm path, it will be stopped on the beam calorimeter, which measures the beam power and thus the current.

First tests of the calorimeter have been performed in order to determine the maximum

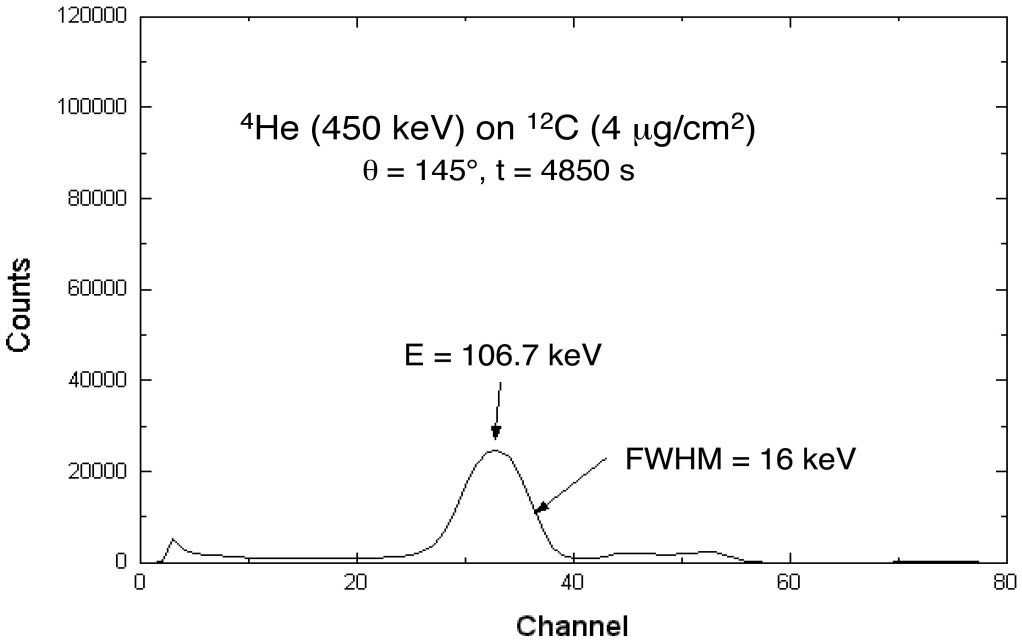

Figure 5: Spectrum of 110 keV alpha particles (measured at INFN-Legnaro)

beam power that can be measured as a function of the temperature difference between the hot side (where the beam is stopped) and the cold side of the calorimeter (kept cold by a cold bath) and to determine the stability of the feedback parameters. In addition to the beam current, we have to know very precisely the density of the target. For this reason a test chamber, identical to the final one, but with different flanges along the target length, has been built in order to measure the pressure profile of the gas inside the chamber without beam. During the cross section measurement, the gas density along the beam path will be determined with a silicon detector.

The germanium detector, a 150% ultra low background crystal, will be positioned at 5 mm from the target chamber. Inside the chamber, a lead collimator will be placed between the beam and the detector in order to shield the detector from gamma rays due to background reactions on the entrance collimator or on the calorimeter cap. Furthermore, thanks to this inner shield, the detector will be mostly sensitive to gammas coming at 55^{O} with respect to the beam direction. This layout makes the measurement almost independent on angular distribution effects. In particular, the systematic uncertainty is reduced from 10 % (detector at 90^{O} or 0^{O}) to 5 %.

2.3 Si detector

As explained in the description of the gas target used to study the $^{14}\mathrm{N}(\mathrm{p},\gamma)^{15}\mathrm{O}$ reaction, it is known that the target density can vary when an intense ion beam impinges on it. This

effect was deeply investigated and it is expected to be of the order of 10 % if the dissipated power is about 20 mW/mm. In order to get rid of systematic errors, we decided to measure the product of the beam intensity times the gas target density via Rutherford scattering by using a Silicon detector. Due to geometrical constraints and to the need of a reasonable life time for the detector, we decided to use a double scattering configuration: the first process being the scattering of ^{4}He beam on ^{3}He target and the latter the scattering of ^{4}He scattered particles on a very thin C layer, placed close to the detector. A special device, made of a thin copper tube with a collimator on both apertures (one facing the beam and the other close to the C foil), was machined by the INFN Genova workshop and it will be positioned inside the gas target at 20^o with respect to the beam axis. The device will be movable along the chamber itself giving the possibility of exploring the whole target length of about 21 cm, viewing approximately 5 cm at each different measurement. The detector, 25 mm^2 surface and 100 μm thickness, will be placed at the end of the target chamber behind a collimator. The angles, distances and collimator diameter were selected in order to maximize the energy of the double scattered alpha particles and to obtain a reasonable final rate on the detector. The detector was selected with an entrance layer as thin as possible in order to loose only a very small fraction of the alpha particle energy and with a relatively small surface to keep its capacitance as low as possible. The preamplifier was developped by the INFN Milano electronic laboratory and it has been tuned to reach the best signal to noise ratio for low energy alpha particles. As a matter of fact, the double scattered particles to be detected will have energies in the range 110-250 keV. The feasibility of such measurement was studied at the Legnaro INFN Laboratory by using a 450 keV ^{4}He beam on a thin C target. The alpha particles back-scattered at 145^o have an energy of about 110 keV. The spectrum measured with the silicon detector (Figure 5) proves the possibility of detecting such low energy alpha particles. The detector and the mechanical device have then been mounted at Gran Sasso Luna facility. This way we could test the electronic noise in the final configuration, i.e. with all the pumps and the calorimeter working and with 1 mbar He gas in the target. The measured noise was, at most, equivalent to 25 keV, well below the energy to be detected.

2.4 Acquisition system

We developped for this measurement a new multi-parametric data acquisition system (DAQ), based on the commercial software Kmax (Sparrow). This software provides an environment for instrument control and data management with high level support for modular instrumentation, event-by-event data acquisition, data sorting, data histogramming and analysis.

We have created a Graphical User Interface to configure independent control panels and distribute them on different pages. This allows a good separation of specific tasks like ADC set-up and Histogram analysis and reduces the risk of unwanted changes of critical parameters. Each page is equipped with control widgets such as buttons, digital displays, meters, etc., associated with Command Sequences to execute specific funtions when the control is activated or its value modified.

The communication to the CAMAC front-end electronics is obtained by the SCSI interface via a SCSI bus crate controller (Jorway 73A). The analog to digital conversion

is based on commercial ADC (ORTEC AD413A) with FERA readout. This ADC has 13 bits conversion range and a total conversion time of 24 μs (without zero suppression). ADC readout is performed by a FERA system driver (ORTEC CMC203), that includes a dual port fast memory unit for data buffering. The events are successively read via the CAMAC dataway and stored into the Kmax event data stream. All events are then written to a list mode file (for offline analysis) and sorted into histograms for a run time control of the measurement.

3 The ^{25}Mg(p,γ)^{26}Al reaction

^{25}Mg(p,γ)^{26}Al is the slowest reaction of the Mg-Al cycle, the key one to rule the efficiency of the cycle. The β^+ decay of ^{26}Al ($t_{1/2}$=7·10^5 year) to the excited state of ^{26}Mg gives rise to a 1.8 MeV γ ray, one of the most important line for γ astronomy.

Two are the reasons which makes the low energy measurement of this cross section so relevant: the 1.8 MeV full sky map taken by the satellites which look at the γ sky and the anomalous meteoritic abundance of ^{26}Mg.

The reaction is going to be studied first in Bochum, down to the center of mass energy of 180 keV, with a germanium detector. The results of these measurements, mainly the ones on the beam induced background, will point to the detector to be used in the underground measurement al low energy: either germanium array or large BGO.

4 Electron screening for deuterated metals

For nuclear reactions studied in the laboratory the target nuclei and the projectiles are usually in the form of neutral atoms or molecules and ions, respectively. The electron clouds surrounding the interacting nuclei reduce the height of the Coulomb barrier and lead to a higher cross section, $\sigma_{\rm s}(E)$, than would be the case for bare nuclei, $\sigma_{\rm b}(E)$, with an exponential enhancement factor:

$$f_{\rm lab}(E) = \sigma_{\rm s}(E)/\sigma_{\rm b}(E) \simeq E(E+U_{\rm e})^{-1}\exp(\pi\eta\, U_{\rm e}/E), \qquad (2)$$

where $U_{\rm e}$ is an electron screening potential energy and η is the Sommerfeld parameter.

Recently, the electron screening effect on the $d(d,p)t$ reaction has been studied with deuterium implanted in various metals [17] [18]. The resulting $S(E)$ data show an exponential enhancement, however the extracted U_e values are about one order of magnitude larger than the value U_e =25±5 eV found in the corresponding gas target experiment [19]. In order to test these surprising results, we started already three years ago a complete experimental program at the 100 kV accelerator of the Bochum Tandem Laboratory [20][21][22].

In particular, we have studied the electron screening effect on the $d(d,p)t$ reaction in about 60 deuterated elements. As compared to measurements performed with a gaseous deuterium target, a large effect has been observed in all the metals [23], while a small (gaseous) effect is found for the insulators and semiconductors. In addition, we measured the screening for the metals Co and Pt as a function of the sample temperature, between

20 °C and 340 °C. All data show a decrease of the screening, i.e. the U_e value, with increasing temperature [23].

In summary, all data on the enhanced electron screening in deuterated metals can be explained quantitatively by the Debey model applied to quasi-free metallic electrons.

References

[1] R. Bonetti et al. (LUNA Coll.), Phys. Rev. Lett. 82(1999)5205

[2] C. Casella et al. (LUNA Coll.), Nucl. Phys. A 706(2002)203

[3] A. Formicola et al. (LUNA Coll.) Phys. Lett. B 591(2004)61

[4] C. Angulo and P. Descouvemont, Nucl. Phys. A 690(2001)755

[5] A.M. Mukhamedzhanov et al., Phys. Rev. C 67(2003)065804

[6] E.G. Adelberger et al., Rev. Mod. Phys. 70(1998)1265

[7] C. Angulo et al. (NACRE Coll.), Nucl. Phys. A 656(1999)3

[8] G. Imbriani et al. (LUNA Coll.), Astronomy and Astrophysics 420(2004)625

[9] S. Degl'Innocentiet al., Phys. Lett. B 590(2004)13

[10] J.N. Bahcall and M. Pinsonneault, Phys. Rev Lett. 92(2004)121301

[11] J.N. Bahcall et al., astro-ph/0412440

[12] U. Schroeder et al., Nucl. Phys. A 467(1987)240.

[13] C. Casella et al. (LUNA Coll.), Nucl. Instr. Meth. A 489(2002)160

[14] J.Gorres et al., Nucl. Instr. Meth. 177(1980)295

[15] G. Fiorentini et al., astro-ph/0310753

[16] M. Hilgemeier et al., Z. Phys. A 329(1988)243

[17] H. Yuki et al., JETP Lett. 68(1998)823

[18] K. Czerski et al., Europhys. Lett. 54(2001)449

[19] U. Greife et al., Phys. A 351(1995)107

[20] F. Raiola et al., Eur. Phys. J. A 13(2002)377

[21] F. Raiola et al., Phys. Lett. B 547(2002)193

[22] F. Raiola et al., Eur. Phys. J. A19(2004)283

[23] F. Raiola et al., submitted to Phys. Lett. B

5 Publications and Conferences

1. A. Formicola et al., "Astrophysical S-factor of $^{14}N(p,\gamma)^{15}O$", Phys. Lett. B 591(2004)61
2. G. Imbriani et al., "The bottleneck of the CNO burning and the age of the Globular Clusters", Astronomy and Astrophysics 420(2004)625
3. D. Bemmerer et al., "Feasibility of low energy radiative capture experiments at the LUNA underground accelerator facility", submitted to Eur. Phys. J
4. F. Raiola et al., "Electron screening in $d(d,p)t$ for deuterated metals: temperature effects", submitted to Phys. Lett. B
5. C. Broggini, XXI Int. Conf. on Neutrino Phy. and Astr., Neutrino 2004, Paris
6. C. Broggini, Work. on Frontier objects in Astrophys. and Part. Phys., Vulcano
7. C. Broggini, Work. on Exp. Nucl. Astr., Chall. and Opportunities, Karlsruhe
8. C. Broggini, NOW2004, Neutrino Oscillation Workshop, Otranto
9. F. Confortola, XC Congresso della Soc. Italiana di Fisica, Brescia
10. F. Confortola, 21st Meeting Between Astrophysicists and Nuclear Physicists, Brussel
11. P. Corvisiero, 19th European Conf. on few-body problems in physics, Groningen
12. P. Corvisiero, INPC 2004, Goteborg
13. H. Costantini, Nuclei in the Cosmos, 8th Int. Symp. on Nucl. Astr., Vancouver
14. A. Formicola, Annual Meeting of the German Physical Society, University of Cologne
15. G. Gervino, II Int. Work. DICE2004, Castello di Piombino, Piombino
16. C. Gustavino, Vth Rencontres du Vietnam, Part. Phys. and Astrophysics, Hanoi
17. R. Menegazzo, 21st Meeting Astrophysicists and Nuclear Physicists, Brussel
18. P. Prati, ECT Work.: "Advances and Challenges in Nucl. Astrophysics", Trento
19. P. Prati, 5th Italy-Japan Symp., Rec. Achiev. and Perspect. in Nucl. Phys., Napoli
20. C. Rolfs, Granada workshop on nuclear astrophysics, Granada
21. F. Strieder, Annual Meeting of the German Physical Society, University of Cologne
22. F. Strieder, Forschungszentrum Rossendorf, Dresden
23. F. Terrasi, 5th It.-Japan Symp., Rec. Achiev. and Perspect. in Nucl. Phys., Napoli
24. H.P. Trautvetter, ECT Work.,"Adv. and Chall. in Nucl. Astrophysics", Trento

THEORY GROUP

R.Aloisio, Z.Berezhiani, V.Berezinsky, P. Ciarcelluti, M. P. Costantini, G. Di Carlo, A.Galante, L. Gianfagna, A.F.Grillo, F.Mendez, F. Nesti, N. Rossi, A. Sakharov, F.Vissani.

The activity of the group in year 2004 has concerned research in the fields: Astroparticle Physics (mainly in Iniziativa Specifica FA51), Particle Phenomenology (mainly in IS PI21) and Computer simulations of Lattice Gauge Theory (in IS GS11). In addition, a research activity on Planck Scale Kinematics and Phenomenology is continuing, also partly included in year 2004 in IS GS11.

In 2005 a partial rearrangement of IS will take place: IS GS11 ceases activity and the scientific activity on lattice field theory will take place in IS PI12, while a new IS (comprising also Roma1 and SISSA groups), GS51, has been started, devoted to Phenomenology near the Planck Scale.

The activities are more specifically reported below.

1 Astroparticle Physics

The Astroparticle group of LNGS in 2004 included R.Aloisio, V.Berezinsky, M.L.Costantini, F.Vissani and visitors V.Dokuchaev (Institute for Nuclear Research, Moscow), Yu.Eroshenko (Institute for Nuclear Research, Moscow), B.Hnatyk (Lviv University, Ukraine), S.Grigorieva (Institute for Nuclear Research, Moscow) and A.Gazizov (DESY, Germany). The group worked in close collaboration with A.Vilenkin (Tufts University, USA), M.Kachelriess (MPI, Munich), P.Blasi (Arcetri Observatory, Firenze), G.Senjanović (ICTP, Trieste), A.Strumia (Pisa University) and others

Scientific work

The main field of the work is astroparticle physics, including neutrino oscillations, physics in underground detectors, massive neutrinos, ultra high energy cosmic rays, topological defects, and high energy neutrino astrophysics. From several works finished in 2004 two following results can be mentioned

In the work by Aloisio and Berezinsky the diffusive propagation of UHECR in the intergalactic magnetic fields has been systematically studied. The propagation theorem is proved, according to which diffuse spectrum has a universal form independent of the mode of propagation, when distance between sources becomes much smaller than all propagation lengths. The spectra in diffusion approximation are calculated analytically. The paper is published in Ap.J. 612 (2004) 900.

In a series of works by Aulakh, Bajc, Melfo, Senjanović and Vissani, fermion masses and in particular neutrino masses in SO(10) are investigated. Interesting indications for type

II seesaw were obtained. In order to exploit the predictions of the minimal supersymmetric SO(10) model, a detailed calculation of the mass spectrum has been performed (Phys.Rev. D70, 035007).

Conferences, seminars and other activities

R.Aloisio works as the scientific secretary of the LNGS scientific committee

V.Berezinsky works as an editor of Int. Journal "Astroparticle Physics"

F.Vissani works (together with C.Cattadori) as the organizer of the LNGS seminar

R.Alosio presented the invited talks at CRIS-04 conference in Catania,

V.Berezinsky presented the invited lecture at DESY Theory workshop "Particles and Cosmology" in DESY (Germany), a course of lectures at ISAPP 2004 in LNGS, invited talks at the European Conference on Very High Energy Cosmic Rays (Greece), at CRIS-04 (Catania), QUARKS-04 in Moscow and at UHECR symposium at Leeds.

M.L.Costantini gave an invited talk at IFAE 04 in Torino.

F.Vissani was an organizer of ICTP Summer School on Astroparticle Physics in Trieste (with G.Senjanovic et al), and of the Summer Institute at LNGS: Particles Gravity and Cosmology, (with Z.Berezhiani et al). He acted as a convenor of Parallel Session on "Absolute Neutrino Masses" at NOW2004, Otranto (with A.Giuliani). F.Vissani presented an invited talk at ECT* (Trento) for the International Workshop on Fundamental Interactions, and a summary talk for the working group on "Flavors and neutrinos" at the "4th meeting EuroGDR Supersymmetry", in LNF (Frascati).

Journal and Proceedings publications in 2004

1. R. Aloisio, V. Berezinsky, M. Kachelriess,
FRAGMENTATION FUNCTIONS IN SUSY QCD AND UHECR SPECTRA PRODUCED IN TOP-DOWN MODELS
Phys.Rev. D69 (2004) 094023

2. R. Aloisio, V. Berezinsky,
DIFFUSIVE PROPAGATION OF UHECR AND THE PROPAGATION THEOREM
Astroph. J, 612 (2004) 612.

3. R. Aloisio, P. Blasi, A. V. Olinto,
NEUTRALINO ANNIHILATION AT THE GALACTIC CENTER REVISITED
JCAP 0405 (2004) 007

4. R. Aloisio,
MULTIWAVELENGTH OBSERVATION OF WIMP ANNIHILATION
Proceedings of 10th Marcel Grossman Meeting

5. R. Aloisio, V. Berezinsky, M. Kachelriess,
ULTRA HIGH ENERGY COSMIC RAY SPECTRA IN TOP-DOWN MODELS

6. V.S.Berezinsky, S.I.Grigorieva, B.I.Hnatyk,
EXTRAGALACTIC UHE PROTON SPECTRUM AND PREDICTION FOR IRON NUCLEI FLUX AT $10^8 - 10^9$ GeV Astropart.Phys. 21 (2004) 617-625

7. V.Berezinsky, A.Gazizov, S. Grigorieva,
PROPAGATION AND SIGNATURES OF ULTRA HIGH ENERGY COSMIC RAYS
Nucl. Phys B (Proc. Suppl) 136 (2004) 147.

8. V. Berezinsky, V. Dokuchaev, Y. Eroshenko,
COSMOLOGICAL ORIGIN OF SMALL-SCALE CLUMPS AND DM ANNIHILATION
Proceedings of the 6th RESCEU International Symposium on "Frontier in Astroparticle Physics and Cosmology", eds. K. Sato and S. Nagataki (Universal Academy Press Inc.: Tokyo, Japan, 2004), p241-248

9. M. L. Costantini, A. Ianni, F. Vissani,
SN1987A AND THE PROPERTIES OF NEUTRINO BURST
Phys.Rev. D70 (2004) 043006

10. F. Cavanna, M. L. Costantini, O. Palamara, F. Vissani,
NEUTRINOS AS ASTROPHYSICAL PROBES
Surveys High Energ.Phys. 19 (2004) 35-54

11. F. Vissani,
NEUTRINOS MASSES AND MIXING: WHAT DO THEY MEAN?
Eur.Phys.J.C33 (2004) 857

12. C.Aulakh, B.Bajc, A.Melfo, G.Senjanović, F.Vissani,
THE MINIMAL SUPERSYMMETRIC GRAND UNIFIED THEORY
Phys.Lett.B588 (2004) 196

13. B.Bajc, A.Melfo, G.Senjanović, F.Vissani,
THE MINIMAL SUPERSYMMETRIC GRNAD UNIFIED THEORY Phys.Rev.D70 (2004) 035002

14. B.Bajc, G.Senjanović, F.Vissani,
PROBING THE NATURE OF THE SEESAW IN RENORMALIZABLE SO(10)
Phys.Rev.D70 (2004) 093002

Preprints of 2004

1. R.Aloisio, V.Berezinsky,
ANTI-GZK EFFECT IN ULTRA HIGH ENERGY COSMIC RAYS DIFFUSIVE PROPAGATION
astro-ph/0412578

2. V.Berezinsky, V.Dokuchaev,
HIGH-ENERGY NEUTRINOS AS OBSERVATIONAL SIGNATURE OF MASSIVE BLACK HOLE FORMATION

astro-ph/0401310

3. V.Berezinsky, M.Narayan, F.Vissani,
LOW SCALE GRAVITY AS THE SOURCE OF NEUTRINO MASSES?
hep-ph/0401029

4. M.L.Costantini, F.Vissani,
EXPECTED NEUTRINO SIGNAL FROM SUPERNOVA REMNANT RX J1713.7-3946 AND FLAVOR OSCILLATIONS
astro-ph/0411761

5. M.Cirelli, G.Marandella, A.Strumia, F.Vissani,
PROBING OSCILLATIONS INTO STERILE NEUTRINOS WITH COSMOLOGY, ASTROPHYSICS AND EXPERIMENTS
astro-ph/0403158

6. APS Neutrino Study [with F.Vissani],
THEORY OF NEUTRINOS
hep-ph/0412099

2 Particle Phenomenology

During this year the activity of the group, which included Z. Berezhiani, P. Ciarcellutti, L. Gianfagna, F. Nesti and A. Sakharov, was mainly devoted to different problems of particle astrophysics and cosmology. The following results can be mentioned.

Z. Berezhiani together with A. Dolgov (INFN Ferrara) suggested the mechanism for the generation of the large scale cosmic magnetic fields. The seeds for the cosmic magnetic could be generated in the primeval plasma slightly before hydrogen recombination. Non-zero vorticity, necessary for that, might be created by the photon diffusion in the second order in the temperature fluctuations or by isocurvature perturbations. The spectrum of resulting seed fields was calculated and it was concluded that a reasonable galactic dynamo is needed to amplify the seed fields by 8-9 orders of magnitude in order to explain the magnitudes of coherent magnetic fields in galaxies.

Z. Berezhiani and P. Ciarcelluti have studied cosmological implications of the mirror world, an identical copy of the observed particle world which interacts with the latter only gravitationally. The mirror baryons, being invisible for ordinary observer, could constitute dark matter of the universe, with specific implications for for the large scale structure (LSS) of the Universe and the cosmic microwave background (CMB). It was given a complete numerical calculations by a special computational code for the LSS power spectrum and the CMB angular anisotropies in the cases of dark matter entirely constituted by mirror baryons, and for the case of mixed cold dark matter and mirror dark matter model.

Z. Berezhiani, in collaboration with A. Drago and G. Pagliara (Ferrara), proposed a model to explain the gravitational wave signals observed by EXPLORER and NAUTILUS

detectors during the year 2001. The sudden variations in the composition and structure of an hybrid star can be triggered by its rapid spin-down, induced by r-mode instabilities. The discontinuity of this process is due to the surface tension between hadronic and quark matter and in particular to the overpressure needed to nucleate new structures of quark matter in the mixed phase. The consequent mini-collapses in the star can produce highly energetic gravitational wave bursts.

A. Sakharov with collaborators, J. Ellis (CERN), N.E. Mavromatos (London) and D.V. Nanopoulos (Texas) discussed that possible patterns of violation of the Lorentz invariance and of the equivalence principle due to the interaction of the propagating particle with the foamy space-time fluctuations expected in quantum gravity theories. These violations may not be universal, and different types of energetic particles may violate Lorentz invariance and the equivalence principle by varying amounts. The phenomenological implications of these phenomena were also discussed.

Participation in conferences

Int. Conf. "Frontier Science 2004: Physics and Astrophysics in Space", Monteporzio Catone, Italy, 14-19 June 2004, poster presentation of P. Ciarcelluti "STRUCTURE FORMATION, CMB AND LSS IN MIRROR DARK MATTER SCENARIO"

Gran Sasso Summer Institute on "Particles, Gravity and Cosmology", LNGS, Assergi, Italy, 30 Aug - 10 Sept 2004, talks of P. Ciarcelluti "MIRROR BARYONS AS DARK MATTER", F. Nesti "SO(10) model for fermion masses and mixing" and A. Sakharov "ASTROPHYSICAL PROBES OF QUANTUM GRAVITY"

Int. Workshop on Neutrino Oscillations NOW 2004, Conca Specchiula, Otranto, Italy, 11-17 Sept. 2004, invited talk di F. Nesti "SO(10) MODEL FOR FERMION MASSES AND MIXING"

Int. Workshop on Particle Physics and the Early Universe COSMO'04, Toronto, Canada, 17-21 Sept. 2004, talk di A. Sakharov "ASTROPHYSICAL PROBES OF QUANTUM GRAVITY"

Int. Conf. on "Theoretical Particle Physics and Cosmology", Tbilisi, Georgia, 20-25 Sept. 2004, invited talk di Z. Berezhiani "SUPERSYMMETRIC SO(10) MODEL FOR FERMION MASSES AND MIXING"

DESY Theory Workshop 2004 on Particle Cosmology "Dark Matter, Dark Energy, Early Universe, High Energy Cosmic Rays", DESY, Hamburg, Germany, 28 Sept - 1 Oct 2004, invited talk di A. Sakharov "ASTROPHYSICAL PROBES OF QUANTUM GRAVITY"

Publications

1. Z. Berezhiani, A.D. Dolgov,
GENERATION OF LARGE SCALE MAGNETIC FIELDS AT RECOMBINATION EPOCH
Astropart. Phys. 21, 59-69 (2004)

2. L. Gianfagna, M. Giannotti, F. Nesti,
MIRROR WORLD, SUPERSYMMETRIC AXION AND GAMMA RAY BURSTS,
JHEP 0410, 044 (2004)

3. Z. Berezhiani,
MIRROR WORLD AND ITS COSMOLOGICAL CONSEQUENCES,
Int. J. Mod. Phys. A19, 3775-3806 (2004)

4. Z. Berezhiani, P. Ciarcelluti, D. Comelli, F.L. Villante,
STRUCTURE FORMATION WITH MIRROR DARK MATTER: CMB AND LSS
Int. J. Mod. Phys. D22, 1334-1342 (2004)

5. P. Ciarcelluti,
COSMOLOGY WITH MIRROR DARK MATTER I: LINEAR EVOLUTION OF PERTURBATIONS
Sep 2004. 33pp., e-Print Archive: astro-ph/0409629, accepted in Int. J. Mod. Phys. D

6. P. Ciarcelluti,
COSMOLOGY WITH MIRROR DARK MATTER II: COSMIC MICROWAVE BACKGROUND AND LARGE SCALE STRUCTURE
Sep 2004. 36pp., e-Print Archive: astro-ph/0409630, accepted in Int. J. Mod. Phys. D

7. P. Ciarcelluti,
STRUCTURE FORMATION, CMB AND LSS IN A MIRROR DARK MATTER SCENARIO
Sep 2004. 8pp. e-Print Archive: astro-ph/0409633, to be published in Frascati Physics Series, Proc. Int. Conf. "Frontier Science 2004: Physics and Astrophysics in Space", Monteporzio Catone, Italy, 14-19 June 2004

8. J. Ellis, N.E. Mavromatos, D.V. Nanopoulos, A.S. Sakharov,
SPACE-TIME FOAM MAY VIOLATE THE PRINCIPLE OF EQUIVALENCE
Int. J. Mod. Phys. A19, 4413-4430 (2004)

9. J. Ellis, N.E. Mavromatos, D.V. Nanopoulos, A.S. Sakharov,
SYNCHROTRON RADIATION AND QUANTUM GRAVITY
Nature 428, 386 (2004)

10. J. Ellis, N.E. Mavromatos, D.V. Nanopoulos, A. Sakharov,
BRANY LIOUVILLE INFLATION
New J. Phys. 6, 171 (2004)

1.] M.Yu. Khlopov, S.G. Rubin, A.S. Sakharov,
PRIMORDIAL STRUCTURE OF MASSIVE BLACK HOLE CLUSTERS
Jan 2004. 17pp. e-Print Archive: astro-ph/0401532, accepted in Astropart. Phys.

12. E. Sarkisyan, A.S. Sakharov,
ON SIMILARITIES OF BULK OBSERVABLES IN NUCLEAR AND PARTICLE COLLISIONS
Oct 2004. 14pp. e-Print Archive: hep-ph/0410324

13. A. Drago, G. Pagliara, Z. Berezhiani,

SHORT GRAVITATIONAL WAVE BURSTS INDUCED BY R-MODE SPIN-DOWN OF HYBRID STARS
May 2004. 6pp. e-Print Archive: gr-qc/0405145, to be published in Phys. Rev. D

3 Computer Simulations of Lattice Gauge theories

During year 2004 this activity was pursueded by: G. Di Carlo, A. Galante in collaboration with V. Azcoiti and V. Laliena (Zaragoza).

The activity mainly regarded non-zero baryon density QCD. A new variant of the well known Hasenfraz-Karsch action has been introduced that allows some step forward toward the determination of the critical line in the Temperature-Baryon density plane. Studying a system in an extended parameter space, an easier, and possibly safer, extrapolation to the region of non-zero baryon density, impossible to be accessed with standard numerical schemes, should be attained. A study in three dimensional Gross-Neveu model and in 4 Flavours QCD has produced encouraging results; the method and these results are the subject of a paper that has appeared in JHEP[2] and of two talks given at the LATTICE 2004 Conference[4,5].

A further report[3], in which the study of the deconfinig phase transition of 4 Flavours QCD is extended in the Temperature-Chemical potential plane up to values of the quark chemical potential as large as 270 MeV, is in advanced stage of preparation. We find a clear first order line separating the usual chiral broken phase from a chiral symmetrical deconfined phase, that should be a quark-gluon plasma phase.

We plan to extend the use of this approach to the more physically interesting case of 2+1 flavours; moreover we are considering the possibility of using it for the study of condensed matter systems described by a partition function with a complex action, like the repulsive Hubbard model that is considered as a paradigm model for superconductor with high critical temperature (H-Tc superconductivity).

Journal and Proceedings publications in 2004

1. V. Azcoiti, G. Di Carlo, A. Galante,V. Laliena,
THETA DEPENDENCE OF CP^9 MODEL
Phys. Rev. D69 (2004) 056006.
2. V. Azcoiti, G. Di Carlo, A. Galante,V. Laliena,
FINITE DENSITY QCD: A NEW APPROACH
JHEP 0412 (2004) 010
3) V. Azcoiti, G. Di Carlo , A. Galante , V Laliena,
PHASE DIAGRAM OF QCD WITH FOUR QUARK FLAVOURS AT FINITE TEMPERATURE AND BARYON DENSITY
in preparation.
4) V. Azcoiti,G. Di Carlo, A. Galante, V. Laliena,
TESTING NEW STRATEGIES IN FINITE DENSITY
Talk presented at Lattice2004, Fermilab, June 21-26, 2004, to appear in Nucl.Phys. B(Proc.Suppl), hep-lat/0409160:.

5)V. Azcoiti, G. Di Carlo, A. Galante, V. Laliena,
NEW IDEAS IN FINITE DENSITY QCD
, Talk presented at Lattice2004, Fermilab, June 21-26, 2004, to appear in Nucl.Phys. B(Proc.Suppl), hep-lat/0409158.
6) V. Azcoiti, G. Di Carlo, A. Galante, V. Laliena,
NEW ADVANCES IN NUMERICAL SIMULATIONS OF θ-VACUUM SYSTEMS
LATTICE 03, Tsukuba, July 2003, Nucl. Phys. B129-130 (Proc. Suppl.) (2004) 680.

4 Planck Scale Kinematics and Phenomenology

This activity during 2004 was included in IS GS11. From 2005 a new IS has been formed (GS51, national coordinator A.F.Grillo, with sections in Roma1 and Trieste) completely devoted to this research theme. and concerned the analysys of phenomenological consequences, in particular in Ultra High Energy Cosmic Ray Physics, of possible departures from (special) relativistic invariance at energy-momentum scales near the Planck Mass. The persons involved are R. Aloisio (partly, main activity in FA51), A. Galante (partly), A. Grillo and F. Mendez, in collaboration with P. Blasi (IAF, Arcetri) and P.L. Ghia (IFSI and INFN Torino).

The activities in 2004 mainly involved the analysis of the so-called Doubly (or Deformed) Special Relativity-DSR models which are momentum space relativistic theories where, apart from the (low energy) speed of light, there exist a second invariant qantity chosen to be the Planck mass. These theories are expected to incorporate some aspects of Quantum Gravity.

A. Grillo has been invited to give lectures on the subject at the 49th Karpacz School held in February 2004 in Ladek Zdnoy (Poland). A. Grillo has given an invited talk at the Vulcano 2004 workshop, while A. Galante has been invited to report at CRIS 2004 in Catania.

Journal and Proceedings publications in 2004

1. R. Aloisio, P. Blasi, A. Galante, P.L. Ghia, A.F. Grillo,
QUANTUM-GRAVITY PHENOMENOLOGY AND HIGH ENERGY PARTICLE PROPAGATION.
Nucl.Phys. Proc.Suppl. 136: 344-349, 2004 Catania 2004, "GZK and surroundings" 344-349 e-Print Archive: astro-ph/0410413
2)R. Aloisio, A. Galante, A.F. Grillo, E. Luzio, F. Mendez,
APPROACHING SPACE TIME THROUGH VELOCITY IN DOUBLY SPECIAL RELATIVITY.
Phys. Rev. D70: 125012,2004 e-Print Archive: gr-qc/0410020
3)R. Aloisio, J.M. Carmona, J.L. Cortes, A. Galante, A.F. Grillo, F. Mendez,
PARTICLE AND ANTIPARTICLE SECTORS IN DSR1 AND KAPPA-MINKOWSKI SPACE-TIME.
Published in JHEP 0405:028, 2004 e-Print Archive: hep-th/0404111
4)R. Aloisio, P. Blasi, A. Galante, A.F. Grillo,
PHENOMENOLOGY OF SPACE-TIME FLUCTUATIONS.

10th Marcel Grossmann Meeting on Recent Developments in Theoretical and Experimental General Relativity, Gravitation and Relativistic Field Theories (MG X MMIII), Rio de Janeiro, Brazil, 20-26 Jul 2003. e-Print Archive: gr-qc/0401082
5)J. Gamboa, M. Loewe, F. Mendez,
QUANTUM THEORY OF TENSIONLESS NONCOMMUTATIVE P-BRANES.
Phys.Rev.D70:106006,2004
6)Jose Manuel Carmona, Jose Luis Cortes, Ashok Das, Jorge Gamboa,
Fernando Mendez MATTER-ANTIMATTER ASYMMETRY WITHOUT DEPARTURE FROM THERMAL EQUILIBRIUM.
e-Print Archive: hep-th/0410143
7)Ashok Das, Jorge Gamboa, Fernando Mendez, Justo Lopez-Sarrion,
CHIRAL BOSONIZATION FOR NONCOMMUTATIVE FIELDS.
JHEP 0405:022,2004 e-Print Archive: hep-th/0402001

UNDERSEIS - Underground Seismic Array

M. Abril[a], G. Alguacil[a], W. De Cesare[b], C. Fischione[c], M. Martini[b], R. Muscente[d], P. Rotella[c], R. Scarpa[e], F. Tronca[d]

[a] Istituto Andaluz de Geofisica - Granada, Spain
[b] Osservatorio Vesuviano, INGV - Napoli, Italy
[c] Dipartimento di Fisica, Università dell'Aquila - Italy
[d] Parco Scientifico e Tecnologico d'Abruzzo - L'Aquila, Italy
[e] Dipartimento di Fisica, Università di Salerno - Italy

Abstract

This report describes a geophysical instrument under installation in the underground physics laboratories of Gran Sasso (LNGS-INFN), located in the seismic zone of central Apennines, Italy. This instrument is aimed to monitor seismic radiation with very high sensitivity; it is a small aperture seismic array composed by 20 three-components short period seismomenters (Mark L4C-3D).

1 Introduction

The physics of earthquakes is based on the measurements of radiated seismic waves and ground displacement associated with this phenomena. The inertial pendulum is the oldest and most diffused instrument used to measure the main features of seismic waves. The advantages of this instrument are the simplicity of the theory, the high sensitivity, the robust design and the simple calibration methods, in spite of the quite reduced frequency band and linearity (Wielandt, 1983). Other instruments based on different physical principles, such as strainmeters and gyroscopes, are only partially used by seismologists (Benioff, 1935; Farrell, 1969, Aki and Richards, 1980). Networks of short period seismometers are as far the most diffused system to monitor local and regional seismicity (Lee and Stewart, 1981). Broad-band instruments make up a powerful system to study the details of seismic sources and also to study large earthquakes at global scale (Lee and Wallace, 1995). Moreover arrays of seismometers and accelerometers are used to study the details of sources and radiation patterns of earthquakes, nuclear underground explosions and volcanic activity (Bolt, 1976; Chouet, 1996). Strainmeters and tiltmeters (Agnew, 1986) are used to study the lower frequencies radiated from seismic sources and allow to detect slow earthquakes and strain steps (i.e. anelastic deformations around seismic sources).

At present, the seismic activity of central Apennines, and in particular of the Gran Sasso massif, is relatively low, as compared to other seismically active areas of Europe such as Turkey or central Greece. Three seismic swarms were monitored in August 1992, June 1994 and October 1996, with the largest earthquake having $M_L = 4.2$. These swarms are the largest events occurred since 1985 in this region. However, this area experienced destructive earthquakes in the past: a magnitude 7 event occurred in 1703. Close to this region, the 1915 Avezzano earthquake ($M_S = 6.8$) occurred, causing more than 15,000 victims. On average, about 1 microearthquake per day above $M_L = 1$ occurs, within 20 Km radius from LNGS-INFN. The facilities existing in the laboratories, and the seismotectonics features of the Gran Sasso massif, make them an excellent site for studies related to the physics of earthquake source, wave propagation in a complex medium and seismic monitoring.

2 The Underground Seismic Array

A seismic array is a set of seismographs distributed over an area of the Earth's surface at spacing narrow enough so that the signal waveform may be correlated between adjacent seismometers (Aki and Richards, 1980).

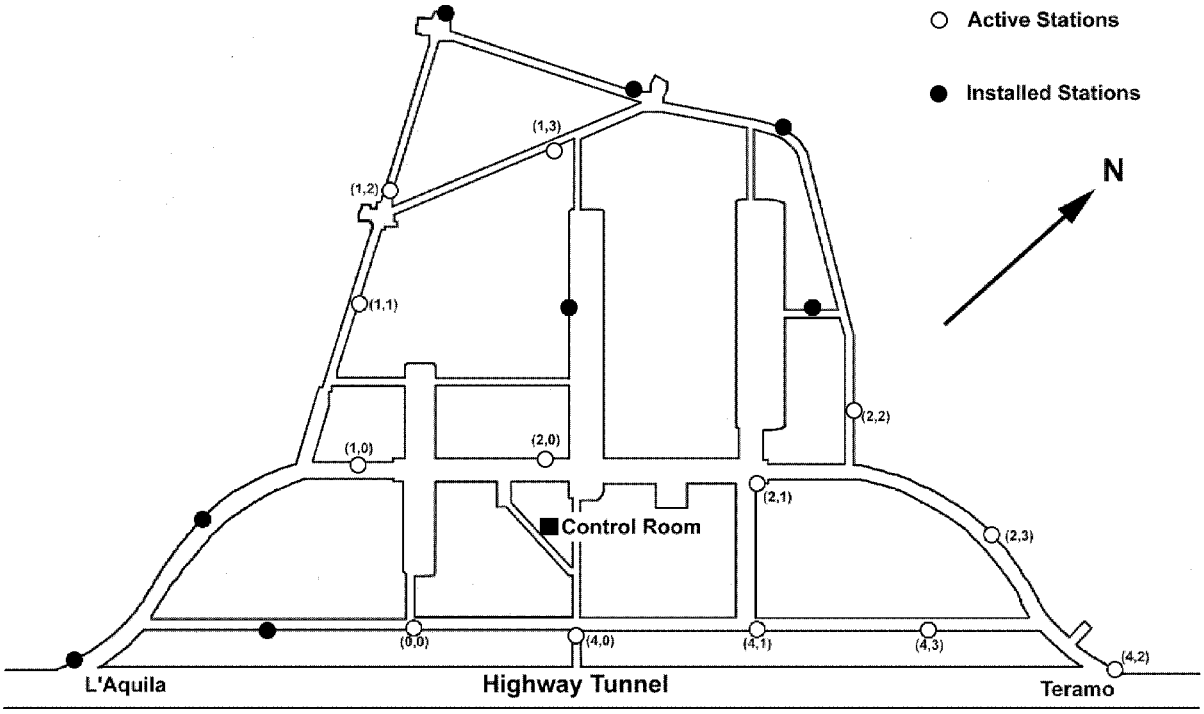

Figure 1: Map of the Underground Seismic Array. The notation (n,m) shows the line number (n) and the station number (m).

The main advantages of such geometrical configurations are the improvement of signal-to-noise ratio and the possibility to perform a detailed analysis of wave propagation and

composition. The development of large aperture seismic arrays such as LASA in Montana, USA (Green et al., 1965) and NORSAR in Norway (Kedrov and Ovtchinnikov, 1990) led to many improvements in the knowledge of Earth's structure (Aki et al., 1977) other than to monitor underground nuclear explosions. More recent developments of these arrays make use of low number of sensors and smaller apertures in order to reduce the effects of lateral inhomogeneities (Mykkeltveit, 1985). The need to monitor local seismicity in the very large underground physics laboratories of LNGS-INFN led to some preliminary experiments to understand the site response; a L-shaped array along the way to access the LNGS, having spatial extension of 10.5 km, was deployed in 1993. This array was formed by 17 three component short period digital seismic stations spaced 600 m (De Luca et al., 1997). In the same region, from 1992 to 2001, a digital seismic network equipped with a maximum of 18 3D short period seismic stations was installed.

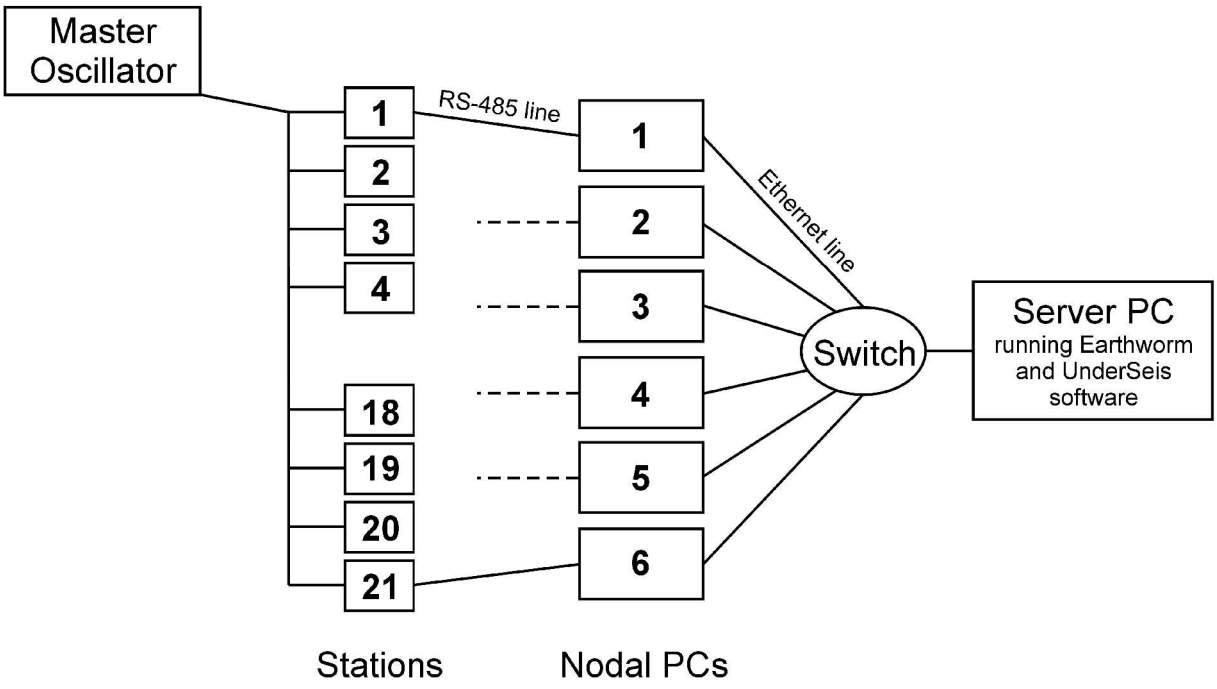

Figure 2: Block scheme of the Underground Seismic Array.

Two important features of seismic response in the region have been observed: a substantial homogeneity of spectral response from underground linear array and, for S waves, an average decrease of amplitudes with respect to the data recorded at the surface, in the band 1-8 Hz. In particular the horizontal components are reduced by a factor 4, while the vertical one is reduced by a factor 2. Strain monitoring, in the same region, through GPS, EDM, levellings and microgravimetry has been also carried out. The optimal array configuration is generally obtained through a compromise between the need of sampling coherent portions of wavefield and the need for adequate azimuthal resolution, which requires a large antenna aperture. However we were limited by the geometry of the underground laboratories, so we decided to start with 21 receivers. In consequence, the underground seismic array has a small aperture (400 m x 600 m) and the average spacing

between the short period seismographs is about 90 m (Fig. 1), thus allowing to resolve wavelenghts in the range $180 - 500m$ which correspond to phase velocity $0.2 - 10\frac{km}{sec}$ (the frequency response is in the range $1 - 20Hz$).

Figure 3: Underground Seismic Array components and control room.

At present, we have completely developed the electronics and the data acquisition system, which constitute an original project. Each seismometer is linked, through a 24 bits A/D board, to an industrial PC which is, in its turn, connected to a serial communication line via a RS-485 standard. The PCs placed at the head of each serial line (nodal PCs) transmit data to a server through an ethernet network. Time syncronization is provided by a Master Oscillator controlled by an atomic clock (Fig. 4). Earthworm package is used for real time data processing and transmission. High quality data have been recorded since May 2002, including local and regional earthquakes. In particular the 31 October, 2002, Molise ($M_W = 5.8$ earthquake) and its aftershocks have been recorded at this array. Array techniques such as polarization and frequency-slowness analyses with the ZLCC algorithm indicate the high performance of this array, as compared to the national seismic network,

for analyzing the main source parameters of earthquakes located up to distances of few hundreds of km.

Figure 4: The Underground Array seismic stations acquire data simultaneously. The time syncronization is controlled by a Master Oscillator: it takes a 1 pps input signal from an atomic clock located in the labs and generates codified time signals which are send to the single stations in order to provide simultaneous data acquisition.

3 Preliminary data analysis.

3.1 Polarization analysis Molise earthquake, ($M_W = 5.8$) October 31, 2002.

A preliminary polarization analysis was performed on data from the Molise October 31 mainshock (only 4 stations active at the moment). The location results are in good agreement with the National network location.

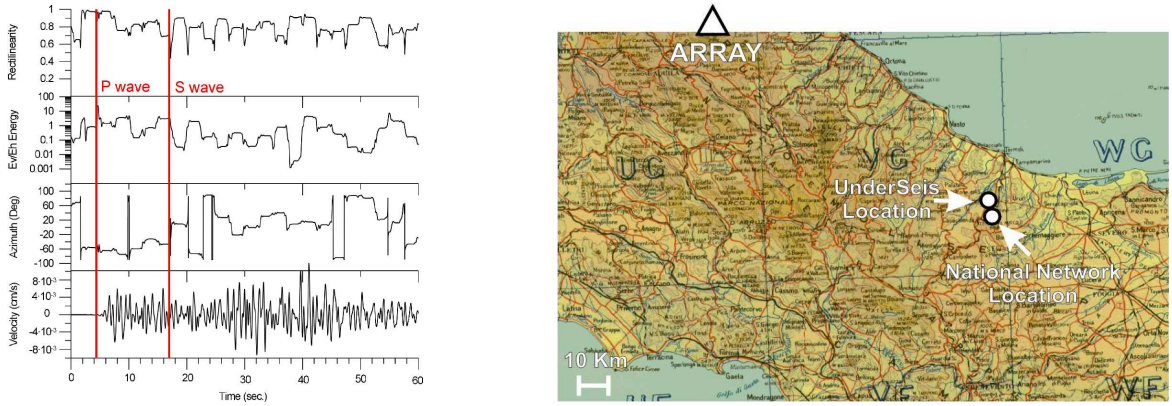

Figure 5: Polarization analysis results and location map.

3.2 ZLCC analysis local earthquake, ($M = 2.4$) November 20, 2002.

A preliminary ZLCC analysis was performed on data from a local earthquake, November 20, 2002 (13 stations active at the moment). The location results are in good agreement with the National network location.

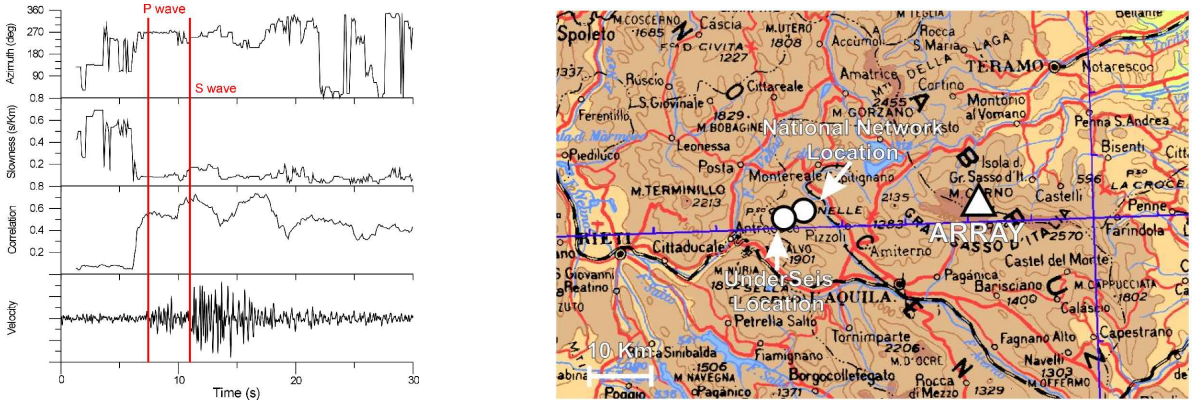

Figure 6: ZLCC analysis results and location map.

3.3 wwwunderseis.lngs.infn.it

Since a couple of months is finally available the internet site of the UnderSeis experiment. In this site you can find the detailed description of the instrument, a bulletin of the last events recorded, a database of the recorded events and some interactive java applets able to do an online analysis of the events stored in the database.

4 Conclusions.

The dense small-aperture seismic array is a powerful high-sensitivity instrument designed and presently under realization and installation. The underground location beneath Gran Sasso has been proved to be an ideal site, in spite of the local noise sources due to human activity, to record seismic waves from regional and local microearthquakes. Its location is rather unique in the world, due to the close distance from active fault segments of the seismogenetic zone of central Apennines. The scientific goals of this multichannel seismic observational system are an improvement of the seismotectonical knowledge of a high potential seismogenetic region of Italy, and a very detailed study of the physical processes leading to seismic ruptures in the area. Moreover the installation of this underground seismic array will allow an experimental study of wave propagation phenomena within a complex medium, leading to results of relevant interest for seismic hazard evaluation in areas of complex geology, for physics of earthquake process, with particular reference to the study of rupture preparation and for all relevant precursory phenomena, seismic radiation and earthquake waveform modeling for hazard reduction.

References

[1] Agnew D. C., 1986. *Strainmeters and tiltmeters*. Rev. Geophys. 24, 579-624.

[2] Aki K. and Richards P., 1980. *Quantitative seismology: Theory and methods*. Freeman, San Francisco, California, 932 pp.

[3] Aki K., Christoffersson A. and Husebye E. S., 1977. *Determination of the three dimensional seismic structure of the lithosphere*. J. Geophys. Res. 82, 277-296.

[4] Benioff H., 1935. *A linear strain seismographs*. Bull. Seism. Soc. Am. 25, 283-309.

[5] Bolt B. A., 1976. *Nuclear explosions and earthquakes. The parted veil*. Freeman, San Francisco.

[6] Capon J., 1969. *High resolution frequency-wavenumber spectrum analysis*. Proc. IEEE 57, 1408-1418.

[7] Chouet B., 1996. *New methods and future trends in seismological volcano monitoring*. In "Monitoring and mitigation of volcano hazards", R. Scarpa and R. Tilling (Eds.), Springer-Verlag, New York.

[8] Chouet B., G. Saccorotti, M. Martini, P. Dawson, G. De Luca, G. Milana and R. Scarpa (1997). *Source and path effects in the wavefields of tremar and explosions at Stromboli Volcano, Italy*. J. Geophys. Res., 102, 15,129-15,150.

[9] De Luca G., Scarpa R., Del Pezzo E. and Simini M., 1997. *Shallow structure of Mt. Vesuvius volcano, Italy, from seismic array analysis*. Geophys. Res. Lett. 24,481-484.

[10] De Luca G., Del Pezzo E., Di Luccio F., Margheriti L., Milana G. and Scarpa R., 1998. *Site response study in Abruzzo (centraI Italy): underground array versus surface stations*. J. Seismol., 2, 223-226.

[11] Farrell W. E., 1969. *A gyroscopic seismometer: measurements during the Borrego earthquake*. Bull. Seism. Soc. Am. 59, 1239-1245.

[12] Green Jr., Frosh B. A. and Romney C. F., 1965. *Principles of an experimental large aperture seismic array*. Proc. IEEE 53, 1821-1833.

[13] Kedrov O. K. and V. M. Ovtchinnikov, 1990. *An on-line analysis system for three component seismic data: method and preliminary results*. Bull. Seism. Soc. Am. 80, 2053-2071.

[14] Lee W. H. K. and Stewart S. W., 1981. *Principles and applications of microearthquake networks*. Academic Press, New York, 293 pp.

[15] Lay T. and Wallace T. C., 1995. *Modern Global Seismology*. Academic Press, New York, 517 pp.

[16] Mikkeltveit S., 1985. *A new regional array in Norway: design, work and results from analysis of data from a provisional installation, in The Vela Program*. A twenty- Five Review of Basic Research, edited by U. A. Kerr (Defence Advanced Research Project Agency), 546-553.

[17] Milana G., Barba S., Del Pezzo E. and Zambonelli E., 1996. *Site response from ambient noise measurements: new perspectives from an array study in CentraI Italy*. Bull. Seism. Soc. Am. 86, 1-9.

[18] Schmidt R. O., 1986. *Multiple emitter location and signal parameter estimation*. IEEE Trans Antennas Propagation 34, 276-280.

[19] Wielandt E., 1983. *Design principles of electronic inertial seismometers*. In H. Kanamori and E. Boschi (Eds.) "Earthquakes: Observation, Theory and Interpretation". Proc. Int. School of Phys. "E. Fermi", North Holland, Amsterdam.

[20] Scarpa R. et al., 2004. *UNDERSEIS: The Underground Seismic Array*. Seism. Res. Lett. Volume 75, n. 4, July/August 2004.

Heidelberg - Moscow Experiment. First Evidence for Lepton Number Violation and the Majorana Character of Neutrinos

H.V. Klapdor-Kleingrothaus[a] and I.V. Krivosheina[a,b]

[a] Max-Planck Institut für Kernphysik, Heidelberg, Germany
[b] Institute of Radiophysical Research, Nishnij Novgorod, Russia
Spokesman of the Collaboration; E-mail: H.Klapdor@mpi-hd.mpg.de
Home-page: http://www.mpi-hd.mpg.de.non_acc/

Abstract

Nuclear double beta decay provides an extraordinarily broad potential to search for beyond-standard-model physics. *The occurrence of the neutrinoless decay* ($0\nu\beta\beta$) mode has fundamental consequences: first **total lepton number is not conserved**, and second, **the neutrino is a Majorana particle**. Further the effective mass measured allows to put an absolute scale of the neutrino mass spectrum. In addition, *double beta experiments yield sharp restrictions also for other beyond standard model physics*. These include SUSY models (R-parity breaking and conserving), leptoquarks (leptoquark-Higgs coupling), compositeness, left-right symmetric models (right-handeld W boson mass), test of special relativity and of the equivalence principle in the neutrino sector and others. **First evidence for neutrinoless double beta decay was given in 2001, by the HEIDELBERG-MOSCOW experiment**. The HEIDELBERG-MOSCOW experiment is the *by far most sensitive* $0\nu\beta\beta$ experiment since more than 10 years. It was operating 11 kg of enriched ^{76}Ge in the GRAN SASSO Underground Laboratory. The analysis of the data taken from 2 August 1990 - 20 May 2003, is presented here. The collected statistics is 71.7 kg y. The background achieved in the energy region of the Q value for double beta decay is 0.11 events/ kg y keV. *The two-neutrino accompanied half-life* is determined on the *basis of more than 100 000 events* to be $(1.74._{-0.16}^{+0.18}) \times 10^{21}$ *years*. **The confidence level for the** *neutrinoless* **signal has been improved to a 4.2 σ level**. The half-life is $T_{1/2}^{0\nu} = (1.19_{-0.23}^{+0.37}) \times 10^{25}$ *years*. **The effective neutrino mass deduced is (0.2 - 0.6) eV (99.73% c.l.)**, with the consequence that neutrinos have degenerate masses. The sharp boundaries for other beyond SM physics, mentioned above, are comfortably competitive to corresponding results from high-energy accelerators like TEVATRON, HERA, etc.

1 Introduction

Since 40 years huge experimental efforts have gone into the investigation of nuclear double beta decay which probably is the most sensitive way to look for (total) lepton number violation and probably the only way to decide the Dirac or Majorana nature of the neutrino. It has further perspectives to probe also other types of beyond standard model physics. This thorny way has been documented recently in some detail [27, 36, 29].

The HEIDELBERG-MOSCOW experiment, proposed already in 1987[8], has been looking for double beta decay of ^{76}Ge since August 1990 until November 30, 2003 in the Gran Sasso Underground Laboratory. It was using the largest source strength of all double beta experiments at present, and has reached a record low level of background, not only for Germanium double beta decay search. It has demonstrated this during more than a decade of measurements and is since more then ten years the most sensitive double beta decay experiment worldwide. The experiment was since 2001 operated only by the Heidelberg group, which also performed the analysis of the experiment from its very beginning.

The experiment has been carried out with five high-purity p-type detectors of Ge enriched to 86% in the isotope ^{76}Ge (in total 10.96 kg of active volume). These were the first enriched high-purity Ge detectors ever produced. So, the experiment starts from the cleanest thinkable source of double beta emitter material, which at the same time is used as detector of $\beta\beta$ events.

A description of the experimental details has been given in [1, 2, 3, 9]. This will not be repeated in this report, instead we concentrate on the results and their consequences. But let us just mention some of the most important features of the experiment here.

1. Since the sensitivity for the $0\nu\beta\beta$ half-life is $T^{0\nu}_{1/2} \sim a \times \epsilon\sqrt{\frac{Mt}{\Delta E B}}$ (and $\frac{1}{\sqrt{T^{0\nu}}} \sim \langle m_\nu \rangle$), with a denoting the degree of enrichment, ϵ the efficiency of the detector for detection of a double beta event, M the detector (source) mass, ΔE the energy resolution, B the background and t the measuring time, the sensitivity of our 11 kg *of enriched* ^{76}Ge experiment corresponds to that of an at least 1.2 ton *natural* Ge experiment. After enrichment - the other most important parameters of a $\beta\beta$ experiment are: energy resolution, background and source strength.

2. The high energy resolution of the Ge detectors of 0.2% or better, assures that there is no background for a $0\nu\beta\beta$ line from the two-neutrino double beta decay in this experiment, in contrast to most other present experimental approaches, where limited energy resolution is a severe drawback.

3. The efficiency of Ge detectors for detection of $0\nu\beta\beta$ decay events is close to 100 % (95%, see [2]).

4. The source strength in this experiment of 11 kg is the largest source strength ever operated in a double beta decay experiment.

5. The background reached in this experiment, is 0.113±0.007 events /kg y keV (in the period 1995-2003) in the $0\nu\beta\beta$ decay region (around $Q_{\beta\beta}$). This is the lowest limit ever obtained in such type of experiment.

6. The statistics collected in this experiment during 13 years of stable running is the largest ever collected in a double beta decay experiment. The experiment took data during $\sim$ 80% of its installation time.

7. The Q value for neutrinoless double beta decay has been determined recently with high precision [31].

2 Data and Analysis

The total sum spectrum measured over the full energy range of all five detectors for the period November 1995 to May 2003 is shown in Ref. [1, 2, 3]. The identified lines are indicated with their source of origin (in [17]).

Fig. 1 shows the part of the spectrum around $Q_{\beta\beta}$, in the range 2000 - 2060 keV, measured in the period August 1990 to May 2003 and November 1995 to May 2003. Non-integer numbers in the sum spectra are simply a binning effect.

The spectra shown in Fig. 1 result from summing the individual runs taken with the detectors (2142 runs for the right spectrum), and finally summing for the right spectrum the sum spectra of the different detectors (in total 9 570 data sets).

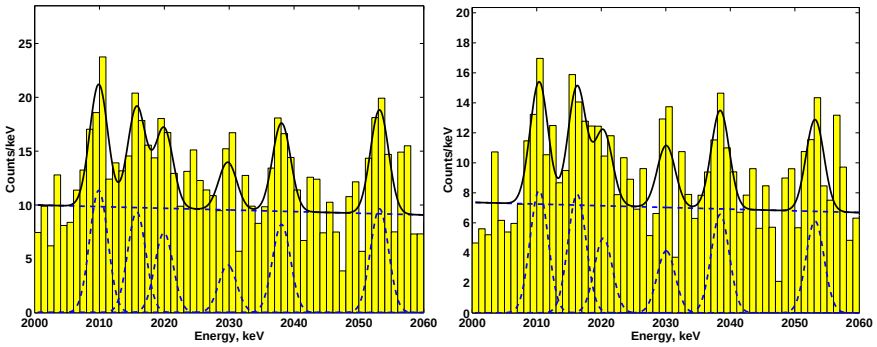

Figure 1: The total sum spectrum of all five detectors (in total 10.96 kg enriched in ^{76}Ge), for the period: left: November 1990 to May 2003 (71.7 kg y) in the range 2000 - 2060 keV right: - November 1995 to May 2003 (56.66 kg y) in the range 2000 - 2060 keV and its fit (see text and [1, 2, 3]).

In the measured spectra (Fig.1) we see in the range around $Q_{\beta\beta}$ the ^{214}Bi lines at 2010.7, 2016.7, 2021.8, 2052.9 keV, the line at $Q_{\beta\beta}$ and a candidate of a line at $\sim$ 2030 keV (see also [12, 18])[1]. The spectra have been analyzed by *different methods*: Least Squares Method, Maximum Likelihood Method (MLM) and Feldman-Cousins Method. The analysis is performed *without subtraction of any background*. We always process background-plus-signal data since the difference between two Poissonian variables does *not* produce a Poissonian distribution [32]. This point has been sometimes overlooked. So, e.g., in [41] a formula is developed making use of such subtraction and as a consequence the analysis given in [41] provides overestimated standard errors.

The improvement of the present analysis (for details see [1, 2, 3]) compared to our paper from 2001 [4, 5, 6], is described in detail in [1, 2, 3]. One reason lies in the stricter conditions for accepting data into the analysis. The second reason is a better energy

[1]The objections raised after our first paper [4] concerning these lines and other points, by Aalseth et al. (Mod.Phys.Lett.A17:1475-1478,2002 and hep-ex/0202018 v.1), **have been shown to be wrong already** in [7] and in [6], and later in [12] and [18]. So this 'criticism' was already history, before we reached the higher statistics presented in this paper.

calibration of the individual runs. The third reason is the refined summing procedure of the individual data sets mentioned above and the correspondingly better energy resolution of the final spectrum. The signal strength seen in the *individual* detectors in the period 1990-2003 is shown in [1].

3 Results

3.1 Full Spectra

Fig.1 shows together with the measured spectra in the range around $Q_{\beta\beta}$ (2000 - 2060 keV), the result of the fit of this energy range. A linear decreasing shape of the background as function of energy was chosen corresponding to the complete simulation of the background performed in [17] by GEANT4 (see Fig.2). In the fits in Fig.1, the peak positions, widths and intensities are determined simultaneously, and also the *absolute* level of the background.

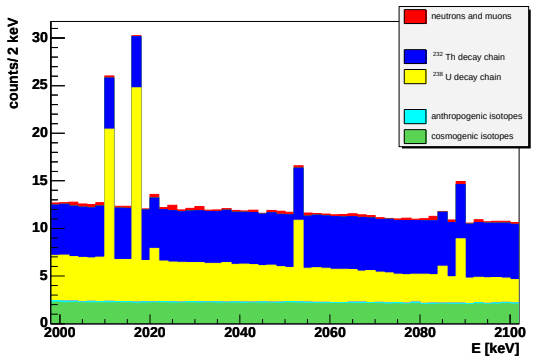

Figure 2: Monte Carlo simulation of the background in the range of $Q_{\beta\beta}$ by GEANT4, including all known sources of background in the detectors and the setup. This simulation [17] seems to be the by far most extensive and complete one ever made for any double beta experiment. The background around $Q_{\beta\beta}$ is expected to be flat, the only lines visible should be some weak ^{214}Bi lines (from [17]).

The signal at $Q_{\beta\beta}$ in the full spectrum at $\sim$ 2039 keV **reaches a 4.2 σ confidence level** for the period 1990-2003 (28.8 $\pm$ 6.9) events, and of 4.1 σ for the period 1995-2003 (23.0 $\pm$5.7) events. The results of the new analysis are consistent with the results given in [4, 5, 6]. The intensities of all other lines are given in [2, 3].

We have given a detailed comparison of the spectrum measured in this experiment with other Ge experiments in [18]. It is found that the most sensitive experiment with natural Ge detectors [13], and the first experiment using enriched (not yet high-purity) ^{76}Ge detectors [14] find essentially the same background lines (^{214}Bi etc.), but *no* indication for the line near $Q_{\beta\beta}$. This is consistent with the rates expected from the present experiment due to their lower sensitivity: $\sim$0.7 and $\sim$1.1 events, respectively. It is also consistent with the result of the IGEX ^{76}Ge experiment [15], which collected only a statistics of 8.8 kg y, before finishing in 1999, and which should expect $\sim$ 2.6 events, which they might

have missed. Their published half-life limit is overestimated as result of an arithmetic mistake (see [16]).

3.2 Time Structure of Events

There are at present *no other* running experiments (with reasonable energy resolution) which can - not to speak about their lower sensitivity - *in principle* give *any further-going* information in the search for double beta decay than shown *up to this point:* namely a line at the correct energy $Q_{\beta\beta}$. Also most future projects cannot determine more. The HEIDELBERG-MOSCOW experiment developed some *additional tool* of independent verification. The method is to exploit the time structure of the events and to select $\beta\beta$ events by their pulse shape exploiting neuronal net methods. The result is shown in Fig.3 (see [1, 2, 3]). Except a line which sticks out sharply near $Q_{\beta\beta}$, *all* other lines are very strongly suppressed. The probability to find $\sim$7 events in two neighboring channels from background fluctuations is

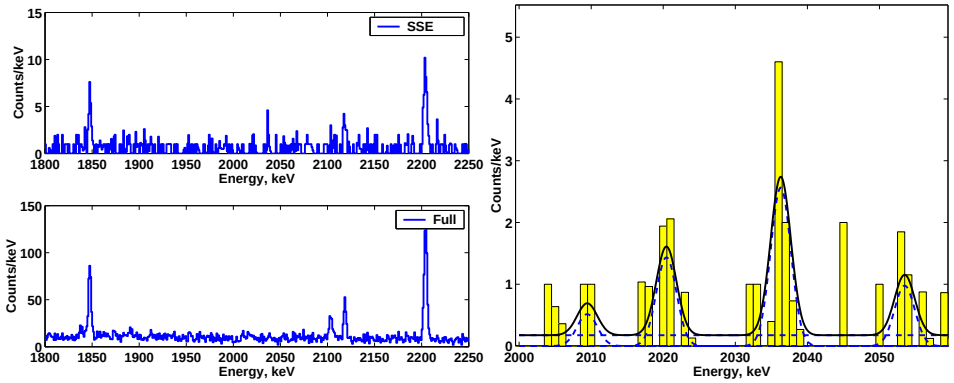

Figure 3: Left top: The pulse-shape selected spectrum of single site events measured with detectors 2,3,4,5 from 1995-2003, see text. Left below: The full spectrum measured with detectors 2,3,4,5 from 1995-2003. Right: As in left top figure, but energy range 2000-2060 keV, to be compared to Fig. 1, right (see [1, 2, 3]).

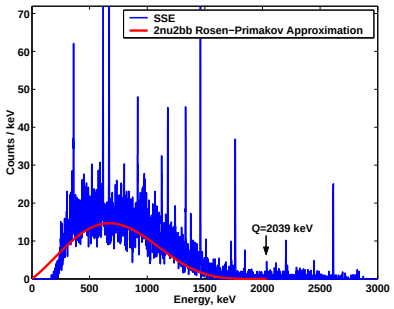

Figure 4: The pulse-shape selected spectrum measured with detectors 2,3,4,5 from 1995$\div$2003 in the energy range of (100$\div$3000) keV, see text and [1].

calculated to be 0.013%. Thus, we see a line near $Q_{\beta\beta}$ at a 3.8σ level.

The energy of this line determined by the spectroscopy ADC is slightly below $Q_{\beta\beta}$, but still within the statistical variation for a weak line (see [18]). This can be understood

as result of ballistic effects (for details see[24]). Obviously the method also fulfills the criterium to select properly the *continuous* $2\nu\beta\beta$ *spectrum* (see Fig. 4).

The 2039 keV line as a single site events signal cannot be the double escape line of a γ-line whose full energy peak would be expected at 3061 keV, since no indication of a line is found there in the spectrum measured up to 8 MeV (see [2, 3]).

4 Half-Life of Neutrinoless Double Beta Decay of ^{76}Ge

We have shown in chapter 3.2 that the signal found at $Q_{\beta\beta}$ is consisting of single site events and is not a γ line. The signal does not occur in the Ge experiments *not* enriched in the double beta emitter ^{76}Ge [13, 11, 18], while neighbouring background lines appear consistently in these experiments.

On this basis we translate the observed numbers of events into half-lives for neutrinoless double beta decay. In Table 1 we give the half-lives deduced from the full data sets taken in the years 1995-2003 and in 1990-2003 and of some partial data sets. In all cases the signal is seen consistently. Also given are the deduced effective neutrino masses. The result obtained **is consistent** with the limits given earlier [10], and with the results given in [4, 5, 6].

Concluding **we confirm**, with **4.2σ (99.9973% c.l.) probability**, our claim from 2001 [4, 5, 6] **of first evidence for the neutrinoless double beta decay mode**.

5 Consequences for Particle Physics, Neutrino Physics and Other Beyond Standard Model Physics

Lepton number violation: *The most important consequence* of the observation of neutrinoless double beta decay is, that **lepton number is not conserved**. This is fundamental for particle physics, and for the early Universe, e.g. for leptogenesis.

Majorana nature of neutrino: Another fundamental consequence is that **the neutrino is a Majorana particle** (see, e.g. [38, 39, 40]). Both of these conclusions are *independent of any* discussion of nuclear matrix elements. It has been discussed that the Majorana nature of the neutrino tells us that spacetime does realize a construct that is central to construction of supersymmetric theories [33].

Effective neutrino mass: The matrix element enters when we derive a *value* for the effective neutrino mass - making the *most natural assumption* that the $0\nu\beta\beta$ decay amplitude is dominated by exchange of a massive Majorana neutrino. The half-life for the neutrinoless decay mode is under this assumption given by [22, 23]

$$[T^{0\nu}_{1/2}(0^+_i \to 0^+_f)]^{-1} = C_{mm}\frac{\langle m\rangle^2}{m_e^2} + C_{\eta\eta}\langle\eta\rangle^2 + C_{\lambda\lambda}\langle\lambda\rangle^2 + C_{m\eta}\langle\eta\rangle\frac{\langle m\rangle}{m_e} + C_{m\lambda}\langle\lambda\rangle\frac{\langle m\rangle}{m_e} + C_{\eta\lambda}\langle\eta\rangle\langle\lambda\rangle,$$

$$\langle m\rangle = |m^{(1)}_{ee}| + e^{i\phi_2}|m^{(2)}_{ee}| + e^{i\phi_3}|m^{(3)}_{ee}|, \quad (1)$$

where $C_{mm}, C_{\eta\eta}, ...$ denote nuclear matrix elements squared, which can be calculated, (see, e.g. [27, 35, 34], for a review). Ignoring contributions from right-handed weak currents, on the right-hand side of eq.(1) only the first term remains.

Table 1: Half-life for the neutrinoless decay mode and deduced effective neutrino mass from the HEIDELBERG-MOSCOW experiment (the nuclear matrix element of [22] is used). Shown are in addition to various accumulated total measuring times also the results for four *non-overlapping* data sets: the time periods 11.1995-09.1999 and 09.1999÷05.2003 for *all* detectors, and the time period 1995÷2003 for two sets of detectors: 1+2+4, and 3+5. *) denotes best value.

Significance $[kg\,y]$	Detectors	$T^{0\nu}_{1/2}$ $[y]$ (3σ range)	$\langle m \rangle$ [eV] (3σ range)	Conf. level (σ)
Period 8.1990 ÷ 5.2003				
71.7	1,2,3,4,5	$(0.69 - 4.18) \times 10^{25}$ $1.19 \times 10^{25*}$	(0.24 - 0.58) 0.44^{*}	4.2
Period 11.1995 ÷ 5.2003				
56.66	1,2,3,4,5	$(0.67 - 4.45) \times 10^{25}$ $1.17 \times 10^{25*}$	(0.23 - 0.59) 0.45^{*}	4.1
51.39	2,3,4,5	$(0.68 - 7.3) \times 10^{25}$ $1.25 \times 10^{25*}$	(0.18 - 0.58) 0.43^{*}	3.6
42.69	2,3,5	$(0.88 - 4.84) \times 10^{25}$ (2σ range) $1.5 \times 10^{25*}$	(0.22 - 0.51) (2σ range) 0.39^{*}	2.9
28.27	1,2,4	$(0.67 - 6.56) \times 10^{25}$ (2σ range) $1.22 \times 10^{25*}$	(0.19 - 0.59) (2σ range) 0.44^{*}	2.5
28.39	3,5	$(0.59 - 4.29) \times 10^{25}$ (2σ range) $1.03 \times 10^{25*}$	(0.23 - 0.63) (2σ range) 0.48^{*}	2.6
Period 11.1995 ÷ 09.1999				
26.59	1,2,3,4,5	$(0.43 - 12.28) \times 10^{25}$ $0.84 \times 10^{25*}$	(0.14 - 0.73) 0.53^{*}	3.2
Period 09.1999 ÷ 05.2003				
30.0	1,2,3,4,5	$(0.60 - 8.4) \times 10^{25}$ $1.12 \times 10^{25*}$	(0.17 - 0.63) 0.46^{*}	3.5

Using the nuclear matrix element from [22, 23], we conclude from the half-life given above the effective mass $\langle m \rangle$ to be $\langle m \rangle = (0.2 \div 0.6)\,\mathrm{eV}$ (99.73% c.l.), with **best value of $\sim$ 0.4 eV**.

The matrix element given by [22] was the *prediction closest to* the *later* measured $2\nu\beta\beta$ decay half-life of $(1.74^{+0.18}_{-0.16}) \times 10^{25}$ y [17, 9]. It underestimates the 2ν matrix elements by 32% and thus these calculations will also underestimate (to a smaller extent) the matrix element for $0\nu\beta\beta$ decay, and consequently correspondingly overestimate the (effective) neutrino mass. Allowing conservatively for an uncertainty of the nuclear matrix element of $\pm$ 50% the range for the effective mass may widen to $\langle m \rangle = (0.1 \text{ - } 0.9)\,\mathrm{eV}$ (99.73% c.l.).

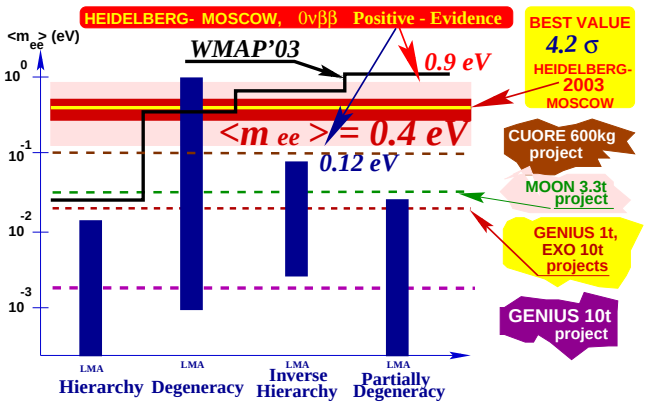

Figure 5: The impact of the evidence obtained for neutrinoless double beta decay (best value of the effective neutrino mass $\langle m \rangle = 0.4\,\mathrm{eV}$, 3σ confidence range (0.1 - 0.9) eV - allowing already for an uncertainty of the nuclear matrix element of $\pm$ 50%) on possible neutrino mass schemes. The bars denote allowed ranges of $\langle m \rangle$ in different neutrino mass scenarios, still allowed by neutrino oscillation experiments (see [26, 47]). All models except the degenerate one are excluded by the new $0\nu\beta\beta$ decay result. Also shown is the exclusion line from WMAP, plotted for $\sum m_\nu < 1.0\,eV$ [48] (which is according to [61] too strict). WMAP does not rule out any of the neutrino mass schemes. Further shown are the expected sensitivities for the future potential double beta experiments CUORE, MOON, EXO and the 1 ton and 10 ton project of GENIUS [27, 29, 55] (from [47]).

Neutrinos degenerate in mass: With the value deduced for the effective neutrino mass, the HEIDELBERG-MOSCOW experiment excludes several of the neutrino mass scenarios allowed from present neutrino oscillation experiments (see Fig. 5, and Fig.1 in [47]), – allowing only for degenerate mass scenarios [26, 47, 25].

Other beyond Standard Model Physics: Assuming *other* mechanisms to dominate the $0\nu\beta\beta$ decay amplitude, which have been studied extensively in our group, and other groups, in recent years, the result allows to set stringent limits on parameters of SUSY models, leptoquarks, compositeness, masses of heavy neutrinos, the right-handed W boson and possible violation of Lorentz invariance and equivalence principle in the neutrino sector. For a further discussion and for references we refer to [27, 28, 29, 30].

6 Conclusion - Perspectives

Recent information from many *independent* sides seems to condense now to a nonvanishing neutrino mass of the order of the value found by the HEIDELBERG-MOSCOW experiment. This is the case for the results from CMB, LSS, neutrino oscillations, particle theory and cosmology (for a detailed discussion see [1, 2, 3]). To mention a few examples: Neutrino oscillations require in the case of degenerate neutrinos common mass eigenvalues of m $>$ 0.04 eV. An analysis of CMB, large scale structure and X-rays from clusters of galaxies yields a 'preferred' value for $\sum m_\nu$ of 0.6 eV [49]. WMAP yields $\sum m_\nu < 1.0$ eV [48], SDSS yields $\sum m_\nu < 1.7$ eV [61]. Theoretical papers require degenerate neutrinos with m $>$ 0.1, or 0.2 eV or 0.3 eV [44, 50, 51, 43], and the recent alternative cosmological concordance model requires relic neutrinos with mass of order of eV [52]. As mentioned already earlier [37, 2] the results of double beta decay and CMB measurements together indicate that the neutrino mass eigenvalues have the same CP parity, as required by the model of [44]. Also the approach of [60] comes to the conclusion of a Majorana neutrino. The Z-burst scenario for ultra-high energy cosmic rays requires $m_\nu \sim$ 0.4 eV [45, 46], and also a non-standard model (g-2) has been connected with degenerate neutrino masses $>$0.2 eV [42]. The neutrino mass determined from $0\nu\beta\beta$ decay is consistent also with present models of leptogenesis in the early Universe [56].

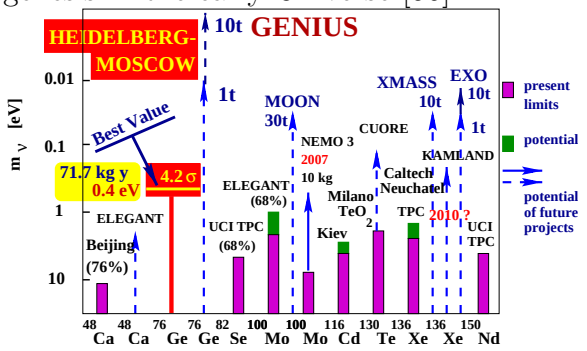

Figure 6: Present sensitivity, and expectation for the future, of the most promising $\beta\beta$ experiments. Given are limits for $\langle m \rangle$, except for the HEIDELBERG-MOSCOW experiment where the measured *value* is given (3σ c.l. range and best value). Framed parts of the bars: present status; not framed parts: future expectation for running experiments; solid and dashed lines: experiments under construction or proposed, respectively. For references see [27, 5, 6].

Future: With the HEIDELBERG-MOSCOW experiment, *the era of small smart experiments is over.* Fig. 6 shows the present result and a comparison to the potential of the most sensitive other double beta decay experiments and the possible potential of some future projects. It is visible that the presently running experiments have hardly a chance, to reach the sensitivity of the HEIDELBERG-MOSCOW experiment. New approaches and considerably *enlarged* experiments would be required to fix the $0\nu\beta\beta$ half life with higher accuracy. **This will, however, only marginally improve the precision of the deduced neutrino mass**, because of the uncertainties in the nuclear matrix elements, which probably hardly can be reduced to less than 50%.

One has to keep in mind further, that **no more can be learnt** on *other* beyond standard model physics parameters from future more sensitive experiments. The reason is that there is **a half-life** now, and **no more a limit** on the half-life, which could be further reduced.

From future projects one has to require that they should be able to differentiate between a β and a γ signal, or that the tracks of the emitted electrons should be measured. At the same time, as is visible from the present information, the energy resolution should be *at least* in the order of that of Ge semiconductor detectors, or better. These requirements exclude at present calorimeter experiments like CUORE, CUORICINO, which *cannot* differentiate between a β and γ signal, etc, but also experiments like EXO [59], *if* the latter will not be able to reconstruct the tracks of the electrons, as it seems at present. The NEMO project *can* see tracks, but unfortunately has at present only a small efficiency, and a low energy resolution of more than 200 keV. The most sensitive future project, is probably the GENIUS project, proposed already in 1997 [53, 57, 58, 54, 55, 28, 27].

A GENIUS Test Facility, (which could already be used to search for cold dark matter by the annual modulation effect) has started operation with 10 kg of natural Germanium detectors in liquid nitrogen in Gran-Sasso on May 5, 2003 [21, 20, 19].

However, if one wants to get *independent* evidence for the neutrinoless double beta decay mode, one would probably, wish to see the effect in *another* isotope, which would then simultaneously give additional information also on the nuclear matrix elements. In view of these considerations, future efforts to obtain *deeper* information on the process of neutrinoless double beta decay, would require *a new experimental approach, different from all, what is at present persued.*

7 Acknowledgement:

The authors would like to thank all colleagues, who have contributed to the experiment over the last 15 years.

Our thanks extend also to the technical staff of the Max-Planck Institut für Kernphysik and of the Gran Sasso Underground Laboratory. We acknowledge the invaluable support from BMBF and DFG, and LNGS of this project. We are grateful to the former State Committee of Atomic Energy of the USSR for providing the enriched material used in this experiment.

References

[1] H.V. Klapdor-Kleingrothaus, I.V. Krivosheina, A. Dietz et al., Phys. Lett. B 586 (2004) 198-212.

[2] H.V. Klapdor-Kleingrothaus, A. Dietz, I.V. Krivosheina et al., NIM A 522 (2004) 371-406.

[3] H.V. Klapdor-Kleingrothaus, in Proc. of BEYOND03, Castle Ringberg, Germany, 9-14 June 2003, *Springer* (2004), ed. H.V. Klapdor-Kleingrothaus, 307.

[4] H.V. Klapdor-Kleingrothaus et al. Mod. Phys. Lett. A 16 (2001) 2409-2420.

[5] H.V. Klapdor-Kleingrothaus, A. Dietz, I.V. Krivosheina, Part. and Nucl. 110 (2002) 57-79.

[6] H.V. Klapdor-Kleingrothaus, A. Dietz, I.V. Krivosheina, Foundations of Physics 31 (2002) 1181-1223 and Corrigenda, 2003.

[7] H.V. Klapdor-Kleingrothaus et al., hep-ph/0205228

[8] H.V. Klapdor-Kleingrothaus, Proposal, MPI-1987-V17, September 1987.

[9] HEIDELBERG-MOSCOW Coll., Phys. Rev. D 55 (1997) 54.

[10] H.V. Klapdor-Kleingrothaus et al., (HEIDELBERG-MOSCOW Coll.), Eur. Phys. J. A 12, 147 (2001) and in Proc. of 3-rd Int. Conf. DARK2000, H.V. Klapdor-Kleingrothaus, ed., (Springer, Heidelberg, 2001) pp. 520-533.

[11] H.V. Klapdor-Kleingrothaus et al., Nucl. Instr. Meth. 510A (2003) 281.

[12] H.V. Klapdor-Kleingrothaus et al., Nucl. Instr. Meth. 511 A (2003) 335.

[13] D. Caldwell, J. Phys. G 17 (1991) S137-S144.

[14] A.A.Vasenko et al., Mod.Phys.Lett.A5 (1990)1299; I.Kirpichnikov, Preprint ITEP (1991).

[15] C.E. Aalseth et al., Phys. Rev. D65 (2002) 092007.

[16] H.V. Klapdor-Kleingrothaus et al., Phys. Rev. D70 (2004) 078301.

[17] Ch. Dörr, H.V. Klapdor-Kleingrothaus, Nucl. Instr. Meth. A513 (2003) 596.

[18] H.V. Klapdor-Kleingrothaus et al., Phys. Lett. 578 B (2004) 54 and NIM A510 (2003) 281.

[19] H.V. Klapdor-Kleingrothaus, CERN Courier 43 N6 (2003) 9 and hep-ph/0307329, *"'Naked' Crystals go Underground".*

[20] H.V. Klapdor-Kleingrothaus et al., Nucl. Instr. Meth. A 511 (2003) 341-346.

[21] H.V. Klapdor-Kleingrothaus et al., Nucl. Instr. Meth. A 530 (2004) 410-418.

[22] A. Staudt, K. Muto, H.V. Klapdor-Kleingrothaus, Eur. Lett. 13 (1990) 31.

[23] K. Muto, E. Bender, H.V. Klapdor, Z. Phys. A 334 (1989) 187.

[24] H.V. Klapdor-Kleingrothaus et al., in preparation.

[25] H.V. Klapdor-Kleingrothaus, H. Päs, A.Yu. Smirnov, Phys. Rev. D 63 (2001) 073005; in Proc. of DARK'2000, Heidelberg, 10-15 July, 2000, Germany, ed. H.V. Klapdor-Kleingrothaus, Springer, Heidelberg (2001) 420-434.

[26] H.V. Klapdor-Kleingrothaus, U. Sarkar, Mod. Phys. Lett. A 16 (2001) 2469.

[27] H.V. Klapdor-Kleingrothaus, "60 Years of Double Beta Decay - From Nuclear Physics to Beyond the Standard Model", World Scientific, Singapore (2001) 1281 pages.

[28] H.V. Klapdor-Kleingrothaus, Int. J. Mod. Phys. A 13 (1998) 3953.

[29] H.V. Klapdor-Kleingrothaus, Springer Tracts in Modern Physics, 163 (2000) 69-104, Springer-Verlag, Heidelberg, Germany (2000).

[30] H.V. Klapdor-Kleingrothaus, U. Sarkar, hep-ph/0302237.

[31] G. Douysset et al., Phys. Rev. Lett. 86 (2001) 4259;J.G. Hykawy et al., Phys. Rev. Lett. 67 (1991) 1708; G. Audi, A.H. Wapstra, Nucl. Phys. A 595 (1995) 409-480; R.J. Ellis et al., Nucl. Phys. A 435 (1985) 34-42.

[32] M.D. Hannam, W.J. Thompson, Nucl. Instr. Meth. A 431 (1999) 239-251.

[33] D.V. Ahluwalia, in Proc. of BEYOND'02, Oulu, Finland, 2-7 Juni, 2002, IOP, Bristol, 2003, ed. H.V. Klapdor-Kleingrothaus, 143-160; D.V. Ahluwalia, M. Kirchbach, Phys. Lett. B529 (2002) 124.

[34] K. Muto, H.V. Klapdor, in "Neutrinos", Graduate Texts in Contemporary Physics", ed. H.V. Klapdor, Berlin, Germany: Springer (1988) 183-238.

[35] K. Grotz, H.V. Klapdor, "Die Schwache Wechselwirkung in Kern-, Teilchen- und Astrophysik", B.G. Teubner, Stuttgart (1989), "The Weak Interaction in Nuclear, Particle and Astrophysics", IOP Bristol (1990), Moscow, MIR (1992) and China (1998).

[36] H.V. Klapdor-Kleingrothaus, A. Staudt, "Teilchenphysik ohne Beschleuniger", B.G. Teubner, Stuttgart (1995), "Non–Accelerator Particle Physics", IOP Pub., Bristol and Philadelphia (1995) and 2. ed. (1998), Moscow, Nauka, Fizmalit (1998).

[37] H.V. Klapdor-Kleingrothaus, in Proc. of Int. Conf. BEYOND'02, Oulu, Finland, 2-7 Jun. 2002, IOP, Bristol, 2003 ed. H.V. Klapdor-Kleingrothaus, 215.

[38] J. Schechter, J.W.F. Valle, Phys. Rev. D 25 (1982) 2951-2954.

[39] M. Hirsch, H.V. Klapdor-Kleingrothaus, Phys.Lett. B398 (1997) 311; Phys.Rev. D57 (1998) 1947; M. Hirsch, H.V. Klapdor-Kleingrothaus, St. Kolb, Phys.Rev. D57 (1998) 2020.

[40] G. Bhattacharyya, H.V. Klapdor-Kleingrothaus, H. Päs, A. Pilaftsis, Phys. Rev. D 67 (2003) 113001 and hep-ph/0402071 in Proc. of Int. Worksh. on Astr. and HE Phys. (AHEP-2003), Valencia, Spain, 14-18 Oct 2003.

[41] Yu. Zdesenko et al., Phys. Lett. B 546 (2002) 206-215.

[42] E. Ma, M. Raidal, Phys. Rev. Lett. 87 (2001) 011802; Erratum-ibid. 87 (2001) 159901.

[43] E. Ma in Proc. of Intern. Conf. BEYOND'02, Oulu, Finland, 2-7 Jun. 2002, IOP, Bristol, 2003, and BEYOND 2003, Ringberg Castle, Tegernsee, Germany, 9-14 Juni 2003, Springer, Heidelberg, Germany, 2004, ed. H.V. Klapdor-Kleingrothaus.

[44] R.N. Mohapatra, M.K. Parida, G. Rajasekaran, (2003) hep-ph/0301234.

[45] D. Fargion et al., in Proc. of DARK2000, Heidelberg, Germany, July 10-15, 2000, Ed. H.V. Klapdor-Kleingrothaus, *Springer*, (2001) 455-468 and in Proc. of Beyond the Desert 2002, BEYOND02, Finland, June 2002, IOP 2003, and BEYOND03, Ringberg Castle, Tegernsee, Germany, 9-14 Juni 2003, Springer, Germany, 2003, ed. H.V. Klapdor-Kleingrothaus.

[46] Z.Fodor, S.D.Katz, A.Ringwald, Phys.Rev.Lett. 88 (2002) 171101; Z.Fodor et al., *JHEP* (2002) 0206:046; in Proc. of Intern. Conf. Beyond the Desert 02, BEYOND'02, Oulu, Finland, 2-7 Jun 2002, IOP, Bristol, 2003, ed. H V Klapdor-Kleingrothaus and hep-ph/0210123.

[47] H. V. Klapdor-Kleingrothaus, U. Sarkar, Mod. Phys. Letter. A18 (2003) 2243.

[48] S.Hannestad, CAP 0305(2003)920030 004, in Proc. of 4th Int. Conf. BEYOND03, Ringberg Castle, Germany, Springer, Germany, 2003, ed. H.V. Klapdor-Kleingrothaus.

[49] S.W. Allen, R.W. Schmidt, S.L. Bridle, astro-ph/0306386.

[50] K.S. Babu, E. Ma and J.W.F. Valle, Phys. Lett. B 552 (2003) 207-213.

[51] M. Hirsch et al., Phys. Rev. D69 (2004) 093006.

[52] A. Blanchard, M. Douspis, M. Rowan-Robinson, S. Sarkar, astro-ph/0304237.

[53] H.V. Klapdor-Kleingrothaus in Proc. of BEYOND'97, Castle Ringberg, Germany, 8-14 June 1997, ed. by H.V. Klapdor-Kleingrothaus et al.,IOP Bristol (1998) 485-531, and Int. J. Mod. Phys. A13 (1998) 3953.

[54] H.V. Klapdor-Kleingrothaus, J. Hellmig et al.,J. Phys. G24 (1998) 483-516.

[55] H.V. Klapdor-Kleingrothaus et al. MPI-Report MPI-H-V26-1999, hep-ph/9910205, in Proc. of the 2nd Int. Conf. BEYOND'99, Castle Ringberg, Germany, 6-12 June 1999, eds. H.V. Klapdor-Kleingrothaus and I.V. Krivosheina, IOP Bristol (2000) 915-1014.

[56] M.N. Rebelo, Proc. of BEYOND'2003, Castle Ringberg, Germany, July 2003, ed. H.V. Klapdor-Kleingrothaus, Springer, Heidelberg (2004) 267.

[57] H.V. Klapdor-Kleingrothaus, M. Hirsch, Z. Phys. A 359 (1997) 361-372.

[58] J. Hellmig, H.V. Klapdor-Kleingrothaus, Z. Phys. A 359 (1997) 351-359.

[59] G. Gratta, ApPEC Paris, France 22.01.2002, and in Proc. of LowNu2, Dec. 4-5 (2000) Tokyo, Japan, ed: Y. Suzuki, World Scientific (2001) p.98.

[60] R. Hofmann, hep-ph/0401017 v.1.

[61] M. Tegmark et al., astro-ph/0310723, subm. Phys. Rev. D.

List of Edited Proceedings (2004)

1. H.V. Klapdor-Kleingrothaus (ed.), BEYOND the DESERT 2003, Proc. of the Fourth Tegernsee International Conference on Particle Physics Beyond the Standard Model, Accelerator, Non-Accelerator and Space Apporoaches in the New Millenium, Castle Ringberg, Tegernsee, Germany, 9-14 June, 2003, Heidelberg, Germany: Springer (2004) 1117 pp.

2. H.V. Klapdor-Kleingrothaus and D. Arnowitt (eds.), Dark Matter in Astro- and Particle Physics., Proc. of 5th Heidelberg Dark Matter International Conference - DARK2004, Texas, USA, 3 - 9 October, 2004, Heidelberg, Germany: Springer (2005).

List of Publications (2004)

1. H.V. Klapdor-Kleingrothaus, I.V. Krivosheina, A. Dietz, O. Chkvorets, Phys. Lett. B 586 (2004) 198 - 212 and hep-ph/0404088, *"Search for neutrinoless double beta decay with enriched ^{76}Ge in Gran Sasso 1990-2003."*

2. H.V. Klapdor-Kleingrothaus, A. Dietz, I.V. Krivosheina, O. Chkvorets, Nucl. Instrum. Meth. A 522 (2004) 371-406 and hep-ph/0403018, *"Data Acquisition and Analysis of the ^{76}Ge Double Beta Experiment in Gran Sasso 1990-2003."*

3. H.V. Klapdor-Kleingrothaus, I.V. Krivosheina, A. Dietz, C. Tomei, O. Chkvoretz, H. Strecker, INFN, Laboratori Nazionali del Gran Sasso, Annual Report 2003, 109-136 and hep-ph/0404062, *"Search For Neutrinoless Double Beta Decay With Enriched ^{76}Ge 1990-2003 – HEIDELBERG-MOSCOW-Experiment."*

4. H.V. Klapdor-Kleingrothaus, A. Dietz, I.V. Krivosheina, Phys. Rev. D 70 078301 (2004) and hep-ph/0403056, *"Critical View to "The IGEX neutrinoless double beta decay experiment: Prospects for next generation experiments".*

5. G. Bhattacharyya, H.V. Klapdor-Kleingrothaus, H. Päs, A. Pilaftsis, AHEP2003/007 in Electronic proc. of International Workshop on Astroparticle and High-Energy Physics (AHEP-2003), Valencia, Spain, 14-18 Oct 2003 and hep-ph/0402071, *"Double beta decay and the extra-dimensional seesaw mechanism."*

6. H.V. Klapdor-Kleingrothaus, A. Dietz, I.V. Krivosheina, C. Dörr, C. Tomei, Phys. Lett. B 578 (2004) 54-62 and hep-ph/0312171, *"Support of Evidence for Neutrinoless Double Beta Decay."*

7. H.V. Klapdor-Kleingrothaus, in Proc. of 21st International Conference on Neutrino Physics and Astrophysics "Neutrino 2004", 14 - 19 June 2004, Collége de France, Paris, France, World Scientific (2005), *"First evidence for neutrinoless double beta decay, with enriched ^{76}Ge in Gran Sasso 1990-2003."*

List of Conference Contributions 2004

1. H.V. Klapdor-Kleingrothaus, International Workshop "Physics of High Energy Density in Matter", Hirschegg, Austria, 1-6 February 2004, *"New Results from the Search for Neutrinoless Double Beta Decay - and World Status of the Absolute Neutrino Mass."*

2. H.V. Klapdor-Kleingrothaus, at Incontri di Fisica delle Alte Energie (IFAE 2004), Turin, Italy, 14-16 April, 2004, *"Final Results from the Search for Neutrinoless Double Beta Decay (Status of the HEIDELBERG-MOSCOW Experiment 2004)."*

3. H.V. Klapdor-Kleingrothaus, at International Workshop "Fundamental Interactions", ECT, Trento, Italy, 21 -25 June 2004, *"Evidence for Neutrinoless Double Beta Decay - and Consequences."*

4. H.V. Klapdor-Kleingrothaus, at 10th International Symposium on "Particle, Strings and Cosmology" (PASCOS'04), Nath Fest, 16 - 22 August 2004, Boston, USA, World Scientific (2005), eds. P. Nath et al., *"First Evidence for Lepton Number Violation - The ^{76}Ge Double Beta Experiment in Gran Sasso 1990-2003."*

5. H.V. Klapdor-Kleingrothaus, at Fifth International Heidelberg Conference on "Dark Matter in Astro and Particle Physics", DARK 2004, 3 - 9 October 2004, College Station, TX, USA: Springer (2005), eds: H.V. Klapdor-Kleingrothaus and D. Arnowitt, *"First Evidence for Lepton Number Violation - The ^{76}Ge Double Beta Experiment in Gran Sasso 1990-2003."*

6. H.V. Klapdor-Kleingrothaus, at 21st International Conference on Neutrino Physics and Astrophysics "Neutrino 2004", 14 - 19 June 2004, Collége de France, Paris, France, World Scientific (2005), *"First evidence for neutrinoless double beta decay, with enriched ^{76}Ge in Gran Sasso 1990-2003."*

7. H.V. Klapdor-Kleingrothaus, at 5th International Workshop on the Identification of Dark Matter, idm 2004, 6-10 September 2004, Edinburgh Scotland, World Scientific (2005), eds: N. Spooner et al., *"First Evidence for Lepton Number Violation and the Majorana Character of Neutrinos."*

8. H.V. Klapdor-Kleingrothaus, at Second Europhysics Neutrino Oscillation Workshop, NOW 2004, Bari, Italy, September 11-17, 2004, World Scientific (2005), eds: G.L. Fogli et al., *"Neutrinoless Double Beta Decay: Experimental Results (HEIDELBERG-MOSCOW Experiment, Gran Sasso)."*

9. H.V. Klapdor-Kleingrothaus, DPG, Nuclear Physics, Spring Meeting, Köln, Germany, 11 März 2004, *"New Results from the Search for Neutrinoless Double Beta Decay (Status of HEIDELBERG-MOSCOW Experiment 2003)."*

10. H.V. Klapdor-Kleingrothaus, DPG, Teilchenphysik, Spring Meeting, Mainz, Germany, 31 März 2004, *"Final Result of the HEIDELBERG-MOSCOW Double Beta Experiment 1990-2003, Evidence for Neutrinoless Double Beta Decay."*

List of Invited Colloquium and Seminar Talks (2004)

1. H.V. Klapdor-Kleingrothaus, Kolloquium at INFN, GRAN SASSO, Italy, March 2004, *"News from the Search for Neutrinoless Double Beta Decay (Status of the HEIDELBERG-MOSCOW Experiment 2003."*

2. H.V. Klapdor-Kleingrothaus, Meeting of the Fachbeirat MPI für Kernphysik, MPI Heidelberg, GERMANY, 27 April 2004, *"Final Result of the HEIDELBERG-MOSCOW Double Beta Experiment 1990-2003, Evidence for Neutrinoless Double Beta Decay."*

3. H.V. Klapdor-Kleingrothaus, MPI Heidelberg, Germany, 6 May, 2004, *"On the Analysis of the HEIDELBERG-MOSCOW Double Beta Experiment 1990-2003."*

4. H.V. Klapdor-Kleingrothaus, Kolloquium, Universität Giessen, Germany, 17 Mai 2004, *"Evidenz für Neutrinolosen Doppelbetazerfall von Atomkernen-Physik jenseits des Standardmodells der Teilchenphysik."*

5. H.V. Klapdor-Kleingrothaus, Kolloquium at Los Alamos National Lab., USA, 23 August, 2004, *"First Evidence for Neutrinoless Double Beta Decay and Consequences for Particle Physics."*

List of Invited of Talks at Conferences, 2004

1. H.V. Klapdor-Kleingrothaus, International Workshop "Physics of High Energy Density in Matter", Hirschegg, Austria, 1-6 February 2004, *"New Results from the Search for Neutrinoless Double Beta Decay - and World Status of the Absolute Neutrino Mass."*

2. H.V. Klapdor-Kleingrothaus, on Incontri di Fisica delle Alte Energie (IFAE 2004), Turin, Italy, 14-16 Aprily, 2004, *"Final Results from the Search for Neutrinoless Double Beta Decay (status of the HEIDELBERG-MOSCOW Experiment 2004)."*

3. H.V. Klapdor-Kleingrothaus, on International Workshop "Fundamental Interactions", ECT, Trento, Italy, 21 -25 June 2004, *"Evidence for Neutrinoless Double Beta Decay - and Consequences."*

4. H.V. Klapdor-Kleingrothaus, on 10th International Symposium on "Particle, Strings and Cosmology" (PASCOS'04), Nath Fest, 16 - 22 August 2004, Boston, USA, *"First Evidence for Lepton Number Violation - The ^{76}Ge Double Beta Experiment in Gran Sasso 1990-2003."*

5. H.V. Klapdor-Kleingrothaus, on Fifth International Heidelberg Conference on "Dark Matter in Astro and Particle Physics", DARK 2004, 3 - 9 October 2004, College Station, TX, USA, *"First Evidence for Lepton Number Violation - The ^{76}Ge Double Beta Experiment in Gran Sasso 1990-2003."*

6. H.V. Klapdor-Kleingrothaus, on 21st International Conference on Neutrino Physics and Astrophysics "Neutrino 2004", 14 - 19 June 2004, Collége de France, Paris, France, *"First evidence for neutrinoless double beta decay, with enriched ^{76}Ge in Gran Sasso 1990-2003."*

7. H.V. Klapdor-Kleingrothaus, on 5th International Workshop on the Identification of Dark Matter, idm 2004, 6-10 September 2004, Edinburgh Scotland, *"First Evidence for Lepton Number Violation and the Majorana Character of Neutrinos."*

8. H.V. Klapdor-Kleingrothaus, on Second Europhysics Neutrino Oscillation Workshop, NOW 2004, Bari, Italy, September 11-17, 2004, *"Neutrinoless Double beta Decay: Experimental Results (HEIDELBERG-MOSCOW Experiment, Gran Sasso)."*

List of Seminars at Heidelberg University by Prof. H.V. Klapdor-Kleingrothaus (2003-2004)

1. Seminar für Mittlere Semester (WS 2003-2004): "Masse und Natur des Neutrinos"

2. Seminar für Mittlere Semester (SS 2004) "NEUTRINOS - in TEILCHEN - und ASTROPHYSIK"

The GENIUS-Test-Facility and the HDMS Detector in GRAN SASSO

H.V. Klapdor-Kleingrothaus[a,*], I.V. Krivosheina[a,b], V. Mironov[a,c], V. Bednyakov[c], H. Strecker[a] and C. Tomei[a,d]

[a] Max-Planck Institut für Kernphysik, Heidelberg, Germany
[b] Institute of Radiophysical Research, Nishnij Novgorod, Russia
[c] Institute of Nuclear Problems, Dubna, Russia
[d] LNGS, Gran Sasso, Italy,
[*] Spokesman of the Collaboration; E-mail: H.Klapdor@mpi-hd.mpg.de
Home-page: http://www.mpi-hd.mpg.de.non_acc/

Abstract

After the installation of **the first four naked** high purity Germanium detectors in liquid nitrogen in the GRAN SASSO Underground Laboratory in the **GENIUS-Test-Facility** (GENIUS-TF-I) on May 5, 2003, an improved setup **GENIUS-TF-II** with now **six** detectors (15 kg), has been installed on October 14, 2004. This is the first time ever that this novel technique aiming at extreme background reduction in search for rare decays is going to be tested underground. The GENIUS-TF experiment, aims to search for the annual modulation of the Dark Matter signal. The **HDMS (Heidelberg Dark Matter Search experiment)** is the only experiment worldwide, operating *an enriched* ^{73}*Ge detector* and is looking for spin-dependent WIMP-neutron interactions. Results for the measurement Febr. 2001 - July 2003 are presented. **They improve the best existing present limits for low WIMP masses.**

1 Introduction

The present status of further cold dark matter search, of investigation of neutrinoless double beta decay and of low-energy solar neutrinos all require new techniques of *drastic* reduction of background in the experiments. For this purpose we proposed the GENIUS (GErmanium in liquid NItrogen Underground Setup) project in 1997 [2]. The idea is to operate 'naked' Ge detectors in liquid nitrogen (as applied **routinely already for more than 20 years by the CANBERRA Company** for technical functions tests [1]), and thus, by removing all materials from the immediate vicinity of the Ge crystals, to reduce the background considerably with respect to conventionally operated detectors. The liquid nitrogen acts both as a cooling medium and as a shield against external radiactivity.

Monte Carlo simulations for the GENIUS project, and investigation of the *new physics potential* of the project **have been performed in great detail**, and have been published elsewhere [2, 3]. We were **the first** to show (in our HEIDELBERG low-level facility already **in 1997**) that such device can be used for spectroscopy [2].

A small scale version of GENIUS, the GENIUS-Test-Facility has the goal to confirm, the claimed evidence for WIMP dark matter from the DAMA experiment[9]. A detailed description of the GENIUS-TF project is given in[5, 6]. In section 2 we give a decription of GENIUS-TF-II. In section 3 we discuss our recent results from the HDMS experiment operating an enriched ^{73}Ge detector and looking for spin-dependent WIMP-neutron interactions [11, 13].

2 The GENIUS-TF-II Setup

The first four detectors had been installed in liquid nitrogen on 5.05.2003 (see Fig.1-upper part). This has been reported in Cern Courier and [6]. The data acquisition system we developed in 2002 for GENIUS-TF and GENIUS is decribed in detail in [7]. In October 2004 we have installed a new setup GENIUS-TF-II (see Fig 1-lower part, and Fig. 2), containing in contrast to the earlier setup now **six naked** Ge detectors, and, as most important improvement **a second copper vessel**, for further shielding of the Radon (see [4]). Each detector has a weight of 2.5 kg. The depth of the core of the detectors was reduced to guarantee a very low threshold. The inner shielding by bricks of monocristalline Germanium is used also in this setup. First results seem to show a reduction of the ^{222}Rn background.

Figure 1: Upper part - left and right: Taking out the crystals from the transport dewars and fixing the electrical contacts in the clean room of the GENIUS-TF building - from left to right: H. Strecker, I. Krivosheina, H.V. Klapdor-Kleingrothaus. Middle: **The first four contacted naked Ge detectors** before installation into the GENIUS-TF setup. Bottom part - left and right: View from the top of the new GENIUS-TF-II setup in the more Radon-clean beta-beta room, during installation in october 2004. Middle: **The first six contacted naked Ge detectors.**

The problem of diffusion of ^{222}Ra into the setup GENIUS-TF-I *could not be solved satisfactorily* during the first half of 2004. At present, in the low-energy region, microphonics still causes some problem, which would **be, as the ^{222}Ra background, very serious for any full GENIUS-like experiment.** Also this problem was not solved in 2003 and the first half of 2004. We are presently working on the reduction of the problem for the GENIUS-TF-II application in dark matter search, by pulse shape analysis methods.

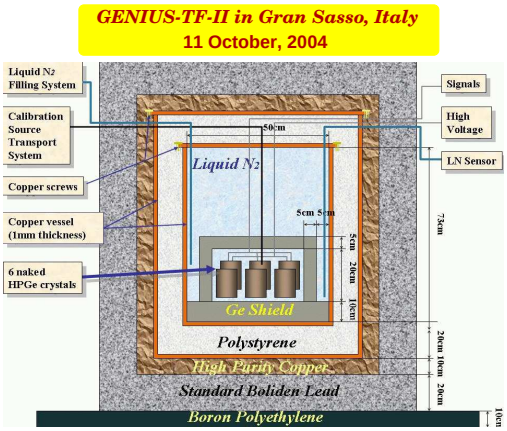

Figure 2: Cross section of the new setup GENIUS-TF-II.

3 The HEIDELBERG Dark Matter Search Experiment (HDMS)

The HDMS project [8] operates a small p-type enriched ^{73}Ge crystal (enriched to 86%), surrounded by a well-type natural Ge crystal, both being mounted in the same copper cryostat. This configuration reduces the background by the shielding provided by the outer crystal, and by the anti-coincidence between the two detectors. The final setup was operated from February 2001 to July 2003 (85.5 kg d). Fig. 3 shows the spectrum collected during this time. The data set is divided into three measuring periods of 30.9, 29.5 and 27.6 kg d, respectively. The latter period is obviously less affected by the background of X-rays from ^{68}Ge.

Fig.3-right, shows the determined limits on WIMP-neutron spin-dependent coupling from the last partial data set, for different values of the spin factors $\langle S_n \rangle$ and $\langle S_p \rangle$. Fig.4, shows the sensitivities of HDMS in the framework of mixed spin-dependent (SD) WIMP-neutron and spin-independent (SI) WIMP-nucleon couplings (see [13]).

4 Conclusions

The GENIUS-TF experiment [6, 5] will be - in addition to DAMA [9] - the *only* experiment which will be able to probe the annual modulation signature in a foreseeable future. The much discussed cryodetector experiments, have at present hardly a chance to look for modulation because the mass used and projected in these experiments is still by far too low (see also [14]).

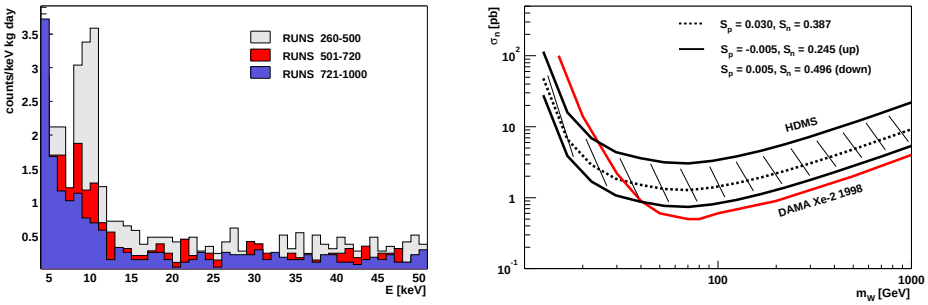

Figure 3: Left: Anti-coincidence spectra from the HDMS experiment (see [11, 12]). Right: Experimental limits on WIMP-neutron SD coupling from the HDMS experiment (data from runs 721-1000). The result of the DAMA Xenon experiment [10] is shown as comparison (from [11, 12]).

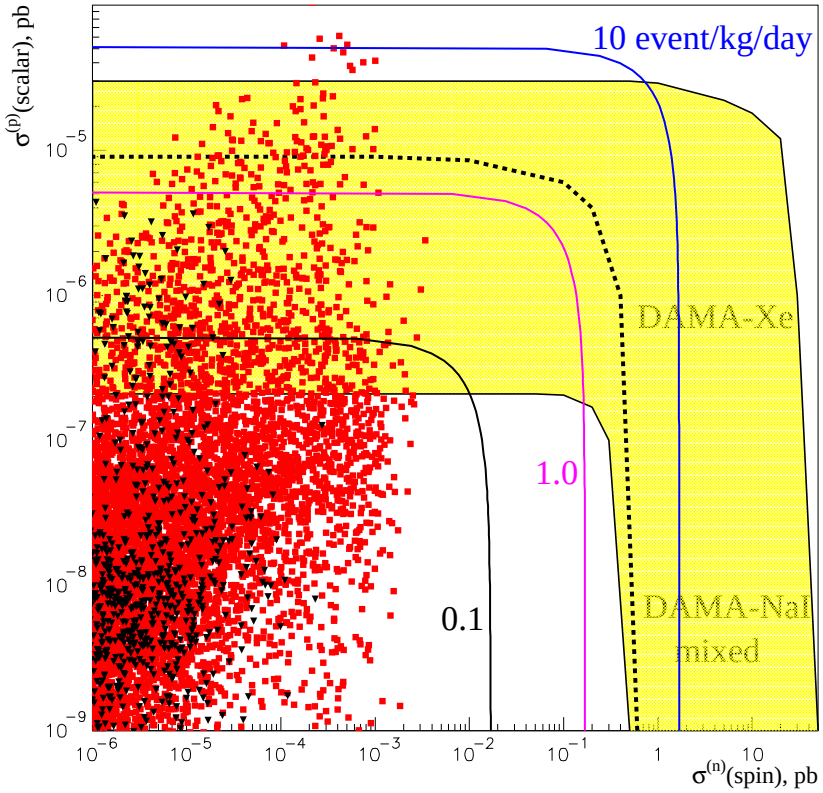

Figure 4: Right: The solid lines (marked with numbers of $R(15, 50)$ in events/kg day) show the sensitivities of the HDMS setup with ^{73}GeV in the framework of mixed SD WIMP-neutron and SI WIMP-nucleon couplings together with the DAMA-NaI allowed region for sub-dominant SD WIMP-neutron coupling ($\theta = \pi/2$). The *present HDMS* result cuts already part of the DAMA allowed range. The scatter plots give correlations between $\sigma^p_{\rm SI}$ and $\sigma^n_{\rm SD}$ in the effMSSM for $m_\chi < 200$ GeV. The squares (red) correspond to sub-dominant relic neutralino contribution $0.002 < \Omega_\chi h_0^2 < 0.1$ and triangles (black) correspond to WMAP relic neutralino density $0.094 < \Omega_\chi h_0^2 < 0.129$. The dashed line from [10] shows the DAMA-^{129}Xe (1998) exclusion curve for $m_{\rm WIMP} = 50$ GeV (from [13]).

A new GENIUS-TF-II setup has been installed in October 14, 2004 with additional shielding against radon and additional two Ge detectors in liquid nitrogen in the GRAN SASSO, increasing the total mass to 15 kg. This is the first time that this novel technique is applied under realistic background conditions of an underground laboratory.

The HDMS (HEIDELBERG Dark Matter Search) project runs an enriched ^{73}Ge detector in Gran Sasso, looking for *spin-dependent* WIMP-neutron interaction. The measurement over the period 2001-2003 improved the best up to now existing limits, by the ^{129}Xe DAMA measurement, in the range of low WIMP masses. At present efforts are going on to improve the sensitivity of HDMS, to be able to restrict the SUSY prediction region (see Fig. 2).

Acknowledgement:
The authors would like to thank their colleaques from MPI Heidelberg: Herrn Theo Apfel, Michael Reissfelder, Michael Saueressig for their help during installation of GENIUS-TF-II. and also the technical staff of the Max-Planck Institut für Kernphysik and of the Gran Sasso Underground Laboratory. We acknowledge the invaluable support from BMBF and DFG, and LNGS of this project. We are grateful to the former State Committee of Atomic Energy of the USSR for providing the monocristalline Ge shielding material used in this experiment.

References

[1] J.Verplancke, **CANBERRA Company,** *priv. commun. 5.03.2004.*

[2] H.V. Klapdor-Kleingrothaus, Proc. of BEYOND'97, Castle Ringberg, eds. H.V. Klapdor-Kleingrothaus et al. *IOP* (1998)485, *Int. J. Mod. Phys.* **A13** (1998) 3953. H.V. Klapdor-Kleingrothaus, J.Hellmig, M.Hirsch, **GENIUS-Proposal 20 Nov. 1997**; *J. Phys.* **G24** (1998) 483; H.V. Klapdor-Kleingrothaus, CERN Courier, Nov. 1997, 16.

[3] H.V. Klapdor-Kleingrothaus, "60 Years of Double Beta Decay - From Nuclear Physics to Beyond the Standard Model Particle Physics", WS (2001) 1281 p. H.V. Klapdor-Kleingrothaus, *Spring. Tr. Mod. Phys.* **163** (2000) 69.

[4] H.V. Klapdor-Kleingrothaus et al., Subm for publ. (2005)

[5] H.V. Klapdor-Kleingrothaus et al., *Nucl. Instrum. Meth.* **A 481** (2002) 149-159.

[6] H.V. Klapdor-Kleingrothaus et al., *Nucl. Instrum. Meth.* **A 511** (2003) 341; Proc. BEYOND02, IOP 2003, ed. H.V. Klapdor-Kleingrothaus, 499. *Nucl. Instrum. Meth.* **A 530** (2004) 410-418 and **A 508** (2003) 343-352, CERN Courier, 2003.

[7] T. Kihm, V. Bobrakov, H.V. Klapdor-Kleingrothaus, *Nucl. Instrum. Meth.* **A 498** (2003) 334.

[8] H. V. Klapdor-Kleingrothaus et al., *Astr. Phys.* **18** (2003) 525.

[9] R. Bernabei et al., *Riv. Nuovo Cim.* **26** (2003) 1; *Phys. Lett.* **B 424** (1998) 195; **450** (1999) 448; **480** (2000) 23.

[10] R. Bernabei *et al. Phys. Lett.* **B 436** (1998) 379.

[11] H.V. Klapdor-Kleingrothaus et al., to be publ. (2005) and Gran Sasso Ann. Rep. 2003, INFN (2004) 99.

[12] C. Tomei, Diss. L'Aquila University, 2004.

[13] V. Bednyakov, H.V. Klapdor-Kleingrothaus, *Phys. Rev.* **D** 70 (2004) 096006.

[14] H.V. Klapdor-Kleingrothaus, *Int. J. Mod. Phys.* **A17** (2002) 3421-3431 (2002).

5 List of Books and Proceedings 2004

1. H.V. Klapdor-Kleingrothaus (ed.), BEYOND the DESERT 2003, Proc. of the Fourth Tegernsee International Conference on Particle Physics Beyond the Standard Model, Accelerator, Non-Accelerator and Space Apporoaches in the New Millenium, Castle Ringberg, Tegernsee, Germany, 9-14 June, 2003, Heidelberg, Germany: Springer (2004) 1117 pp.

2. H.V. Klapdor-Kleingrothaus and D. Arnowitt (eds.), Dark Matter in Astro- and Particle Physics., Proc. of 5th Heidelberg Dark Matter International Conference - DARK2004, Texas, USA, 3 - 9 October, 2004, Heidelberg, Germany: Springer (2005).

6 List of Publications 2004

1. H.V. Klapdor-Kleingrothaus, C. Tomei, I.V. Krivosheina, O. Chkvorets, Nucl. Instrum. Meth. A 530 (2004) 410 - 418, *The GENIUS-test-facility - first results on background from ^{222}Rn daughters".*

2. V.A. Bednyakov and H.V. Klapdor-Kleingrothaus, hep-ph/0404102 and Phys. Rev. D 70 (2004) 096006, *"On dark matter search after DAMA with Ge-73".*

7 List of Conference Contributions in 2004

1. I.V. Krivosheina, International Workshop "Physics of High Energy Density in Matter", Hirschegg, Austria, 1-6 February 2004, *"GENIUS-TF - a New Generation of Ge Detectors."*

2. H.V. Klapdor-Kleingrothaus, at Incontri di Fisica delle Alte Energie (IFAE 2004), Turin, Italy, 14-16 April, 2004, *"Final Results from the Search for Neutrinoless Double Beta Decay (Status of the HEIDELBERG-MOSCOW Experiment 2004)."*

3. H.V. Klapdor-Kleingrothaus, at International Workshop "Fundamental Interactions", ECT, Trento, Italy, 21 -25 June 2004, *"Evidence for Neutrinoless Double Beta Decay - and Consequences."*

4. H.V. Klapdor-Kleingrothaus, at 10th International Symposium on "Particle, Strings and Cosmology" (PASCOS'04), Nath Fest, 16 - 22 August 2004, Boston, USA, World Scientific (2005), eds. P. Nath et al., *"First Evidence for Lepton Number Violation - The ^{76}Ge Double Beta Experiment in Gran Sasso 1990-2003."*

5. H.V. Klapdor-Kleingrothaus and I.V. Krivosheina, at Fifth International Heidelberg Conference on "Dark Matter in Astro and Particle Physics", DARK 2004, 3 - 9 October 2004, College Station, TX, USA, Heidelberg, Germany: Springer (2005), eds: H.V. Klapdor-Kleingrothaus and D. Arnowitt, *"The GENIUS-Test-Facility and the HDMS Detector in GRAN SASSO."*

6. H.V. Klapdor-Kleingrothaus, at 21st International Conference on Neutrino Physics and Astrophysics "Neutrino 2004", 14 - 19 June 2004, Collége de France, Paris, France, World Scientific (2005), *"First evidence for neutrinoless double beta decay, with enriched ^{76}Ge in Gran Sasso 1990-2003."*

7. H.V. Klapdor-Kleingrothaus and I.V. Krivosheina, at 5th International Workshop on the Identification of Dark Matter, idm 2004, 6-10 September 2004, Edinburgh Scotland, World Scientific (2005), eds: N. Spooner et al., *"The GENIUS-Test-Facility and the HDMS Detector in GRAN SASSO."*

8. I.V. Krivosheina, at Second Europhysics Neutrino Oscillation Workshop, NOW 2004, Bari, Italy, September 11-17, 2004, World Scientific (2005), eds: G.L. Fogli et al., *"GENIUS Test Facility in GRAN SASSO after one year of operation."*

9. H.V. Klapdor-Kleingrothaus and C. Tomei, DPG, Teilchenphysik, Spring Meeting, Mainz, Germany, 31 März 2004, *"Latest Results from the Heidelberg Dark Matter Search (HDMS) Detector."*

10. I.V. Krivosheina DPG, Teilchenphysik, Spring Meeting, Mainz, Germany, 30 März 2004, *"GENIUS Test Facility in GRAN SASSO After Ten Months of Operation."*

8 List of Invited Colloquium and Seminar Talks and of Invited of Talks at Conferences

1. H.V. Klapdor-Kleingrothaus, Kolloquium at INFN, GRAN SASSO, Italy, March 2004, *"News from the Search for Neutrinoless Double Beta Decay (Status of the HEIDELBERG-MOSCOW Experiment 2003."*

2. H.V. Klapdor-Kleingrothaus, Meeting of the Fachbeirat MPI für Kernphysik, MPI Heidelberg, GERMANY, 27 April 2004, *"Final Result of the HEIDELBERG-MOSCOW Double Beta Experiment 1990-2003, Evidence for Neutrinoless Double Beta Decay."*

3. H.V. Klapdor-Kleingrothaus, MPI Heidelberg, Germany, 6 May, 2004, *"On the Analysis of the HEIDELBERG-MOSCOW Double Beta Experiment 1990-2003."*

4. H.V. Klapdor-Kleingrothaus, Kolloquium, Universität Giessen, Germany, 17 Mai 2004, *"Evidenz für Neutrinolosen Doppelbetazerfall von Atomkernen-Physik jenseits des Standardmodells der Teilchenphysik."*

5. H.V. Klapdor-Kleingrothaus, Kolloquium at Los Alamos National Lab., USA, 23 August, 2004, *"First Evidence for Neutrinoless Double Beta Decay and Consequences for Particle Physics."*

9 List of Invited Talks at Conferences in 2004

1. I.V. Krivosheina, International Workshop "Physics of High Energy Density in Matter", Hirschegg, Austria, 1-6 February 2004, *"GENIUS-TF a New Generation of Ge Detectors."*

2. H.V. Klapdor-Kleingrothaus, on Incontri di Fisica delle Alte Energie (IFAE 2004), Turin, Italy, 14-16 Aprily, 2004, *"Final Results from the Serach for Neutrinoless Double Beta Decay (status of the HEIDELBERG-MOSCOW Experiment 2004)."*

3. H.V. Klapdor-Kleingrothaus, on International Workshop "Fundamental Interactions", ECT, Trento, Italy, 21 -25 June 2004, *"Evidence for Neutrinoless Double Beta Decay - and Consequences."*

4. H.V. Klapdor-Kleingrothaus, on 10th International Symposium on "Particle, Strings and Cosmology" (PASCOS'04), Nath Fest, 16 - 22 August 2004, Boston, USA, *"First Evidence for Lepton Number Violation - The ^{76}Ge Double Beta Experiment in Gran Sasso 1990-2003."*

5. H.V. Klapdor-Kleingrothaus, on Fifth International Heidelberg Conference on "Dark Matter in Astro and Particle Physics", DARK 2004, 3 - 9 October 2004, College Station, TX, USA, *"The GENIUS-Test-Facility and the HDMS Detector in GRAN SASSO."*

6. H.V. Klapdor-Kleingrothaus, on 21st International Conference on Neutrino Physics and Astrophysics "Neutrino 2004", 14 - 19 June 2004, Collége de France, Paris, France, *"First evidence for neutrinoless double beta decay, with enriched ^{76}Ge in Gran Sasso 1990-2003."*

7. H.V. Klapdor-Kleingrothaus, on 5th International Workshop on the Identification of Dark Matter, idm 2004, 6-10 September 2004, Edinburgh Scotland, *"The GENIUS-Test-Facility and the HDMS Detector in GRAN SASSO."*

8. I.V. Krivosheina on Second Europhysics Neutrino Oscillation Workshop, NOW 2004, Bari, Italy, September 11-17, 2004, *"GENIUS Test Facility in GRAN SASSO after one year of operation."*

10 List of Seminars at Heidelberg University in 2004)

1. Seminar für Mittlere Semester (WS 2003-2004):
   "Masse und Natur des Neutrinos"

2. Seminar für Mittlere Semester (SS 2004)
   "Neutrinos - in Teilchen - und Astrophysik"

GIGS. The Interferometric Station at LNGS

Antonella Amoruso[a,b], Luca Crescentini[a,c,d]

[a] Dip.to di Fisica Univ. di Salerno, Salerno - Italy
[b] INFN - Gruppo collegato dell'Aquila, L'Aquila - Italy
[c] INFN - LNGS, L'Aquila - Italy
[d] Spokeperson

Abstract

Since several years two Michelson-type laser interferometers, operating as geodetic extensometers, are working at LNGS. The two orthogonal baselines, striking N66E and N24W, are 90-m long. Nominal sensitivity is about 3×10^{-12} and recording rate is 5Hz. Until 1999 one interferometer measured difference in extension between the two baselines in an equal-arm configuration, since then two independent unequal-arm interferometers are monitoring extension along the two orthogonal directions.

Tidal analysis of strain data has been performed using different codes in order to evidence the fluid core resonance (FCR) effect in the diurnal tidal band and study the resonance function. The unusual depth of the station largely reduces contamination caused by atmospheric effects in the diurnal band of recorded tides. Predicted ocean loading effects are small, mainly for one of the two monitored directions. In this condition an uncomplete removal of oceanic tidal loading and atmospheric effects is expected to affect results less severely than in other stations.

Preliminary analyses show that values of the FCR period are consistent with but slightly lower than those previously published and values of the quality factor Q are more realistic than those obtained from gravity data. Ocean loading corrections suggest supplement by local tidal models.

1 Introduction

The Free Core Nutation (FCN) is a rotational eigenmode which appears in addition to the well-known Chandler period (≈ 435 days). This mode is due to the pressure coupling between the liquid core and the solid mantle which acts as a restoring force. The FCN causes a resonance on the Earth response to tidal forcing whose period T_{FCR} (situated in the diurnal tidal band) and quality factor Q depend on the core-mantle boundary (CMB) ellipticity, the Earth's inelasticity, and the viscomagnetic coupling of the CMB.

The FCN has been observed using tidal gravimetry, because the amplitude and phase of some diurnal tides of lunisolar origin are perturbed by the resonance process, and Very Long Baseline Interferometry (VLBI), which allows to measure changes in the Earth orientation. From these Earth orientation parameters, the nutations can be determined; and from the nutation coefficients it is possible to investigate the FCN. Both methods suggest that the eigenperiod is around 430 sidereal days, instead of the 460-sidereal-day period which is theoretically predicted for a hydrostatically prestressed Earth ([4]). However, gravimetry gives a quality factor usually smaller than VLBI. In other words, gravimetry suggests that the Earth is more inelastic than expected from VLBI. Strain data are more affected by local effects (e.g. topographic distortion of the strain field) than gravimetric data, but changes of the Love and Shida numbers (which give the Earth response to tidal forcing and whose computed values depend on the Earth model) at frequencies near to resonance induce relative disturbances in strain that are about ten times larger than in gravity tide. In this latter case, resonance effects are often comparable with uncertainties on ocean loading.

We have used about 4-year data from the geodetic interferometers at Gran Sasso to make a preliminary tidal analysis devoted to the determination of T_{FCN} and Q. Data span is sufficient to resolve a few tidal lines around the resonance frequency.

2 Data analysis and results

Strain data are affected by the ground deformation induced by temperature and pressure fluctuations. This problem can be particularly severe when looking for signals having periods around 24 hours. In the case of the Gran Sasso interferometers, a comparison of the power spectral density of strain data, atmospheric pressure and temperature indicates that environmental effects in the diurnal tidal band should be very low (see Fig. 1).

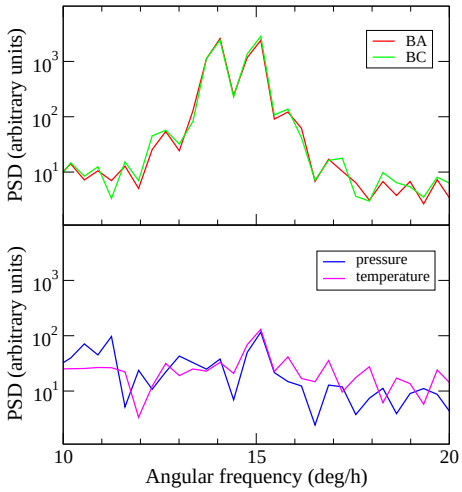

Figure 1. Power spectral density of strain data, pressure and temperature obtained by averaging PSDs of three 35d-long records.

This suggestion is supported by the not so large amplitude of the 24-hour period component of strain data, caused by the environmental effects and a very weak tidal wave (namely S1). In the preliminary analysis shown here we have neglected any environmental effect, but we are going to overcome this limitation.

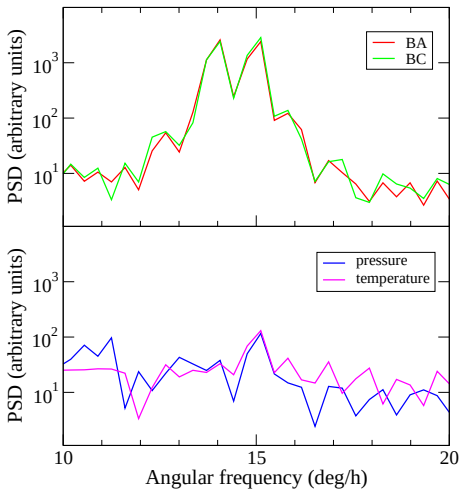

Figure 1. Power spectral density of strain data, pressure and temperature obtained by averaging PSDs of three 35d-long records.

The cavity effects on both interferometers are expected to be negligible, because end monuments stay more than one diameter away from the end face of the interferometer tunnels. The topographic effects are expected to be negligible for BA and to reduce measured strain by 20-40% for BC ([3]).

We have performed preliminary analysis of two data sets, the former spanning 1514 days from 1999 to 2004 (BA interferometer) and the latter 1293 days from 2000 to 2004 (BC interferometer), taking into account ocean loading tides effects on strain records. Ocean loading tides have been computed using GOTIC2 ([6]) with Earth models 1066A and GB and global ocean models NAO.99b and CSR4.0. Since minor Ψ_1 and Φ_1 constituents of the diurnal tidal band under investigation are not computed by GOTIC2, ocean loading tides for Ψ_1 and Φ_1 are estimated by interpolating tidal parameters for the nearby K_1 and J_1 constituents. The parameters of the transfer function Earth tides - instrument in the diurnal tidal band have been estimated using three different codes: ETERNA 3.40 ([9], without despiking the data records), VAV ([8], with two iterations after the first analysis), and ACS ([1]). Figure 2 shows amplitude factors and phase lag of tidal constituents in the diurnal tidal band for BA and BC interferometers, obtained using ACS, without and with ocean loading correction in two Earth-ocean model combinations. Similar results have been obtained using ETERNA and VAV.

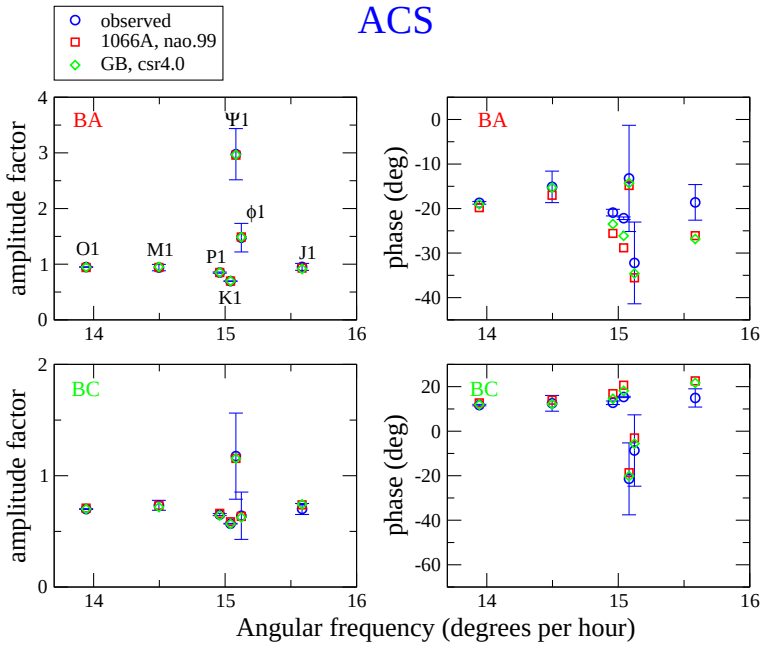

Figure 2.

The amplitude factor is the ratio between the observed amplitude and the amplitude computed for an elastic Earth model (Fig. 3), in which case the phase lag is -17.3 deg for BA and 12.7 deg for BC.

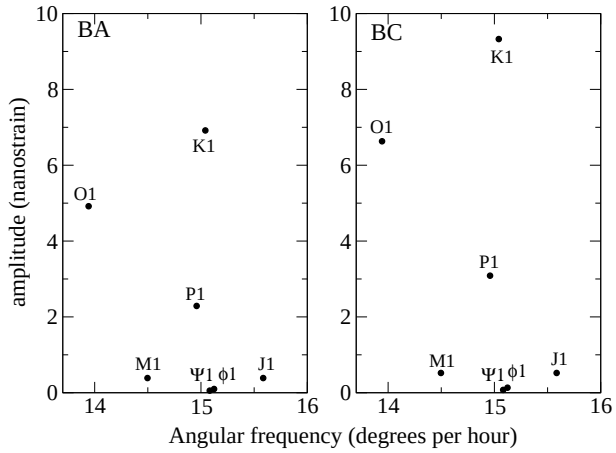

Figure 3.

Predicted ocean loading amounts to a few percent of the predicted tidal deformation for an elastic Earth, so that uncertainties on ocean loading are not expected to severely affect the results. The only exception is given by J_1 (a small tidal component), which however appears unreliable, thus indicating that inclusion of a proper local tidal model for the Adriatic Sea is necessary. The same improvement is suggested by the phase lag of Ψ_1, Φ_1, and J_1 as obtained after ocean loading correction.

Observed amplitude factors contain the FCR effect and several indirect effects due e. g. to topography, heterogeneities etc. For example, amplitude factors far from the resonance are about 0.7 for BC, as expected because of local topography. These indirect effect are almost the same in the diurnal tidal band and can be eliminated by considering the ratio of the amplitude factor of any diurnal wave to that of O_1, which is far from resonance.

The diurnal tidal strain can be expressed by ([7])

$$\varepsilon(\alpha) = \{C(f)\cos H + D(f)\sin H\}\, F$$

where

$$C(f) = a_0 + f_2\left\{a_1\left(f_1 - f\right) + b_1 f_1/2Q\right\}$$

$$D(f) = b_0 + f_2\left\{b_1\left(f_1 - f\right) + a_1 f_1/2Q\right\}$$

$$f_2 = \left(f - f_0\right) / \left\{\left(f_1 - f\right)^2 + \left(f_1/2Q\right)^2\right\}$$

Here H is the hour angle of the Moon or the Sun, f_0 is the O_1 frequency and f_1 is the FCR frequency. The unknown parameters a_0, a_1, b_0, and b_1 depend on the Love and Shida numbers (including the strength of the FCR), station latitude and instrumental azimuth.

The parameters concerning the fluid core resonance effects on diurnal strain tides have been estimated by minimizing a L1-norm cost function including both the ratios of the amplitude factors and the phase lags, with and without correction for ocean loading. The cost function has been minimized using ASA ([5]). Many inversions starting from random points of the parameter space have been performed, end points have been plotted versus related costs, and regions of the parameter space that give a good fit have been identified. Figure 4 shows T_{FCR} $(= 1/f_1)$ and $\log Q$ obtained using data from Fig. 2.

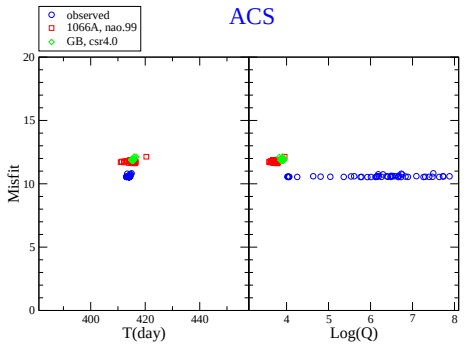

Figure 4.

An example of comparison between observations and theory is in Fig. 5.

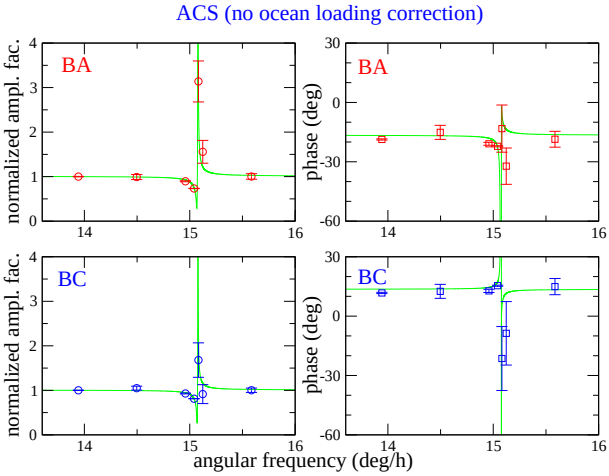

Figure 5.

We are still working on data pre-analysis, inclusion of local tidal models for the Adriatic Sea, and assesment of uncertainties on retrieved parameters by Monte Carlo techniques. Preliminary results show that:

1. Ocean loading correction does not lower misfit, suggesting supplement by local tidal models
2. Values of the FCN period are consistent with but slightly lower than those previously published ([7] and references therein).
3. Values of the quality factor Q are consistent with results in [2].

References

[1] Amoruso A., L. Crescentini, and R. Scarpa, Removing tidal and atmospheric effects from Earth deformation measurements, *Geophys. J. Int.*, **140**, 493-499, 2000.

[2] Florsch N., and J. Hinderer, Bayesian estimation of the free core nutation parameters from the analysis of precise tidal gravity data, *Phys. Earth Planet. Int.*, **117**, 21-35, 2000.

[3] Harrison J. C., Cavity and topographic effects in tilt and strain measurements, *J. Geophys. Res.*, **81**, 319-328, 1976.

[4] Hinderer J., J. P. Boy, P. Gegout, P. Defraigne, F. Roosbeek, and V. Dehant, Are the free core nutation parameters variable in time?, *Phys. Earth Planet. Int.*, **117**, 37-49, 2000.

[5] Ingber L., Simulated annealing: Practice versus theory, *Mathl. Comput. Modelling*, **18**, 29-57, 1993.

[6] Matsumoto K., T. Sato, T. Takanezawa, and M. Ooe, GOTIC2: A program for computation of oceanic tidal loading effect, *J. Geod. Soc. Japan*, **47**, 243-248, 2001.

[7] Mukai A., S. Takemoto, and T. Yamamoto, Fluid core resonance revealed from a laser extensometer at the Rokko-Takao station, Kobe, Japan, *Geophys. J. Int.*, **156**, 22-28, 2004.

[8] Venedikov A. P., J. Arnoso, and R. Vieira, VAV: a program for tidal data processing, *Computers and Geosciences*, **29**, 487-502, 2003.

[9] Wenzel H.-G., Tha nanogal software: Earth tide data processing package ETERNA 3.30, *Bull. Inf. Marees Terrestres*, **124**, 9425-9439, 1996.

OPERA

METU, Ankara, Turkey
M. Guler, M. Serin-Zeyrek, P. Tolun, M.T. Zeyrek

LAPP, IN2P3-CNRS and Université de Savoie, Annecy, France
A. Degre, J.Damet, D. Duchesneau, J. Favier, M. Lavy, H. Pessard

L'AQUILA University and INFN, LAquila, Italy
A. Di Giovanni, N. Di Marco, P. Monacelli

Bari University and INFN, Bari, Italy
M. Ieva, M.T. Muciaccia, M. De Serio, S. Simone

IHEP, Beijing, China PR
S.L. Lu, J. Ren, S.J. Zhou

Humboldt University, Berlin, Germany
K. Winter

Bern University, Bern, Switzerland
K. Borer, M. Hess, U. Moser, K. Pretzl, T. Waelchli, M. Weber

Bologna University and INFN, Bologna, Italy
G. Giacomelli, G. Mandrioli, L. Patrizii, P. Serra, M. Sioli, G. Sirri

IIHE (ULB-VUB), Brussels, Belgium
G. Van Beek, P. Vilain, G. Wilquet

JINR, Dubna, Russia
D. Bardin, I. Boudagov, G. Chelkov, Y. Gornouchkine, Z. Kroumchtein, A. Nozdrin, A. Olchevski, A. Sadovski.

LNF, Frascati, Italy
F. Bersani Greggio, B. Dulach, A. Franceschi, F. Grianti, A. Paoloni, M. Spinetti, F. Terranova, L. Votano

LNGS, Assergi, Italy
N. Ferrari, C. Gustavano, D. Orlandi,

Toho University, Funabashi, Japan
S. Ogawa, H. Shibuya

Märkische Fachhochschule FB Elektrotechnik, Hagen, Germany
K. Schauties, H. Sohlbach, H. Woltersdorf

Israeli group c/o Technion, Haifa, Israel
J. Goldberg

Hamburg University, Hamburg, Germany
C. Ballhausen, F.W. Buesser, J. Ebert, K. Hagner, B. Koppitz, B. Naroska, W. Schmidt-Parzefall, R. van Staa, R. Zimmermann

Shandong University, Jinan, Shandong, China PR
C.F. Feng, Y. Fu, M. He, J.Y. Li, L. Xue

Aichi Educational University, Kariya, Japan
K. Kodama, N. Ushida

Kobe University, Kobe, Japan
S. Aoki, T. Hara

IPNL, IN2P3-CNRS and Université C. Bernard Lyon I, Villeurbanne, France
A.Autiero,L. Chaussard, Y. Déclais, C. Heritier,I. Laktineh, J. Marteau, P. Royole-Degieux
Münster University, Münster, Germany
P. Boschan, N. Bruski, D. Frekers

Nagoya University, Nagoya, Japan
K. Hoshino, M. Komatsu, M. Miyanishi, M. Nakamura, T. Nakano, K. Niwa, O. Sato, T. Toshito

"Federico II" University and INFN, Naples, Italy
M. Ambrosio, S. Buontempo, N. D'Ambrosio, G. De Lellis, G. De Rosa, F. Di Capua, P. Migliozzi, C. Pistillo, L. Scotto Lavina, G. Sorrentino, P. Strolin, V. Tioukov

Neuchatel University, Neuchatel, Switzerland
J. Busto, M. Hauger, J. Janiscko, F. Juget, J-L. Vuilleumier, J-M. Vuilleumier

Institute of Nuclear Power Engineering, Obninsk, Russia
S. Aplin, V. Galkine, V. Saveliev, M. Zaboudko

LAL, IN2P3-CNRS and Université Paris-Sud, Orsay, France
J. Boucrot, J.E. Campagne, A. Cazes, A. Lucotte, J.P. Repellin

Padova University and INFN, Padova, Italy
R. Brugnera, R. Ciesileski, F. Dal Corso, S. Dusini, C. Fanin, A. Garfagnini, A. Longhin, L. Stanco

"La Sapienza" University and INFN, Rome, Italy
P. Righini, G. Rosa

Fachbereich Physik der Universitaet Rostock, Rostock, Germany
M. Beyer, H. Schroeder, R. Waldi, R. Zimmermann

Salerno University and INFN, Salerno, Italy
E. Barbuto, C. Bozza, G. Grella, G. Romano, S. Sorrentino

Sofia University, Sofia, Bulgaria
D. Kolev, R.Tsenov

IRES, IN2P3-CNRS and Université Louis Pasteur, Strasbourg, France
R. Arnold, E. Baussan, M. Dracos, J.L. Guyonnet, J.P. Engel, B. Dorion

Utsunomiya University, Utsunomiya, Japan
Y. Sato, I. Tezuka

Rudjer Boskovic Institute (IRB), Zagreb, Croatia
K. Jakovcic, A. Ljubicic, M. Stipcevic

Abstract

The OPERA experiment has been designed for an appearance search of $\nu_\mu \leftarrow \nu_\tau$ oscillations in the parameter region indicated by Super-Kamiokande as the explanation of the zenith dependence of the atmospheric neutrino deficit. OPERA is a long baseline experiment being constructed at the Gran Sasso Laboratory in the CNGS neutrino beam from the CERN SPS. The detector design is based on a massive lead/nuclear emulsion target. Nuclear emulsion are used as high resolution tracking devices, for the direct observation of the decay of the τ leptons produced in ν_τ charged-current interactions. Electronic detectors are used to locate the event in the emulsions. Magnetized iron spectrometers measure charge and momentum of muons. The discovery potential of OPERA originates from the observation of a ν_τ signal with very low background level. The direct observation of $\nu_\mu \leftarrow \nu_\tau$ appearance will constitute a milestone in the study of neutrino oscillations. The OPERA experiment will also search for $\nu_\mu \leftarrow \nu_e$ with a sensitivity a factor two better than current limits from CHOOZ. During 2004 the OPERA collaboration made important progresses on the construction of the detector components and the installation in Hall C of LNGS.

1 Design Principles

The OPERA experiment [1] is designed for the direct observation of ν_τ appearance from $\nu_\mu \to \nu_\tau$ oscillations in the CNGS long-baseline beam from the CERN SPS to the Gran Sasso laboratory.

The measurements of atmospheric neutrino fluxes performed by the Super-Kamiokande experiment indicate a deficit of muon neutrinos with a zenith angle distribution consistent with $\nu_\mu \to \nu_\tau$ oscillations with $\Delta m^2_{23} = 1.3 - 3.0 \times 10^{-3} eV^2$ (90% C.L.) and full mixing.

MACRO, Soudan2 and K2K experiments also made observations compatible with this result. Therefore the primary goal of OPERA is to obtain direct evidence for ν_τ appearance, which would confirm the oscillation hypothesis and its nature. An important byproduct is the search for $\nu_\mu \to \nu_e$ oscillations which could lead to a first measurement of the mixing angle θ_{13}.

A long baseline of 732 Km is used between the neutrino source (the CERN beam line) and the detector (located in the Gran Sasso underground laboratory), in order to be sensitive to the oscillation parameters indicated by the Super-Kamiokande data. The CNGS neutrino beam has been optimized for the detection of ν_τ charged current (CC) interactions and provides an average ν_μ energy of about 20 GeV. For the evaluation of the performance of the experiment an integrated fluence of 2.25×10^{20} protons on target is assumed, corresponding to 5 years SPS operation in shared mode. However, ongoing studies at CERN aim to obtain a beam intensity upgrade equivalent to a factor 1.5.

The main principle of the ν_τ search is the direct detection of the decay of the τ lepton produced by CC interactions. This is achieved by a massive (about 1.8 Kton) neutrino target based on the Emulsion Cloud Chamber (ECC) design which combines, in a sandwich-like cell, the high-precision tracking capabilities of nuclear emulsions (two 40 μm layers on both sides of 200 μm plastic base) and the large target mass provided by the lead plates (1 mm thick). This technique has been recently demonstrated to be effective for τ detection by the DONUT Collaboration.

The basic element of the target structure is the brick, made out of consecutive series of ECC cells with transverse dimensions of 10.2×12.7 cm^2. Bricks are arranged in planar structures (walls), which are interleaved with electronic tracker planes. These planes are built from vertical and horizontal strips of extruded plastic scintillator 2.6 cm wide, read out by wavelength-shifting fibers coupled with photodetectors at both ends. The main purposes of the target tracker are to provide a trigger for neutrino interactions, localize the particular brick in which the neutrino interacted and perform a first muon tracking within the target. The selected brick is then extracted from the target for the emulsion development and scanning in a quasi-online sequence. Large emulsion areas can be scanned with automatic microscopes equipped with fast track-recognition processors. This technique allows for the search of the tau decay topology and, at the same time, for the measurement of the event kinematic. Tracks momenta are measured from their multiple scattering in the brick and electron and gamma energies from showers development. The total number of bricks amounts to 206,336 resulting in a target mass of 1766 tons.

Figure 1 shows the side view of the OPERA detector, which is arranged in two independent supermodules. Each supermodule includes a block of 31 walls+scintillator

planes, followed downstream by a magnetized iron spectrometer. The spectrometers are used for the identification of muons and to measure their charge and momentum. Each spectrometer consists of a dipolar magnet made of two iron walls interleaved with pairs of precision trackers. Particle trajectories are measured by these trackers, consisting of vertical drift tube planes. Resistive Plate Chambers (RPC) with inclined strips, called XPC, are combined with the precision trackers to provide unambiguous track reconstruction in space. Moreover, planes of RPCs (Inner Tracker) are inserted between the magnet iron plates. They allow a coarse tracking inside the magnet to identify muons and ease track matching between the precision trackers. They also provide a measurement of the tail of the hadronic energy leaking from the target and of the range of muons which stop in the iron.

The OPERA design is optimized to achieve low background levels for the tau appearance search. The experiment aims at the analysis of all the single-prong tau decay modes (e,μ,h). Signal events are classified as long or short decays depending on whether the tau track traverses an emulsion sheet or not. The main background sources are charm production in CC interactions, hadronic interactions in lead and large-angle muon Coulombian scatterings. These events are rejected by the identification of the primary lepton in CC interactions and either by requiring the presence of a tau-like kink topology (long decays) or by an impact parameter method (short decays). In addition a kinematic analysis is used to enhance the signal-to-background ratio. Overall a total background of 0.7 events is expected. If $\nu_\mu \to \nu_\tau$ oscillations occur, the average number of detected signal events ranges from 3.1 (at $\Delta m^2 = 1.3 \times 10^{-3} eV^2$) to 16.4 (at $\Delta m^2 = 3.0 \times 10^{-3} eV^2$) and corresponds to 7.3 events for the Super-Kamiokande best fit value ($\Delta m^2 = 2.0 \times 10^{-3} eV^2$, full mixing).

For what concerns the search for $\nu_\mu \to \nu_e$ oscillations, still after a five years run, OPERA will be able to constrain the θ_{13} mixing angle at the level $\theta_{13} < 0.06$ at 90% C.L. (for $\Delta m^2 = 2.5 \times 10^{-3} eV^2$, $\sin^2 2\theta_{23} = 1$).

2 Detector construction progress in 2004

The OPERA experiment was approved in 2001. During 2002 the Collaboration completed the detector design, tests and optimization phase resulting in a two supermodules configuration. Important progresses were made in 2003, as foreseen by the construction schedule; in February 2003 the detector installation started in Hall C and has been going with the assembly of the magnetic spectrometers and the RPC system. At the end of 2003 the lower return yokes of the two magnets had been installed together with the connecting support structure. Two vertical RPC planes had been positioned and fully instrumented. The installation of the mechanical structure started after the completion of the first spectrometer. By august 2004 the upper and lower support rails together with the dumping structure have been mounted and aligned. After this operation most of the activities in the underground hall were halted to allow for the safety works in Hall C. These modifications of the LNGS infrastructures have been planned by the Commissioner appointed by the Italian government (July 2003) with the task of ensuring LNGS to be compliant with safety and environmental rules. The installation of the second magnet

was resumed in autumn 2004 and completion is planned in spring 2005.

The target tracker modules, assembled in Strasbourg (IRES), are being mounted in the underground detector (see section 4). The target walls are being built and the first wall has been delivered at LNGS and mounted in November 2004. The first of the two Brick Manipulator system has been built in Annecy (LAAP) and is currently under test, the second manipulator is under construction. The pre-series production of the precision tracker for the spectrometers has started in Hamburg (8 modules glued, 2 modules wired) and the preparation for mass production and for assembling is finished. Mass production started in January 2005. The production speed is expected to reach two modules/week. The design of the Brick Assembly Machine (BAM) was completed, the tendering procedure has been accomplished, the industry has been selected and the construction has started (see paragraph on BAM status).

The mass production of nuclear emulsions started in April 2003 and will end in 2005. An underground facility for their refreshing (the erasure of the cosmic ray tracks accumulated during the production) was set up in the Tono mine in Japan. After production at Fuji Inc., the emulsion sheets are refreshed and then sent to Gran Sasso where an emulsion storage area, located in the hall B of LNGS, was built in summer 2003. The first set of refreshed emulsions (1.5 millions of emulsion sheets) have been shipped from Japan to Gran Sasso at the end of 2004 and has arrived in the underground laboratory on January the 8th 2005. The development of the scanning systems has improved significantly. A peak scanning power of 20 cm^2/h has been reached by the european laboratories while the current scanning speed at 90% efficiency is of the order of 10 cm^2/h. The development of the Japanese scanning system is also well in progress. The OPERA installation will end in 2006, when the first neutrinos from the CNGS beam are expected.

3 Spectrometer status

During 2004, the OPERA Spectrometers were well advanced in terms of installation and services developments. The RPC detectors were installed with a refined optimisation which was quickly reached. The installation of RPC in the first spectrometer ended on middle May, in advance of at least 3 weeks on the official schedule. Globally, 462 detectors, 3 m^2 each, were installed in single walls of 70 m^2. Each detector was carefully selected after strong tests before being chosen for installation (see Annual Report 2003). Moreover, after the transportation in the underground laboratory, each one was rechecked against gas leakage and High Voltage shorts and disconnections. At the end of May only 2 of the 462 detectors had some problems (breaking of gas inlet) which had to be recovered. Together with the RPC, vertical and horizontal layers of cupper strips were positioned inside the iron walls of the magnet, for a total of 12320 channels. Finally 220 probes for temperature and several for Hall measurements, have also been placed. Gas piping systems have been installed in the lateral edges of the iron walls. Figure 2 shows the completed first Spectrometer of OPERA.

During June, some tests have been performed in few rows of the installed RPC. Unfortunately, the results were not conclusive of the actual performances of the analysed detectors, since the gas quantity to flow was too small. For the time being a complete

test is foreseen in order to analyse with cosmics (1 Hz/m^2/hour) at least 4 layers of RPC. During June and July the installation of the mechanical structure was done, with the careful positioning of the top parts of the magnet, coils etc. .

In September the installation of the 2nd Spectrometer started. However, it has been immediately stopped due to the concomitance of the Commissioner works in Hall C. The installation resumed at the end of November and it immediately reached the full velocity. At the present time (end of January 2005) more than half of the second Spectrometer has already been installed. During 2004, the problem of high RPC rejection rate, during the strong tests they underwent, had to be faced. Several batches of RPC produced during the summer suffered of an exceptional high level of rejection (almost 50% on some kind of RPC), probably due to hot climate conditions. These detectors were actually correctly working but had the presence of single spots of high rates, few cm diameter wide. Long period tests, lasting 460 days, were done on some of the detectors with "hot spot". Results seem to show that these chambers are becoming really noisy after some time. The collaboration decided to put aside these detectors and to go for a extended production.

The electronic system for the RPC was completely defined during 2004. The racks for the Front End boards, the power supply and the controller cards for triggering and data acquisition will be placed on the top of the Spectrometers.

At present, it is foreseen to switch on the magnets in summer 2005, to start the commissioning of the RCP system at the same time, in order to be ready to take cosmic data at the end of the year 2005.

4 Target Tracker installation

The OPERA Target Tracker, in charge of pointing to the right lead/emulsion brick to be extracted from the detector target, is under construction since the beginning of 2004. This construction will last up to the end of 2005. The first tests for the Target Tracker installation at LNGS have started in September 2004. The Target Tracker is composed by 62 walls, each one associated with one brick wall. Each Target Tracker wall contains four horizontal and for vertical modules defining a sensitive area of about 7x7 m^2. The Target Tracker modules enclose 64 scintillator strips readout by Wave Length Shifting fibres and multianode photomultipliers. For the whole Target Tracker, 496 modules, 992 photomultipliers, 31200 scintillator strips and about 300 km WLS fibre are needed. The photomultipliers and both ends of the WLS fibres are located in two end-caps/module specifically constructed for this purpose. The high yield and low absorption WLS fibres come from Kuraray company while the multianode photomultipliers (8x8 channels) are provided by Hamamatsu. The tests of the delivered photomultipliers, the high voltage modules and the front-end electronics are under the responsibility of Universities of Bern and Neuchtel. The scintillator strip production is done by AMCRYS-H and the quality control is performed by JINR-Dubna. The end-caps are produced by Ariane under the supervision of ULB-Brussels. The assembly of the Target Tracker modules is made at IReS-Strasbourg. Two production chains producing two modules per day are necessary in order to respect the OPERA schedule. After production, each module is tested and

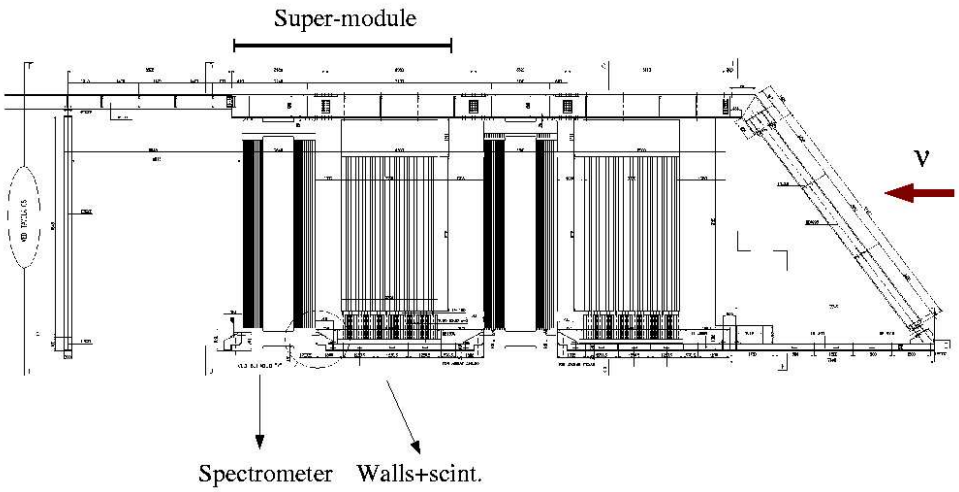

Figure 1: Side view of the OPERA detector

Figure 2: 19th of May 2004. First Spectrometer completed.

calibrated using an electron spectrometer produced for this purpose. Up to the end of 2004, almost half of the module production has been finished. To test the installation procedure at LNGS underground laboratory, Target Tracker modules have been sent there end of August 2004. The strategy adopted by the experiment consists of mounting the Target Tracker walls outside the detector and inserting them one by one when needed. In this way, a brick-Target Tracker wall interference is limited and several teams can work in parallel. For this purpose, the Target Tracker group has installed in Hall C a mounting platform and a wall storage arch. The first Target Tracker wall insertion test has been done the 16th of September 2004 (figure 3). With this successful test, the wall insertion procedure has been validated. It has also been proved that this operation was faster than all expectations and that the OPERA schedule could be less tight than expected. After the insertion of the first Target Tracker wall the activities have been stopped due to waterproofing works done in front of Hall C. At the end of 2004 investigations have been done to understand residual deformations of the Target Tracker walls and the way to remove them. During this period, the wall attachment system inside the detector has been finalized.

Figure 3: Insertion of the first Target Tracker wall inside the OPERA detector.

5 BAM project activity in 2004

The Brick Assembly Machine (BAM) is an automatic system whose aim is the mass production of about 207000 brick of the OPERA detector in about 220 working days. This means about 960 brick a day, i.e. a production rate of about 1 brick each 30 seconds for 8 working hours a day. A brick is formed by pile of 56 lead sheets interleaved with 57 emulsion films. The pile has to be built within 50 micron piling precision and with no additional deformation in the lead sheets (10 micron flatness) and no distortion nor chemical effects on the emulsion films while automatic handling occurs. During 2004 the prototyping phase of BAM and brick packaging was terminated. Till June two packaging options for the pile packaging were studied: vacuum and mechanical packaging. After severe tests on robustness and reproducibility of the packaging dimensions, a final choice was done towards the mechanical packaging. The final solution is based on the use of a metallic (aluminum) structure being laid around the pile. The pile is protected by a 1 mm black polyethylene sheet all around in order to avoid direct contact of emulsion films with Al and to guarantees a first layer of light tightness to the films. Once closed with PE and Al, the pile is then wrapped with two layers of Al adhesive tape which guarantee the total light and gas tightness of the packaging. Tests in this direction were performed showing the absolute safety of such packaging for the emulsion films. Accelerated aging tests were also performed at 33 ^{o}C for 4 months showing no degradation of emulsion performances. In parallel, emulsion-lead compatibility tests were performed in order to validate the choice of the lead hardener. PbCa, PbSb and PbAgAl samples were studied. No effect in mechanical packaging was detected, while PbCa showed poisoning effects in vacuum packaging. PbSb was the final choice showing no poisoning effect in any packaging and being an intermediate value of hardness with respect to other two options. Concerning the brick production, several tenths of bricks were produced in manual and semiautomatic mode, both for measurements with test beams and for BAM packaging tests. In the November test beam first bricks with mechanical procedure in semiautomatic mode were produced, showing a relevant level of reproducibility in terms of dimensions with a sigma at level of about 100 microns. The BAM construction was started in November in the firm site, starting with the assembling of first piling pressing station and using two anthropomorphic robots and a manual pressing unit. The final layout of the BAM (see figure 4) was designed by the firm and matched with the BAM site infrastructures in collaboration with the LNGS engineers. The construction of several BAM components has started and is on schedule with respect to the official OPERA planning of activity.

In parallel to the activity above mentioned, the BAM site preparation in LNGS was started. Regular monthly meetings were performed in LNGS to define the specs of all the infrastructures needed for the correct working condition of the BAM. Civil engineer, electric networking, air conditioning system, safety sensor networking were defined in close collaboration with LNGS engineers. Specs documentations were produced; tendering and ordering phases were closed. Construction phase is now in progress and final delivery of the site is expected in spring 2005 Figure 5 shows the starting and present conditions of the BAM LNGS site.

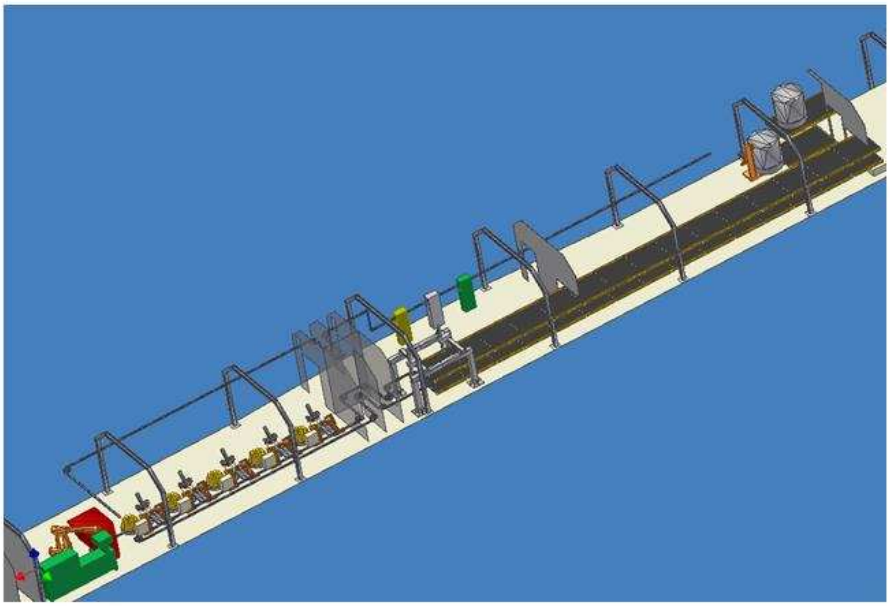

Figure 4: BAM final layout.

6 Status of European Scanning System Project

The project aims to develop a high-speed automatic system for the scanning of thin nuclear emulsions exposed to perpendicularly impinging particles, working at a speed of $\approx 20 cm^2/h$ (more than a factor of 20 better than in the past) and with sub-micron precision. The various components are industrially produced in order to replicate the system in all participating laboratories. The project can be divided into 4 main sections: optics; motorized mechanical stage; image acquisition and processing; tracking. The system makes use of optical components normally employed in biological applications, adapted to work on large surfaces. A modified optical bench hosts the illumination system and is equipped with a granite bracket to sustain the optical system. The image is formed on a CMOS camera, mounted on top of the optical tube. A flat aberration-free image is obtained, resulting in a field of view of 310x390 m^2 divided into a matrix of 1280x1024 squared pixels. The motorized mechanical stage covers an area of 20x20 cm^2 in the horizontal plane and a distance of a few cms along the vertical axis. The settling time of the horizontal XY stage is less than 80 ms for a 300 μm-step and the positioning reproducibility is about 0.3μm. The speed of the vertical Z-axis depends on the camera frame rate (up to 500 fps). Images are grabbed and processed by a programmable vision processor. For each field of view, several images of the emulsion are taken at almost equidistant depths: an optical tomography is thus obtained and allows to reconstruct the trajectories of particle tracks in 3D as sequences of aligned black clusters of given size and shape drowned in a sea of background clusters. A dedicated software controls the movements of the XY stage

Figure 5: May 04 and December 04 pictures of BAM site work in progress.

and the Z-axis, is responsible for image grabbing and processing and performs the online tracking through an asynchronous data-taking scheme that allows the parallel execution of several tasks. At Gran Sasso a scanning station is being installed. In 2004 one microscope has been put into operation; in 2005 the installation of at least 6 microscopes is foreseen to test the configuration which should be used for the analysis of the changeable sheets. The European Scanning System is operational since the beginning of 2004. A total of 15 microscopes have already been installed in the INFN scanning laboratories (Bari, Bologna, LNGS, Naples, Rome, Salerno) and in the joint European laboratories (Bern, Lyon, Neuchtel). The installation of 10 other microscopes is foreseen in 2005. The systems will continuously run for 5 years following the daily brick extraction from the OPERA target.

7 List of Publications

1. *Next generation long baseline experiments on the path to leptonic CP violation P. Migliozzi and F. Terranova, Phys. Lett. B563 (2003) 73.*

2. *The OPERA cosmic ray test facility at Gran Sasso R. Brugnera et al, Nucl. Inst. and Meth. A 533 (2004) 221.*

3. *Ageing and recovering of Glass RPC A. Candela et al, Nucl. Inst. and Meth. A 533 (2004) 116.*

4. *Performance of glass RPC operated in streamer mode with four-fold gas mixtures containing SF6 C. Gustavino et al, Nucl. Inst. and Meth. A 517 (2004) 111.*

5. *The quality control tests for the RPCs of the OPERA experiment A. Bergnoli et al, Nucl. Inst. and Meth. A 533 (2004) 203.*

6. *Long term operation test of RPCs for the OPERA experiment G. Barichello et al, Nucl. Inst. and Meth. A 533 (2004) 42.*

References

[1] M. Guler *et al.*, OPERA proposal, CERN/SPSC 2000-028, SPSC/P318, LNGS P25/2000.

CRESST. Dark Matter Search

G. Angloher [a], C. Bucci [d], P. Christ [a], C. Cozzini [b], F. von Feilitzsch [c], D. Hauff [a], S. Henry [b], Th. Jagemann [c], J. Jochum [e], H. Kraus [b], B. Majorovits [b], J. Ninkovic [a], F. Petricca [a], W. Potzel [c], F. Pröbst [a], Y. Ramachers [b, *], M. Razeti [c], W. Rau [c], W. Seidel [a, +], M. Stark [c], L. Stodolsky [a], A. J. B. Tolhurst [b], W. Westphal [c], H. Wulandari [c]

[a] *MPI für Physik, Föhringer Ring 6, 80805 Munich, Germany*
[b] *University of Oxford, Department of Physics, Oxford OX1 3RH, U.K.*
[c] *Technische Universität München, Physik Department, D-85747 Garching, Germany*
[d] *Laboratori Nazionali del Gran Sasso, I-67010 Assergi, Italy*
[e] *Eberhard-Karls-Universität Tübingen, D-72076 Tübingen, Germany*
[+] *Spokesperson E-mail address: seidel@mppmu.mpg.de*
[*] *present address: University of Warwick, Coventry CV4 7AL, U.K.*

Abstract

The aim of CRESST (**C**ryogenic **R**are **E**vent **S**earch with **S**uperconducting **T**hermometers) is to search for particle Dark Matter and to contribute to the elucidation of its nature. The experiment is located at the 'Laboratori Nazionali del Gran Sasso' (LNGS), Italy, and it uses low background cryogenic detectors with superconducting phase transition thermometers for the direct detection of WIMP-nucleus scattering events.

1 The Dark Matter Problem

The search for Dark Matter and the understanding of its nature is of central interest for particle physics, astronomy and cosmology. There is strong evidence for its existence on all scales, ranging from dwarf galaxies, through spiral galaxies like our own, to large scale structures. The history of the universe is difficult to reconstruct without Dark Matter, be it Big Bang Nucleosynthesis or structure formation.

Particle physics provides a well motivated candidate with the lightest SUSY-particle, the "neutralino". Generically, such particles are called WIMPs (Weakly Interacting Massive Particles). WIMPs are expected to interact with ordinary matter by elastic scattering on nuclei. All direct detection schemes have focused on this possibility.

Conventional methods for direct detection rely on the ionization or scintillation caused by the recoiling nucleus. This leads to certain limitations connected with the low ionization or scintillation efficiency of the slow recoil

nuclei. The cryogenic detectors developed for the first phase of CRESST (CRESST-I) measure the deposited energy calorimetrically, independent of ionization, and allow a detection of much smaller recoil energies. When the cryogenic measurement of the deposited energy is combined with a measurement of scintillation light an extremely efficient discrimination of the nuclear recoil signals from radioactive background signals can be obtained. This type of detectors is beeing used in the upcoming phase CRESST-II.

2 Detection Principle

The low temperature calorimetric detectors consist of a target crystal, the so-called absorber, an extremely sensitive superconducting phase transition thermometer, and a weak thermal coupling to a heat bath to allow thermal relaxation of the system after an interaction. The thermometer is made of a tungsten film evaporated onto the absorber crystal. Its temperature is stabilized in the transition region from the superconducting to the normal conducting state, which occurs at termeratures of about 10 mK. A typical width of the transition region is about 1 mK. A small temperature rise (typically some μK), e.g. from a WIMP nucleus scattering event, leads to an increase of resistance, which is measured with a SQUID based readout. For the first phase of CRESST, which ended in Feb. 2001, 262 g sapphire detectors have been developed at the institute. These detectors provided an excellent energy resolution of 133 eV at 6 keV and a very low energy threshold of 600 eV.

In the upcoming second phase CRESST-II, we are using 300 g scintillating $CaWO_4$ crystals as absorbers. The scintillating crystal is equipped with a superconducting tungsten phase transition thermometer for the detection of the phonons created by particle interactions in the scintillating crystal. The scintillation light is measured in coincidence with a separate cryogenic detector, optimized for light detection. Fig. 1 schematically shows the setup of this composite detector. Starting with a proof of principle experiment in 1998, the technique of simultaneous measurement of phonons and scintillation light has been developed at the institue.

The important advantage of the simultaneous detection of phonons and scintillation light is that it offers an extremely efficient suppression of the radioactive background. The ratio of the energy in the phonon channel and the energy in the light channel depends on the type of interaction. Nuclear recoils, such as WIMP or neutron scattering events, emit substantially less scintillation light than fully ionizing interactions, e.g. γ or β interactions do. As the overwhelming part of the backgroud consists of β and γ interactions,

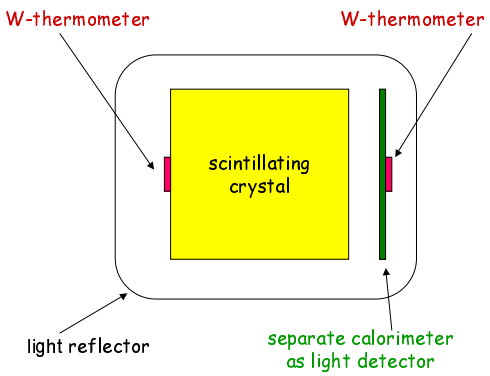

Figure 1: Sketch of the detector setup for the coincident detection of phonons and scintillation light. This novel concept will be used in CRESST-II. It allows to effieciently discriminate nuclear recoils signals from radioactive backgrounds.

this phonon/light technique provides a very effective method of background suppression. Fig. 2 illustrates this novel detection method. With this proof of principle device, a 99.7 % suppression of ionizing background in the energy range from 15 and 25 keV , and 99.9 % at energies above 25 keV has been demonstrted.

Compared to the alternative approach of simultaneous measurement of phonons and charge in a semiconductor crystal, which is applied in the experiments CDMS and Edelweiss-II, the method developed for CRESST-II has the important advantage that it does not suffer from dead layers at the surface. A reduced charge collection for ionizing events occurring close to the surface in semiconducting crystals may lead to a false identification of low energetic γ's and β's as nuclear recoils. The result in Fig. 2, which was obtained with a gamma and beta source, confirms that the supression also works for low energy electrons impinging onto the crystal surface.

3 The CRESST Setup in Gran Sasso

The central part of the CRESST installation is the cryostat, sketched in figure 3. The low temperature generated in the mixing chamber of the dilution refrigerator is transferred into the radiopure cold box, which houses

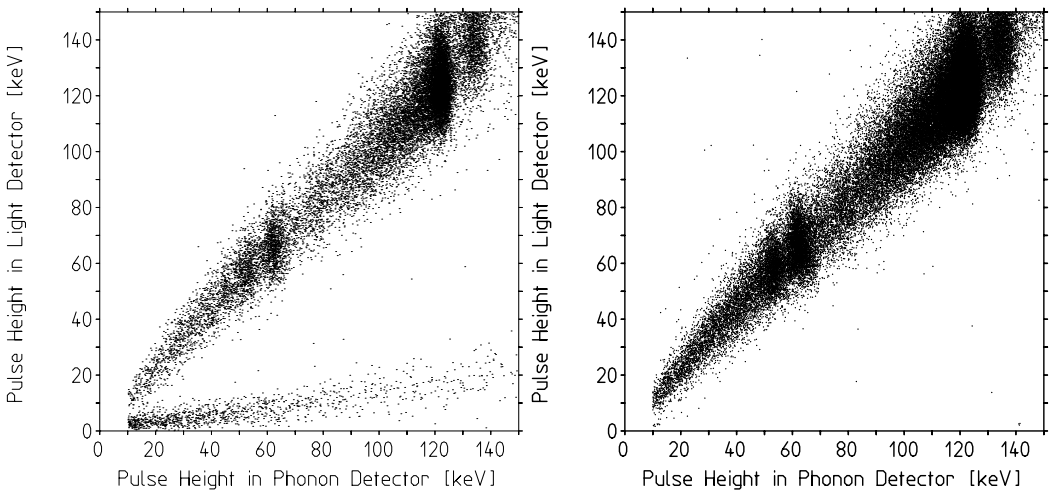

Figure 2: Coincident detection of phonons and scintillation light with a 6 g proof of principle $CaWO_4$ detector. Left fig.: The upper band of events is due to irradiation of the $CaWO_4$ crystal with electrons and gammas, whereas the lower band with lower light yield, is from nuclear recoils caused by a neutron source. Removing the neutron source (right fig.), confirms that there is no leakage of ionizing events into the nuclear recoil region.

the detectors, via a 1.5 m long cold finger, protected by thermal radiation shields, all fabricated of low background copper. Two internal cold shields consisting of low level lead are attached to the mixing chamber and to a thermal radiation shield at liquid N_2 temperature, respectively, in order to block any line-of-sight from the non-radiopure parts of the dilution refrigerator to the detectors inside the cold box. The design completely avoids potentially contaminated cryogenic liquids inside the cold box.

An extensive passive shielding of low background copper and lead surrounds the cold box and serves to shield radioactivity from the surrounding rock. The entire shilding is inclosed inside a gas-tight radon box, that is flushed with boil of N_2 gas and maintained at a small overpressure. Special care has been taken to minimize above ground exposure of the construction materials of the cold box and the shielding to cosmic rays, in order to avoid activation.

Figure 4 schematically shows the CRESST experimental building. The cryostat is installed in a two level faraday cage to shield electromagnetic interference. The ground level inside the faraday cage is equipped as a class-100 clean room, in order to minimize contamination of the detectors and cold box during mounting. The head of the cryostat extends into the first

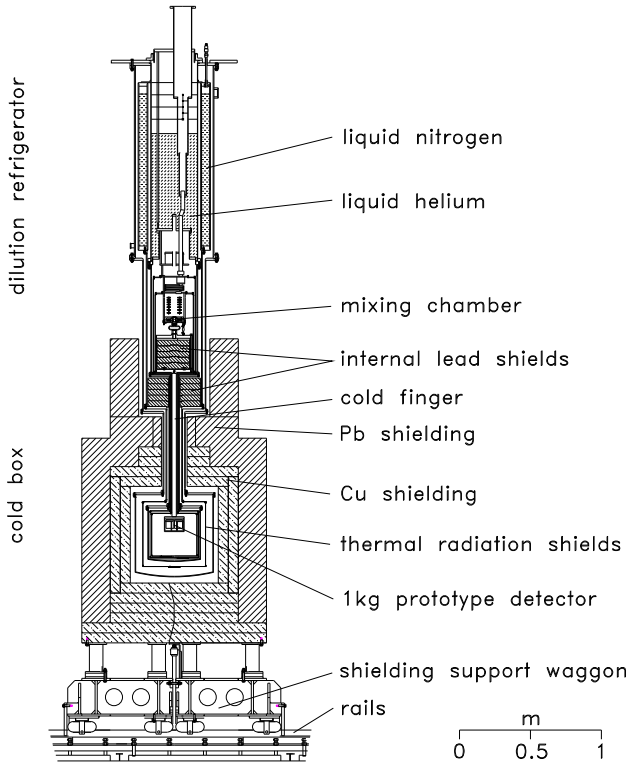

Figure 3: Layout of the CRESST ^{3}He/^{4}He dilution refrigerator and low background cold box with its shielding.

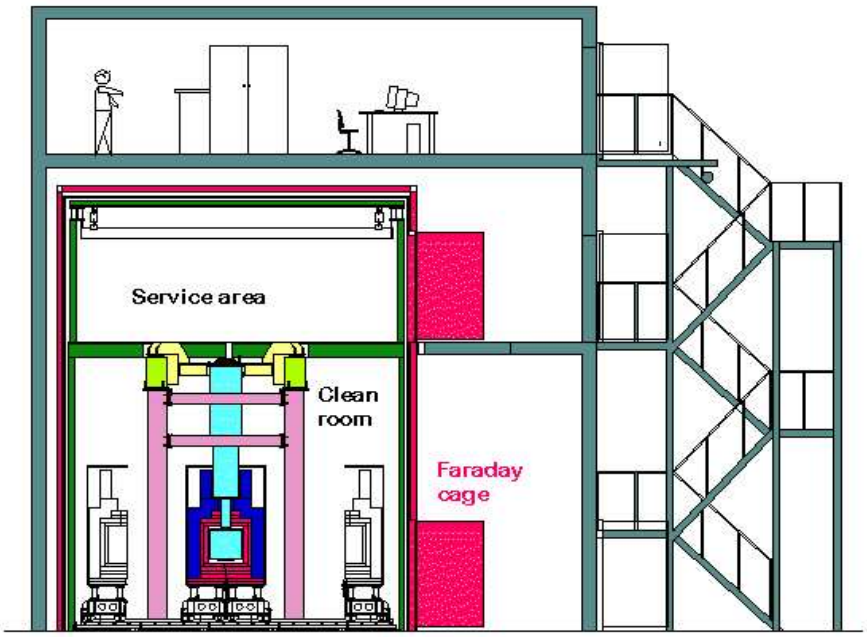

Figure 4: Schematic drawing of the three level CRESST building in hall B of the Gran Sasso Underground Laboratory.

floor of the farady cage, which is outside the clean room to simplify servicing of the cryostat. The first floor also houses the sensitive analog electronics. The gas handling system of the cryostat and the DAQ is outside the faraday cage. In the top floor, of the experimantal building a laminar flow work place is installed which serves to assemble and rebond detectors under clean conditions.

The setup is now beeing upgraded for the experimental program of CRESST-II, which will use 33 of such 300 g phonon/light detector modules. The upgrade includes the installation of a 66 channel SQUID readout system in the existing cryostat, the installation of a neutron shield and a muon veto and a new multichannel electronics and DAQ. The cryostat with the upgraded shielding is shown schematically in fig. 5. The upgrade started in 2004 and will be completed in 2005.

4 Preparations for CRESST-II

Starting in spring 2001, the CRESST set-up had to be moved from hall B to hall A within LNGS. After completion of this move the cryostat was still

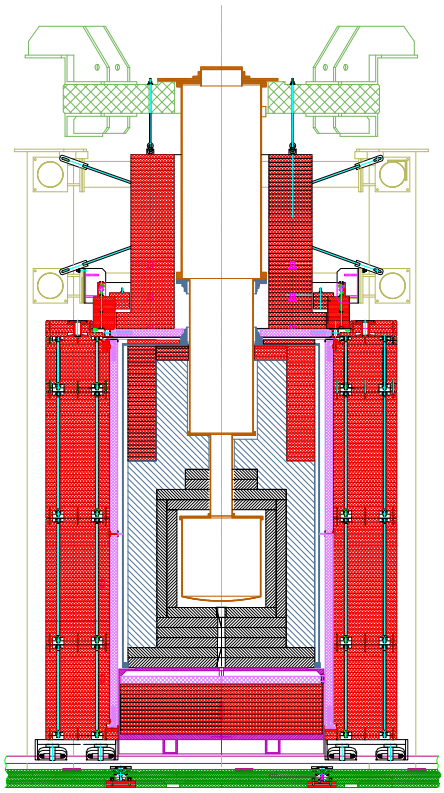

Figure 5: Dilution refrigerator and low background cold box with its shielding upgraded for CRESST-II. The gas tight radon box enclosing the Cu (shown in grey) and Pb (blue) shielding will be completely covered by a plastic scintillator μ-veto (pink) and 50 cm of poly ethylen (red).

equipped with the four SQUID readout system of CRESST-I, which at most allows to run two detectors in parallel. In the beginning of 2002 operation started again with testing and optimization of 300 g $CaWO_4$ prototype detector modules for CRESST-II. In 2002 and 2003 a series of runs was made to optimize the performande of the detector modules. The mounting systems of the crystals again tuned out to be a very critical issue, and it introduced spurious events. In the last run at the end of 2003 the problem was solved. An additional run with two detectors was performed in 2004 with a net exposure of 20.5kg days. Form factor effects effectively limit the energy transfer to the heavy tungsten nuclei in elastic WIMP nucleus scattering to energies below 40 keV. We obtained 16 events in the nuclear recoil acceptance band in the relevant energy region between 12 keV and 40 keV. The cryostat is still without neutron shield and this rate of 0.87 events per kg and day is consistent with the predicted neutron background. Moreover, most of this recoil events have a clear light signal associated with the phonon signal as expected for neutron generated recoils. Neutron events in this energy range are dominantly oxyxgen recoils, whereas WIMPs with spin independent interaction almost exclusively ($\sigma \propto A^2$) recoil off tungsten nuclei. We have measured a very large quenching factor of $Q \approx 40$ for W-recoils, whereas the quenching factor for oxygen recoils is $Q = 7.3$ at mK temperatures and $Q \approx 10$ at room temperature. If a similar quenching factor applies for the tungsten recoils at low temperature, there should be no light emission observed in the 12 to 40 keV region within the detection limit. The exclusion plot derived from this run is shown infig. 6.

The detector was calibrated with external ^{57}Co (122 keV γ's) and ^{60}Co (1.1 MeV and 1.3 MeV γ's) sources. With electric heater pulses the energy calibration is extended over the complete energy range of interrest. Periodically injected heater pulses also serve to confirm the stability of the calibration and to measure the trigger efficiency close to threshold. The phonon channel had a detection threshold for reoils of 3 keV at 100% efficiency and the threshold of the light channel was 8 keV for γ andβ interactions. As shown in fig. 7, the phonon channel exhibited an energy resolution of 1 keV at a 46.53 keV peak from an external ^{210}Pb contamination during the whole measuring period.

Since this detectors can clearly discriminate background from alpha particles and pgamma background one can obtain a background free alpa spectrum. In this spectrum we could unambigously detect the natural α-decay of ^{180}W.A half-life of $T_{1/2} = (1.8 \pm 0.2) \times 10^{18}$ y and an energy release of Q = (2516.4 $\pm$ 1.1 (stat.) $\pm$ 1.2 (sys.)) keV have been measured. The limits on the decay of other Tungsten isotopes could be improved by more than a foactor 50 over present limits.

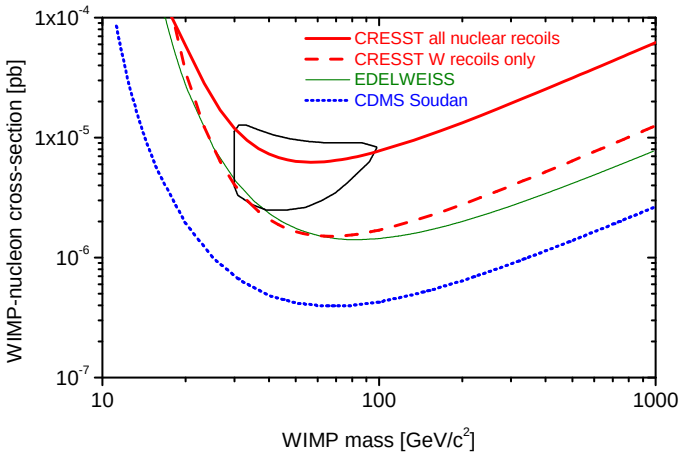

Figure 6: Exclusion plot for spin independent WIMP interaction, derived from 8.11 kg days of data from one 300 g CRESST-II detector module. The area above the curve is excluded at 90% c.l. For comparison, the DAMA positive evidence is shown and also the limits from other cryogenic experiments, CDMS and EDELWEISS.

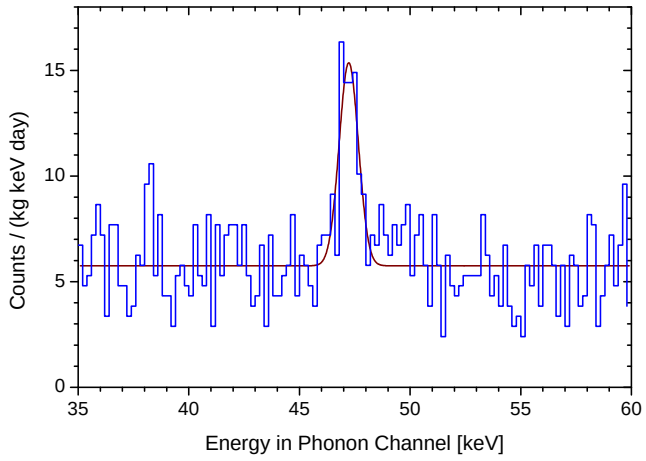

Figure 7: Energy spectrum of the phonon channel of a 300 g $CaWO_4$ detector. The peak at 46.53 keV, with a rate of 3.2 counts/day, is from an external ^{210}Pb contamination. The agreement with the nominal decay energy and the good resolution confirms the energy calibration and its stability.

5 Publications

-Limits on WIMP dark matter using scintillating CaWO cryogenic detectors with active background suppression G.Angloher et al. accepted for publication in Journal of Astroparticle Physics
-Detection of Natural Alpha Decay of Tungsten C. Cozzini et al. accepted for publication in Phys. Rev. B
-CRESST-II: dark matter search with scintillating absorbers G. Angloher et al. NIM A Vol. 520 Nos. 1-3
-Light detector development for CRESST-II, F. Petricca et al. , NIM A Vol. 520 Nos. 1-3

CUORICINO and CUORE. Neutrinoless double beta decay searches with low temperature detectors

R. Ardito[1,2], C. Arnaboldi[1], D. R. Artusa[3], F. T. Avignone III[3], M. Balata[4], I. Bandac[3], M. Barucci[5], J.W. Beeman[6], F. Bellini[14], C. Brofferio[1], C. Bucci[4], S. Capelli[1], F. Capozzi[1], L. Carbone[1], S. Cebrian[7], M. Clemenza[1], C. Cosmelli[14], O. Cremonesi[1], R. J. Creswick[3], I. Dafinei[14], A. de Waard[8], M. Diemoz[14], M. Dolinski[6,11], H. A. Farach[3], F. Ferroni[14], E. Fiorini[1], G. Frossati[8], C. Gargiulo[14], E. Guardincerri[10], A. Giuliani[9], P. Gorla[7], T.D. Gutierrez[6], E. E. Haller[6,11], I. G. Irastorza[7], E. Longo[14], G. Maier[2], R. Maruyama[6,11], S. Morganti[14], S. Nisi[4], C. Nones[1], E. B. Norman[13], A. Nucciotti[1], E. Olivieri[5], P. Ottonello[10], M. Pallavicini[10], V. Palmieri[12], E. Pasca[5], M. Pavan[1], M. Pedretti[9], G. Pessina[1], S. Pirro[1], E. Previtali[1], B. Quiter[6,11], L. Risegari[5], C. Rosenfeld[3], S. Sangiorgio[9], M. Sisti[1], A. R. Smith[6], S. Toffanin[12], L. Torres[1], G. Ventura[5], N. Xu[6], and L. Zanotti[1]

1. Dipartimento di Fisica dell'Università di Milano-Bicocca e Sezione di Milano dell'INFN, Milano I-20126, Italy
2. Dipartimento di Ingegneria Strutturale del Politecnico di Milano, Milano I-20133, Italy
3. Dept.of Physics and Astronomy, University of South Carolina, Columbia, South Carolina, USA 29208
4. Laboratori Nazionali del Gran Sasso, I-67010, Assergi (L'Aquila), Italy
5. Dipartimento di Fisica dell'Università di Firenze e Sezione di Firenze dell'INFN, Firenze I-50125, Italy
6. Lawrence Berkeley National Laboratory, Berkeley, California, 94720, USA
7. Laboratorio de Fisica Nuclear y Altas Energias, Universidàd de Zaragoza, 50009 Zaragoza, Spain
8. Kamerling Onnes Laboratory, Leiden University, 2300 RAQ, Leiden, The Netherlands

9. Dipartimento di Fisica e Matematica dell'Università dell'Insubria e Sezione di Milano dell'INFN, Como I-22100, Italy

10. Dipartimento di Fisica dell'Università di Genova e Sezione di Genova dell'INFN, Genova I-16146, Italy

11. University of California, Berkeley, California 94720, USA

12. Laboratori Nazionali di Legnaro, I-35020 Legnaro (Padova), Italy

13. Lawrence Livermore National Laboratory, Livermore, California, 94550, USA

14. Dipartimento di Fisica dell'Università di Roma e Sezione di Roma 1 dell'INFN, Roma I-16146, Italy

Abstract

CUORE is a bolometric experiment aiming at the search of neutrinoless double beta decay of ^{130}Te with a sensitivity on the Majorana neutrino effective mass of the order of 20-30 meV. The CUORE detector will consist of an array of 988 TeO_2 bolometers arranged in a cylindrical configuration of 19 towers of 52 5×5×5 cm^3 crystals each. A slightly modified tower of CUORE, named CUORICINO, has been already built in 2002 and is taking data at LNGS since 2003. Besides being a crucial test of the CUORE concept, CUORICINO is also a sensitive experiment on $\beta\beta(0\nu)$ of ^{130}Te. It consists of 44 cubic TeO_2 crystals of 5×5×5 cm^3 and 18 crystals of 3×3×6 cm^3 arranged in a single 13 storey tower. With a mass of 40.7 kg it is the largest mass detector operating at low temperature ($\sim$ 10 mK). The progress achieved during 2004 for CUORE and CUORICINO is reported.

1 Introduction

The results of the neutrino oscillation experiments have provided strong evidence that neutrinos undergo flavor-changing oscillations and therefore have non-zero mass. However, such experiments can only determine the differences in the masses of the neutrinos, not the absolute scale of neutrino mass which can only be directly inferred by beta decay end point spectral shape measurements, or in the case of Majorana neutrinos, by the observation and measurement of the neutrinoless double-beta decay half-life. By using the mixing angles and mass differences yielded by the oscillation experiments it is possible to predict with good accuracy a range of values of the effective mass of the Majorana electron neutrino which could be tested by the next generation $\beta\beta(0\nu)$ experiments. In particular it is possible to conclude that at least one species of neutrino has a mass greater than 55 meV while nothing can be deduced about the important issue of whether the neutrino and anti-neutrino are distinct particles (i.e. Dirac type) or not (Majorana type). Neutrinoless double beta decay (DBD) experiments seem therefore to be still the only way to answer both the question of the neutrino mass scale and of its nature.

Consisting of an array of 988, 750 g, TeO_2 bolometers operating at $\sim$10 mK, the CUORE experiment is designed with a sensitivity capable of probing most of the range suggested by oscillation experiment results. The large natural abundance of ^{130}Te (33.87%)

eliminates the requirement for the very expensive isotopic enrichment required in all of the other proposed next generation experiments. The proposed array has a cylindrical structure consisting of 19 towers of 52 detectors each.

One such tower has been successfully constructed and is being operated at LNGS as an independent experiment called CUORICINO since spring 2003. In 3 years of operation CUORICINO will reach a half-life sensitivity for neutrinoless double-beta decay of 6.4×10^{24} years (1σ), corresponding to an average value of $|\langle m_\nu\rangle|$ of the order of 0.3 eV. This will be superior to the present upper bound on the effective electron-neutrino mass set by the ^{76}Ge experiments.

The current year (2004) was of crucial importance both for CUORICINO and CUORE. CUORICINO restated data taking with the full available mass (40.7 kg) in April 2004, after complete repair of the wiring system problem (thermalizers failure). It is presently taking data with a duty cycle better than 60%. On the other hand, CUORE was approved by the LNGS Scientific Committee in April 2004 and by the INFN Scientific Committee in September 2004. Complete funding for the CUORE cryostat was also granted by INFN in September 2004. CUORE has no more to be considered therefore as a project but as an actual experiment.

2 Neutrinoless Double Beta Decay

Neutrinoless double beta decay is a lepton violating process in which a nucleus (A,Z) decays into its isobar (A,Z+2) with the emission of two electrons and no neutrino. This leads to a sharp line in the sum energy spectrum of the two electrons. The decay rate of this process can be expressed as

$$\tau_{1/2}{}^{-1} = G^{0\nu}(Q,Z)|M^{0\nu}|^2|\langle m_\nu\rangle|^2 \tag{1}$$

where $G^{0\nu}(Q,Z)$ is the exactly calculable phase space factor while $|M^{0\nu}|^2$ is the nuclear matrix element whose calculations are still quite uncertain. Of particular interest for neutrino Physics is the dependence on the inverse square of the effective neutrino mass $|\langle m_\nu\rangle|$, which can be expressed in terms of the elements of the neutrino mixing matrix as follows:

$$|\langle m_\nu\rangle| \equiv ||U^L_{e1}|^2 m_1 + |U^L_{e2}|^2 m_2 e^{i\phi_2} + |U^L_{e3}|^2 m_3 e^{i\phi_3}|, \tag{2}$$

where $e^{i\phi_2}$ and $e^{i\phi_3}$ are the Majorana CP–phases ($\pm$ 1 for CP conservation), $m_{1,2,3}$ are the Majorana neutrino mass eigenvalues and U^L_{ej} are the coefficients of the Pontecorvo-Maki-Nakagawa-Sakata (PMNS) neutrino mixing matrix, determined from neutrino oscillation data. Recent global analyses of all oscillation experiments [1, 2, 3, 4, 5, 6, 7, 8, 9, 10] yield on average:

$$|\langle m_\nu\rangle| = |(0.70\pm0.03)m_1 + (0.30\pm0.03)m_2 e^{i\phi_2} + +(<0.05)m_3 e^{i\phi_3}| \tag{3}$$

Since neutrino oscillation experiments can only yield neutrino mass eigenvalue differences squared, they imply two possible patterns, or hierarchies, the normal ($m_1 \approx m_2 << m_3$) and the inverted one ($m_1 << m_2 \approx m_3$). The mass parameter measured in solar oscillation experiments, δ_{solar}, is m_2^2–m_1^2 in the normal hierarchy case and m_3^2–m_2^2 in the inverted

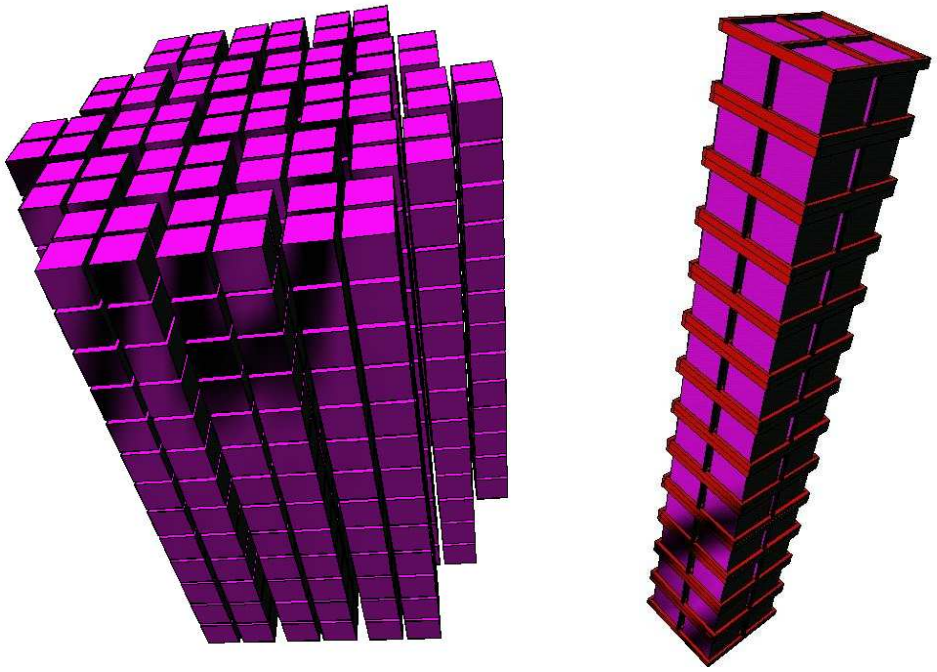

Figure 1: The CUORE detector (left) and one of its 19 towers (right).

case. That measured in atmospheric neutrino experiments, δ_{atm}, is then approximately m_3^2–m_1^2 in both cases. If we neglect U_{e3}^L, and also note that experimentally, $\delta_{solar} << \delta_{atm}$, two useful approximate expressions for $|\langle m_\nu \rangle|$ result:

$$|\langle m_\nu \rangle| = m_1 |0.70 + 0.3 e^{i\phi_2}(1 + \delta^2_{solar}/m_1^2)| \tag{4}$$

for normal hierarchy and

$$|\langle m_\nu \rangle| = \sqrt{m_1^2 + \delta^2_{atm}} |0.70 e^{i\phi_2} + 0.3 e^{i\phi_3}| \tag{5}$$

for inverted hierarchy.

If one uses the value, δ_{atm}=2×10^{-3}, equation (5) implies that $|\langle m_\nu \rangle|$ could have a minimum value as large as 0.045 eV, which implies a minimum sensitivity acceptable for next generation experiments on neutrinoless DBD.

No evidence for neutrinoless DBD has been reported so far [11, 12, 13, 14], with the only exception of a claimed discovery of the decay of ^{76}Ge reported by a subset of the Heidelberg-Moscow collaboration [15]. This claim has been disputed by various authors [1, 16, 17] and also by other members of the same Heidelberg-Moscow Collaboration [18]. It was however confirmed by a new recently published analysis [19, 20]. Due to the smallness of the signal and to the presence of not completely understood peaks in the same energy region (with similar statistical significance) it is possible to conclude that only new results from the presently running (CUORICINO and NEMO3) or from the next generation experiments will possibly turn off the discussion.

3 Low Temperature Detectors

As can be easily deduced from the 1σ sensitivity formula

$$S_{0\nu}^{1\sigma} = \ln 2 \frac{N_A \eta \epsilon}{A} \sqrt{\frac{Mt}{B\Gamma}} \tag{6}$$

where η is the isotopic abundance, ϵ the detection efficiency, M the detector mass, t the measure time, B the background level (per unit mass, energy and time) and Γ the energy resolution, the most effective approach to $\beta\beta(0\nu)$ is represented by direct experiments based on the use of "calorimeters" [21] in which the detector itself is made of a material containing the double beta active nucleus.

Suggested in 1984[22] in order to enlarge the number of $\beta\beta(0\nu)$ active isotopes for which the calorimetric approach could be possible, cryogenic detectors have shown a constantly improving performance. In a very naive approach they consist of a suitable (massive) absorber in good thermal contact with a proper phonon detector (temperature sensor). When made of diamagnetic and dielectric crystals, these bolometers are characterized by a heat capacity which, at low temperature, is proportional to the cube of the ratio between the operating and Debye temperatures [23, 24, 25] and can become so small that even the small energy released by a single particle interaction in the form of heat generates a measurable increase of temperature. Cryogenic detectors offer therefore a wide choice of DBD candidates, since the only requirement is that the candidate nucleus be part of a compound which can be grown in the form of a crystal with reasonable thermal and mechanical properties, low temperature detectors (LTD) offer a wide choice of DBD candidates. In particular, because of its high transition energy (2528.8 $\pm$ 1.3 keV) [26] and large natural isotopic abundance (33.8 %)[27], ^{130}Te is the best candidate and was chosen for CUORE and CUORICINO. Other isotopes (e.g. ^{100}Mo and ^{150}Nd) seem however of particular interest for $\beta\beta(0\nu)$ searches and their inclusion as a part the CUORE project is under study.

4 CUORE (Cryogenic Underground Observatory for Rare Events)

Consisting of an array of 988 TeO_2 bolometers arranged in a cylindrical configuration of 19 towers of 52 crystals each (Fig. 1), CUORE will be a second generation experiment on $\beta\beta(0\nu)$ with a sensitivity in the $|\langle m_\nu \rangle|$ range suggested by neutrino oscillation experiments. The single CUORE detector will consist of a $5\times5\times5$ cm^3 crystal of TeO_2 acting both as a detector and source of the decay. The detectors will be supported in a copper frame and grouped in modules of 4 bolometers, so that each tower will be a stack of 13 modules. The crystal temperature change will be recorded with Neutron Transmutation Doped (NTD) germanium thermistors. All TeO_2 bolometers will be housed in a common dilution refrigerator and operated at a temperature of 8–10 mK. The total mass of ^{130}Te contained in CUORE will be approximately 203 kg.

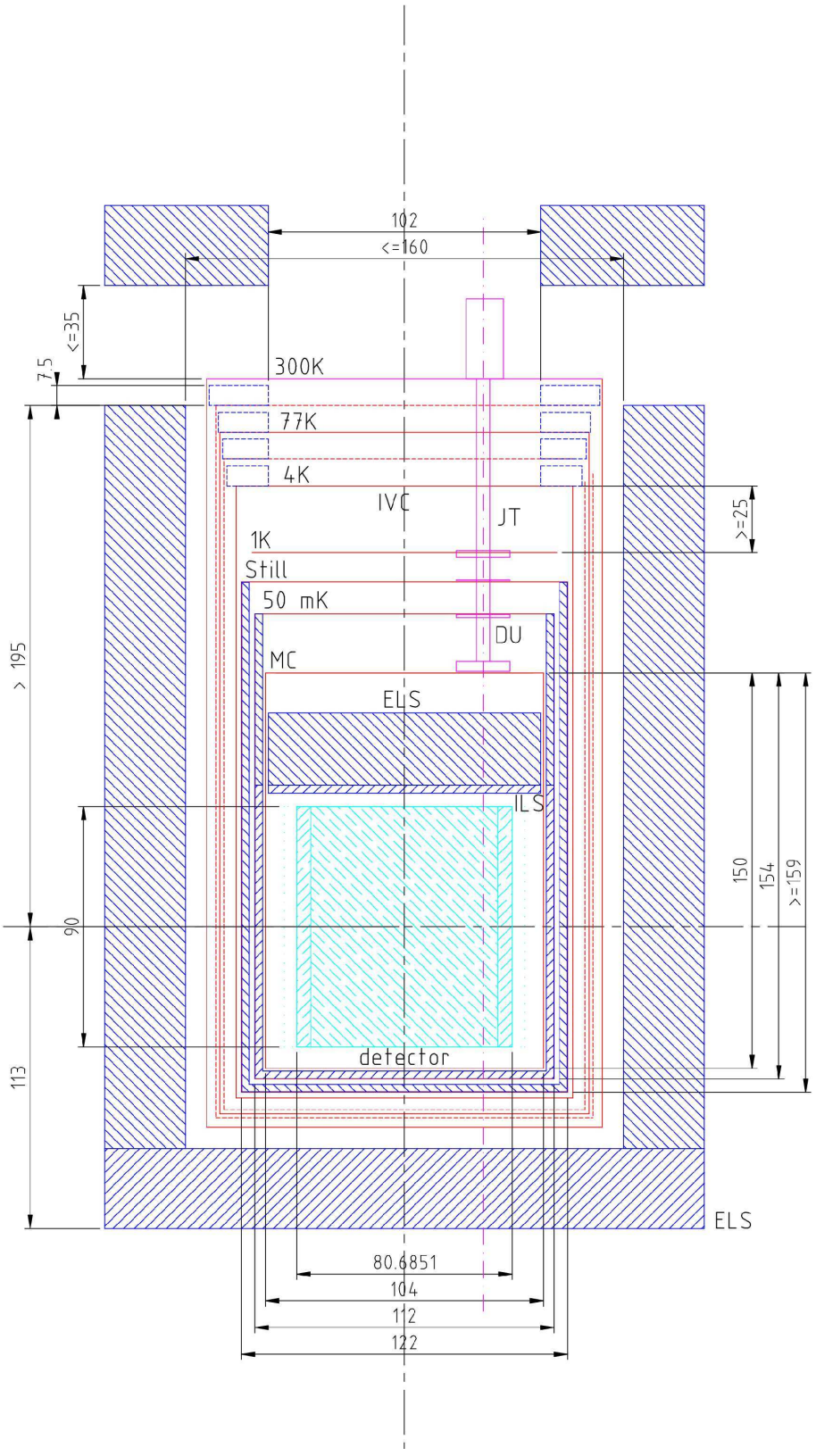

Figure 2: The CUORE cryogenic and radiation shield setup.

The CUORE dilution refrigerator will be built with selected, low activity materials and shielded from environmental and material radioactivity by means of heavy shields held both at low and room temperature (Fig. 2). The relevant details of the CUORE detector as well as the background issues, electronics, DAQ and data-analysis can be found in the CUORE proposal [28].

The expected CUORE $\beta\beta(0\nu)$ sensitivities according to different detector performance and background levels are summarized in table 1. The actual background level that can be presently foreseen just rescaling the CUORICINO results (i.e. assuming to simply assemble 13 CUORICINO towers without any improvement) but taking into account the different structure of the CUORE cryogenic setup is shown in table 2.

A straighforward reduction of this background to a level of the order of 0.01 counts/keV/kg/y is expected as a result of the improvement of the surface cleaning techniques, currently under investigation (a reduction by about an order of magnitude of the crystal and copper surface contamination is required). A more radical change of the surface treatment procedures or the development of active methods for the suppression of surface contributions, resulting in a further improvement by an order of magnitude, cannot be excluded but will require a more extensive and long dedicated R&D. In this respect, the preliminary results concerning the development of Surface Sensitive TeO_2 Detectors [29] looks very promising.

The CUORE experiment was proposed to the LNGS Scientific Committee (LNGSSC) and to the INFN *Commissione Nazionale Scientifica II* (CSN2) in September and November 2003, repectively. It was approved by the LNGSSC in March 2004 subject to the possibility to demonstrate that, compared to CUORICINO, copper (TeO_2 crystal) surface contamination can be reduced by about a factor of 10 (4) within one (two) year. An area of about 10×10 m^2 in the southern wing of Hall A (just near CRESST, in the region once occupied by GNO) was accorded for the location of the CUORE setup inside the underground laboratories (Fig. 3).

Scientific approval of the CUORE project was accorded by CSN2 in June 2004 followed, in September 2004 by the complete approval of the CUORE plan of activities and costs. Complete funding for the CUORE cryostat was also granted by INFN in September 2004. Two new Italian groups, Roma "La sapienza" and Genova, officially joined the CUORE collaboration in June and September respectively.

Table 1: Expected CUORE $\beta\beta(0\nu)$ sensitivity (5 years). B is the background rate and Δ is the FWHM energy resolution. The $|\langle m_\nu\rangle|$ interval is evaluated according to different QRPA nuclear matrix element calculations.

B(counts/keV/kg/y)	Δ(keV)	$T_{1/2}$(y)	$\lvert\langle m_\nu\rangle\rvert$ (meV)
0.01	10	1.5×10^{26}	23–118
0.01	5	2.1×10^{26}	19–100
0.001	10	4.6×10^{26}	13–67
0.001	5	6.5×10^{26}	11-57

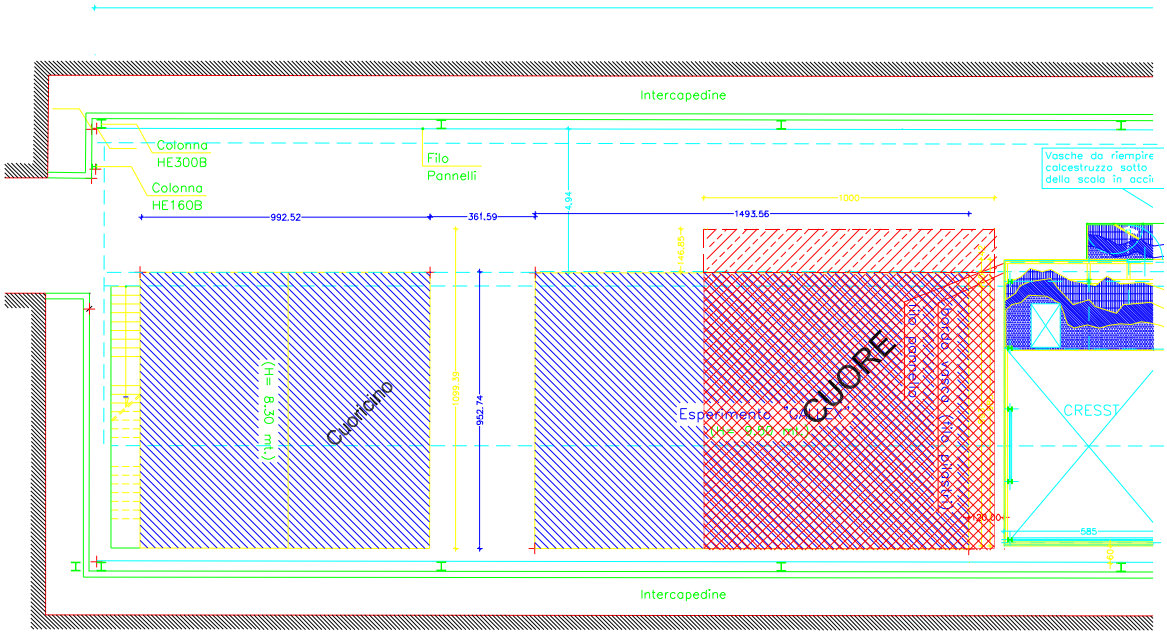

Figure 3: Detail of the south wing of the hall A of the underground Laboratori Nazionali del Gran Sasso, showing the final location of CUORE.

An R&D program aiming at the construction of an enriched core of CUORE (144 central crystals) was presented in July to the American National Science Foundation. It is worthwhile to mention that this option would practically double the CUORE sensitivity on the half-life for $\beta\beta(0\nu)$ of ^{130}Te . Finally, the CUORE scientific motivations and the plan of activities and costs was presented to the American Department of Energy in November 2004.

Table 2: Expected CUORE background contributions in the $\beta\beta(0\nu)$ energy region for different sources. Background rates are obtained by assuming the presently available limits for material bulk contaminations and simply rescaling to the CUORE structure the CUORICINO results on surface contamination.

	B(10^{-3} counts/keV/kg/y)
Detector and setup material bulk	2.39 ± 0.07
TeO_2 crystal surface	16 ± 8.4
Copper surface	58 ± 6.6

4.1 CUORE activities in 2004

CUORE activities in 2004 were mainly devoted to the preliminary design of the hut and cryogenic system, to the study of possible improvements of the detector structure and performance and to the study of possible methods of reduction of the (surface) background contributions. The design of the CUORE DAQ card prototypes (to be tested on the CUORICINO setup) was also completed and the material selection program for all the CUORE setup components started. We will summarize here only the activities concerning the optimization of the detector structure and the analysis of the surface backgrond contributions.

4.1.1 Optimization of the CUORE detector structure

The baseline detector structure described in the CUORE proposal [28] is based on the experience gathered in the course of several years of development of TeO_2 bolometers of increasing mass, culminated with the CUORICINO detector. However, several aspects of the CUORE detectors can be improved substantially (e.g. single element reproducibility) with a contained effort. An intense program of optimization of the detector structure was therefore started in 2004, involving all aspects of the single module structure and of its assembly procedure in the final CUORE towers. Dedicated measurements the mechanical response of the present structure design and calculations of the expected response of various alternate solutions to it were carried out. Test prototypes are under construction and are going to be verified next year in our R&D setup at LNGS. Mechanical tolerances for all the detector parts (TeO_2 crystals and copper mounting structure) as well as geometrical parameters of the final detector structure will be therefore soon fixed. Dedicated measurements for the selection of the best doping level for the CUORE NTD thermistors were also carried out in our Hall C test setup at LNGS. Moreover, innovative eutectic couplings between Ge thermistors and TeO_2 crystals by means of thin gold layers, which could lead to better detector reproducibility, are also under study. The possibility to increase the mass of the single CUORE detector by a factor of two ($6\times6\times6$ cm^3 TeO_2 crystals) without spoiling its performance was tested in June 2004. As expected the increased mass didn't deteriorate the detector response (crystals reached a good base temperature and, despite their small pulse amplitude, showed an extremely good energy resolution: about 4 keV FWHM at the 2615 keV ^{208}Tl line) but resulted in a more critical mechanical behaviour. The larger crystal option was therefore abandoned. Tests for the possible inclusion of crystals containing compounds of $\beta\beta(0\nu)$ candidates other than ^{130}Te (mainly Nd) were also carried out. Test results were not conclusive and will be perfectioned in the near future.

4.1.2 Reduction of the surface background contributions

The most important objective of the next CUORE activities program consists in the development of methods to control and reduce the radioactive background due to surface material contaminations. Three main solutions can be devised:

- improvement of the quality of the copper and TeO_2 crystal surface treatment;

- design of single CUORE elements with a radically innovative structure with a substantially reduced surface and mass;
- development of bolometers able to identify events originated at the detector surface.

A program of optimization of the surface cleaning methods, combined with a more sensitive diagnostic method for low surface contamination levels, was continued with promising results in 2004. As discusse above, the possibility to develop a modified CUORE structure characterized by a reduced mass and surface of the coper parts was also studied, even if this option looks less promising in obtaining radical reductions of the background level. Finally the development of active shields in the form of thin, large-area, ultrapure, Ge or Si bolometers, surrounding the TeO_2 crystals and allowing the identification events originating from maerial surface was considered.

4.1.3 Surface cleaning

The program of surface cleaning of the detector materials close to the TeO_2 bolometers, was originally started in the second run of MiDBD and has been perfectioned in CUORICINO with satisfactory results in terms of background reduction. As described above however, the background level obtained in CUORICINO is not enough to guarantee the CUORE sensitivity goal and an improvement of the cleaning methods of both the TeO_2 crystals and of the Copper parts directly faced to them is necessary. Pure materials are going to be selected both for the mechanical and chemical procedures. Moreover, fast diagnostic methods based on the ICPMS technique are being developed to test the effectiveness of the cleaning treatments.

A dedicated measurement with a bolometric setup ("Radioactivity Array Detector" or RAD) cleaned with an improved procedure based on the use of ultrapure materials was carried out at LNGS at the end of summer. The RAD consists in a 2-plane array made of 8 $5\times5\times5$ cm^3 TeO_2 crystals, with a structure almost identical to that of CUORICINO (fig. 4). A nice feature of the RAD is that it can be mounted inside the hall C cryostat, as a standalone system, together with other detectors housed in an independent mounting structure. In this manner it is possible to exploit the hall C facility simultaneously for different CUORE measurements. The preparation of the first run of the RAD started in June. The crystals were etched with nitric acid (removing about 10 micron on the surfaces) and then polished with a SiO_2 powder. The copper mounting structure was etched and successively treated through electroerosion removing from 10 to 30 microns on the surfaces. The materials used for these treatments were previously selected for their U and Th contamination on the basis of HPGe spectrometry and ICPMS. All the operations - including detector assembly - were performed in the same clean room. Once cooled in the hall C refrigerator, one of the eight crystals disconnected. The other 7 crystals worked properly with an average energy resolution (FWHM at 2.6 MeV) of about 10 keV. The measurement in hall C lasted for about 2 months (September-November), totalling a live time of 7700 hours on the sum background spectrum of the 7 crystals. The RAD background was compared with that measured by Cuoricino crystals, yielding the following results:

- below the 2615 keV ^{208}Tl line (the so called γ-region) the measured background was by far higher with respect to CUORICINO; this is completely justified by the reduced internal and external shielding of the hall C refrigerator. The ^{208}Tl line itself showed a counting rate of 0.03 c/h to be compared with the average 0.007 c/h of the CUORICINO crystals. Similarly in the DBD region the hall C counting rate was 0.8 c/keV/kg/y compared to the 0.18 c/keV/kg/y of CUORICINO.

- between 2.7 and 4 MeV, a region where CUORICINO shows a continuous background ascribed to degraded alphas from external surface contamination, a continuum similar to that of CUORICINO was observed. A peak at 3.2 MeV ascribed to an internal ^{190}Pt contamination of the crystals produced during crystal grow in a Platinum crucible, was observed both RAD and CUORICINO.

- between 4 and 5 MeV a deep change was observed between CUORICINO and RAD: the asymmetric peaks (bumps) produced by the ^{238}U surface contamination of the CUORICINO crystals disappeared. Two almost gaussian peaks at 4.1 and 4.7 MeV were clearly visible above the continuum. These two peaks, which are probably present also in CUORICINO but hidden by the ^{238}U bumps, can be ascribed to bulk contamination of the TeO_2 crystans, consisting of long living isotopes of Th (i.e. ^{232}Th and ^{230}Th).

- between 5 and 6 MeV the background is by far dominated by the 5.3 and 5.4 MeV lines of ^{210}Po . The first line is due to a contamination external to the crystals and correspond to an energy deposition of the emitted alphas (i.e. no recoil contribution). The latter is due instead to a surface/internal contamination of the crystals where also the nuclear recoil participates to the energy deposition. These two contaminations have been always observed in our detectors with large differences in counting rates from crystal to crystal. Apparently no correlation exists with background rates in the 2.7-4 region.

- above 6 MeV once again a consistent reduction of the counting rate with respect to Cuoricino is observed, this in agreement with the interpretation of a decrease of the crystal surface contamination.

In conclusion, the results of this first measurement with the RAD can be interpreted in terms of a clear improvement of a factor 4 in the reduction of the crystal surface contamination and of only a slight improvement in the reduction of the sources responsible for the counting rate in the continuum between 2.7 and 4 MeV. It should be stressed that, for what concerns the crystal surface contamination, this result is in the range required for the CUORE sensitivity goal. Indeed when extrapolated to the CUORE array the crystal surface contamination measured with the RAD yields a contribution to the overall background in the DBD region of less than few 10^{-3} c/keV/kg/y. Furthermore, the reduced background allowed a new, more sensitive, evaluation of TeO_2 crystal internal contamination resulting in ^{232}Th ¡ $3\ 10^{-14}$ g/g and ^{238}U ¡ $1\ 10^{-14}$ g/g. The RAD has therefore proved to be a powerful diagnostic tool to test background achievements for CUORE. In future this same array will be used to test other background sources and or other surface cleaning techniques. The next run is indeed intended to verify the

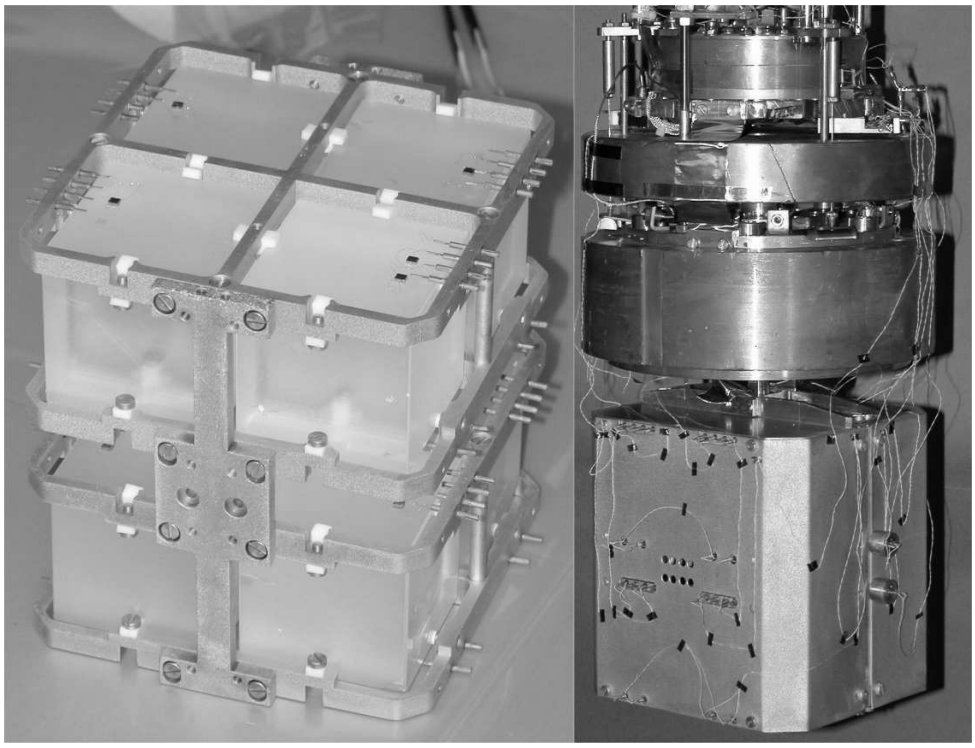

Figure 4: The Radioactivity Array Detector (RAD).

radioactivity of small components like gold bonding wires, PTFE and Si heaters. A large amount of material (10, 100 times more than that required for detector construction) will be placed on the top and bottom copper covering of the RAD, so that the pieces will face directly the TeO_2 crystals. In a month it will be possible to have very sensitive limits on both surface and bulk contamination of these components.

4.1.4 Development of surface sensitive TeO_2 elements

The basic idea of the method consists in the realization of active Ge (or Si) shields completely surrounding the TeO_2 crystals in order to get rid of possible events originating at te detector surface by means of the anti-coincidence technique. In principle this can be achieved by thermally coupling these active shields to the main TeO_2 detector. The Ge or Si auxiliary bolometers would be attached at the main crystal providing almost complete coverage without a dedicated holder. In this way, a composite bolometer would be realized with multiple read-out, capable to distinguish the origin of the event (active shields or TeO_2 crystal) by means of the comparison among pulses coming from the different elements. A degraded alpha coming from outside would release its energy in the shield, originating a thermal pulse that, seen by the shield thermistor, would be much higher than a pulse corresponding to the same energy released directly in the main TeO_2 crystal.

In order to reduce the readout channels, the six thermistors of the shields could be connected in series or in parallel. In this way, the total number of channels would simply double and would represent a tolerable complication. The size of the auxiliary bolome-

ters would be $50\times50\times0.3$ mm^3 or $60\times60\times0.3$ mm^3: therefore, the main crystal plus the shields would form a cube with a side only 0.6 mm larger than the main crystal alone, preserving the general CUORE structure and rendering the assembling procedure substantially unchanged. This proposed solution has the potential to control the problem of the surface radioactivity relying on a technological improvement of the detector rather than on a better cleanness of the employed materials.

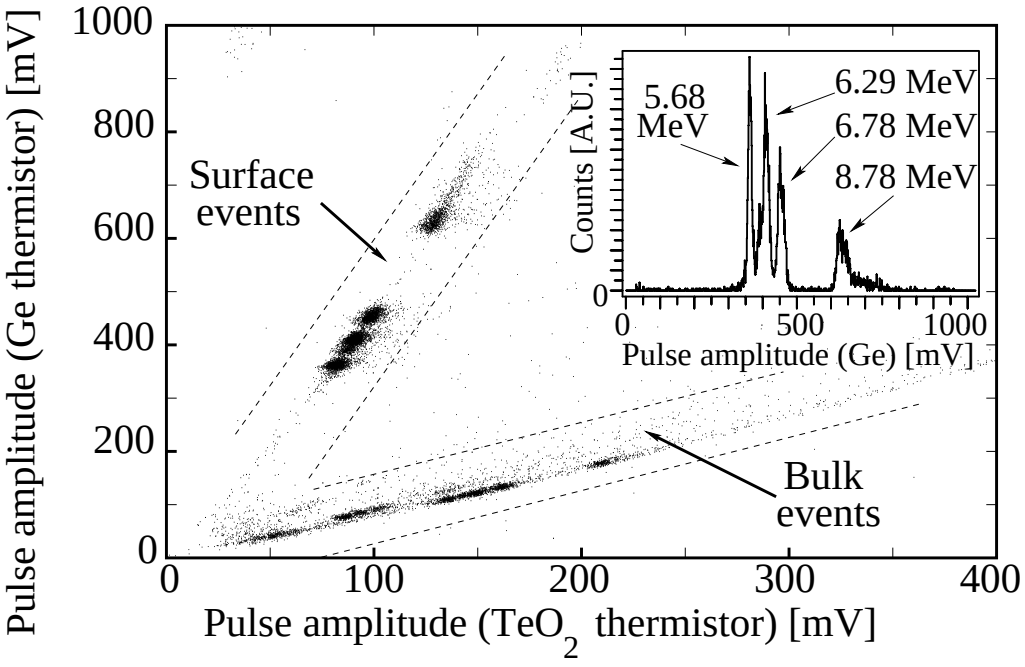

Figure 5: Scatter plot of the pulse amplitudes from TeO_2 thermistor versus the pulse amplitudes from shield thermistor obtained with a 12 g TeO_2 surface sensitive detector.

In order to test the method, several small scale prototype detectors were realized. In all of them the main absorber consisted of a TeO_2 single crystal, with masses ranging from 12 g ($2\times2\times0.5$ cm^3) to 48 g ($2\times2\times2$ cm^3). A Ge or Si single crystal with a 1.5×1.5 cm^2 surface and 500 μm thickness was glued at a 2×2 cm^2 face by means of four epoxy spots (1 mm diameter and 50 μm thick). Neutron Transmutation Doped (NTD) Ge thermistors were glued at the main absorbers and at the auxiliary Ge or Si bolometers with six epoxy spots (0.5 mm diameter and 50 mm thickness). The NTD chip size was $3\times1.5\times1$ mm^3 in all cases. The coupling of the main absorber to the heat bath was realized by means PTFE blocks, as in the CUORICINO modules. The Ge or Si active layers were exposed to α particles. The source was obtained by a shallow implant of ^{224}Ra nuclides onto a piece of copper tape, facing the Ge or Si layer. ^{224}Ra is an a emitter with a half life of 3.66 d in equilibrium with its α and β emitting daughters. The main α lines are at 5.68, 6.29, 6.78 and 8.78 MeV. Two weak lines sum up at about 6.06 MeV. The detector typical operation

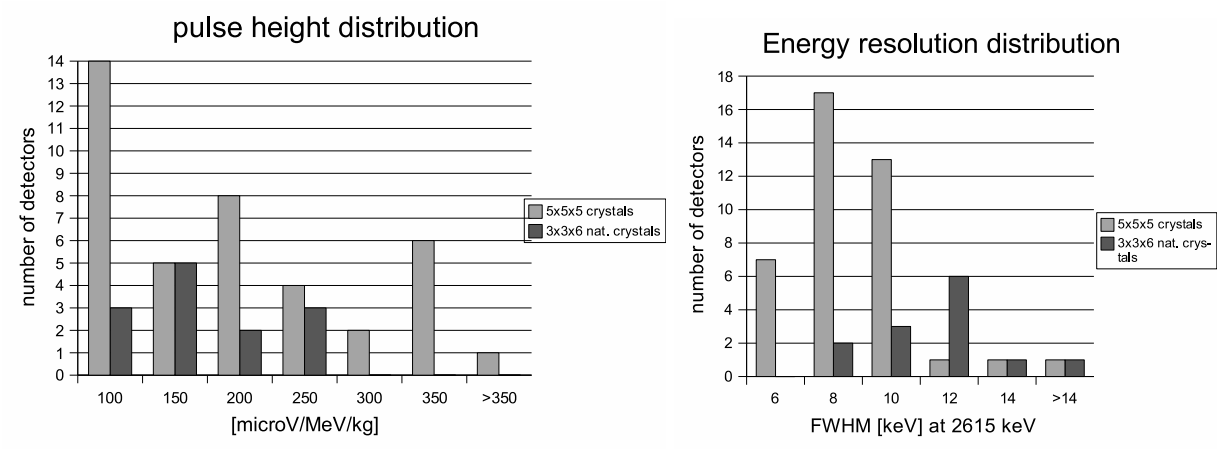

Figure 6: Distribution of the single detector energy responses (left) and energy resolutions (FWHM) at the ^{208}Tl 2615 keV line (right) for the second (2004) CUORICINO run.

temperatures were T $\sim$25 mK. No remarkable differences were observed between Ge and Si shields. In particular, the scatter plot obtained with a 12 g TeO_2 absorber (2×2×0.5 cm^3 dimension) is shown in fig. 5. The fast pulses coming from the active Ge layer had a rise time of $\sim$6.5 ms and a decay time of $\sim$40 ms, while the pulses coming from the main absorber were remarkably slower (rise time $\sim$9.7 ms, decay time $\sim$70 ms. The two bands, corresponding to surface and bulk events, are well separated and the 4 main α lines of the source are clearly appreciable. This measurements demonstrates therefore the power of this technique in identifying surface events. The possibility to improve the effectiveness of the method by using also rise time selection is under study. In fact, by this kind of analysis the fast surface events can be cleanly separated by the slow bulk events and this could help to get rid also of the main absorber thermistor, reducing the read-out channel to one as in the conventional case.

5 CUORICINO

Besides being a conclusive test of CUORE, CUORICINO is also a sensitive experiment on $\beta\beta(0\nu)$ of ^{130}Te . Installed at LNGS during 2002 and cooled down for the first time in January 2003, CUORICINO is providing important results concerning both the technical performance of the bolometric tower, the $\beta\beta(0\nu)$ background level and origin, and the $\beta\beta(0\nu)$ of ^{130}Te .

CUORICINO is a tower of 13 planes containing 62 crystals of TeO_2 ; 44 of them are cubes of 5 cm on a side while the dimensions of the others are 3×3×6 cm^3 . All crystals are made with natural paratellurite, apart from two 3×3×6 cm^3 crystals, which are enriched in ^{128}Te and two others of the same size enriched in ^{130}Te , with isotopic abundance of 82.3 % and 75 %, respectively. The total mass of TeO_2 in CUORICINO is 40.7 kg, the largest by more than an order of magnitude than anycryogenic detector.

In order to shield against the radioactive contaminants from the materials of the refrigerator, a 10 cm layer of Roman lead, with ^{210}Pb activity of <4 mBq kg^{-1} [30],

was inserted inside the cryostat immediately above the CUORICINO tower. A 1.2 cm lateral layer of the same lead is framed around the array to reduce the activity of the thermal shields. The cryostat is externally shielded by two layers of Lead of 10 cm minimal thickness. The background due to environmental neutrons is reduced by a layer of Borated Polyethylene of 10 cm minimum thickness. The refrigerator operates inside a Plexiglass anti-radon box flushed with clean N_2, and inside a Faraday cage to reduce electromagnetic interference.

Thermal pulses are recorded by means of Neutron Transmutation Doped (NTD) Ge thermistors thermally coupled to each crystal. Possible detector response instabilities are controlled by means of voltage pulses generated across heater resistors attached to each bolometer by high stability pulse generators. A tagging of these stabilizing signals is made by the acquisition system. The detector temperature is stabilized by means of a dedicated feedback circuit.

The front-end electronics for all the $3\times3\times6$ cm^3 and for 20 of the $5\times5\times5$ cm^3 detectors is maintained at room temperature while a *cold electronics* stage (located in a box at $\sim$100 K near the detector to reduce the noise due to microphonics) is used for the remaining 24 crystals.

CUORICINO is operated at a temperature of $\sim8 \pm 1$ mK. A routine energy calibration is performed at the beginning and at the end of each background measurement period ($\sim$two weeks) by irradiating the detector with ^{232}Th and/or ^{60}Co sources placed in immediate contact with the refrigerator (fig. 8).

During the first cool down in Spring 2003, 12 of the $5\times5\times5$ cm^3 and one of the $3\times3\times6$ cm^3 crystals were disconnected because of a problem in the thermalisation stages. In order to collect crucial informations on the detector performance and background level, data taking was continued with a detector reduced mass. The thermalizers problem was fully solved at the beginning of 2004 and the CUORICINO was cooled down again in April with only 2 of the 13 detectors still disconnected. The distributions of the single detector energy responses and energy resolutions for thi second CUORICINO run are shown in Fig. 6.

Due to a serious accident occurred to the CUORICINO Helium liquefier in Spetember, we were compelled to disconnect it from the cryogenic setup and switch to manual refilling of the Helium main bath. Since then, two shifters are always needed at LNGS to follow the detector operation. On the other hand, the nice surprise is that starting with the liquefier disconnection the experiment duty cycle (just background measurement) has steadily increased to about 60%. We have therefore decided to continue with manual refilling while relying on the use of the liquid Helium produced by an external Helium liquefier (kindly shared with the CRESST Collaboration).

The total statistics so far collected and analyzed corresponds to an effective exposure of 10.85 kg $\times$year. The background spectra, after the anticoincidence cut, are separately shown for the $5\times5\times5$ cm^3 and $3\times3\times6$ cm^3 detectors in fig. 7). The detail of the sum spectrum of the $5\times5\times5$ cm^3 and $3\times3\times6$ cm^3 crystals in the $\beta\beta(0\nu)$ region is shown in Fig. 9. The lines at 2447 and 2615 keV from the decays of ^{214}Bi and ^{208}Tl, and also the weak line at 2505 keV due to the sum of the two γ lines of ^{60}Co are clearly visible. The background at the energy of neutrinoless DBD is of 0.18 ± 0.01 counts kg^{-1} keV^{-1} y^{-1}.

No peak was observed at the ^{130}Te $\beta\beta(0\nu)$ energy implying a 90% C.L. lower limit of

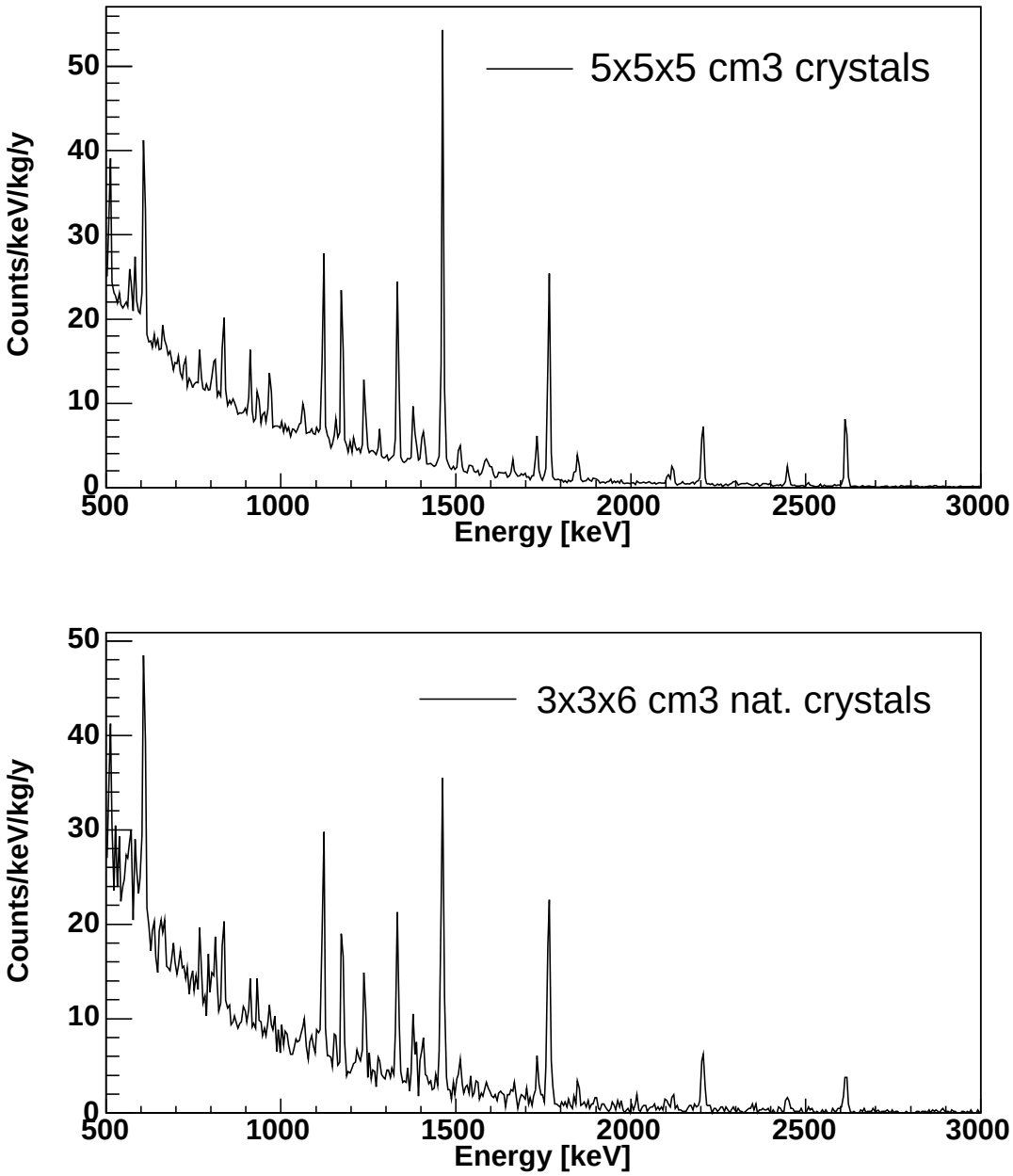

Figure 7: Background sum spectra, after anticoincidence cut, for $5\times5\times5$ cm^3 and $3\times3\times6$ cm^3 CUORICINO crystals.

1.8×10^{24} years on the lifetime for this decay. The upper bounds on the effective mass of the electron neutrino that can be extracted from this result depend strongly on the values adopted for the nuclear matrix elements. Considering all the theoretical calculations apart from those based on the shell model whose validity for heavy nuclei is sill under discussion, it is possible toindicate an interval of 0.2 to 1.1 eV, which partially covers the mass range of 0.1 to 0.9 eV indicated by H.V. Klapdor-Kleingrothaus et al. [20].

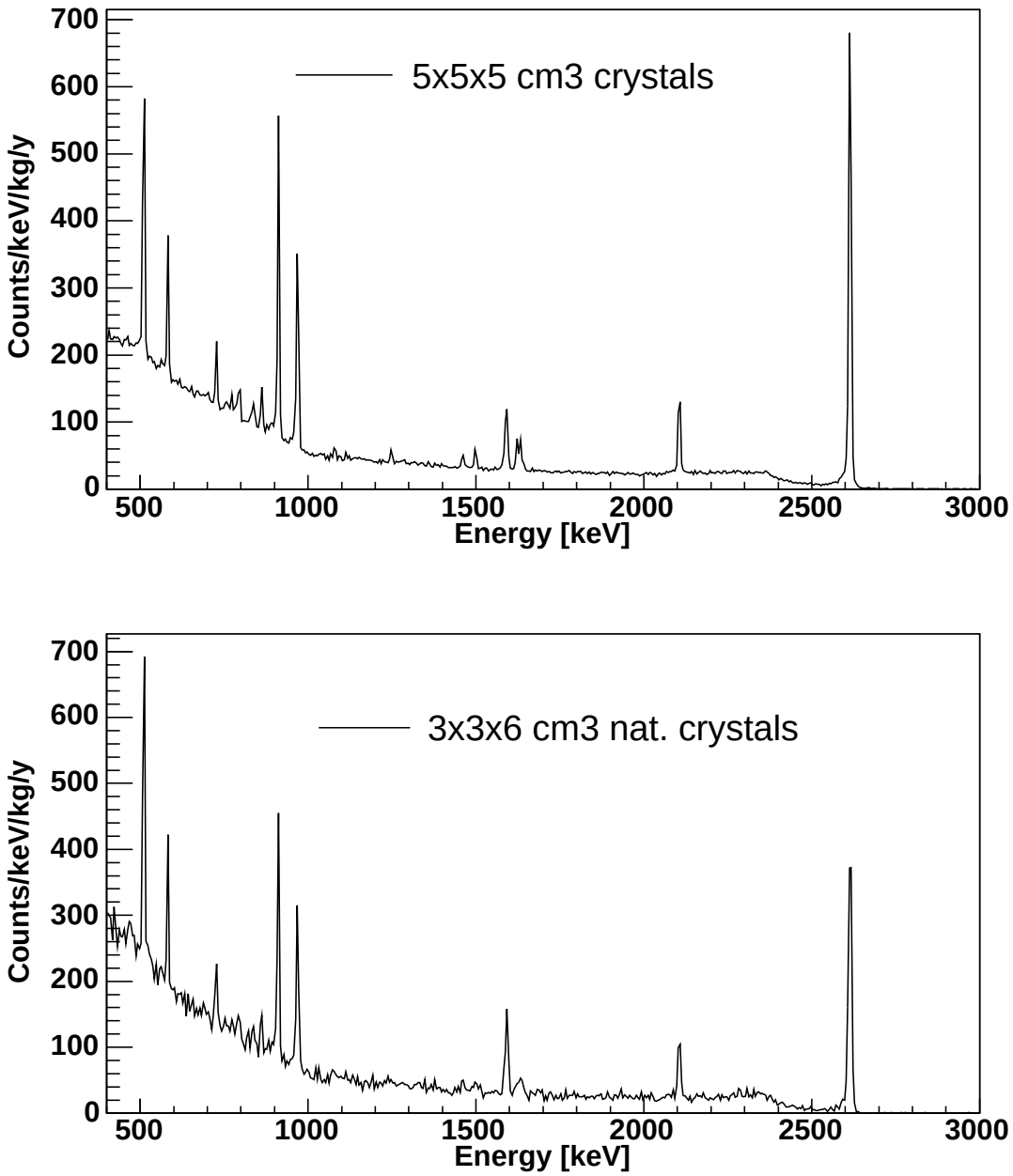

Figure 8: Calibration sum spectra (^{232}Th γ-source), after anticoincidence cut, for 5×5×5 cm^3 and 3×3×6 cm^3 CUORICINO crystals.

5.1 Conclusions

The excellent results of CUORICINO in terms of detector performance and $\beta\beta(0\nu)$ sensitivity are the best proof of the actual feasibility of a larger scale experiment like CUORE. Improvements with respect to the present CUORICINO design are still possible and are under study. In particular an improvement of the background level by at least an order

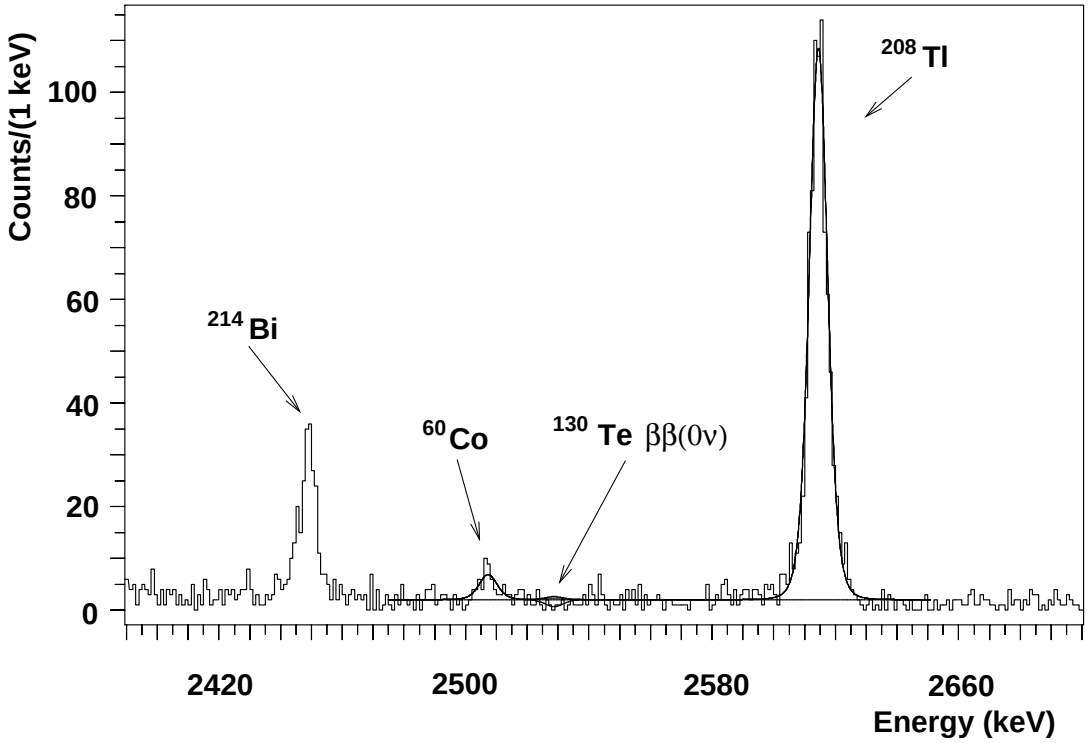

Figure 9: Spectrum of the sum of the two electron energies in the region of neutrinoless DBD

of magnitude is required in order to fulfil the CUORE sensitivity goal and a big effort is being dedicated by the CUORE collaboration to the development of new active and passive techniques of background reduction. In this respect, the CUORICINO background results, especially when coupled with those of dedicated runs for the study of the background contributions in bolometric systems, could be crucial in identifying the background sources and allow us to reach the required sensitivity for CUORE.

We would like to thank the Laboratori Nazionali del Gran Sasso for generous hospitality and support. We would like to acknowledge also the help of C. Callegaro, G.Ceruti, G. Galotta, R. Gaigher, S. Parmeggiano, M. Perego, B. Romualdi and A. Rotilio in various stages of the CUORICINO experiment.
This experiment has been partly supported by the Commission of European Communities under contracts FMRX-CT98-03167 and HPRN-CT-2002-00322, by the U.S. Dept. of Energy under Contract number DE-AC03-76 SF000 98 and by the National Science Foundation.

6 List of 2004 Publications

1. C. Arnaboldi et al., *First Results on Neutrinoless Double Beta Decay of* ^{130}*Te with the Calorimetric Cuoricino Experiment*, Phys. Lett. B 584 (2004) 260.

2. C. Arnaboldi et al., *A New Limit on the neutrinoless $\beta\beta$ -decay of ^{130}Te* , Submitted to Phys. Rev. Lett. (hep-ex/050110)

3. L. Foggetta et al., *Surface-sensitive macrobolometers for the identification of external charged particles*, Submitted to Appl. Phys. Lett.

4. C. Arnaboldi et al., *The temperature stabilization system of CUORICINO, an array of macro bolometers*, Submitted to IEEE Trans. Nucl. Science.

5. C. Arnaboldi et al., *CUORE: Cryogenic Underground Observatory for Rare Events*, Proposal to the LNGS and INFN Scientific Committees, Milano Gennaio 2004.

6. O. Cremonesi et al., *New CUORICINO results and the CUORE project*, Proc. of Noon2004, Tokyo, February 2004, Japan.

7. E. Previtali et al., *CUORICINO: a new large bolometer array for astroparticle physics*, Proc. of the "9th Pisa Meeting on Advanced Detectors: Frontier Detectors for Frontier Physics", NIM A 518 (2004) 256.

8. C. Brofferio et al., *CUORICINO status and CUORE prospects*, Proc. of Now2004, Conca Specchiulla (Otranto), September 2004, Italy.

9. M. Pedretti et al., *Search for neutrinoless double beta decay of Te-130 with low temperature detectors: Cuoricino and CUORE experiments*,Proc. of INPC 2004, Goteborg, June 2004, Sweden.

10. E. Fiorini et al., *Results of Cuoricino and prospects for CUORE*, Proc. of "Neutrino 2004",College de France, Paris, June 2004, France.

11. S. Cebrian et al., *Results from Cuoricino and perspectives for CUORE*, Proc. of "IDM2004", Edinburgh, September 2004, Scotland.

12. P. Gorla et al., *Cuoricino and CUORE detectors: developing big arrays of large mass bolometers for rare events physics*, Proc. of the "9th Topical Seminar on Innovative Particle and Radiation Detectors", Siena, May 2004, Italy.

13. S. Pirro et al., *Cleanliness, backgrounds and surface contamination in CUORE*, Proc. of the "Topical Workshop in Low Radioactivity Techniques", Sudbury, December 2004, Canada.

References

[1] F. Feruglio, A. Strumia and F.Vissani, Nucl.Phys.B 637 (2002) 345

[2] F. Feruglio et al., Nucl.Phys.B 659 (2003) 359.

[3] F. Joaquim, Phys.Rev. D 68 (2003) 033019.

[4] C. Giunti, hep-ph/0308206.

[5] S. Pascoli and S.T.Petkov, Phys.Lett. B 544 (2004) 239.

[6] S. Pascoli and S.T.Petkov, Phys.Lett. B 580 (2004) 280.

[7] J. Bahcall and C.Pena-Garay, J.High En.Phys JHEP 11 (2004) 4.

[8] J. Bahcall et al., Phys.Rev.D 70 (2004) 033012.

[9] H. Murayama and C.Pena-Garay, Phys.Rev.D 69 (2004) 031301.

[10] J. Suhonen and O.Civitarese, Phys.Rep. 300 (1998) 123.

[11] V.I. Tretyak and Yu.G.Zdesenko, At.Data Nucl.Data Tables 80 (2002) 83.

[12] A.S. Barabash, Phys.of Atom.Nuclei 27 (2004) 438.

[13] S.R.Elliott and P.Vogel, Ann.Rev.Part.Sci. 53 (2002) 115.

[14] S.R. Elliott and J.Engel, J.Phys.G:Nucl.Part.Phys. 30 (2004) 183.

[15] H.V. Klapdor-Kleingrothaus et al., Mod.Phys.Lett.A 16 (2001) 2409.

[16] C.E. Aalseth et al., Mod.Phys.Lett.A 17 (2002) 1475.

[17] C.E. Aalseth et al., Phys.Lett.B 546 (2002) 206.

[18] A.M. Bakaliarov et al., hep-ex/0309016.

[19] H.V. Klapdor-Kleingrothaus et al., Phys.Lett.B 586 (2004) 2004.

[20] H.V. Klapdor-Kleingrothaus et al., Nucl.Instrum.and Meth. 522 (2004) 367.

[21] G.F. Dell'Antonio and E. Fiorini, Suppl. Nuovo Cim. 17 (1960) 132.

[22] E. Fiorini and T. Niinikoski, Nucl. Instrum. and Meth. 224 (1984) 83.

[23] D. Twerenbold, Rep. Prog. Phys. 59 (1996) 349; N. Booth, B. Cabrera and E. Fiorini, Ann. Rev. of Nucl. Sci. 46 (1996) 471.

[24] Proc. of the IX International Workshop on Low Temperature Detectors, Ed. by F. Scott Porter, D. McCammon, M. Galeazzi and C.K. Stahle, Madison (Wisconsin) 22-27 July 2001. Amer. Inst. of Phys. Vol. 605 (2002)

[25] Proc. of the X International Workshop on Low Temperature Detectors, Ed. by F.Gatti Genoa 6-11 July 2003, to be published on Nucl. Instrum. and Meth.A

[26] G.R. Dyck et al., Phys. Lett. B 245 (1990) 343

[27] R.B. Firestone, C. Baglin and S.F. Chu: Tables of Isotopes (eight edition), 1998 CD-ROM update (1998)

[28] CUORE Collaboration, *CUORE (Cryogenic Underground Observatory for Rare Events): A proposal submitted to the INFN, the us doe and the us nsf by the international CUORE Collaboration*, http://crio.mib.infn.it/wig and hep-ex/0501010.

[29] L. Foggetta et al., *Surface-sensitive macrobolometers for the identification of external charged particles*, Submitted to Appl. Phys. Lett.

[30] A. Alessandrello et al., Nucl.Instrum.and Meth. A 142 (1998) 454.

ERMES

Wolfango Plastino[a,b], Iosif Chereji[c], Stela Cuna[c], Lauri Kaihola[d], Nicolae Lupsa[c], Gabriela Balas[c], Valentin Mirel[c], Petre Berdea[c], Calin Baciu[e]

[a] Department of Physics, University of Roma Tre, Rome (Italy)
[b] National Institute for Nuclear Physics, Section Rome III, Rome (Italy)
[c] National Institute of Research and Development for Isotopic and Molecular Technologies, Cluj-Napoca (Romania)
[d] PerkinElmer Life and Analytical Sciences, Wallac Oy, Turku (Finland)
[e] Faculty of Environmental Sciences, Babes-Bolyai University, Cluj-Napoca (Romania)

Abstract

The usual improvement of the detection sensitivity by an order (or more) of magnitude for the tritium content of water samples can be performed by electrolysis. As the developed batch of cells was provided with a pre-programmable electronic system having an electrolyte level sensor, the pre-set termination condition in the electrolysis can be set in such a way as to ensure in each cell a desired final quantity of water, usually 20-30 % higher than that used for LSC. Three water samples and their duplicates (a tap water, practically with unobservable content of tritium, a rain water with a low level of tritium concentration and a contaminated moisture, collected from a nuclear laboratory) were subjected to two enrichment processes: an electrolysis for l.e. (with EFT ≅11), and an electrolysis for h.e. (with EFT ≅22).

1 Introduction

Tritium is one of the most important global contaminants, produced not only by nuclear bomb tests, but always in increasing amount by fission reactors and nuclear fuel reprocessing as well. It has been established that useful hydrological and meteorological information can be obtained by measuring the natural tritium content of precipitations, surface water and groundwater. In fact, tritium contamination of the environment may be used as a tracer in hydrological investigations or in groundwater dating. Routine tritium analyses in water samples for hydro-geological and hydrological studies are usually performed by liquid scintillation spectrometry. At present, a certain degree of enrichment is essential to obtain adequate net tritium count rates for most of the water samples. Electrolysis is generally used for the enrichment process [1-4].

2 Methods

In order to increase the tritium concentration in the water samples to an easily measurable level, a batch of 5 electrolysis cells was developed [5]. The procedure for electrolytic tritium enrichment of water has to exclude both the isotopic fractionation during the sample treatment and the possible contamination with another water of high ^{3}H concentration. Before the enrichment run, the procedure includes a primary distillation of the samples and after the enrichment, a final distillation. During distillation the temperature should be as high as possible to attain a water recovery close to unit. The distillation and electrolysis cells reservoirs should be separated from the surrounding air as it usually contains water vapor with a higher 3H concentration than that of the sample. With a view to obtain a desired final volume automatically, a pre-programmable electronic system was developed. By using an electrolyte level sensor, this system can switch-off the current through any cell in which the desired volume of electrolyte is attained. Each cell was filled with about 330 mL of the sample water in which 2.5 g NaOH was dissolved for the single step run. The cells were connected in series and a voltage corresponding to 2.2-2.7 volts was applied across each of them from the battery-charger. The current was stabilized at maximum 10 A and was reduced at a half value on the final stage of the electrolysis run. A cooling bath with running tap water (4÷8 °C) was used in order to minimize the lost quantity of evaporated and sprayed water. A total charge of about 977 Ah is theoretically needed for the volume reduction of about 305 mL of water. When the preset level of the remaining electrolyte has been attained in a cell, the current has been automatically interrupted through this cell and the electrolysis has been continued in the remaining cells until the preset levels were attained in each of them. Afterwards the cells were removed from the cooling bath and the enriched samples poured out of the anode vessels into glass flasks and distilled without adding a neutralizing agent.

3 Results and discussion

Three water samples with different contents of tritium were selected for electrolysis enrichment: 1) tap water (presumably with a very low level of tritium content); 2) rain water (with a low tritium content); 3) contaminated moisture collected from the controlled area of a nuclear laboratory, where some sources of high tritium activity were manipulated and stored. From each sample A a replicate B was taken, both of them being distilled and electrolyzed separately: in the former electrolysis for low enrichment (l.e.), and in the latter electrolysis for high enrichment (h.e.). In the electrolysis for h.e., after a first step (during which the volume was reduced from 355 mL to about 50 mL), for the second step of the run the cells were refilled with 305 mL of sample water without adding more NaOH, in order to keep the final electrolyte concentration within the tolerable limits (the initial quantity of NaOH was also 2.5 g as in the electrolysis for l.e.). The enrichment factor (EFT) for the tritium content was calculated by means of the enrichment factor (EFD) for the deuterium content. For the tritium measurements, an ultra low-level liquid scintillation spectrometer Quantulus was used in underground conditions at Gran Sasso National Laboratory, where a 3800 m water equivalent shielding almost fully removes the

cosmic contribution to the background [6-9]. By using the glass vials having some content of ^{40}K, the contribution of the Cherenkov and fluorescence radiation from glass is impossible to remove fully with Quantulus Pulse Shape Analyzer (Fig 1, channels 50-300). Some loss of ^{3}H efficiency will always be associated with such attempts [10].

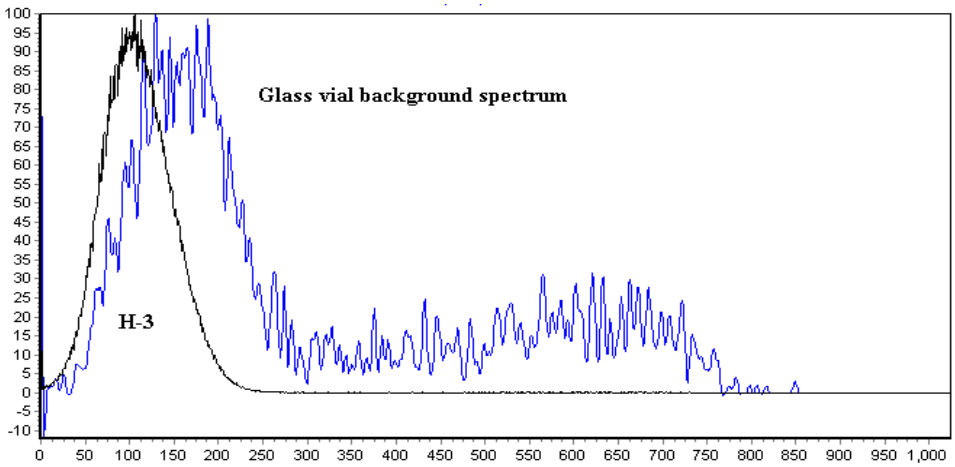

Figure 1: Background sample spectrum in a low potassium glass vial. ^{3}H spectrum corresponds to sample 2. Sample scales are normalized to maximum vertical displacement. Pulse shape analyzer was not active in the runs.

The results were obtained by using non-radioactive polyethylene (PE) vials and a mixture of 10 mL Ultima Gold LLT cocktail with 10 mL of water sample [11]. The mean count rates are given for 2 x 3 repeats of the sample measurements. Sample stayed in counting chamber during each 3 repeat sequence. Counting time for each repeat is 1 h and time difference to the later 3 repeats was 60 h, i.e. 6 h total counting time for each sample. Looking at the background sample spectra and at the corresponding count rates it is clear that there is some extra background in the wide tritium window for sample 1 BKG (Fig 2).

Tap water samples 3 to 8 have no observable tritium concentration, as enrichment does not increase the count rates. A great part of the remaining background signals below Ch.300 rising towards lower channels in the wide tritium window is due to the presence of the radon gas in laboratory air [12]. The nitrogen luminescence by radon alpha particles in the counting chamber produces an identifiable spectral peak in the tritium window. Cocktail itself contains a little ^{40}K, which shows as a rising background in Ch.400-750, but very little in tritium window. The samples were at about the same quench level considering the variation of SQP(E) and therefore, all tritium activity calculations are given for a fixed counting efficiency. The best figure of merit (FOM) is obtained for optimal Ch.20-160 window, with Eff = 22.2 % and mean Bkg = 1.066 CPM: FOM = Eff^2/Bkg = 460, while for wide tritium window FOM = 384.

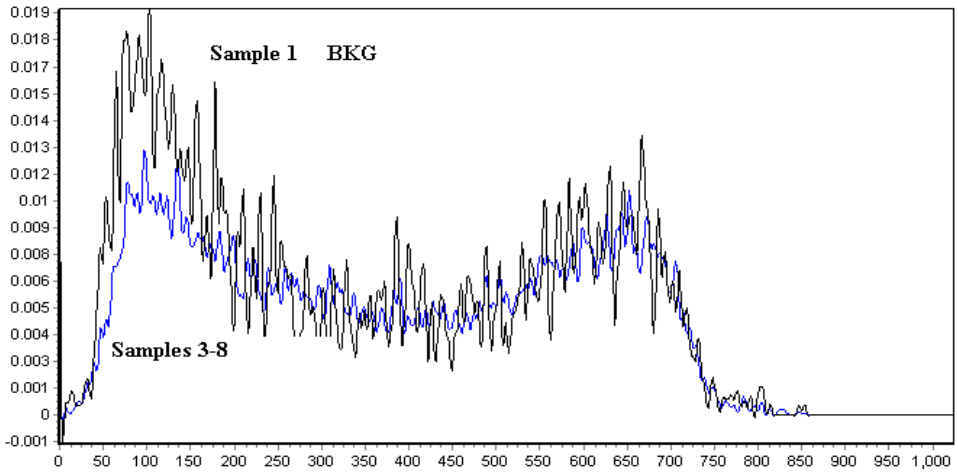

Figure 2: Background spectra of sample 1 BKG and sum of samples 3-8.

The detection sensitivity for the tritium analysis method, given by the minimum detectable activity (MDA) or concentration (MDC), is enhanced by the order of magnitude of the enrichment factor EFT provided by the electrolysis, i.e. MDA or MDC/EFT = 0.95/11 $\cong$ 0.08 Bq kg^{-1} or $\cong$ 0.7 TU for l.e. and MDC/EFT= 0.95/22 = 0.04 Bq kg^{-1} or $\leq$0.4 TU for h.e. where MDA = 0.95 Bq kg^{-1} is calculated for 10 mL volume of water (0.01 kg), in optimal window and with a counting time of 24 h.

4 Conclusions

By comparing the EFT calculated with the aid of the deuterium concentrations (measured by mass spectrometry before and after the enrichment) with the ratios of tritium count rates determined by LSC it is obvious that there is an excellent agreement in the case of samples with a significant content of tritium. The spectra accumulated with the samples in PE vials have revealed some radon and ^{40}K contribution to the background in the tritium window. Without these contributions the background could be reduced at least by 2 times than the mean background obtained. The underground laboratories of Gran Sasso provides an excellent environment for low background measurements, taking into consideration that the cosmic contribution is almost entirely missing. Nevertheless, it seems that only a strict reduction and control of radon in the surrounding air will ensure the best conditions which presume a residual background merely from the inherent radioactivity of the phototubes and of the bedrock [12].

Acknowledgements We wish to thank Prof. Eugenio Coccia, Director of Gran Sasso National Laboratory, for his kind collaboration, and Dr. Nicola Ferrari, Dr. Fausto

Chiarizia of the LNGS for their very useful and precious assistance. The work was funded by EU-LNGS (INFN) (HPRI-CT-2001-00149) LNGS (INFN)-TARI

References

[1] D.J. Groeneveld, Tritium analysis of environmental waters, PhD Thesis, Univ. Grningen, 1977.

[2] G.T. Cook, Ch.J .Passo and B. Carter, in: Handbook of radioactivity analysis, M.F.LAnnunziata ed., Academic Press N.Y. 1995 , pp.358-365.

[3] G. Sauzay and W.R. Schell, Analysis of low level tritium concentration by electrolytic enrichment and liquid scintillation counting, Int.J.Appl.Radiat.Isotopes 23,(1966)25.

[4] C.B. Taylor, Tritium enrichment of environmental waters by electrolysis: development of cathodes exhibiting high isotopic separation and precise measurement of tritium enrichment factors, Proc.Int.Conf. on Low-level radioactivity measurements and applications, High Tatras, oct.1977, pp.131-140.

[5] P.K. Zutshi and J. Sas-Hubicky, A new cathode treatment for the reproducible enrichment of tritium, Int.J.Appl.Radiat.Isotopes 17(12), (1966) 670.

[6] W. Plastino, L .Kaihola, P. Bartolomei and F. Bella, Cosmic background reduction in the radiocarbon measurements by liquid scintillation spectrometry at underground laboratory of Gran Sasso, Radiocarbon 43(2-3), (2001) 157-161.

[7] W. Plastino, L .Kaihola, Surface and underground ultra low level scintillation spectrometry, Radiocarbon, 46(1), (2004) 97-104.

[8] W. Plastino, L .Kaihola, Radiocarbon measurements by liquid scintillation spectrometry at the Gran Sasso National Laboratory, Journal of Environmental Radioactivity, (2005) in press.

[9] C. Arpesella, Background measurements at Gran Sasso Laboratory, Nuclear Physiscs B (Proc.Suppl) 28A (1992) 420-424.

[10] L. Kaihola, Liquid scintillation counting performance using glass vials in the Wallac 1220 Quantulus, in: H. Ross, J.E. Noakes and J.D. Spauling eds. Liquid scintillation Counting and organic scintillators, Chelsea, Michigan, Lewis Publishers, 1991, pp. 495-500.

[11] F. Schonhofer and C. Kralik , Optimisation of liquid scintillation measurements of environmental tritium, Radioactivity & Radiochemistry 10(4) , (1999) 14-17.

[12] W. Plastino, I. Chereji, S. Cuna, L. Kaihola, N. Lupsa, G. Balas, V. Mirel, P. Berdea, C. Baciu, Tritium electrolytic enrichment of environmental waters and liquid scintillation analysis by Quantulus at the Gran Sasso National Laboratory (Italy), Applied Radiation and Isotopes, submitted.

TELLUS. Ground Deformations and their Effects in the near-Earth Space.

V. Sgrigna[a], A. Buzzi[a], L. Conti[a], C. Stagni[a], D. Zilpimiani[b]

[a] Dipartimento di Fisica e Sezione INFN, Università Roma Tre - Italy
[b] Institute of Geophysics, Georgian Academy of Sciences (GAS)
and National Space Agency, Tbilisi - Republic of Georgia

Abstract

This report will describe the activities carried out by the TELLUS team during 2004. They are continuing those concerning ground aseismic creep strain events, observed by the TELLUS tilt network; the ESPERIA space mission project planned and designed for studying Earth near-Earth space interactions; the construction of the particle detector ARINA to be installed on board the Russian satellite RESURS-DK1, which launch is scheduled for next autumn 2005 within the PAMELA mission. ARINA is part of the ESPERIA payload, another one being the LAZIO-EGLE magnetic and particle instruments to be tested in space on board the International Space Station and used for collecting particle and magnetic data. These two instruments have been built during 2004 within a collaboration between the Universities Roma Tre, Perugia and Roma Tor Vergata, and related INFN branches, with the Lazio Region and Polytechnic of Moscow (MEPhI). LAZIO-EGLE thermal, vibration and electromagnetic emission tests have been performed in laboratory both in Italy and in Russia. Launch is scheduled for February 2005. During 2004, on the basis of an ITT of the European Space Agency (ESA), the TELLUS team also submitted as sub-contractor (the prime one being Alenia-Laben S.p.A.) the ARETUSA proposal for a General Study with title " Techniques and Spaceborne Concepts for the Study of Earth-Quake Precursors and Analysis of Associated Atmospheric Effects ". Both the ARETUSA proposal and the construction of the EGLE space magnetometer will be described in the present annual report.

1 The aim of the TELLUS Experiment

The main scientific objective of the TELLUS experiment is the study of Earth's surface rock deformation events (as earthquakes) and their possible effects in the atmospheric, ionospheric, and magnetospheric regions. Electromagnetic emissions (EME) associated with seismic events appear to be and efficient coupling element between the Earth's surface and the surrounding near space. At this purpose continuous mechanical measurements

are performed at three tilt sites of LNGS while pre-seismic EME-wave investigations demand for specific space experiments to be carried out on board of LEO (Low-Earth-Orbit) satellites. But these theoretical aspects have already been discussed in previous TELLUS annual reports [1] and will not be reported here. We only remember here that a space mission project (ESPERIA) has already been performed for the Italian Space Agency (ASI) and one of the ESPERIA instruments (the ARINA particle detector) has been built during 2002. They have been described in the previous LNGS Annual Reports 2002, 2003 [1, 2]. During 2004 another ESPERIA instrument (the EGLE magnetometer) has been built and tested in laboratory, as well as a proposal (ARETUSA) for a general study has been submitted to ESA. Both EGLE and ARINA instruments will be launched during 2005. The first one in February, on board the ISS, and the second one in autumn, on board the Russian satellite RESURS-DK1, within the PAMELA mission. Then, the TELLUS experiment give a contribution to a more general scientific project devoted to study ionospheric and magnetospheric perturbations caused by seismicity, and in particular, to develop a method to reveal short-term earthquake precursors.

2 Experimental Apparatus

During 2003 a first study for a new magnetic sensor and related electronic unit was carried out [1]. On the basis of these preliminary investigations, a new space magnetometer (EGLE) has been built in 2004. It is described briefly in the following. The EGLE magnetometer is accompanied by the LAZIO particle detector. Both the two instruments will perform measurements to monitor the radiation and magnetic environment inside the ISS.

2.1 The EGLE magnetometer

EGLE will be used to measure the intensity and variations of the magnetic field within the ISS, and to correlate these measurements with those of particle fluxes detected by LAZIO. EGLE will be tested in space together with its data acquisition system based on the 1-Wire technology. This magnetometer is constituted by:

- a single axis search coil probe, the EGLE Magnetometer Head (MH)
- an electronic interface with signal conditioning and data acquisition system (EGLE MB box)
- a 2m long cable to connect LAZIO and EGLE
- a 1-Wire to RS232 serial adapter on the LAZIO pc tower.

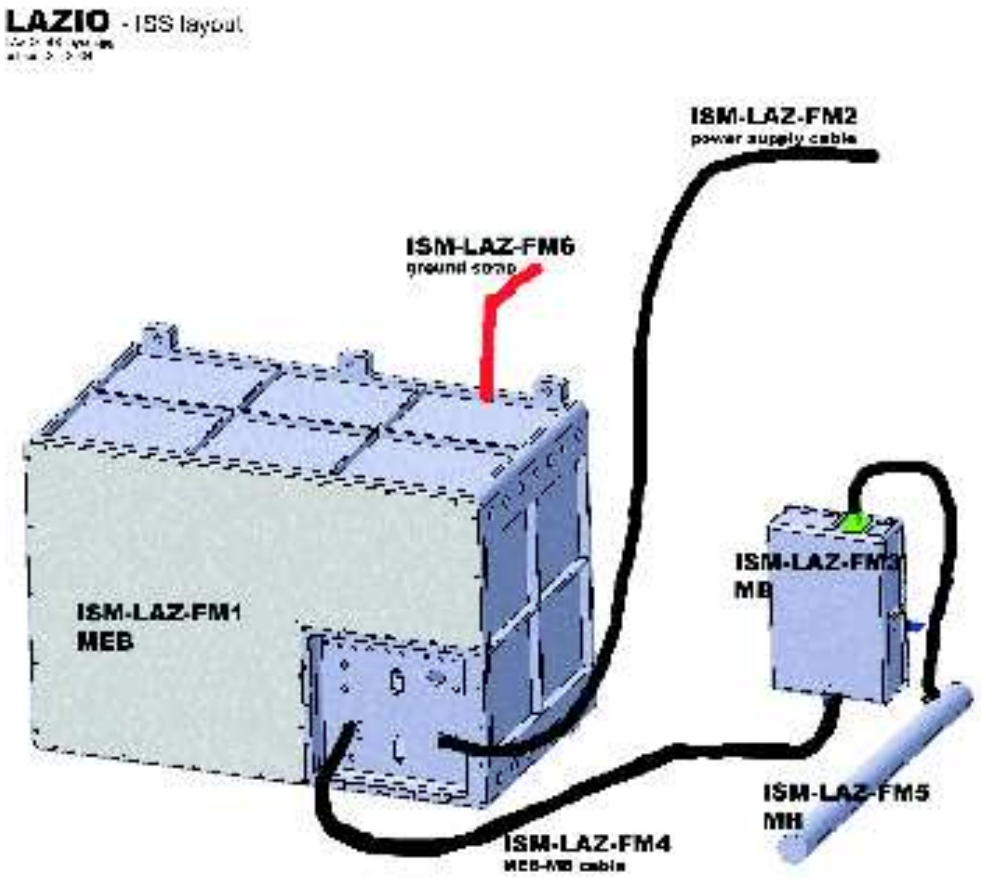

Figure 1: A schematic representation of the LAZIO-EGLE space experiment. The figure shows the LAZIO (MEB) box, EGLE (MB) box , and (MH) probe connection.

The EGLE magnetometer has been planned and designed for automatic measurements of the low frequency component of the magnetic field. Positive characteristics of EGLE are its:

- small dimensions and mass; low power consumption;
- original data acquisition system via 1-Wire technology;
- standard power supply.

2.1.1 EGLE magnetic probe (MH)

The EGLE magnetic probe has been built making use of high-quality components and materials in order to ensure a reliable operation in the outer space during its launch time.

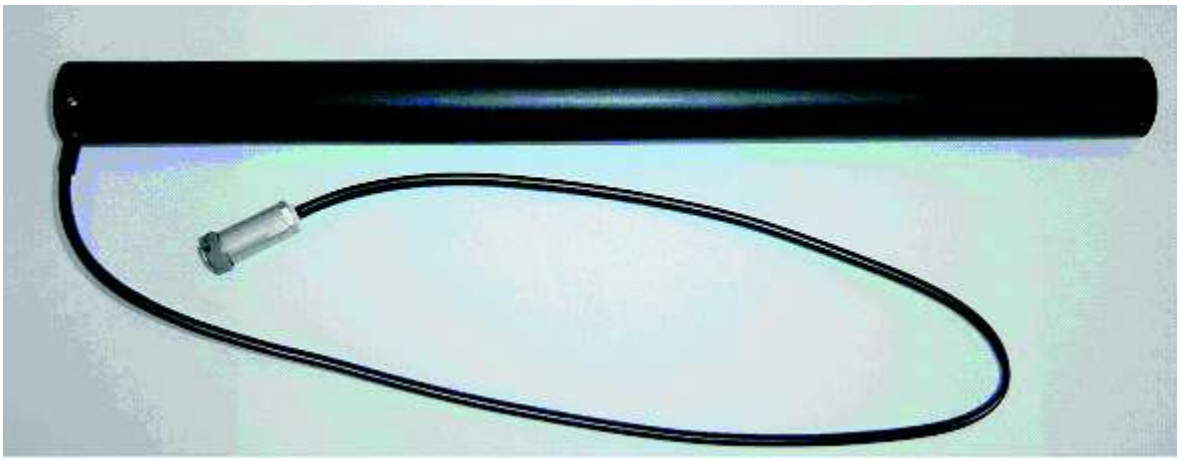

Figure 2: EGLE magnetic probe MH with 0.7m cable connected.

The basic technical specifications of the EGLE probe MH are summarized in figure 3.

Basic technical specifications of the EGLE probe MH	
Frequency band of receiver signals	0.5 ÷ 50000 Hz
Shape of transfer function	linear – flat
Type of output	Symmetrical
Transformation factor at both output terminals:	
▪ at linear part (0.5 – 5 Hz)	f*4 mV/(nT*Hz)
▪ at flat part (5 – 50000 Hz)	20 mV/nT
Transformation factor error:	
▪ at flat part of band pass without edges	≤ ±0.25 dB
▪ at flat part band pass edges	≤ 3 dB
Magnetic noise level, $pT*Hz^{-1/2}$:	
▪ at 5 Hz	≤ 0.4
▪ at 100 Hz	≤ 0.02
▪ at 5 kHz	≤ 0.004
▪ at 50 kHz	≤ 0.02
Nominal output load	≤ 200 pF ≥ 50 kΩ
Power supply voltage	± (15 ± 0.2) V
Power consumption	300 mW
Temperature range of operation	$-30^{\circ}C \div +50^{\circ}C$
Outer dimensions (without prominent parts)	l = 400 mm d = 32 mm
Length of the output cable	0.7 m
Weight	≤ 320 g

Figure 3: Basic Technical Specifications of the EGLE probe

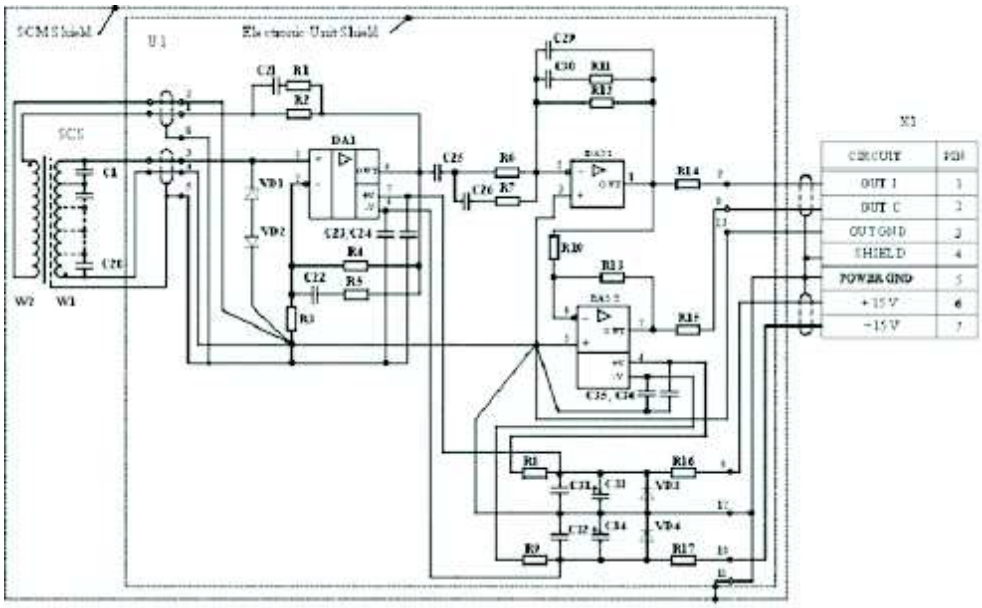

Figure 4: EGLE magnetic probe MH schematic diagram

2.1.2 The EGLE Signal Conditioning and data acquisition system

Magnetic field signals detected by the EGLE (MH) probe are amplified, filtered and acquired by the EGLE signal conditioning and data acquisition board located into the EGLE (MB) box. It allows to collect magnetic field data in the following four frequency bands:

- 1 Hz ÷ 40 Hz
- 0.5 Hz ÷ 5 kHz
- 20 kHz ÷ 40 kHz
- 1 Hz ÷ 20 Hz

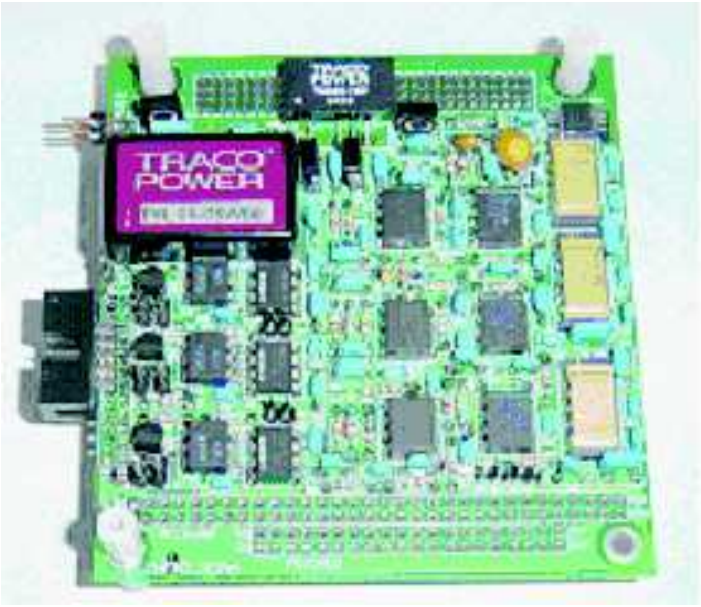

Figure 5: EGLE signal conditioning and data acquisition board

2.1.3 The EGLE 1-Wire technology for both data and power trasmission

The Dallas Semiconductor/Maxim 1-Wire technology uses a single wire (plus ground) to accomplish both communication and power transmission between the central electronic unit and sensors. A single bus master can feed multiple slaves over a single twisted-pair cable. The 1-Wire net is a bus based on a PC or microcontroller communicating digitally over twisted-pair cable with 1-Wire components. The network is defined with an open-drain (wired-AND) master/slave multidrop architecture that uses a resistor pull-up to a nominal 5V supply at the master. A 1-Wire net-based system consists of three main elements: a bus master with controlling software; wiring and associated connectors; and 1-Wire devices. Every slave has a globally unique digital address. The system permits tight control because no node is authorized to speak unless requested by the master, and no communication is allowed between slaves except through the master. Both master and slaves are configured as transceivers permitting bit sequential data to flow in either direction, but only one direction at a time, with data read and written least significant bit (LSB) first. The 1-Wire net is connected to the serial RS-232 CPU port via a 1-Wire to serial adapter. Data on the 1-Wire net is transferred by time slots; a system clock is not required, as each 1-Wire part is self-clocked by its own internal oscillator synchronized to the falling edge of the master. Power for chip operation is derived from the bus during idle communication periods when the DATA line is at 5V by including a half-wave rectifier on each slave.

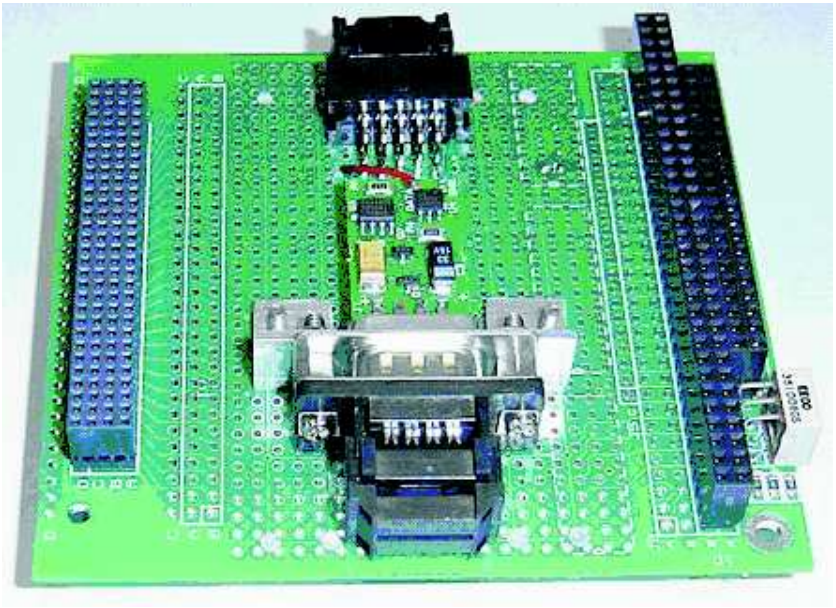

Figure 6: 1-Wire to RS232 serial adapter installed on the LAZIO pc104 tower

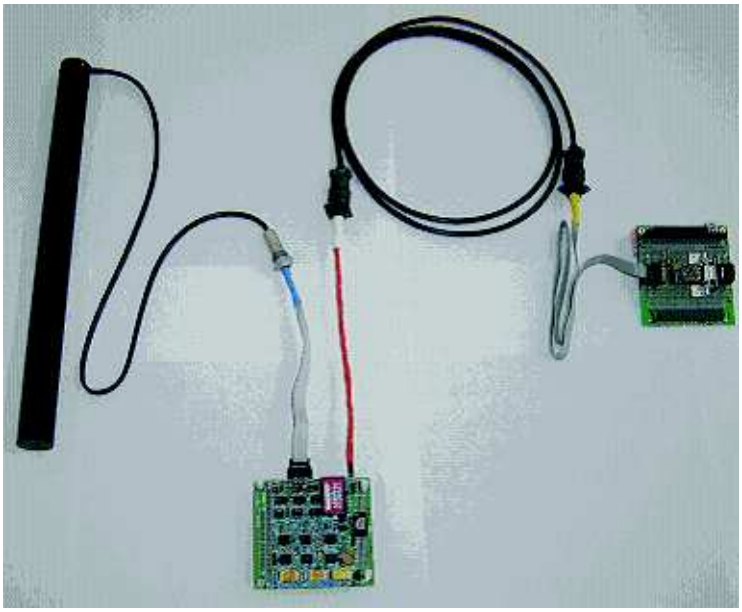

Figure 7: LAZIO-EGLE connections scheme. Magnetic sensor (left), EGLE acquisition board mounted inside the EGLE MB box (bottom), Lazio MEB box - EGLE MB box connection cable (top), 1-Wire-Serial board mounted on the pc tower (right).

2.2 EGLE software

The EGLE software has two main operational modes:

- calibration : This mode is for optimising data acquisition in order to allow changes of the electronic gain at different frequency bands.
- monitoring : Continuous acquisition in the above mentioned 4 frequencies bands.

Data acquisition is done at 16 bits. Is possible to upgrade the EGLE acquisition parameters by re-installing the acquisition software on the MEB pc tower. Magnetic field data will be recorded in the PCMCIA card of LAZIO MEB. EGLE magnetic field data will be analyzed on the ground and then correlated with the LAZIO particle detector measurements.

3 The ARETUSA Proposal

ARETUSA (Analysis of the Relationships between Electromagnetic emission and Tectonic local deformation event Ushering Seismic Activity) is a general study submitted to ESA in December 2004. It is based on the following preliminary statements.

1. Natural disasters are of serious concern to the mankind and the earthquake is one of the most dangerous of them, another one being the effects produced by volcanic eruptions. Therefore any plausible approach suitable to reduce the impact of these disasters deserves great attention.
2. In this frame earthquake prediction becomes one of the most important societal goal of scientists
3. Hence, the Proposal aims at giving a contribution along this direction and on a deterministic basis. Of course, it is not meant to achieve immediately an explicit solution to the problem, that is being studied since decades giving confirmation of its immense complexity.
4. At present some attempts to build a theory of earthquake prediction are far from being defined and generally accepted.
5. But numerous earthquake related phenomena, and in particular the so-called earthquake precursors (or pre-seismic anomalies, or earthquake forerunners), have been observed prior to catastrophic events like earthquakes.
6. These anomalies associated to seismic events have been observed from both ground-based and space measurements and have indicated some degree of positive statistic correlation with the earthquake preparation and occurrence.
7. The Study we are going to propose is based on the detection of the most significant earthquake precursors.

8. Both near-Earth space and ground-based continuous observations of pre-seismic changes will be carried out in the so-called topside ionosphere and in several seismic areas, respectively, within a "unified" physical model of earthquake forerunners.

9. This "unified" model will:

   a describe the preparation phase of an earthquake and involved physical mechanisms;

   b justify the genesis and characteristics of pre-seismic anomalies, together with their relative and absolute reliability as earthquake predictors;

   c allow a fundamental and better understanding of the physics of the lithosphere-atmosphere-ionosphere-magnetosphere interactions.

10. Results, observations and modeling will be used to validate a method for possible future applications in earthquake forecasting and early warning service.

11. So, it is evident that earthquake precursors are not only of fundamental but also of practical importance since earthquake prediction is an extremely important and urgent problem

12. In the present Study we will try to demonstrate consistently a causal relationship with explained physical processes and looking for a correlation between data gathered simultaneously and continuously by space observations and ground-based measurements.

13. From an objective standpoint, once these relationships and correlations will be pointed out, we are confident that the combination of data from both Earth and near-Earth space, with their inherent analysis, can provide the scientific basis to establish a coherent interpretation of the assumed earthquake forerunners and, consequently, to enable and pave the way to future applications and services on a sound scientific basis.

The primary objectives of the Study are:

1. propose a physical model of earthquake forerunners on a scientific and deterministic basis, to define a method for future applications and services in earthquake forecasting;

2. validate such a model, and consequent method, through coordinated and simultaneous ground-based and space observations

The methodology used to achieve these objectives is based on:

1. Ground-based observations of seismic precursors from different ground test sites, by instrument monitoring networks working in different seismic areas of the Earth's surface.

2. Space observations of seismic precursors from data collected on board of dedicated satellites.

3. Search of precursor signals from the coordinated and simultaneous observations of the previous two items.

4. Relative and absolute estimation of the reliability of anomalous signals as earthquake precursors

5. Interpretation of the results within a "unified" physical model and their possible application in earthquake forecasting and early warning service.

4 List of Publications

List of the publications during 2004:

1. Sgrigna, V., R. Console, L. Conti , A.M. Galper, V. Malvezzi, M. Parrot, P. Picozza, R. Scrimaglio, P. Spillantini, D. Zilpimiani, 2004. The ESPERIA Project: a Mission to Investigate the near-Earth Space, in: Earth Observation with CHAMP, Results from Three Years in Orbit, C.Reigberg, H. Luhr, P. Schwintzer, J. Wickert (Editors), Potsdam, August 2004, Springer Geosciences Series, Berlin, pp.407-412.

2. Sgrigna, V., A. BuzziL. Conti, A.V. Guglielmi, O.A. Pokhotelov, 2004. Electromagnetic Signals Produced by Elastic Waves in the Earth's Crust, Nuovo Cimento, 27C, 115-132.

3. Conti, L., Cirella, A., Malvezzi, V., Sgrigna, V., 2004. A model for the propagation of preseismic electromagnetic fields through lithosphericand atmospheric media, 2004. Proc.1st General Assembly, European Geosciences Union, Nice, France, 25-30 April 2004, EGU04-A-04927; NH4.02-1FR4P-0430, p. 337, 2004.

4. Sgrigna, V., Console, R., Buzzi, A., Conti, L., Galper, A.M., Malvezzi, V., Parrot, M., Picozza, P., Scrimaglio, R., Spillantini, P., Zilpimiani, D., 2004. ESPERIA: an equatorial magnetic, plasma and particle mission for monitoring perturbations in the topside ionosphere and for defining the near-Earth magnetic environment, EOS Trans., AGU, vol. 85, GP13A-03, n.17, JA162, 2004 (INVITED).

5. Malvezzi, V., Buzzi, A., Cirella, A., Conti, L., Sgrigna, V., 2004. A physical model of seismo-associated electromagnetic emissions propagating in layered lithospheric and atmospheric media, EOS Trans., AGU, vol. 85, GP21A-02, n.17, JA164, 2004.

6. Sgrigna, V.; The ESPERIA team, 2004. The ESPERIA equatorial, electromagnetic, plasma, and particle mission concerned with detecting preseismic related signals, in: COSPAR04-A-01843 A0.2-0005-04, Programme, pag.26, 35th COSPAR Scientific Assembly, Paris, France, 8 - 25 July 2004

7. Sgrigna, V., 2004. Description and Testing of ESPERIA Instruments (ARINA and LAZIO-SIRAD) in Space, EOS Trans., AGU, vol. 85, T53C-03, n.47, F1795, 2004 (INVITED).

8. Sgrigna, V.; Buzzi, A.; Conti, L.; Picozza, P.; Stagni, C.; Zilpimiani, D., 2005. Ground rock deformation events and their possible effects in the near-Earth space, EGU05-A-06210, EGU General Assembly, Vienna 2005, Austria, 24-29 April, 2005 (INVITED).

References

[1] Sgrigna, V., A. Buzzi, A. Cirella, L. Conti, V. Malvezzi, 2003. TELLUS. Ground deformations and their effects in the near-Earth space, Laboratori Nazionali del Gran sasso, INFN, Annual Report, 2003, pp. 221-228.

[2] Sgrigna, V., Conti, L., Malvezzi, V., 2002. TELLUS. Ground deformations and their effects in the near-Earth space, Laboratori Nazionali del Gran sasso, INFN, Annual Report, 2002, pp. 217-232.